

Flavor changing neutral currents and rare decays of K-mesons

L G Landsberg

DOI: 10.1070/PU2003v046n10ABEH001331

Contents

1. Introduction	995
2. The Standard Model and New Physics	996
2.1 The main ideas of the Standard Model; 2.2 Weak decays and the problem of long distances; 2.3 Physics beyond the Standard Model	
3. Violation of CP invariance	1005
3.1 Direct CP violation in the decays of neutral and charged mesons; 3.2 Indirect CP violation in the $P^0 \rightleftharpoons \bar{P}^0$ mixing of electrically neutral mesons; 3.3 CP nonconservation in the interference of direct decays and mixing processes	
4. Processes involving K- and B-mesons and properties of the unitary triangle	1008
4.1 Data on the CP-violation parameter ϵ_K in $K^0 \rightleftharpoons \bar{K}^0$ mixing; 4.2 Data on the side R_b of the triangle; 4.3 The mixing processes $B_d^0 \rightleftharpoons \bar{B}_d^0$ and $B_s^0 \rightleftharpoons \bar{B}_s^0$; 4.4 Violation of CP invariance and the measurement of asymmetry in the decays $B_d^0 \rightarrow (J/\psi)K_S^0$ and $\bar{B}_d^0 \rightarrow (J/\psi)K_S^0$; 4.5 Prospects for further investigation of the parameters of the unitary triangle	
5. The decays $K^+ \rightarrow \pi^+ \nu \bar{\nu}$ and $K_L^0 \rightarrow \pi^0 \nu \bar{\nu}$	1020
5.1 General considerations; 5.2 The $K \rightarrow \pi \nu \bar{\nu}$ decays in the Standard Model; 5.3 Other rare FCNC decays of kaons; 5.4 Experimental studies of the decays $K^+ \rightarrow \pi^+ \nu \bar{\nu}$ and $K_L^0 \rightarrow \pi^0 \nu \bar{\nu}$ (state of affairs and prospects)	
6. Rare decays of K- and B-mesons, CP violation in the Standard Model and beyond it	1031
6.1 Joint analysis of the data from experiments with K- and B-mesons and searches for manifestations of New Physics; 6.2 Models with New Physics and their influence on the $K \rightarrow \pi \nu \bar{\nu}$ -decay probabilities	
7. Conclusions	1044
8. Appendices	1045
I. Determination of $\sin 2\beta$ in the SM from measurements of the branching ratios for $K^+ \rightarrow \pi^+ \nu \bar{\nu}$ and $K_L^0 \rightarrow \pi^0 \nu \bar{\nu}$; II. Modified formulas for mixing processes and for FCNC decays in MFV models; III. More precise relationship for $BR(K^+ \rightarrow \pi^+ \nu \bar{\nu}) = K_+ B(\lambda_c; \lambda_i)$	
9. Notes added in proof	1048
References	1048

Abstract. Processes with K-mesons that are due to weak flavor changing neutral currents (FCNC) are considered, primarily, the theoretically clean ‘golden decays’ $K^+ \rightarrow \pi^+ \nu \bar{\nu}$ and $K_L^0 \rightarrow \pi^0 \nu \bar{\nu}$. Experimental data for these and other processes violating CP invariance are discussed, and the prospects of future studies are examined. The results of experiments with kaons are compared with those obtained for B-mesons (CP-odd asymmetry in the decays $B_d^0(\bar{B}_d^0) \rightarrow (J/\psi)K_S^0$, $B^0 \rightleftharpoons \bar{B}^0$ mixing). A possible interpretation of the data on the decays $K \rightarrow \pi \nu \bar{\nu}$, $K_L^0 \rightarrow \pi^0 e^+ e^-$, and $K_L^0 \rightarrow \mu^+ \mu^-$ is discussed within the framework of the Standard Model and of New Physics models.

1. Introduction

Processes with neutral currents that do not conserve quark flavors (FCNC — Flavor Changing Neutral Currents), and related rare decays in higher orders of the weak interaction, ($K^0 \rightleftharpoons \bar{K}^0$)- and ($B^0 \rightleftharpoons \bar{B}^0$)-mixing, the violation of CP invariance and studies of the mechanisms of such violation — all these phenomena play an extremely important role in the development of the modern theory of elementary particles, the so-called Standard Model (SM), and, also, in searches for possible manifestations of New Physics (NP) extending beyond the framework of this theory.

In the present review we shall attempt to summarize the results of the principal experiments performed within the past few years and devoted to the study of rare kaon decays related to the general concept of FCNC processes, to various CP violations, to data on the quark mixing matrix and its unitarity, and to other SM ideas. We shall consider the prospects of a new generation of experiments for studying rare kaon decays and, first of all, of theoretically clean processes such as $K \rightarrow \pi \nu \bar{\nu}$, and we shall also compare the expected results of these investigations with certain other experiments involving B-mesons. Comparison of these data with SM predictions and possible NP effects will be performed throughout the entire review. One must bear in

L G Landsberg RF State Scientific Center
‘Institute for High Energy Physics’,
142280 Protvino, Moscow Region, Russian Federation
Tel. (7-096) 771 31 05. Fax (7-096) 774 49 37
E-mail: lgl@mx.ihep.su

Received 9 October 2002, revised 2 July 2003
Uspekhi Fizicheskikh Nauk 173 (10) 1025–1082 (2003)
Translated by G Pontecorvo; edited by A Radzig

mind that this review has been written by an experimentalist and, for this reason, problems of completed and planned experiments will always hold the most central part of the author's attention. Certain details will be dealt with in considering a number of effects, for the same reason.

From a historical standpoint, precisely the absence of neutral currents that do not conserve quark flavors (for example, $K_L^0 \rightarrow \mu^+\mu^-$ decays being extremely rare), and studies of K_L^0 - and \bar{K}^0 -meson mixing played an essential role in the creation of modern ideas concerning quark generations and quark mixing, which underlie the SM.

In this review, and especially in the introductory Section 2, material has been used from well-known monographs [1–7], from a number of recent international conferences [8–23], and from review articles and talks [24–48], containing references to the original publications. The present work represents a further development of the previous review by the author [42], complements it, and is based on new material. Although the two reviews do overlap to a certain extent, we have tried to minimize this effect, and in a number of cases we merely refer the reader to review [42].

2. The Standard Model and New Physics

2.1 The main ideas of the Standard Model

The main ideas of modern elementary particle physics are consistent with the so-called Standard Model¹, which provides a good description of physical phenomena within the scale of masses up to 100 GeV, or even up to several hundred GeV. The SM includes three generations of fundamental particles — quarks and leptons:

- u, d, e, ν_e (first generation),
- c, s, μ , ν_μ (second generation),
- t, b, τ , ν_τ (third generation).

These fundamental families exhibit the same structure, but differ significantly in mass.

Strong interactions between quarks characterized by special quantum numbers — flavors and colors — are realized by the exchange of eight types of massless colored vector gluons. These interactions are described within the framework of the modern theory of strong processes — quantum chromodynamics (QCD) — which at sufficiently small distances (smaller than $1\text{--}2 \text{ GeV}^{-1}$) permits us to perform quite satisfactorily perturbative calculations with account of the leading logarithmic approximation, as well as the next-to-leading one. Color quantum numbers of quarks and gluons make them unobservable in a free state (the concept of confinement). Strong interactions conserve the quark flavors, so that in such processes quarks cannot transform into quarks of other flavors and can only be rearranged into various combinations, be produced in pairs ($q\bar{q}$), or undergo annihilation of such pairs.

Electroweak interactions involving both quarks and leptons are carried by the intermediate bosons W^\pm , Z and the photon γ . An important role in weak interactions must, apparently, also be assumed by scalar Higgs bosons which, however, have yet to be found. In the SM there should exist an observable Higgs boson H^0 . Weak interactions of charged

currents carried by W^\pm -bosons change the quark flavors, as we shall see below.

Now, we shall consider in greater detail the electroweak interactions $SU(2)_L \times U(1)$. The interaction Lagrangian includes left-handed quarks and leptons that group into weak isospin doublets

$$\begin{pmatrix} \nu_e \\ e^- \end{pmatrix}_L, \quad \begin{pmatrix} \nu_\mu \\ \mu^- \end{pmatrix}_L, \quad \begin{pmatrix} \nu_\tau \\ \tau^- \end{pmatrix}_L, \quad (2)$$

$$\begin{pmatrix} u \\ d' \end{pmatrix}_L, \quad \begin{pmatrix} c \\ s' \end{pmatrix}_L, \quad \begin{pmatrix} t \\ b' \end{pmatrix}_L, \quad (3)$$

and right-handed quark and lepton singlets q_R, l_R . Left- and right-handed fermions can be represented as²

$$\psi_L = \frac{1}{2}(1 + \gamma_5)\psi, \quad \psi_R = \frac{1}{2}(1 - \gamma_5)\psi. \quad (4)$$

Electroweak interactions of quarks and leptons are realized by exchanging the heavy gauge intermediate bosons W^\pm and Z^0 and massless photons. These interactions are described by the Lagrangian

$$L[SU(2)_L \times U(1)] = L_{CC} + L_{NC}. \quad (5)$$

The Lagrangian density L_{CC} is determined by the charged weak ($V - A$) current:

$$L_{CC} = \frac{g_2}{2\sqrt{2}}(J_\mu^+ W^{+\mu} + J_\mu^- W^{-\mu}), \quad (6)$$

where

$$J_\mu^+ = (\bar{u}d')_{V-A} + (\bar{c}s')_{V-A} + (\bar{t}b')_{V-A} + (\bar{\nu}_e e)_{V-A} + (\bar{\nu}_\mu \mu)_{V-A} + (\bar{\nu}_\tau \tau)_{V-A}. \quad (7)$$

These interactions, due to the exchange of intermediate W^\pm -bosons, proceed with a change in the quark flavors.

The Lagrangian density L_{NC} of the neutral current has the form

$$L_{NC} = e J_\mu^{\text{em}} A^\mu + \frac{g_2}{2 \cos \vartheta_W} J_\mu^0 Z^\mu, \quad (8)$$

where J_μ^{em} represents the vector electromagnetic current, and J_μ^0 is the neutral weak current with ($V - A$) and ($V + A$) components

$$J_\mu^{\text{em}} = \sum_f Q_f \bar{f} \gamma_\mu f, \quad J_\mu^0 = \sum_f \bar{f} \gamma_\mu (v_f + a_f \gamma_5) f. \quad (9)$$

Here, $v_f = T_3^f - 2Q_f \sin^2 \vartheta_W$ and $a_f = T_3^f$ are the coefficients of the vector and axial components of the neutral weak current, $\sin^2 \vartheta_W = 0.23143 \pm 0.00015$ is the sine squared of the Weinberg angle, $g_2^2/8M_W^2 = G_F/\sqrt{2}$ is the weak interaction Fermi constant, and, finally, Q_f and T_3^f represent the electric charge and the third component of the weak isospin of fermion f .

² Hereinafter the quantity γ_5 is defined as in Ref. [1]:

$$\gamma_5 = \gamma^5 = - \begin{pmatrix} 0 & I \\ I & 0 \end{pmatrix}.$$

We also recall how the weak ($V - A$) current is defined in the SM. The current J_μ^+ corresponding to the weak ($i \rightarrow f$) transition from the initial to the final fermion with $\Delta Q = +1$ contains differences between vector and axial terms such as

$$\bar{f} \gamma_\mu (1 + \gamma_5) i = 2\bar{f}_L \gamma_\mu i_L = \bar{f} \gamma_\mu i - \bar{f} \gamma_5 \gamma_\mu i = V_\mu - A_\mu = (\bar{f} i)_{V-A}.$$

¹ The material of this introductory section is discussed in greater detail in review [42].

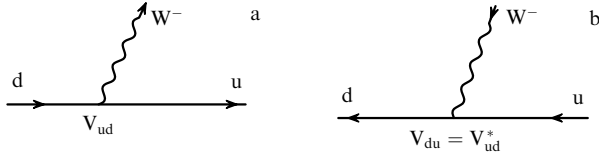


Figure 1. The role of the V_{CKM} matrix elements for the transition amplitudes of $d \rightarrow u$ and $u \rightarrow d$ with the production of W^- -bosons. From the diagrams one can see that $A(d \rightarrow u) \propto V_{ud}$, and $A(u \rightarrow d) \propto V_{du} = V_{ud}^*$ (time reversal results in complex conjugation). For antiquarks, one has $A(\bar{u} \rightarrow \bar{d}) \propto V_{ud}$, and $A(\bar{d} \rightarrow \bar{u}) \propto V_{ud}^*$.

The expressions for weak quark charged currents contain the transformed components of the ‘lower’ quarks d' , s' and b' , determined by the Cabibbo–Kobayashi–Maskawa unitary quark mixing matrix V_{CKM} [49]

$$\begin{pmatrix} d' \\ s' \\ b' \end{pmatrix} = \begin{pmatrix} V_{ud} & V_{us} & V_{ub} \\ V_{cd} & V_{cs} & V_{cb} \\ V_{td} & V_{ts} & V_{tb} \end{pmatrix} \begin{pmatrix} d \\ s \\ b \end{pmatrix} = V_{\text{CKM}} \begin{pmatrix} d \\ s \\ b \end{pmatrix}. \quad (10)$$

Figure 1 illustrates the role played by the elements of the quark mixing matrix in quark transitions. As one can see from this figure, the $d \rightarrow u$ type transition amplitude involving the production of W^- -bosons has the form

$$A(d \rightarrow u) \propto i \frac{g_2}{2\sqrt{2}} \bar{u} V_{ud} \gamma_\mu (1 + \gamma_5) d,$$

while the inverse transitions $u \rightarrow d$ involving the absorption of W^- -bosons are determined by the Hermitian conjugate element $V_{du}^+ = V_{ud}^*$, i.e., the transition amplitude is

$$A(u \rightarrow d) \propto i \frac{g_2}{2\sqrt{2}} \bar{d} V_{ud}^* \gamma_\mu (1 + \gamma_5) u.$$

For antiquarks, the $(\bar{d} \rightarrow \bar{u})$ vertex is determined by the element V_{ud}^* , and the $(\bar{u} \rightarrow \bar{d})$ vertex by the element V_{ud} .

Unitarity of the quark mixing matrix is related to the absence of additional families of fundamental particles and to the conservation of probability (all quark transitions occur in the processes governed by three quark generations). If in nature there existed additional families of fundamental particles interacting with the three quark families (3), then there would be no place left for unitarity of the three-row matrix V_{CKM} , since quark mixing would include new fundamental multiplets. For probability to be conserved it would be necessary to take into account the matrix elements of the respective transitions to these new families, going beyond the limits of the elements of the matrix V_{CKM} .

Unitarity of the V_{CKM} matrix can be written as the condition

$$V_{\text{CKM}}^+ V_{\text{CKM}} = V_{\text{CKM}} V_{\text{CKM}}^+ = 1, \quad (11)$$

which results in a series of relationships for the elements of the quark mixing matrix:

$$\begin{aligned} VV^+ &= \sum_l V_{al} V_{bl}^* = \delta_{ab}, \\ V^+V &= \sum_a V_{al}^* V_{am} = \delta_{lm}, \end{aligned} \quad (12)$$

where $a, b = u, c, t$, and $l, m = d, s, b$. These unitarity relations are discussed in greater detail below.

We note that unitarity of the V_{CKM} matrix is the mathematical basis for the so-called Glashow–Iliopoulos–Maiani mechanism [50] (the GIM mechanism), according to which in the tree approximation (i.e., in the first-order approximation with respect to weak interaction) there exist no neutral currents in SM that change quark flavors. The FCNC terms in the neutral quark currents would have the form $(\bar{d}'s')$, etc. Their absence is due to the unitary relationships.

Indeed, the general form of the neutral weak quark current is written down as

$$\begin{aligned} &(\bar{u}c\bar{t}) \gamma_\mu (a + c\gamma_5) \begin{pmatrix} u \\ c \\ t \end{pmatrix} + (\bar{d}'s'b') \gamma_\mu (a + c\gamma_5) \begin{pmatrix} d' \\ s' \\ b' \end{pmatrix} \\ &= (\bar{u}c\bar{t}) \gamma_\mu (a + c\gamma_5) \begin{pmatrix} u \\ c \\ t \end{pmatrix} \\ &+ (\bar{d}'s'b') V_{\text{CKM}}^+ \gamma_\mu (a + c\gamma_5) V_{\text{CKM}} \begin{pmatrix} d \\ s \\ b \end{pmatrix} \\ &= (\bar{u}c\bar{t}) \gamma_\mu (a + c\gamma_5) \begin{pmatrix} u \\ c \\ t \end{pmatrix} \\ &+ (\bar{d}'s'b') \gamma_\mu (a + c\gamma_5) V_{\text{CKM}}^+ V_{\text{CKM}} \begin{pmatrix} d \\ s \\ b \end{pmatrix}. \end{aligned}$$

The unitarity condition $V_{\text{CKM}}^+ V_{\text{CKM}} = 1$ results in the neutral quark current containing only diagonal terms of the type $(\bar{d}d)_{V-A, V+A}$ and so on. Nondiagonal elements

$$(\bar{u}c)_{V-A, V+A}, \quad (\bar{d}'s)_{V-A, V+A}, \quad \dots$$

(i.e., neutral currents changing quark flavors) are absent owing to the unitarity condition.

However, FCNC processes forbidden in the SM in the first order of the weak interaction (i.e., in the tree approximation) may proceed in the second order, taking into account loop diagrams. They play a very important role in studies of rare kaon decays. In loop diagrams involving virtual u -, c -, and t -quarks, the differences in mass between these quarks violate the compensation for FCNC processes owing to the GIM mechanism. Therefore, the respective decays will take place, but with very small probabilities. We shall deal with these processes in detail in Sections 4 and 5.

Let us note one more important property of the quark (3×3) mixing matrix V_{CKM} : it contains complex matrix elements originated due to the sole nontrivial phase which characterizes V_{CKM} . To see this, we consider the general form of the unitary mixing matrix of a set of n different quarks, namely $(n \times n)$. The total number of degrees of freedom, characterizing a complex unitary $(n \times n)$ matrix amounts to $2n^2 - n - (n^2 - n) = n^2$ (the second term accounts for the unitary relationships for the diagonal matrix elements, while the third term accounts for the same relations for the nondiagonal elements).

Now, of the remaining n^2 parameters, $2n - 1$ represent nonphysical phases which can be removed by redefinition of the nonobservable phases of the quark fields (of $2n$ such phases for the upper and lower quark fields it is possible to choose $2n - 1$ phases arbitrarily). Then, the total number of independent parameters for the unitary $(n \times n)$ mixing matrix equals $n^2 - 2n + 1 = (n - 1)^2$. Here, $n_\theta = (1/2)n(n - 1)$ parameters can be considered independent

mixing angles between various quark ‘generations’ (actually, the number of combinations of n quark indices taken 2 at a time), while the remaining number of parameters $n_\psi = (n-1)^2 - (1/2)(n-1)n = (1/2)(n-1)(n-2)$ can be considered nonvanishing phases of the matrix elements. For $n=3$ (the mixing matrix V_{CKM}), the number of free parameters equals four, with the number of mixing angles being $n_\vartheta = 3$, and the number of phases $n_\psi = 1$.

The standard parametrization of V_{CKM} , recommended in PDG [25], assumes the form

$$V_{\text{CKM}} = \begin{pmatrix} V_{\text{ud}} & V_{\text{us}} & V_{\text{ub}} \\ V_{\text{cd}} & V_{\text{cs}} & V_{\text{cb}} \\ V_{\text{td}} & V_{\text{ts}} & V_{\text{tb}} \end{pmatrix} = \begin{pmatrix} c_{12}c_{13} & s_{12}c_{13} & s_{13}e^{-i\delta} \\ -s_{12}c_{23} - c_{12}s_{23}s_{13}e^{i\delta} & c_{12}c_{23} - s_{12}s_{23}s_{13}e^{i\delta} & s_{23}c_{13} \\ s_{12}s_{23} - c_{12}c_{23}s_{13}e^{i\delta} & -s_{23}c_{12} - s_{12}c_{23}s_{13}e^{i\delta} & c_{23}c_{13} \end{pmatrix}. \quad (13)$$

The four independent parameters characterizing V_{CKM} are the mixing angles ϑ_{12} , ϑ_{13} , ϑ_{23} and the phase δ ; here, the notation $s_{ij} = \sin \vartheta_{ij}$, $c_{ij} = \cos \vartheta_{ij}$ is introduced.

The complex character of certain matrix elements of the V_{CKM} matrix, stipulated by the phase δ , essentially makes it possible to explain processes involving CP violation within the framework of the SM and the phenomenology of the quark mixing matrix. Indeed, CP violation is due to the imaginary part of the matrix element determining the respective process. For example, in CPT-invariant theory, the decay amplitudes corresponding to the decays $K^0 \rightarrow 2\pi$ and $\bar{K}^0 \rightarrow 2\pi$ are of the form

$$A(K^0 \rightarrow 2\pi) = A \exp(i\delta_{\pi\pi}),$$

$$A(\bar{K}^0 \rightarrow 2\pi) = A^* \exp(i\delta_{\pi\pi}),$$

where $\delta_{\pi\pi}$ is the $\pi\pi$ -interaction phase in the final $\pi\pi$ state of these decays. Then, CP violation in weak decays points to $A(K^0 \rightarrow 2\pi) \neq A(\bar{K}^0 \rightarrow 2\pi)$ or to $A \neq A^*$, i.e., the respective amplitudes contain an imaginary part responsible for the CP violation.

From Fig. 1 it also follows that the complex character of the matrix elements of V_{CKM} results in the violation of invariance with respect to time reversal. Note that if there existed only two generations of quarks and if the dimensionality of the quark mixing matrix were $n=2$, then the elements of the mixing matrix would be real ($n_\psi = 0$ for $n=2$) and an explanation of CP nonconservation would have to be found beyond the framework of the model with two quark generations.

In the description of the Cabibbo–Kobayashi–Maskawa matrix within its standard parametrization (13), the following hierarchy of mixing angles occurs:

$$s_{12} = \lambda = 0.222 \pm 0.002, \quad s_{23} = O(10^{-2}), \quad s_{13} = O(10^{-3}). \quad (14)$$

Then, with a high degree of precision $c_{13} = c_{23} = 1$, and the four independent parameters determining the unitary quark mixing matrix V_{CKM} can be chosen as

$$|s_{12}| = \lambda = |V_{\text{us}}|, \quad s_{23} = |V_{\text{cb}}|, \quad s_{13} = |V_{\text{ub}}|, \quad 0 \leq \delta \leq 2\pi. \quad (15)$$

Another very convenient parametrization of the V_{CKM} matrix has been proposed by Wolfenstein [51]. In this parametrization, each element of V_{CKM} (13) is represented as a series expansion in terms of the small parameter $\lambda = 0.222 \pm 0.002$. Then, with an accuracy up to terms on the order of λ^4 , the matrix V_{CKM} assumes the form

$$V_{\text{CKM}} = \begin{pmatrix} 1 - \frac{\lambda^2}{2} & \lambda & A\lambda^3(\rho - i\eta) \\ -\lambda & 1 - \frac{\lambda^2}{2} & A\lambda^2 \\ A\lambda^3(1 - \rho - i\eta) & -A\lambda^2 & 1 \end{pmatrix} + O(\lambda^4). \quad (16)$$

In this representation, the matrix V_{CKM} is determined by four parameters: λ , A , ρ , and η .

In calculating CP-odd effects it is necessary to enhance the precision in the expansion of the matrix elements of V_{CKM} in terms of λ up to $O(\lambda^6)$ or even up to $O(\lambda^7)$. To this end, we require (by definition) the validity to hold true in the relations

$$s_{12} = \lambda, \quad s_{23} = A\lambda^2, \quad s_{13} \exp(-i\delta) = A\lambda^3(\rho - i\eta) \quad (17)$$

in any order of λ . We also introduce in the V_{CKM} matrix (16) the modified parameters

$$\bar{\rho} = \rho \left(1 - \frac{\lambda^2}{2}\right), \quad \bar{\eta} = \eta \left(1 - \frac{\lambda^2}{2}\right). \quad (18)$$

To find the remaining elements of the V_{CKM} matrix in the Wolfenstein representation, we take advantage of the exact formula (13) for the standard parametrization of the V_{CKM} matrix and of the series expansion with a precision up to $O(\lambda^6)$:

$$c_{12} = (1 - s_{12}^2)^{1/2} = 1 - \frac{\lambda^2}{2} - \frac{\lambda^4}{8} + O(\lambda^6), \quad (19)$$

$$c_{23} = 1 - \frac{A^2\lambda^4}{2} + O(\lambda^6), \quad c_{13} = 1 + O(\lambda^6).$$

Applying Eqns (13) and (17)–(19), one can obtain more accurate expressions for the elements of the quark mixing matrix V_{CKM} in the Wolfenstein representation (see Table 1), exhibiting a precision no worse than $O(\lambda^6)$.

One must bear in mind that in accordance with formulas (18) the following expansions are valid:

$$\rho = \bar{\rho} \left(1 + \frac{\lambda^2}{2} + \dots\right), \quad \eta = \bar{\eta} \left(1 + \frac{\lambda^2}{2} + \dots\right).$$

Therefore, by choosing the appropriate precision of the expansion in terms of λ it is possible to represent any elements of the Wolfenstein matrix and their related expressions as one wants, making use of parameters $\bar{\rho}$, $\bar{\eta}$ or ρ , η (see Table 1).

In calculations of the matrix elements of many processes and, in particular, of the effects of CP violation, an important role is played by the quantities

$$\lambda_i = V_{\text{id}} V_{\text{is}}^*, \quad i = c, t \quad (20)$$

entering the amplitudes of quark transitions. Expressions for λ_i in terms of the parameters $\bar{\rho}$, $\bar{\eta}$ are also presented in Table 1.

Table 1. Quark mixing matrix V_{CKM} in the standard representation (13) and in the Wolfenstein representation taking into account relationship (18) in an approximation not inferior to $O(\lambda^6)$.

$V_{ud} = c_{12}c_{13} = 1 - \frac{\lambda^2}{2} - \frac{\lambda^4}{8} + O(\lambda^6)$	$V_{us} = s_{12}c_{13} = \lambda + O(\lambda^7)$	$V_{ub} = s_{13} \exp(-i\delta) = A\lambda^3(\rho - i\eta)$
$V_{cd} = -s_{12}c_{23} - c_{12}s_{23}s_{13} \exp(i\delta)$ $= -\lambda c_{23} - c_{12}A^2\lambda^5(\rho + i\eta)$ $= -\lambda + \frac{A^2\lambda^5}{2} [1 - 2(\rho + i\eta)] + O(\lambda^7)$ $= -\lambda + A^2\lambda^5\left(\frac{1}{2} - \rho\right) - i\eta A^2\lambda^5 + O(\lambda^7)$	$V_{cs} = c_{12}c_{23} - s_{12}s_{23}s_{13} \exp(i\delta)$ $= c_{12}c_{23} - A^2\lambda^6(\rho + i\eta)$ $= 1 - \frac{\lambda^2}{2} - \frac{\lambda^4}{8}(1 + 4A^2) + \frac{A^2\lambda^6}{4} - \lambda^6 A^2\rho - i\eta\lambda^6 A^2$ $\simeq 1 - \frac{\lambda^2}{2} - \frac{\lambda^4}{8}(1 + 4A^2) + O(\lambda^6)$	$V_{cb} = s_{23}c_{13} = A\lambda^2 c_{13}$ $= A\lambda^2 [1 + O(\lambda^6)] = A\lambda^2 + O(\lambda^8)$
$V_{td} = s_{12}s_{23} - c_{12}c_{23}s_{13} \exp(i\delta)$ $= A\lambda^3 - c_{12}c_{23}A\lambda^3(\rho + i\eta)$ $= A\lambda^3 \left[1 - \left(1 - \frac{\lambda^2}{2}\right)(\rho + i\eta)\right] + O(\lambda^7)$ $= A\lambda^3(1 - \bar{\rho}) - i\eta A\lambda^3 + O(\lambda^7)$	$V_{ts} = -s_{23}c_{12} - s_{12}c_{23}s_{13} \exp(i\delta)$ $= -A\lambda^2 c_{12} - c_{23}A\lambda^4(\rho + i\eta)$ $= \left[-A\lambda^2 + \frac{A\lambda^4}{2}(1 - 2\rho)\right] - i\eta A\lambda^4 + O(\lambda^6)$	$V_{tb} = c_{23}c_{13} = 1 - \frac{A^2\lambda^4}{2} + O(\lambda^6)$
<p>Coefficients $\lambda_i = V_{id}V_{is}^*$ ($i = c, t$):</p> $\text{Re } \lambda_t = A^2\lambda^5(-1 + \bar{\rho}) + \frac{1}{2}A^2\lambda^7[1 - 3\bar{\rho} + 2(\bar{\rho}^2 + \bar{\eta}^2)] + O(\lambda^9) \simeq -A^2\lambda^5\left(1 - \frac{\lambda^2}{2}\right)(1 - \bar{\rho}) + O(\lambda^7),$ $\text{Im } \lambda_t = \eta A^2\lambda^5 + O(\lambda^9) = \bar{\eta}A^2\lambda^5\left(1 - \frac{\lambda^2}{2}\right)^{-1} + O(\lambda^9),$ $\text{Re } \lambda_c = -\lambda\left(1 - \frac{\lambda^2}{2}\right) + \lambda^5\left[A^2(1 - \rho) + \frac{1}{8}\right] + O(\lambda^7) \simeq -\lambda\left(1 - \frac{\lambda^2}{2}\right) + O(\lambda^5),$ $\text{Im } \lambda_c = -\eta A^2\lambda^5 = -\bar{\eta}A^2\lambda^5\left(1 - \frac{\lambda^2}{2}\right)^{-1} + O(\lambda^9), \quad \text{Im } \lambda_c = -\text{Im } \lambda_t$		

Direct experimental data on the elements of the quark mixing matrix V_{CKM} are related to the first two rows of the matrix. The other matrix elements related to the decays of t-quarks can be obtained from the unitary relations (12) and from data on other processes proceeding in the highest approximation with respect to weak interaction. We shall write down the respective nondiagonal elements for Eqn (12) explicitly:

$$V_{ud}V_{cd}^* + V_{us}V_{cs}^* + V_{ub}V_{cb}^* = 0, \tag{21}$$

$$V_{ud}V_{td}^* + V_{us}V_{ts}^* + V_{ub}V_{tb}^* = 0, \tag{22}$$

$$V_{cd}V_{td}^* + V_{cs}V_{ts}^* + V_{cb}V_{tb}^* = 0, \tag{23}$$

$$V_{ud}V_{us}^* + V_{cd}V_{cs}^* + V_{td}V_{ts}^* = 0, \tag{24}$$

$$V_{ud}V_{ub}^* + V_{cd}V_{cb}^* + V_{td}V_{tb}^* = 0, \tag{25}$$

$$V_{us}V_{ub}^* + V_{cs}V_{cb}^* + V_{ts}V_{tb}^* = 0. \tag{26}$$

In the Wolfenstein representation for the quark mixing matrix it is convenient to introduce an illustrative geometric interpretation of the unitarity condition for this matrix in the complex $(\bar{\rho}, i\bar{\eta})$ plane — the so-called *unitary triangle*. Consider the unitarity relation (25) and represent it in the form of a sum of three vectors in the complex plane (Fig. 2):

$$\underbrace{V_{ud}V_{ub}^*}_{\mathbf{r}} + \underbrace{V_{cd}V_{cb}^*}_{-\mathbf{b}} + \underbrace{V_{td}V_{tb}^*}_{\mathbf{c}} = 0.$$

Starting from the expressions for the elements of the mixing matrix presented in Table 1, it is possible to show that the quantity $V_{cd}V_{cb}^* = -A\lambda^3 + O(\lambda^7)$ is a real number with a very good accuracy and that vector \mathbf{B} is directed along the $\bar{\rho}$ -axis.

The two other vectors have the form

$$V_{ud}V_{ub}^* = A\lambda^3(\bar{\rho} + i\bar{\eta}), \quad V_{td}V_{tb}^* = A\lambda^3[1 - (\bar{\rho} + i\bar{\eta})].$$

Upon performing the appropriate normalization (division by $-V_{cd}V_{cb}^* = A\lambda^3$), the vector equality in the $(\bar{\rho}, \bar{\eta})$ -plane can be represented as

$$\underbrace{\left(-\frac{V_{ud}V_{ub}^*}{V_{cd}V_{cb}^*}\right)}_{\mathbf{r}} + \underbrace{\left(-\frac{V_{td}V_{tb}^*}{V_{cd}V_{cb}^*}\right)}_{\mathbf{c}} = \underbrace{1}_{\mathbf{1}} \tag{27}$$

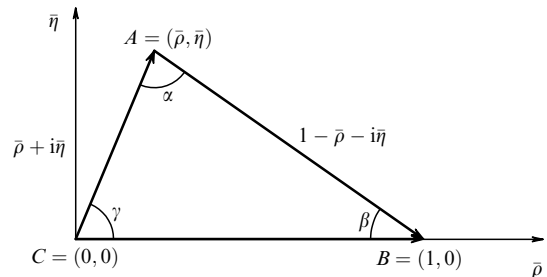


Figure 2. Outline of the unitary triangle ABC based on the unitarity relation (25): $V_{ud}V_{ub}^* + V_{cd}V_{cb}^* + V_{td}V_{tb}^* = 0$, which is represented in the $(\bar{\rho}, \bar{\eta})$ -plane in the vector form: $\mathbf{r} + \mathbf{c} = \mathbf{1}$, where

$$|\vec{CA}| = |\mathbf{r}| = \frac{|V_{ud}V_{ub}^*|}{|V_{cd}V_{cb}^*|} = \frac{|V_{ud}V_{ub}^*|}{A\lambda^3} = (\bar{\rho}^2 + \bar{\eta}^2)^{1/2} = R_b,$$

$$|\vec{AB}| = |\mathbf{c}| = \frac{|V_{td}V_{tb}^*|}{|V_{cd}V_{cb}^*|} = \frac{|V_{td}V_{tb}^*|}{A\lambda^3} = [(1 - \bar{\rho})^2 + \bar{\eta}^2]^{1/2} = R_t,$$

and $|\vec{CB}| = |\mathbf{1}| = 1$.

(see Fig. 2), i.e., in the form of a ‘unitary triangle’ with the sides

$$R_b = |\mathbf{r}| = \sqrt{\bar{\rho}^2 + \bar{\eta}^2} = \frac{|V_{ud}V_{ub}^*|}{|V_{cd}V_{cb}^*|} \simeq \left(1 - \frac{\lambda^2}{2}\right) \frac{1}{\lambda} \left| \frac{V_{ub}^*}{V_{cb}^*} \right|$$

$$= \frac{1}{\sqrt{\sigma}} \frac{1}{\lambda} \left| \frac{V_{ub}}{V_{cb}} \right| \simeq \frac{1}{\lambda} \left| \frac{V_{ub}}{V_{cb}} \right| \simeq \frac{|V_{ub}|}{A\lambda^3}, \quad (28)$$

$$R_t = |\mathbf{c}| = \sqrt{(1 - \bar{\rho})^2 + \bar{\eta}^2} = \frac{|V_{td}V_{tb}^*|}{|V_{cd}V_{cb}^*|} \simeq \frac{1}{\lambda} \left| \frac{V_{td}}{V_{cb}} \right| \simeq \frac{|V_{td}|}{A\lambda^3}$$

and angles α , β , γ [since $V_{ud} \simeq |V_{ud}| \simeq 1 - \lambda^2/2$, $V_{tb} \simeq 1$, $|V_{cd}| \simeq -\lambda$, $V_{cb} \simeq A\lambda^2$, $\sigma = 1/(1 - \lambda^2/2)^2$].

The angles of the unitary triangle are determined by the phases of the matrix elements V_{ub} and V_{td} . As follows from Fig. 2 and relations (16)–(18), one obtains

$$V_{ub} = A\lambda^3(\rho - i\eta) = \frac{A\lambda^3(\bar{\rho} - i\bar{\eta})}{1 - \lambda^2/2} \simeq A\lambda^3(\bar{\rho} - i\bar{\eta})$$

$$= A\lambda^3 R_b \exp(-i\gamma) = |V_{ub}| \exp(-i\gamma) = |V_{ub}| \exp(-i\delta),$$

$$V_{td} = A\lambda^3(1 - \bar{\rho} - i\bar{\eta}) = |V_{td}| \exp(-i\beta) = A\lambda^3 R_t \exp(-i\beta). \quad (29)$$

Further, one can also find that

$$\alpha = \arg\left(-\frac{V_{td}V_{tb}^*}{V_{ud}V_{ub}^*}\right), \quad \beta = \arg\left(-\frac{V_{cd}V_{cb}^*}{V_{td}V_{tb}^*}\right), \quad (30)$$

$$\gamma = \arg\left(-\frac{V_{ud}V_{ub}^*}{V_{cd}V_{cb}^*}\right).$$

Indeed, it is easy to verify that

$$\bar{\rho} + i\bar{\eta} = \mathbf{r} = \left(-\frac{V_{ud}V_{ub}^*}{V_{cd}V_{cb}^*}\right) = |\mathbf{r}| \exp(i\gamma),$$

$$\gamma = \arg\left(-\frac{V_{ud}V_{ub}^*}{V_{cd}V_{cb}^*}\right),$$

$$1 - \bar{\rho} - i\bar{\eta} = \mathbf{c} = \left(-\frac{V_{td}V_{tb}^*}{V_{cd}V_{cb}^*}\right) = |\mathbf{c}| \exp(-i\beta),$$

$$-\beta = \arg\left(-\frac{V_{td}V_{tb}^*}{V_{cd}V_{cb}^*}\right), \quad \beta = \arg\left(-\frac{V_{cd}V_{cb}^*}{V_{td}V_{tb}^*}\right),$$

since $x = |x| \exp(i\varphi)$ and $1/x = |x|^{-1} \exp(-i\varphi)$, and also

$$\alpha = \pi - \gamma - \beta, \quad \exp(i\alpha) = (-1) \exp(-i\beta) \exp(-i\gamma)$$

$$= -\left[\left(-\frac{V_{td}V_{tb}^*}{V_{cd}V_{cb}^*}\right) \frac{1}{|\mathbf{c}|}\right] \left[\left(-\frac{V_{cd}V_{cb}^*}{V_{ud}V_{ub}^*}\right) |\mathbf{r}|\right]$$

$$= -\frac{V_{td}V_{tb}^*}{V_{ud}V_{ub}^*} \frac{|\mathbf{r}|}{|\mathbf{c}|}, \quad \alpha = \arg\left(-\frac{V_{td}V_{tb}^*}{V_{ud}V_{ub}^*}\right).$$

On the basis of the geometry of the unitary triangle in the $(\bar{\rho}, \bar{\eta})$ -plane, the angles α , β , and γ can be expressed via the parameters $\bar{\rho}$, $\bar{\eta}$:

$$\sin 2\alpha = \frac{2\bar{\eta}(\bar{\eta}^2 + \bar{\rho}^2 - \bar{\rho})}{(\bar{\rho}^2 + \bar{\eta}^2)[(1 - \bar{\rho})^2 + \bar{\eta}^2]},$$

$$\sin 2\beta = \frac{2\bar{\eta}(1 - \bar{\rho})}{(1 - \bar{\rho})^2 + \bar{\eta}^2}, \quad (31)$$

$$\sin 2\gamma = \frac{2\bar{\rho}\bar{\eta}}{\bar{\rho}^2 + \bar{\eta}^2} = \frac{2\rho\eta}{\rho^2 + \eta^2}.$$

Applying the theorem of sines

$$\frac{R_b}{\sin \beta} = \frac{R_t}{\sin \gamma} = \frac{1}{\sin \alpha}$$

to the unitary triangle, one can also obtain

$$R_b = \frac{\sin \beta}{\sin \alpha} = \frac{\sin \beta}{\sin(\gamma + \beta)}, \quad R_t = \frac{\sin \gamma}{\sin \alpha} = \frac{\sin \gamma}{\sin(\gamma + \beta)}.$$

Since CP violation is related to the complex character of the V_{CKM} matrix (i.e., to $\bar{\eta} \neq 0$), the parameters of the unitary triangle play a very important role in analyzing processes in which CP symmetry is not conserved. The area S of the triangle and its angles differ from zero only owing to the CP violation and are determined by the degree of this violation: $S = J_{CP}/2$, where J_{CP} is the so-called ‘Jarlskog parameter’ that characterizes the CP violation in the SM. It is possible to show that

$$J_{CP} = |\text{Im}(V_{ud}V_{tb}V_{ub}^*V_{td}^*)| \simeq A^2\eta\lambda^6.$$

Application of the quark mixing matrix in the Wolfenstein representation and parametrization of the unitary triangle (27) in terms of $\bar{\rho}$, $\bar{\eta}$, α , β , γ is, at present, the universal language in which discussions are held of rare K- and B-decays. We shall also take advantage of this language in the present review. However, such a description gives rise to a number of difficulties, some of which are dealt with in Section 5.2. Other methods for parametrization of the unitary triangle are discussed in Ref. [48].

We shall now make a few comments concerning the remaining unitary triangles corresponding to the unitarity relations (21)–(24) and (26). These new unitary triangles have another form and are arranged differently in the $(\bar{\rho}, \bar{\eta})$ -plane. However, they all have the same area $S = J_{CP}/2$. We shall now point out certain practical differences between the properties of various unitarity relations and unitary triangles (see, for example, Ref. [47]).

(1) For relations (22) and (25), all three terms of the sum are of the same order of magnitude:

$$\left. \begin{array}{l} (22) \\ (25) \end{array} \right\} O(\lambda^3) + O(\lambda^3) + O(\lambda^3) = 0.$$

The respective triangles have similar structures: in the limit of $O(\lambda^4)$ they tend toward the relationship

$$A\lambda^3(1 - \rho - i\eta) + (-A\lambda^3) + A\lambda^3(\rho - i\eta) = 0,$$

which is close to Eqn (27). In this approximation both triangles have the same form and differ only in higher approximations with respect to λ .

(2) The individual sum elements for the remaining unitarity relations differ significantly from each other, so that

$$\left. \begin{array}{l} (21) \\ (24) \end{array} \right\} O(\lambda) + O(\lambda) + O(\lambda^5) = 0,$$

$$\left. \begin{array}{l} (23) \\ (26) \end{array} \right\} O(\lambda^2) + O(\lambda^2) + O(\lambda^4) = 0.$$

The respective triangles turn out to be highly elongated, which hinders their application in SM studies or in searches of NP.

Below, any reference to the unitary triangle will imply the unitary triangle (27), shown in Fig. 2, if the exact name of the

triangle is not mentioned explicitly. Precisely this triangle is used in most works on rare K- and B-meson decays. Another unitary triangle based on the unitarity relation (24), namely $V_{ud}V_{us}^* + V_{cd}V_{cs}^* + V_{td}V_{ts}^* = 0$ (i.e., $\lambda_u + \lambda_c + \lambda_t = 0$, where $\lambda_i = V_{id}V_{is}^*$ and $i = u, c, t$), and termed the ‘kaon unitarity triangle’, in spite of its being canted, has also turned out to be useful in analyzing $K \rightarrow \pi\nu\bar{\nu}$ decays.

As already noted, at present there exist no direct data on the matrix elements describing the decays of t-quarks. To determine the parameters of the unitary triangle, data are used on the matrix elements involving t-quarks, which are obtained by analyzing loop FCNC processes proceeding in the highest approximation with respect to weak interaction. Such processes are extremely sensitive to the region of small distances, and they can be influenced by the effects related to NP. This may result in divergences between the parameters of the unitary triangle, which are derived from different decays and weak transitions, when SM ideas are applied.

The divergences indicated (in case they are revealed) will unambiguously confirm the existence of new physical phenomena going beyond the framework of the SM. Therefore, it is important to separate very clearly those results that are little influenced by the region of small distances from those that are potentially sensitive to new energy scales and to new phenomena. Thus, no contribution of t-quarks to relation (21) exists, and all its elements are known from direct measurements. An attempt has been made to use this relation for determining the parameter J_{CP} by a method free from the possible influence of NP [52]. Regretfully, owing to the large difference between the individual components of the sum (21), the accuracy of this determination turned out to be small: $J_{CP} = (2.5 \pm 1.4) \times 10^{-5}$, which corresponds to the phase δ in the V_{CKM} matrix (13) being between 17° and 163° .

Data relevant to the unitary triangle (27) and the determination of its parameters are discussed in greater detail in Section 4. The kaon unitary triangle is examined in Section 5.2.

2.2 Weak decays and the problem of long distances

Determination of the parameters of the V_{CKM} matrix from data on weak decays is not a simple task at all. Quantitative analysis of the amplitudes for weak processes involves the necessity of not only taking into account the region of small distances, where the well-developed technique of perturbative calculations in QCD can be successfully applied, but also taking into account the region of large distances, in which additional exchange of virtual soft gluons occurs and for which there still exist no adequate methods for performing sufficiently accurate calculations.

For estimating the amplitudes of weak hadron decays, a method of operator expansion of amplitudes has been developed, which is described in detail in Refs [26, 27]. This method permits us to factorize the region of small distances ($R < 1/\mu$) and the region of large distances ($R > 1/\mu$), in which the respective calculations can be performed within the framework of perturbative QCD ($R < 1/\mu$) or by less reliable nonperturbative methods ($R > 1/\mu$).

The choice of the parameter μ of the energy scale is discussed below. In doing so, use is made of the low-energy effective weak Hamiltonian exhibiting the following structure:

$$H_{w, \text{eff}} = \frac{G_F}{\sqrt{2}} \sum_i [V_{CKM}^i] C_i(\mu) Q_i.$$

Here, G_F is the Fermi weak-interaction constant, Q_i represents the local current operators determining the decays examined, $C_i(\mu)$ are the so-called Wilson coefficients representing effective coupling constants and being determined by the region of small distances $R < 1/\mu$, and $[V_{CKM}^i]$ is a factor due to the quark mixing matrix (in the case of lepton and semilepton tree decays of hadrons, this factor represents the matrix element V_{ik} of the hadron current participating in the decay, while for nonleptonic decays, in which two quark currents take part, $[V_{CKM}^i] = V_{ik}V_{ij}^*$).

In accordance with the method of operator expansion, the amplitude of the exclusive weak decay $M \rightarrow F$ can be represented as

$$A(M \rightarrow F) = \langle F | H_w | M \rangle = \frac{G_F}{\sqrt{2}} \sum_i [V_{CKM}^i] C_i(\mu) \langle F | Q_i(\mu) | M \rangle, \quad (32)$$

where $\langle F | Q_i(\mu) | M \rangle$ are the hadron matrix elements of the operators $Q_i(\mu)$, determined by the region of large distances $R > 1/\mu$. Thus, in particular, in the case of nonleptonic decays, the local current four-quark operators $Q_i(\mu)$ have the form

$$\begin{aligned} Q_1 &= (\bar{s}_\alpha u_\beta)_{V-A} (\bar{u}_\beta d_\alpha)_{V-A}, \\ Q_2 &= (\bar{s}u)_{V-A} (\bar{u}d)_{V-A}, \\ Q_{3,5} &= (\bar{s}d)_{V-A} \sum_q (\bar{q}q)_{V\mp A}, \\ Q_{4,6} &= (\bar{s}_\alpha d_\beta)_{V-A} \sum_q (\bar{q}_\beta q_\alpha)_{V\mp A}, \\ Q_{7,9} &= \frac{3}{2} (\bar{s}d)_{V-A} \sum_q e_q (\bar{q}q)_{V\pm A}, \\ Q_{8,10} &= \frac{3}{2} (\bar{s}_\alpha d_\beta)_{V-A} \sum_q e_q (\bar{q}_\beta q_\alpha)_{V\pm A}. \end{aligned} \quad (33)$$

Here, α, β denote color indices, e_q are the quark charges, and $V \pm A$ are the Dirac structures $\gamma_\mu (1 \mp \gamma_5)$. Summation over the color indices for color scalars is omitted. Summation over the quark indices q is performed for quarks that are essential for the given process (in the case of K-decays, q stands for u, d, s, and in the case of B-decays $q = u, d, s, c, b$).

Figure 3 shows Feynman diagrams corresponding to the local four-quark operators $Q_1 - Q_{10}$ represented in Eqn (33), as well as diagrams for certain concrete processes dealt with in the present review. Thus, Fig. 3a presents the current-current diagram with W-boson exchange, corresponding to operator Q_2 . Operator Q_1 describes the gluon correction to the tree diagram with W-boson exchange (Fig. 3b). Operators $Q_3 - Q_6$ correspond to the so-called gluon penguin diagrams (Fig. 3c), while operators $Q_7 - Q_{10}$ correspond to electroweak penguin diagrams (Fig. 3d). The introduction of gluon penguin diagrams and revelation of their essential role in the explanation of the selection rule $\Delta T = 1/2$ in $K \rightarrow 2\pi$ decays and in hyperon decays was first performed by Vaĭnshteĭn, Zakharov, and Shifman [53] (see also Ref. [54], where the history of how these diagrams and their titles came into being is presented).

Thus, calculation of a matrix element $A(M \rightarrow F)$ proceeds through two stages:

(1) Taking into account the region of small distances ($R < 1/\mu$), where perturbative QCD can be applied. Calculation of the Wilson coefficients $C_i(\mu)$ is performed quite accurately, taking into account the leading logarithmic

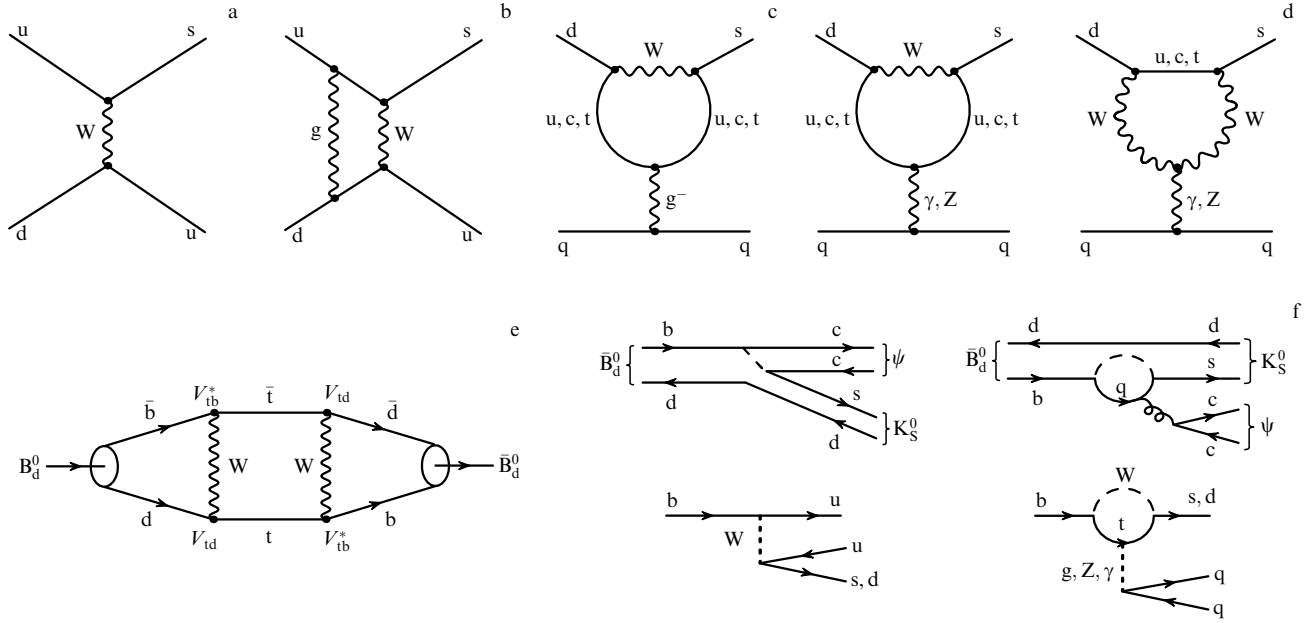


Figure 3. Diagrams of processes related to the local quark operators Q_i [see Eqn (33)], to the mixing of neutral mesons, and to certain B-decays. (a) Current–current tree diagram with W-boson exchange (operator Q_2). (b) Tree diagram with gluon correction (operator Q_1). (c) Gluon loop penguin diagram (operators $Q_3–Q_6$). (d) Electroweak loop penguin diagrams (operators $Q_7–Q_{10}$). (e) Box diagram for neutral meson mixing processes $|P^0\rangle \rightleftharpoons |\bar{P}^0\rangle$ (illustrated by the example of $B_d^0 \rightleftharpoons \bar{B}_d^0$). The matrix element V_{id} of the quark mixing matrix corresponds to the transition $d \rightarrow t$; the matrix element $V_{bt} = V_{tb}^*$ (the contrary for antiquarks) corresponds to the transition $t \rightarrow b$, since complex conjugation corresponds to time reversal. Similar diagrams occur in the case of mixings $K^0 \rightleftharpoons \bar{K}^0$, $D^0 \rightleftharpoons \bar{D}^0$, and $B_s^0 \rightleftharpoons \bar{B}_s^0$. (f) Tree (on the left) and penguin (on the right) diagrams for the decay $\bar{B}^0 \rightarrow (J/\psi) K_S^0$ and other B-decays.

approximation (LLA) [summation of terms, such as $\alpha_s^n (\ln M_W/\mu)^n$] and, also, of the next-to-logarithmic approximation (NLA) [summation of terms such as $\alpha_s^n (\ln M_W/\mu)^{n-1}$]. The summation of terms of the perturbative LLA- and NLA-expansion is implemented by the renormalization group method. Virtual heavy particles (c-, t-quarks, W^{\pm} , Z^0 -bosons, etc.) contribute to the coefficients $C_i(\mu)$.

(2) Taking into account the region of large distances ($R > 1/\mu$), i.e., the estimation of hadron matrix elements $\langle F | Q_i(\mu) | M \rangle$. There exist no reliable methods for calculations in this region, and for estimation of such matrix elements various approximations are applied: lattice QCD, $(1/N_c)$ -expansion, QCD sum rules, chiral perturbative theory (CHPT), etc.

The choice of the parameter μ in Eqn (32) is quite arbitrary: it must be such that, when $R < 1/\mu$, the application of perturbative QCD may be possible. For the decays of R charmed and beauty mesons, the μ scale may correspond to the masses of c- and b-quarks. In the case of K-decays, $\mu \simeq 1–2$ GeV. Here, the final result for $A(M \rightarrow F)$ must not depend on the choice of μ . However, this requirement may not be satisfied in practice, which only results in an additional increase in the uncertainty of calculations.

Thus, when the method of operator expansion is utilized, calculations in the regions of small and large distances are factorized, and the set of problems related to the analysis of large distances happens to be well-defined.

In examining rare decays and processes with violation of CP invariance, an essential role is assumed by loop processes of the box and penguin types, involving the exchange of virtual c- and t-quarks and W^{\pm} -bosons (Fig. 3e). Application of the method of operator expansion within the framework of the SM permits us to represent the respective decay

amplitudes in the form

$$A(M \rightarrow F) = \sum_i B^i \eta_{\text{QCD}}^i V_{ij} V_{ik}^* [F_{\text{SM}}^i], \quad (34)$$

which is a certain modification of formula (32). Here, B^i are nonperturbative parameters describing the respective matrix elements, η_{QCD}^i are the results of QCD calculations within the LLA- and NLA-approximations, $V_{ij} V_{ik}^*$ are the products of elements of the quark mixing matrix that are due to the highest order in the weak interaction for loop processes (see, for instance, Fig. 3e), and F_{SM}^i are universal gauge functions of loop processes — the so-called Inami–Lim functions [55]. These functions are presented in Table 2 (see also Refs [56–58]), in which their application is also indicated for certain decay processes examined below in this review.

Figure 3f demonstrates penguin and tree diagrams for certain B-decays.

2.3 Physics beyond the Standard Model

The results obtained in numerous experiments within the range of energies up to 100 GeV, or even up to several hundred GeV, are consistent with theoretical predictions made within the framework of the SM. At present, only data on the possible existence of neutrino oscillations, mainly obtained in nonaccelerator experiments (experiments with solar and atmospheric neutrinos and experiments at nuclear reactors), go beyond the SM framework and point to the nonconservation of lepton flavors (the mixing of neutrinos of different generations) and to differences in the masses of ν_e , ν_μ , and ν_τ neutrinos. However, for an explanation of the neutrino experiments it is apparently sufficient to perform only an insignificant modification of the SM by introducing neutrino mass.

Table 2. Inami–Lim functions for loop processes.

Inami–Lim functions and QCD corrections in the NLA approximation
$S_0(x_t) = 2.46 \left(\frac{m_t}{170 \text{ GeV}} \right)^{1.52} = 2.38 \pm 0.11, \quad \eta_{tt} = 0.57 \pm 0.01, \quad \eta_B = 0.55;$ $S_0(x_c) = x_c = (2.42 \pm 0.39) \times 10^{-4}, \quad \eta_{cc} = 1.45 \pm 0.38;$ $S_0(x_c; x_t) = x_c \left[\ln \frac{x_t}{x_c} - \frac{3x_t}{4(1-x_t)} - \frac{3x_t^2 \ln x_t}{4(1-x_t)^2} \right] = (2.15 \pm 0.31) \times 10^{-3}, \quad \eta_{tc} = 0.47 \pm 0.04;$ $X_0(x_t) = 1.57 \left(\frac{m_t}{170 \text{ GeV}} \right)^{1.15} = 1.528 \pm 0.053, \quad \eta_X = 0.994;$ $Y_0(x_t) = 1.02 \left(\frac{m_t}{170 \text{ GeV}} \right)^{1.56} = 0.983 \pm 0.046, \quad \eta_Y = 1.012;$ $Z_0(x_t) = 0.71 \left(\frac{m_t}{170 \text{ GeV}} \right)^{1.86} = 0.679 \pm 0.038;$ $E_0(x_t) = 0.26 \left(\frac{m_t}{170 \text{ GeV}} \right)^{-1.02} = 0.266 \pm 0.008$
Application of Inami–Lim functions in calculations for certain weak processes
$(K^0 \rightleftharpoons \bar{K}^0)$ -mixing (ε_K): $S_0(x_t)\eta_{tt}, S_0(x_c)\eta_{cc}, S_0(x_c, x_t)\eta_{ct};$ $(B^0 \rightleftharpoons \bar{B}^0)$ -mixing: $S_0(x_t)\eta_B;$ $K \rightarrow \pi\nu\bar{\nu}$: $X(x_t) = X_0(x_t)\eta_X = 1.52 \pm 0.05;$ $K_L^0 \rightarrow \mu^+\mu^-$: $Y(x_t) = Y_0(x_t)\eta_Y = 1.00 \pm 0.05;$ $K_L^0 \rightarrow \pi^0 1^+ 1^-$: $\tilde{Y}_{7A} = \frac{Y_0(x_t)}{\sin^2 \theta_W} = 4.26 \pm 0.20, \quad \tilde{Y}_{7V} = B_0 + \frac{Y_0(x_t)}{\sin^2 \theta_W} - 4Z_0(x_t) = 4.59 \pm 0.26, \quad B_0 = 3.05 \pm 0.08, \quad \tilde{Y}_{7A}^2 + \tilde{Y}_{7V}^2 = 39.2 \pm 2.9.$ Estimation of the parameter ε' for direct CP violation in $K_L^0 \rightarrow 2\pi$: $X_0(x_t), Y_0(x_t), Z_0(x_t), E_0(x_t)$
<p><i>Note.</i> The parametrization of functions applied is from Ref. [27]; $x_t = (m_t/M_W)^2, x_c = (m_c/M_W)^2$. The effective t-quark mass $m_t = \bar{m}_t(m_t) = 166 \pm 5 \text{ GeV}$ is related to the pole mass $m_t^{\text{pol}} = 174.3 \pm 5.1 \text{ GeV}$ of the t-quark [25], measured in experiments D0 and CDF, by the relationship</p> $m_t = m_t^{\text{pol}} \left[1 - \frac{4}{3} \frac{\alpha_s(m_t)}{\pi} \right]$ <p>(see, for example, Ref. [27]). The following function also contributes to the decay $K^+ \rightarrow \pi^+\nu\bar{\nu}$:</p> $F(x_c) = \frac{2}{3} X(x_c)_{e,\mu} + \frac{1}{3} X(x_c)_\tau = (9.82 \pm 1.78) \times 10^{-4}.$

Thus, neutrino oscillations do not contradict a somewhat modified SM. But, if other processes are revealed that proceed with violation of lepton flavors (for instance, such decays as $\mu^+ \rightarrow e^+\gamma$ or $K_L^0 \rightarrow \mu e$), then the above simple modification of the SM will no longer be sufficient to explain such effects which will already represent a clear manifestation of NP. It is also possible that the data on the existence of direct CP violation in the decays $K^0 \rightarrow \pi\pi$ will not be explicable quantitatively within the SM framework, although there does exist at least a qualitative explanation of these results owing to the complex character of the V_{CKM} matrix. It is too early now to speak about quantitative divergences between experiments and theoretical predictions, since the accuracy of the predictions is still insufficient.

Very important measurements of CP asymmetry in the decay $B_d^0(\bar{B}_d^0) \rightarrow (J/\psi)K_S^0$ and in close processes have been performed in recent experiments at the B-meson e^+e^- factories BaBar and Belle (they are discussed in Section 4). The results of these experiments are in extremely good agreement with SM predictions and are the first quantitative confirmation of the SM in CP-violating processes. Hence, the conclusion may be drawn that the mechanism of CP violation in the SM, related to the complex character of the V_{CKM} matrix, apparently plays a dominant role, at least in certain processes involving quark flavor changing and CP nonconservation at low energies. However, this first success only emphasizes the necessity of quantitative studies of the

CP violation mechanisms in other processes, such as, for example, rare $K \rightarrow \pi\nu\bar{\nu}$ decays, where one may expect surprises. To complete the picture of CP violation, new high-precision experiments are needed.

We shall point out certain problems which, most likely, go beyond the SM framework and whose resolution requires new physical ideas [31]. A very serious problem for the SM is presented by the baryon asymmetry of the Universe, for whose explanation an important role is attributed to the violation of CP invariance [59]. However, for such an explanation the extent of this violation must significantly exceed the SM predictions. Thus, cosmological data indicate that there should exist mechanisms for CP nonconservation differing from the SM mechanism based on the complex character of the elements of the quark mixing matrix. It is possible that these new mechanisms manifest themselves only at very high energies and that they do not influence the properties of decay processes involving K- and B-mesons [31].

Another serious difficulty consists in the violation of CP invariance in strong processes due to an additional term in the SM Lagrangian, which is induced by nonperturbative QCD effects and has the form (see, for example, Refs [31, 34])

$$L_\Theta = \frac{\Theta_{\text{QCD}}}{32\pi^2} \epsilon_{\mu\nu\rho\sigma} F^{\mu\nu a} F^{\rho\sigma a},$$

where $\mu, \nu, \rho, \sigma = 0, 1, 2, 3$, and $a = 1, \dots, 8$. This term violates CP invariance and gives rise, for instance, to the dipole

electric moment of the neutron:

$$d_N \simeq 5 \times 10^{-16} \Theta_{\text{QCD}} e \cdot \text{cm}.$$

The experimental limit for this dipole moment amounts to $d_N < 6.3 \times 10^{-26} e \cdot \text{cm}$ [60], from which it follows that $\Theta_{\text{QCD}} \lesssim 10^{-10}$. Since the quantity Θ_{QCD} is due to nonperturbative effects, it cannot be calculated. Nevertheless, within the SM framework such a small quantity Θ_{QCD} seems unnatural [it is expected to be $O(1)$]. Apparently, the solution of this problem may be related to NP effects.

Thus, in spite of possible ‘dark spots’, on the whole it must be noted that the research carried out during the past decades has turned out to be a triumph for the SM. However, physicists do not doubt the limited character of the SM and the existence of an extremely rich NP, extending beyond its limits.

First of all, a serious disadvantage of the SM consists in the large number of arbitrary parameters pertaining to it: the masses of quarks and leptons, the coupling constants of electroweak, strong, and gravitational interactions, the mass of the Higgs boson, parameters of the quark mixing matrix, and, probably, of the neutrino mixing matrix — 25 parameters in all. This is already quite sufficient to cast doubt on the fundamental character of such a theory.

Besides the great number of free parameters, in spite of its impressive successes, the SM exhibits essential conceptual drawbacks. First of all, it seems that the Higgs sector of this model is of a somewhat too simple character. Actually, it may turn out to be more complex and to include several physically observable Higgs bosons — both neutral and charged. Further, diagrams with virtual boson and fermion loops, determining the masses of Higgs fields, diverge quadratically. Therefore, if no mutual cancellation of these diagrams takes place, then the masses of the Higgs particles will turn out to be very large, which is not acceptable.

The compensation of fermion and boson loops may occur if there exists in nature a new fundamental symmetry between these particles — so-called supersymmetry — in the case of which each fermion (boson) has its respective superpartner: boson (fermion). It may be possible, also, that the Higgs bosons are composite particles. Such theories with technicolor (techniquarks and technigluons connected to each other by extremely strong interactions, with a confinement radius on the order of 10^{-17} cm) also permit us to remove divergences in the masses of Higgs bosons.

Other disadvantages of the SM are related to the ‘gap’ between quarks and leptons and between various types of interactions. In this connection, Grand unified models with common multiplets of quarks and leptons are considered, with unification of electromagnetic, weak and strong interactions at very high energies. It is also possible that at high energies symmetry is restored between right and left currents, i.e., there should exist additional more massive right-handed intermediate W_R -bosons. There may also exist additional generations of fundamental fermions, leptoquarks carrying lepton and baryon charges, new intermediate bosons of scalar, pseudoscalar, and tensor types, various schemes for the nonconservation of lepton flavors, and so forth.

Thus, SM seems to represent a low-energy approximation to a more general theory, which holds valid up to energies of several hundred GeV. We have, probably, come quite close to the range of energies where NP, going beyond the SM framework, may be manifested. New heavy particles and

new effects are expected to be observed in collider experiments of the new generation (see, for example, Refs [1, 4, 29, 31–34, 61–71] and references cited therein, as well as Table 4 in review article [42]):

- new generations of quarks and leptons;
- supersymmetric partners of known particles: squarks, sleptons, photinos, neutralinos, vinos, etc.;
- additional intermediate bosons (S, P, W', Z', W_R , and so on) realizing new types of weak interactions;
- ‘horizontal bosons’ realizing transitions between leptons of different generations and causing processes with nonconservation of lepton flavors;
- additional Higgs bosons (for instance, H^\pm and others);
- leptoquarks of various types, possessing simultaneously baryon and lepton charges;
- the quark structure manifested in the transverse momentum distributions of hard hadron jets;
- theories with extra dimensions; in these models gravitational interactions may become comparable to electroweak interactions already at energies of about several TeV (and not at energies on the order of the Planck mass $M_{\text{Pl}} \sim 10^{19}$ GeV, as predicted in the conventional theory of gravity);
- the formation of ‘black holes’ at high energies (in supercolliders and in cosmic rays).

This list can, certainly, be extended. Direct searches for new heavy particles represent a task of first priority in measurements at colliders, if their energies happen to be sufficient for the production of such particles. Broad research activity is already under way and will be continued at the installations CDF and D0 of the Fermilab $\bar{p}p$ collider and in experiments at the ep-collider HERA. Especially great hopes are attached to construction of the new supercollider LHC (CERN) and also to projects of linear electron colliders of the new generation.

There also exist, however, alternative possibilities — ‘subthreshold’ searches for the manifestations of new particles and phenomena in rare decays of kaons, pions, B-mesons and muons. We shall outline a number of directions in which searches for new effects (NP) in rare decays may proceed, first of all, in rare kaon decays:

- unitarity tests of the quark mixing matrix V_{CKM} ;
- searches for new quark currents participating in weak interactions (for example, pseudoscalar, scalar, and tensor interactions in lepton and semilepton decays of π^- and K-mesons);
- searches for nonstandard direct processes violating CP invariance at a level significantly exceeding SM predictions [for example, T-odd correlations in the decays $K^+ \rightarrow \pi^0 \mu^+ \uparrow \nu_\mu$ with transverse muon polarization and in radiative decays $K^+ \rightarrow \pi^0 \mu^+ \nu_\mu \gamma$, charge asymmetry in the decays $K^\pm \rightarrow 3\pi$ and $\Xi^- \rightarrow \Lambda \pi^-$ ($\bar{\Xi}^- \rightarrow \Lambda \pi^+$)];
- searches for nonconservation of lepton flavors in the decays $K_L^0 \rightarrow \mu e$, $K \rightarrow \pi \mu e$, $\mu \rightarrow e \gamma$, $\mu \rightarrow 3e$, $\mu^+ + (ZA) \rightarrow e^- + (ZA)$, etc.;
- searches for CPT-invariance violation in the systems $K^0 \rightleftharpoons \bar{K}^0$, $B^0 \rightleftharpoons \bar{B}^0$, and $D^0 \rightleftharpoons \bar{D}^0$.

From the point of view of the influence of NP processes on weak kaon and B-meson decays, theoretical models going beyond the SM can be divided into two classes:

- (1) Models of the type of so-called model with Minimal Flavor Violation (MFV) [28, 72–74]. These models contain no new interactions, no new operators, and no new complex phases giving rise to the violation of CP symmetry. Such violation is fully due to the complex character of the V_{CKM}

matrix and is determined by the sole phase inherent in this matrix. In these theories, new physical effects manifest themselves in the form of modifications of the Inami–Lim functions for loop diagrams, contributions to which can now be due to the new heavy objects: chargino, squarks, charged Higgs bosons, etc. The Inami–Lim functions acquire new components F_{NP}^i , and formula (34) for the respective decay amplitudes is modified and assumes now the form

$$A(M \rightarrow F) = \sum_i B^i (\eta_{\text{QCD}}^i) V_{ij} V_{ik}^* [F_{\text{SM}}^i + F_{\text{NP}}^i] \quad (35)$$

(the functions F_{SM}^i and F_{NP}^i are real).

(2) There may exist, however, more complicated extensions of the SM, in which manifestations of new interactions and operators are present, which are absent or strongly suppressed in the SM, new sources of the nonconservation of quark flavors and of CP violations (new complex phases), and new Dirac structures: for example, scalar, pseudoscalar, and tensor weak interactions, right currents, and new fundamental multiplets. In this case further modification of the formula for the amplitudes of decay processes takes place, which now assumes a more general form [28]

$$A(M \rightarrow F) = \sum_i B^i (\eta_{\text{QCD}}^i) V_{ij} V_{ik}^* [F_{\text{SM}}^i + F_{\text{NP}}^i] + \sum_k B_{\text{NP}}^k (\eta_{\text{QCD}}^k)_{\text{NP}} V_{\text{NP}}^k [G_{\text{NP}}^k]. \quad (36)$$

The first sum in this formula coincides with Eqn (35) and reflects the modifications in the SM, which are contained in MFV. The second sum in formula (36) contains all the further extensions of the SM. Functions G_{NP}^k and V_{NP}^k can involve new complex phases and reflect the new mechanisms of CP-symmetry violation in the extended theory.

A more detailed discussion of some of these processes within the framework of the program of K-meson studies [39–42, 75–77] and in related researches is presented in subsequent sections of this review.

3. Violation of CP invariance

Following Refs [1–7, 30–38], we shall consider various types of CP-invariance violation in the decays of pseudoscalar mesons P and \bar{P} with differing flavors ($P = \text{K}, \text{D}, \text{B}$). P - and \bar{P} -mesons correspond to conjugation with respect to flavors (for example, they are characterized by the values of strangeness $S = -1$ and $S = +1$).

3.1 Direct CP violation in the decays of neutral and charged mesons

Let us define the decay amplitudes for the meson states P and the respective CP-conjugate states \bar{P} :

$$A_f = \langle f | H | P \rangle, \quad \bar{A}_{\bar{f}} = \langle \bar{f} | H | \bar{P} \rangle. \quad (37)$$

Violation of CP invariance is manifested in the form of the difference between these amplitudes:

$$A_f \neq \bar{A}_{\bar{f}}. \quad (38)$$

To determine the conditions in which CP violation takes place, we assume that each amplitude (37) represents a sum of

at least two independent amplitudes:

$$A_f = a \exp(i\delta_a) + b \exp(i\delta_b), \quad (39)$$

$$\bar{A}_{\bar{f}} = a^* \exp(i\delta_a) + b^* \exp(i\delta_b).$$

Here, $a = |a| \exp(i\varphi_a)$ and $b = |b| \exp(i\varphi_b)$ are the amplitudes of weak decays for which CP conjugation results in the transformation $a \rightarrow a^*$, $b \rightarrow b^*$ (i.e., in complex conjugation with respect to the ‘weak’ phases: $\varphi_a \rightarrow -\varphi_a$, $\varphi_b \rightarrow -\varphi_b$). The phase factors $\exp(i\delta_a)$ and $\exp(i\delta_b)$ characterize scattering processes in the final state $\langle f | H_{\text{st}} | f \rangle_{\text{in}}$ and do not change under the CP transformation owing to the CP invariance of strong interactions.

The characteristics of decay processes are determined by the squares of absolute values of the respective amplitudes:

$$|A_f|^2 = (a \exp(i\delta_a) + b \exp(i\delta_b)) \times (a^* \exp(-i\delta_a) + b^* \exp(-i\delta_b))$$

$$= |a|^2 + |b|^2 + ab^* \exp[i(\delta_a - \delta_b)] + a^* b \exp[-i(\delta_a - \delta_b)]$$

$$= |a|^2 + |b|^2 + 2 \text{Re}(ab^*) \cos(\delta_a - \delta_b) - 2 \text{Im}(ab^*) \sin(\delta_a - \delta_b),$$

$$|\bar{A}_{\bar{f}}|^2 = (a^* \exp(i\delta_a) + b^* \exp(i\delta_b)) \times (a \exp(-i\delta_a) + b \exp(-i\delta_b))$$

$$= |a|^2 + |b|^2 + 2 \text{Re}(ab^*) \cos(\delta_a - \delta_b) + 2 \text{Im}(ab^*) \sin(\delta_a - \delta_b).$$

The CP asymmetry is determined by the expression

$$\Delta = \frac{|A_f|^2 - |\bar{A}_{\bar{f}}|^2}{|A_f|^2 + |\bar{A}_{\bar{f}}|^2} = \frac{-2 \text{Im}(ab^*) \sin(\delta_a - \delta_b)}{|a|^2 + |b|^2 + 2 \text{Re}(ab^*) \cos(\delta_a - \delta_b)}$$

$$= \frac{-2|a||b| \sin(\varphi_a - \varphi_b) \sin(\delta_a - \delta_b)}{|a|^2 + |b|^2 + 2|a||b| \cos(\varphi_a - \varphi_b) \cos(\delta_a - \delta_b)}. \quad (40)$$

Thus, the violation of CP invariance in weak decays ($\bar{A} \neq A$ and $\Delta \neq 0$) is only revealed if the amplitudes A and \bar{A} contain contributions from at least two independent processes with differing weak phases and phases of strong rescattering in the final state ($\varphi_a \neq \varphi_b$, $\delta_a \neq \delta_b$). CP violation is due to interference between the decay amplitudes a and b in formulas (39). This assertion is of a general character and holds valid not only for meson decays, but in other cases as well: for example, for the decays of hyperons and antihyperons. As we shall further see, decays of electrically neutral mesons P^0 and \bar{P}^0 with transition to one and the same state f_{CP} of definite CP parity are of special interest. Such processes are described by the amplitudes $A_f = \langle f_{\text{CP}} | H | P^0 \rangle$ and $\bar{A}_{\bar{f}} = \langle f_{\text{CP}} | H | \bar{P}^0 \rangle$.

3.2 Indirect CP violation in the $P^0 \rightleftharpoons \bar{P}^0$ mixing of electrically neutral mesons

Now, consider electrically neutral mesons $|P^0\rangle$ and $|\bar{P}^0\rangle$ that are the eigenstates of the strong interaction Hamiltonian³ H_0 , and that are conjugate with respect to the appropriate quark flavors (with respect to strangeness for K^0 and $\bar{\text{K}}^0$, charm for D^0 and $\bar{\text{D}}^0$, and beauty for B^0 and $\bar{\text{B}}^0$). If there were no weak

³ The Hamiltonian H_0 includes strong and electromagnetic interactions: $H_0 = H_{\text{strong}} + H_{\text{em}}$.

interactions H_w changing flavors, $|P^0\rangle$ and $|\bar{P}^0\rangle$ would be stationary states of definite mass M (owing to CPT invariance of strong interactions H_0 , the masses of particles and antiparticles $|P^0\rangle$ and $|\bar{P}^0\rangle$ should be identical). CP transformations for the states $|P^0\rangle$ and $|\bar{P}^0\rangle$ assume the form

$$\text{CP}|P^0\rangle = \exp(i\alpha)|\bar{P}^0\rangle, \quad (41)$$

$$\text{CP}|\bar{P}^0\rangle = \exp(-i\alpha)|P^0\rangle.$$

The choice of the arbitrary phase factor with $\alpha = 0$ is consistent with the condition

$$\text{CP}|P^0\rangle = |\bar{P}^0\rangle, \quad \text{CP}|\bar{P}^0\rangle = |P^0\rangle. \quad (42)$$

In the scientific literature, the choice of the phase factor is often used with $\alpha = \pi$, when

$$\text{CP}|P^0\rangle = -|\bar{P}^0\rangle, \quad \text{CP}|\bar{P}^0\rangle = -|P^0\rangle.$$

Although in this case a number of relations alter their form, the difference in choice of the arbitrary phase will, naturally, not influence the physical results.

Strong interaction is also invariant with respect to the CP transformation. Therefore, it is possible to introduce superpositions of $|P^0\rangle$ and $|\bar{P}^0\rangle$, characterized by certain values of CP parity:

$$|P_1^0\rangle = \frac{1}{\sqrt{2}}[|P^0\rangle + |\bar{P}^0\rangle], \quad (43)$$

$$|P_2^0\rangle = \frac{1}{\sqrt{2}}[|P^0\rangle - |\bar{P}^0\rangle].$$

Indeed, from expressions (42) it follows that

$$\text{CP}|P_1^0\rangle = |P_1^0\rangle \quad (\text{CP-even states}),$$

$$\text{CP}|P_2^0\rangle = -|P_2^0\rangle \quad (\text{CP-odd states}).$$

Owing to the change of flavors in weak interactions, ($P^0 \rightleftharpoons \bar{P}^0$)-mixing occurs via common intermediate states ($|P^0\rangle \rightleftharpoons |X\rangle \rightleftharpoons |\bar{P}^0\rangle$). Therefore, a complete description of the $|P^0\rangle \rightleftharpoons |\bar{P}^0\rangle$ system is given by the expression

$$|\psi(t)\rangle = a(t)|P^0\rangle + \bar{a}(t)|\bar{P}^0\rangle. \quad (44)$$

Here, matrix notation is applied for the meson wave functions, namely

$$|P^0\rangle = |1\rangle = \begin{pmatrix} 1 \\ 0 \end{pmatrix}, \quad |\bar{P}^0\rangle = |2\rangle = \begin{pmatrix} 0 \\ 1 \end{pmatrix}.$$

The wave function $|\psi(t)\rangle$ is determined by the Schrödinger equation with the Hamiltonian $\hat{H} = \hat{H}_0 + \hat{H}_w$ which includes both weak and strong interactions:

$$i \frac{d}{dt} |\psi(t)\rangle = \hat{H}|\psi(t)\rangle. \quad (45)$$

We note that in the case of stationary states the Hamiltonian \hat{H} is Hermitian, and the solution of the Schrödinger equation (45) takes the form

$$\psi(t) = \psi(0) \exp(-iMt),$$

where M is the mass of the respective eigenstate. Since, when weak interactions are switched on, the states $\psi(t)$ are no

longer stationary and decay exponentially with time, the Hamiltonian \hat{H} is not Hermitian:

$$\hat{H} = \hat{M} - \frac{i}{2} \hat{\Gamma}.$$

The respective eigenvalues are given in a complex form

$$\lambda = M - \frac{i}{2} \Gamma,$$

$$\psi(t) = \psi(0) \exp(-i\lambda t) = \psi(0) \exp\left(-\frac{1}{2} \Gamma t\right) \exp(-iMt),$$

and the appropriate probability

$$|\psi(t)|^2 = |\psi(0)|^2 \exp(-\Gamma t)$$

decreases exponentially with time, owing to weak decays.

In our case, when the mixing of

$$|P^0\rangle = \begin{pmatrix} 1 \\ 0 \end{pmatrix}, \quad |\bar{P}^0\rangle = \begin{pmatrix} 0 \\ 1 \end{pmatrix}$$

is dealt with, the Hamiltonian has a matrix form

$$\begin{aligned} \hat{H} = \hat{A} = \hat{M} - \frac{i}{2} \hat{\Gamma} &= \begin{pmatrix} A_{11} & A_{12} \\ A_{21} & A_{22} \end{pmatrix} \\ &= \begin{pmatrix} M_{11} & M_{12} \\ M_{21} & M_{22} \end{pmatrix} - \frac{i}{2} \begin{pmatrix} \Gamma_{11} & \Gamma_{12} \\ \Gamma_{21} & \Gamma_{22} \end{pmatrix}, \end{aligned} \quad (46)$$

where $\hat{M} = \hat{M}^\dagger$ and $\hat{\Gamma} = \hat{\Gamma}^\dagger$ are Hermitian matrices, and the corresponding matrix elements are defined as

$$\langle P^0 | \hat{A} | \bar{P}^0 \rangle = (1 \ 0) \begin{pmatrix} A_{11} & A_{12} \\ A_{21} & A_{22} \end{pmatrix} \begin{pmatrix} 0 \\ 1 \end{pmatrix} = A_{12},$$

$$\langle P^0 | \hat{A} | P^0 \rangle = (1 \ 0) \begin{pmatrix} A_{11} & A_{12} \\ A_{21} & A_{22} \end{pmatrix} \begin{pmatrix} 1 \\ 0 \end{pmatrix} = A_{11},$$

and so forth.

Below we shall assume CPT invariance of the total Hamiltonian $\hat{H} = \hat{H}_0 + \hat{H}_w$ to hold valid. In this case $M_{11} = M_{22} = M$, $\Gamma_{11} = \Gamma_{22} = \Gamma$, and $A_{11} = A_{22} = A = M - (i/2)\Gamma$. From the matrices \hat{M} and $\hat{\Gamma}$ being Hermitian it follows that M and Γ are real quantities, and $M_{21} = M_{12}^*$, $\Gamma_{21} = \Gamma_{12}^*$. The eigenstates $|P_\lambda\rangle$ of the complex Hamiltonian \hat{H} correspond to complex eigenvalues $\lambda = M - (i/2)\Gamma$ and represent resonances with definite masses and decay widths:

$$|P_\lambda^0(t)\rangle = \exp(-iMt) \exp\left(-\frac{1}{2} \Gamma t\right) |P_\lambda^0(0)\rangle \quad (47)$$

(for reasons of brevity, we shall further denote $|P_\lambda^0(0)\rangle$ as $|P_\lambda^0\rangle$).

If CP invariance were conserved in weak processes resulting in ($P^0 \rightleftharpoons \bar{P}^0$) mixing, then $|P_\lambda^0\rangle$ would coincide with the CP eigenstates $|P_1^0\rangle$ and $|P_2^0\rangle$. Mixing processes are determined by box loop diagrams (Fig. 3e). The imaginary parts of these diagrams lead to violation of CP invariance in mixing, so the states $|P_\lambda^0\rangle$ no longer have definite CP parity and are the superpositions of $|P_1^0\rangle$ and $|P_2^0\rangle$. Such a violation of CP invariance has been termed *indirect* CP violation.

The states $|P_\lambda^0\rangle$ can be represented as

$$|P_\lambda^0\rangle = p|P^0\rangle + q|\bar{P}^0\rangle = \begin{pmatrix} p \\ q \end{pmatrix}, \quad |p|^2 + |q|^2 = 1. \quad (48)$$

Indirect violation of CP invariance results in

$$\left| \frac{q}{p} \right| \neq 1 \tag{49}$$

(unlike the states (43) with definite CP parity, for which $|q/p| = 1$).

To find the eigenstates $|P_\lambda^0\rangle$ of the complex Hamiltonian \hat{H} , corresponding to the eigenvalues λ , one applies the stationary Schrödinger equation:

$$\hat{H}|P_\lambda^0\rangle = \lambda|P_\lambda^0\rangle = \left(M - \frac{i}{2}\Gamma \right) |P_\lambda^0\rangle. \tag{50}$$

In the matrix form, this equation becomes

$$\begin{pmatrix} A_{11} & A_{12} \\ A_{21} & A_{22} \end{pmatrix} \begin{pmatrix} p \\ q \end{pmatrix} = \begin{pmatrix} A & A_{12} \\ A_{21} & A \end{pmatrix} \begin{pmatrix} p \\ q \end{pmatrix} = \begin{pmatrix} \lambda & 0 \\ 0 & \lambda \end{pmatrix} \begin{pmatrix} p \\ q \end{pmatrix},$$

and it reduces to the system of homogeneous equations

$$\begin{aligned} (A - \lambda)p + A_{12}q &= 0, \\ A_{21}p + (A - \lambda)q &= 0, \end{aligned} \tag{51}$$

which has a nontrivial solution, if the determinant of the system equals zero:

$$\begin{vmatrix} A - \lambda & A_{12} \\ A_{21} & A - \lambda \end{vmatrix} = 0,$$

or

$$\lambda^2 - 2A\lambda + A^2 - A_{12}A_{21} = 0. \tag{52}$$

From relation (52) it is possible to determine the eigenvalues λ :

$$\begin{aligned} \lambda &= A \pm \sqrt{A^2 - A^2 + A_{12}A_{21}} = A \pm \sqrt{A_{12}A_{21}} \\ &= M - \frac{i}{2}\Gamma \pm \sqrt{A_{12}A_{21}}. \end{aligned} \tag{53}$$

We now introduce the notation

$$\begin{aligned} \sqrt{A_{12}A_{21}} &= \left[\left(M_{12} - \frac{i}{2}\Gamma_{12} \right) \left(M_{12}^* - \frac{i}{2}\Gamma_{12}^* \right) \right]^{1/2} \\ &= -A = -\text{Re } A - i \text{Im } A \end{aligned} \tag{54}$$

(where $\text{Re } A > 0$, and $\text{Im } A > 0$). Then one arrives at

$$\begin{aligned} \lambda - A &= \pm \sqrt{A_{12}A_{21}} \\ &= \pm \left[\left(M_{12} - \frac{i}{2}\Gamma_{12} \right) \left(M_{12}^* - \frac{i}{2}\Gamma_{12}^* \right) \right]^{1/2} = \mp A, \\ \lambda &= A \mp (\text{Re } A + i \text{Im } A) = M \mp \text{Re } A - \frac{i}{2}(\Gamma \pm 2 \text{Im } A). \end{aligned} \tag{55}$$

We now denote the two eigenvalues for the solution of the Schrödinger equation (50) with definite masses and lifetimes [corresponding to the signs ‘ \pm ’ in formula (53)] as follows

$$\begin{aligned} \lambda_S &= M_S - \frac{i}{2}\Gamma_S = (M - \text{Re } A) - \frac{i}{2}(\Gamma + 2 \text{Im } A), \\ \lambda_L &= M_L - \frac{i}{2}\Gamma_L = (M + \text{Re } A) - \frac{i}{2}(\Gamma - 2 \text{Im } A). \end{aligned} \tag{56}$$

The differences in mass and decay widths for the two states $|P_S^0\rangle$ and $|P_L^0\rangle$, corresponding to the eigenvalues λ_S and λ_L , are thus seen to be

$$\Delta m = M_L - M_S = 2\text{Re } A, \quad \Delta\Gamma = \Gamma_L - \Gamma_S = -4 \text{Im } A. \tag{57}$$

The differences in mass and widths between the $|P_S^0\rangle$ and $|P_L^0\rangle$ states are determined by the real parts of the amplitudes described by box diagrams (Fig. 3e).

In the general form for the wave functions of mixed states $|P_{S,L}^0\rangle = p|P^0\rangle \pm q|\bar{P}^0\rangle$, which are solutions of the Schrödinger equation (50) and correspond to the eigenvalues λ_S and λ_L , the coefficients p, q are determined from relations (51):

$$\begin{aligned} \frac{q}{p} &= \frac{\lambda_S - A}{A_{12}} = \frac{\sqrt{A_{12}A_{21}}}{A_{12}} = \left(\frac{A_{21}}{A_{12}} \right)^{1/2} \\ &= \left(\frac{M_{12}^* - (i/2)\Gamma_{12}^*}{M_{12} - (i/2)\Gamma_{12}} \right)^{1/2} = \frac{-A}{M_{12} - (i/2)\Gamma_{12}} \\ &= -\frac{\Delta m - (i/2)\Delta\Gamma}{2M_{12} - i\Gamma_{12}} = \frac{M_{12}^* - (i/2)\Gamma_{12}^*}{-A} = -\frac{2M_{12}^* - i\Gamma_{12}^*}{\Delta m - (i/2)\Delta\Gamma}. \end{aligned} \tag{58}$$

We now introduce the notation

$$\frac{q}{p} = \left(\frac{M_{12}^* - (i/2)\Gamma_{12}^*}{M_{12} - (i/2)\Gamma_{12}} \right)^{1/2} = \frac{1 - \varepsilon}{1 + \varepsilon}. \tag{59}$$

Here, the parameter ε determines the extent to which CP invariance is violated. Indeed, as $\varepsilon \rightarrow 0$, the equalities $M_{12} = M_{12}^*$ and $\Gamma_{12} = \Gamma_{12}^*$ are valid, i.e., the matrix elements are real quantities, $q/p = 1$, and the wave functions $|P_{S,L}^0\rangle$ reduce to the CP eigenstates $|P_{1,2}^0\rangle$ of definite CP parity (CP parity is conserved).

From formulas (48) and (59) it is possible to find the solutions for $|P_{S,L}^0\rangle$:

$$\begin{aligned} |P_{S,L}^0\rangle &= p \left[|P^0\rangle \pm \frac{1 - \varepsilon}{1 + \varepsilon} |\bar{P}^0\rangle \right] \\ &= \frac{p}{1 + \varepsilon} \left[(1 + \varepsilon)|P^0\rangle \pm (1 - \varepsilon)|\bar{P}^0\rangle \right]. \end{aligned} \tag{60}$$

The normalization condition $|p|^2 + |q|^2 = 1$ for these functions reduces to

$$|p|^2 + \left| \frac{1 - \varepsilon}{1 + \varepsilon} \right|^2 |p|^2 = 1,$$

from which one finds

$$\frac{|p|^2}{|1 + \varepsilon|^2} [2(1 + |\varepsilon|^2)] = 1.$$

This results in the formula

$$\frac{|p|}{|1 + \varepsilon|} = \frac{1}{\sqrt{2(1 + |\varepsilon|^2)}}. \tag{61}$$

Then with an accuracy up to an insignificant phase factor we have the result

$$|P_{S,L}^0\rangle = \frac{1}{\sqrt{2(1 + |\varepsilon|^2)}} \left[(1 + \varepsilon)|P^0\rangle \pm (1 - \varepsilon)|\bar{P}^0\rangle \right]. \tag{62}$$

If, with the aid of formulas (43), one expresses $|P^0\rangle$ and $|\bar{P}^0\rangle$ via $|P_{1,2}^0\rangle$ and $|P_{2,1}^0\rangle$, then

$$\begin{aligned} |P_{S,L}^0\rangle &= \frac{1}{\sqrt{2(1+|\varepsilon|^2)}} [(1+\varepsilon)|P^0\rangle \pm (1-\varepsilon)|\bar{P}^0\rangle] \\ &= \frac{1}{\sqrt{2(1+|\varepsilon|^2)}} [(|P^0\rangle \pm |\bar{P}^0\rangle) + \varepsilon(|P^0\rangle \mp |\bar{P}^0\rangle)] \\ &= \frac{1}{\sqrt{1+|\varepsilon|^2}} [|P_{1,2}^0\rangle + \varepsilon|P_{2,1}^0\rangle], \end{aligned} \quad (63)$$

i.e., one can see directly that mixing gives rise, in the corresponding wave function, to a component of opposite CP parity, which is proportional to the CP-violation parameter ε .

For the quantity A in formulas (54) and (57), the following relations hold valid:

$$\begin{aligned} 4A^2 &= 4\left(M_{12} - \frac{i}{2}\Gamma_{12}\right)\left(M_{12}^* - \frac{i}{2}\Gamma_{12}^*\right) \\ &= 4\left[(\operatorname{Re} M_{12} + i\operatorname{Im} M_{12}) - \frac{i}{2}(\operatorname{Re} \Gamma_{12} + i\operatorname{Im} \Gamma_{12})\right] \\ &\quad \times \left[(\operatorname{Re} M_{12} - i\operatorname{Im} M_{12}) - \frac{i}{2}(\operatorname{Re} \Gamma_{12} - i\operatorname{Im} \Gamma_{12})\right] \\ &= 4\left[\left(\operatorname{Re} M_{12} + \frac{1}{2}\operatorname{Im} \Gamma_{12}\right) + i\left(\operatorname{Im} M_{12} - \frac{1}{2}\operatorname{Re} \Gamma_{12}\right)\right] \\ &\quad \times \left[\left(\operatorname{Re} M_{12} - \frac{1}{2}\operatorname{Im} \Gamma_{12}\right) - i\left(\operatorname{Im} M_{12} + \frac{1}{2}\operatorname{Re} \Gamma_{12}\right)\right] \\ &= 4\left[(\operatorname{Re} M_{12})^2 + (\operatorname{Im} M_{12})^2 - \frac{1}{4}(\operatorname{Re} \Gamma_{12})^2 - \frac{1}{4}(\operatorname{Im} \Gamma_{12})^2\right] \\ &\quad - 4i[\operatorname{Re} M_{12} \operatorname{Re} \Gamma_{12} + \operatorname{Im} M_{12} \operatorname{Im} \Gamma_{12}] \\ &= [4|M_{12}|^2 - |\Gamma_{12}|^2] - 4i \operatorname{Re}(M_{12}\Gamma_{12}^*), \\ 4A^2 &= 4(\operatorname{Re} A + i\operatorname{Im} A)^2 \\ &= (2\operatorname{Re} A)^2 - \frac{1}{4}(4\operatorname{Im} A)^2 - i(2\operatorname{Re} A)(-4\operatorname{Im} A) \\ &= (\Delta m)^2 - \frac{1}{4}(\Delta\Gamma)^2 - i\Delta m\Delta\Gamma. \end{aligned}$$

Comparison of these expressions with each other reveals that

$$\begin{aligned} 4|M_{12}|^2 - |\Gamma_{12}|^2 &= (\Delta m)^2 - \frac{1}{4}(\Delta\Gamma)^2, \\ \Delta m\Delta\Gamma &= 4\operatorname{Re}(M_{12}\Gamma_{12}^*). \end{aligned} \quad (64)$$

The data for the two states $|P_{S,L}^0\rangle$ arose due to $|P^0\rangle \rightleftharpoons |\bar{P}^0\rangle$ mixing are given in Table 3. Table 4 presents the information on various processes involving direct and indirect violation of CP invariance in experiments with K^0 -mesons (see Refs [78–89]).

In concluding this section, we note that considering the weak interactions \hat{H}_w to be small perturbations, one can obtain in the Weisskopf–Wigner approximation in the second order with respect to \hat{H}_w the expressions for the matrix elements of the mass matrix \hat{M} and of the decay

matrix $\hat{\Gamma}$ [2]:

$$\begin{aligned} M_{ab} &= \langle a|H_0|b\rangle\delta_{ab} + \langle a|H_w|b\rangle + P' \sum_i \frac{\langle a|H_w|i\rangle\langle i|H_w|b\rangle}{M - E_i}, \\ \Gamma_{ab} &= 2\pi \sum_j \langle a|H_w|j\rangle\langle j|H_w|b\rangle \delta(M - E_j). \end{aligned} \quad (65)$$

Here, $|P^0\rangle = |1\rangle$, $|\bar{P}^0\rangle = |2\rangle$, $a, b = 1, 2$, and P' is the principal value of the sum. Thus, the mass matrix is determined by transitions of $|P^0\rangle$ and $|\bar{P}^0\rangle$ to virtual off-mass-shell states $|i\rangle$, while the decay matrix is determined by decays into real on-mass-shell states $|j\rangle$.

3.3 CP nonconservation in the interference of direct decays and mixing processes

The violation of CP invariance may also result from the interference between the amplitude of direct decay to a final state with definite CP parity f_{CP} and the amplitude of mixing processes and subsequent decay to the same final state. This violation of CP invariance is revealed in the asymmetry:

$$a_{f_{CP}} = \frac{\Gamma(\bar{P}^0 \rightarrow f_{CP}) - \Gamma(P^0 \rightarrow f_{CP})}{\Gamma(\bar{P}^0 \rightarrow f_{CP}) + \Gamma(P^0 \rightarrow f_{CP})} \neq 0. \quad (66)$$

For characterizing such processes the quantity

$$\lambda_{f_{CP}} = \frac{q\bar{A}}{pA} \quad (67)$$

is introduced, where A and \bar{A} are defined by formulas (37). Violation of CP invariance takes place if $\lambda_{f_{CP}} \neq 1$. Here, as we have already seen, indirect invariance violation in mixing corresponds to $|q/p| \neq 1$, while direct violation results in $|\bar{A}/A| \neq 1$.

Violation of CP invariance due to interference is most conspicuous if $|q/p| \simeq 1$ and $|\bar{A}/A| \simeq 1$ and, consequently, $|\lambda_{f_{CP}}| = 1$, but here $\operatorname{Im} \lambda_{f_{CP}} \neq 0$ and $\lambda_{f_{CP}} \neq 1$. The quantity $\operatorname{Im} \lambda_{f_{CP}}$ is determined by the relative phase between the mixing amplitude and the amplitude of direct decay, while the corrections due to strong interactions, which hinder the analysis, turn out to be very small.

Further, we shall illustrate this type of violation of CP invariance by taking advantage of the example of asymmetry $a_{f_{CP}}$ in the decays of $|B^0\rangle$ and $|\bar{B}^0\rangle$ into the states of charmonium and of the K^0 -meson [$(J/\psi)K_S^0$, $(J/\psi)K_L^0$, and others] and of the example of the rare decay $K_L^0 \rightarrow \pi^0\nu\bar{\nu}$.

4. Processes involving K- and B-mesons and properties of the unitary triangle

Direct experimental data on the elements of the quark mixing matrix V_{CKM} , relative to the first two rows of this matrix, were obtained in studying the superallowed vector β -decays of nuclei in transitions such as $O^+ \rightarrow O^+$, β -decays of neutrons and π^+ -mesons ($|V_{ud}|$), semilepton decays of K -mesons and hyperons ($|V_{us}|$), semilepton decays of charmed particles, neutrino and antineutrino reactions and decays of W^\pm -bosons with the production of charmed particles ($|V_{cs}|$ and $|V_{cd}|$), inclusive decays $B \rightarrow X_u l \bar{\nu}_l$ and $B \rightarrow X_u l \nu_l$, and exclusive semilepton decays of B -mesons ($|V_{cb}|$, $|V_{ub}|$ and $|V_{ub}|/|V_{cb}|$).

Table 3. Data on $|P^0\rangle \leftrightarrow |\bar{P}^0\rangle$ mixing.

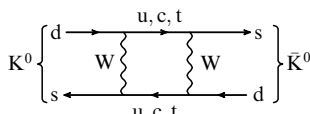
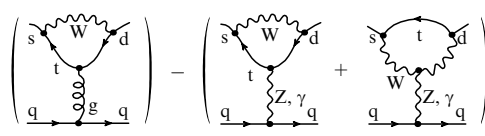
Eigenstates of the $(P^0\rangle \leftrightarrow \bar{P}^0\rangle)$ system and their characteristics	
$ P_S^0\rangle = p P^0\rangle + q \bar{P}^0\rangle = \frac{1}{\sqrt{2(1+ \varepsilon ^2)}} [(1+\varepsilon) P^0\rangle + (1-\varepsilon) \bar{P}^0\rangle] = \frac{1}{\sqrt{1+ \varepsilon ^2}} [P_1^0\rangle + \varepsilon P_2^0\rangle], \quad \lambda_S = M_S - \frac{i}{2}\Gamma_S = (M - \text{Re} A) - \frac{i}{2}(\Gamma + 2\text{Im} A);$	
$ P_L^0\rangle = p P^0\rangle - q \bar{P}^0\rangle = \frac{1}{\sqrt{2(1+ \varepsilon ^2)}} [(1+\varepsilon) P^0\rangle - (1-\varepsilon) \bar{P}^0\rangle] = \frac{1}{\sqrt{1+ \varepsilon ^2}} [P_2^0\rangle + \varepsilon P_1^0\rangle], \quad \lambda_L = M_L - \frac{i}{2}\Gamma_L = (M + \text{Re} A) - \frac{i}{2}(\Gamma - 2\text{Im} A);$	
$ P_1^0\rangle = \frac{1}{\sqrt{2}} [P^0\rangle + \bar{P}^0\rangle], \quad P_2^0\rangle = \frac{1}{\sqrt{2}} [P^0\rangle - \bar{P}^0\rangle];$	
$\left[\left(M_{12}^* - \frac{i}{2}\Gamma_{12}^* \right) \left(M_{12} - \frac{i}{2}\Gamma_{12} \right) \right]^{1/2} = -A, \quad \frac{q}{p} = \frac{1-\varepsilon}{1+\varepsilon} = \sqrt{\frac{M_{12}^* - (i/2)\Gamma_{12}^*}{M_{12} - (i/2)\Gamma_{12}}} = -\frac{\Delta m - (i/2)\Delta\Gamma}{2M_{12} - i\Gamma_{12}} = -\frac{2M_{12}^* - i\Gamma_{12}^*}{\Delta m - (i/2)\Delta\Gamma}.$	
Difference in mass and decay widths of $ P_L^0\rangle$ and $ P_S^0\rangle$:	
$\Delta m = M_L - M_S = 2\text{Re} A, \quad \Delta\Gamma = \Gamma_L - \Gamma_S = -4\text{Im} A, \quad (\Delta m)^2 - \frac{1}{4}(\Delta\Gamma)^2 = 4 M_{12} ^2 - \Gamma_{12} ^2, \quad \Delta m \times \Delta\Gamma = 4\text{Re}(M_{12} \times \Gamma_{12}^*)$	
Mixing for the $(K^0\rangle \leftrightarrow \bar{K}^0\rangle)$ system	
$ K_S^0\rangle$ and $ K_L^0\rangle$ states: $\Delta m_K = M_{K_L} - M_{K_S} = (3.489 \pm 0.008) \times 10^{-15} \text{ GeV}, \quad \Delta\Gamma_K = \Gamma_{K_L} - \Gamma_{K_S} = (-7.361 \pm 0.010) \times 10^{-15} \text{ GeV};$ $2\Delta m_K \simeq -\Delta\Gamma_K$ (experiment), $2 M_{12} = \Gamma_{12} $ (from Eqn (64)); $\text{Im}\Gamma_{12} \ll \text{Re}\Gamma_{12}, \quad \text{Im}M_{12} \ll \text{Re}M_{12}$ (from the smallness of ε_K); $\left \frac{q}{p} \right _K \simeq 1 + \frac{2 \Gamma_{12} ^2}{4 M_{12} ^2 + \Gamma_{12} ^2} \text{Im} \frac{M_{12}}{\Gamma_{12}} \simeq 1 + \text{Im} \frac{M_{12}}{\Gamma_{12}} \simeq 1 - 2\text{Re} \varepsilon_K;$ $ K_S^0\rangle = \frac{1}{\sqrt{2(1+ \varepsilon_K ^2)}} [(1+\varepsilon_K) K^0\rangle + (1-\varepsilon_K) \bar{K}^0\rangle] = \frac{1}{\sqrt{1+ \varepsilon_K ^2}} [K_1^0\rangle + \varepsilon_K K_2^0\rangle],$ $ K_L^0\rangle = \frac{1}{\sqrt{2(1+ \varepsilon_K ^2)}} [(1+\varepsilon_K) K^0\rangle - (1-\varepsilon_K) \bar{K}^0\rangle] = \frac{1}{\sqrt{1+ \varepsilon_K ^2}} [K_2^0\rangle + \varepsilon_K K_1^0\rangle],$ $ K_0\rangle = \frac{1}{2p} [K_S^0\rangle + K_L^0\rangle], \quad \bar{K}_0\rangle = \frac{1}{2q} [K_S^0\rangle - K_L^0\rangle]$	
Mixing for the $(B^0 \leftrightarrow \bar{B}^0)$ system	
Two types of B^0 -mesons: $ B_d^0\rangle = \bar{b}d\rangle, \quad \bar{B}_d^0\rangle = b\bar{d}\rangle; \quad B_s^0\rangle = \bar{b}s\rangle, \quad \bar{B}_s^0\rangle = b\bar{s}\rangle; \quad \Delta\Gamma_B/\Gamma_B \ll 1, \quad \Delta\Gamma_B \ll \Delta M_d, \quad \Gamma_{12} \ll M_{12}.$ Only $ B_d^0\rangle \leftrightarrow \bar{B}_d^0\rangle$ mixing has been observed. Therefore we present data for the B_d^0 -meson. Since the difference in lifetime between the two states originated due to mixing is very small, they differ only in mass: $ B_H^0\rangle = p B^0\rangle - q \bar{B}^0\rangle$ (Heavy), $ B_L^0\rangle = p B^0\rangle + q \bar{B}^0\rangle$ (Light); $\Delta M_d = M_{B_H} - M_{B_L} = (0.489 \pm 0.008) \times 10^{12} \text{ s}^{-1} = (3.22 \pm 0.05) \times 10^{-4} \text{ eV};$ $M_{B_H} = M_d + \frac{\Delta M_d}{2}, \quad M_{B_L} = M_d - \frac{\Delta M_d}{2}, \quad \Gamma_{H,L} \simeq \Gamma_B, \quad \left(\frac{q}{p} \right)_B = -\frac{M_{12}^*}{ M_{12} } \left(1 - \frac{1}{2} \text{Im} \frac{\Gamma_{12}}{M_{12}} \right).$ The states are produced as pure B^0 - and \bar{B}^0 -mesons: $ B^0(0)\rangle = \frac{1}{2p} (B_H^0\rangle + B_L^0\rangle), \quad \bar{B}^0(0)\rangle = \frac{1}{2q} (B_L^0\rangle - B_H^0\rangle),$ $ B^0(t)\rangle = \frac{1}{2p} \exp(-iM_d t) \exp\left(-\frac{\Gamma_B t}{2}\right) \left[\exp\left(-\frac{i\Delta M_d t}{2}\right) B_H^0\rangle + \exp\left(\frac{i\Delta M_d t}{2}\right) B_L^0\rangle \right] = \exp(-iM_d t) \exp\left(-\frac{\Gamma_B t}{2}\right) \left[\cos\frac{\Delta M_d t}{2} \cdot B^0\rangle + i\frac{q}{p} \sin\frac{\Delta M_d t}{2} \cdot \bar{B}^0\rangle \right],$ $ \bar{B}^0(t)\rangle = \frac{1}{2q} \exp(-iM_d t) \exp\left(-\frac{\Gamma_B t}{2}\right) \left[\exp\left(\frac{i\Delta M_d t}{2}\right) B_L^0\rangle - \exp\left(-\frac{i\Delta M_d t}{2}\right) B_H^0\rangle \right] = \exp(-iM_d t) \exp\left(-\frac{\Gamma_B t}{2}\right) \left[\cos\frac{\Delta M_d t}{2} \cdot \bar{B}^0\rangle + i\frac{p}{q} \sin\frac{\Delta M_d t}{2} \cdot B^0\rangle \right]$	

In processes of the tree type, no significant contribution from NP effects, which could be revealed in the region of small distances, are expected. Therefore, such tree processes can be used for determining the respective matrix elements of V_{CKM} in the SM, although the task is rendered difficult by the necessity of calculations in the region of large distances (see Section 2.2). The difficulties in calculations hinder the theoretical analysis and increase the systematic uncertainties. In the reduction of uncertainties and enhancement of the precision and reliability of analysis, a determinant role must be played by the further development of theoretical methods for describing decays, in particular, the significant progress to be expected in lattice QCD calculations.

The values of matrix elements related to the decays of t-quarks have not been measured directly⁴. At present, they can only be derived from the unitary relations and from data on loop processes which proceed in the higher orders with respect to weak interactions (rare K- and B-decays, $K^0 \leftrightarrow \bar{K}^0$ - and $B^0 \leftrightarrow \bar{B}^0$ -mixing effects, processes violating CP invariance). This information is used to find the position of the vertex A of the unitary triangle (see Fig. 2) that fully

⁴ The value for $|V_{tb}|$ obtained in direct experiments at the Fermilab collider is 0.99 ± 0.15 [25]. But, the value derived from the diagonal unitary relation $|V_{td}|^2 + |V_{ts}|^2 + |V_{tb}|^2 = 1$ is much more accurate, owing to the smallness of $|V_{td}|^2$ and $|V_{ts}|^2$: $|V_{tb}| = 1$ up to an uncertainty of 2×10^{-3} .

Table 4. Processes violating CP symmetry in the decays of K^0 -mesons.

<p>(1) Direct and indirect CP violation in decays $K_L^0 \rightarrow 2\pi$:</p> $ K_L^0\rangle \sim K_2^0\rangle + \varepsilon_K K_1^0\rangle.$ $\begin{array}{cc} \downarrow & \downarrow \\ 2\pi & 2\pi \\ \text{direct} & \text{indirect} \end{array}$	
<p>Violation of CP invariance in decays $K^0 \rightarrow 2\pi$:</p> $\langle \pi\pi H K_L^0 \rangle = \frac{\langle \pi\pi H K_2^0 \rangle + \varepsilon_K \langle \pi\pi H K_1^0 \rangle}{\sqrt{1 + \varepsilon_K ^2}},$ $\langle \pi\pi H K_S^0 \rangle = \frac{\langle \pi\pi H K_1^0 \rangle + \varepsilon_K \langle \pi\pi H K_2^0 \rangle}{\sqrt{1 + \varepsilon_K ^2}} \simeq \frac{\langle \pi\pi H K_1^0 \rangle}{\sqrt{1 + \varepsilon_K ^2}},$ $\frac{\langle \pi\pi H K_L^0 \rangle}{\langle \pi\pi H K_S^0 \rangle} = \varepsilon_K + \frac{\langle \pi\pi H K_2^0 \rangle}{\langle \pi\pi H K_1^0 \rangle}.$	<p>Diagram illustrating the mechanism of indirect CP violation in ($K^0 \rightleftharpoons \bar{K}^0$) mixing ($\Delta S = 2$). The violation of CP invariance is determined by the imaginary part of the respective amplitude and is characterized by the parameter $\varepsilon_K = 2.282 \times 10^{-3}$. The parameter ε_K is determined from the measurement of the interference between the decays $K_L^0 \rightarrow 2\pi$ and $K_S^0 \rightarrow 2\pi$.</p>
<p>Parameters:</p> $\eta_{+-} = \frac{\langle \pi^+ \pi^- H K_L^0 \rangle}{\langle \pi^+ \pi^- H K_S^0 \rangle} = \varepsilon_K + \frac{\langle \pi^+ \pi^- H K_2^0 \rangle}{\langle \pi^+ \pi^- H K_1^0 \rangle}$ $= \varepsilon_K + \frac{i}{\sqrt{2}} \frac{\text{Im} A_2}{\text{Re} A_0} \exp [i(\delta_2 - \delta_0)] = \varepsilon_K + \varepsilon',$ $\eta_{00} = \frac{\langle \pi^0 \pi^0 H K_L^0 \rangle}{\langle \pi^0 \pi^0 H K_S^0 \rangle} = \varepsilon_K + \frac{\langle \pi^0 \pi^0 H K_2^0 \rangle}{\langle \pi^0 \pi^0 H K_1^0 \rangle}$ $= \varepsilon_K - i\sqrt{2} \frac{\text{Im} A_2}{\text{Re} A_0} \exp [i(\delta_2 - \delta_0)] = \varepsilon_K - 2\varepsilon';$ $ \eta_{+-} = (2.276 \pm 0.017) \times 10^{-3}, \quad \varphi_{+-} = 43.3^\circ \pm 0.5^\circ;$ $ \eta_{00} = (2.262 \pm 0.017) \times 10^{-3}, \quad \varphi_{00} - \varphi_{+-} = -0.1^\circ \pm 0.8^\circ;$ $R = \frac{ \eta_{+-} ^2}{ \eta_{00} ^2} = 1 + 6 \text{Re} \frac{\varepsilon'}{\varepsilon_K} = 1.00996 \pm 0.00096, \quad \varepsilon' = \frac{i}{\sqrt{2}} \frac{\text{Im} A_2}{\text{Re} A_0} \exp [i(\delta_2 - \delta_0)]$ <p>is the parameter of direct CP violation in decays $K_L^0 \rightarrow 2\pi$.</p>	 <p>Penguin diagrams describing the mechanism of direct CP violation in $K^0 \rightarrow 2\pi$ decay ($\Delta S = 1$). The amplitudes of $K^0 \rightarrow 2\pi$ and $\bar{K}^0 \rightarrow 2\pi$ have the form $\langle 2\pi; I H K^0 \rangle = A_I \exp(i\delta_I)$, $\langle 2\pi; I H \bar{K}^0 \rangle = A_I^* \exp(i\delta_I)$, where $I = 0, 2$ is the isotopic spin of the 2π-system, and δ_I is the phase of the strong $\pi\pi$-scattering in the state with isospin I. Direct CP violation is characterized by $\varepsilon' = (i/\sqrt{2}) (\text{Im} A_2 / \text{Re} A_0) \exp [i(\delta_2 - \delta_0)]$. The quantity ε' is due to the difference between the amplitudes determined by the ‘gluon penguin’ (exchange of g) and the ‘electroweak penguin’ (exchange of Z, γ).</p>
<p>Measurement of ε':</p> $R = \frac{\Gamma(K_L^0 \rightarrow \pi^+ \pi^-) / \Gamma(K_S^0 \rightarrow \pi^+ \pi^-)}{\Gamma(K_L^0 \rightarrow \pi^0 \pi^0) / \Gamma(K_S^0 \rightarrow \pi^0 \pi^0)} = \frac{ \eta_{+-} ^2}{ \eta_{00} ^2} = \frac{ \varepsilon_K ^2 (1 + \text{Re}(\varepsilon'/\varepsilon_K))^2 + (\text{Im}(\varepsilon'/\varepsilon_K))^2}{ \varepsilon_K ^2 (1 - 2 \text{Re}(\varepsilon'/\varepsilon_K))^2 + 4(\text{Im}(\varepsilon'/\varepsilon_K))^2} \simeq \frac{1 + 2 \text{Re}(\varepsilon'/\varepsilon_K)}{1 - 4 \text{Re}(\varepsilon'/\varepsilon_K)} \simeq 1 + 6 \text{Re} \frac{\varepsilon'}{\varepsilon_K}, \quad \text{Re} \frac{\varepsilon'}{\varepsilon_K} = \frac{1}{6}(R - 1).$	
<p>Experimental data for $\text{Re}(\varepsilon'/\varepsilon_K) \times 10^4$:</p> <p>$23 \pm 6.5$ (NA31 [78]), 7.4 ± 5.9 (E731 [79]), 20.7 ± 2.8 (KTeV [80]), 14.7 ± 2.2 (NA48 [81]), 16.6 ± 1.6 (mean weighted value).</p>	
<p>Thus, the experimental data yield $\langle \text{Re}(\varepsilon'/\varepsilon_K) \rangle_{\text{expt}} = (16.6 \pm 1.6) \times 10^{-4}$; CM theoretical calculations yield $\text{Re}(\varepsilon'/\varepsilon_K)_{\text{SM}} = (5 - 30) \times 10^{-4}$ [82]; other estimates yield $\text{Re}(\varepsilon'/\varepsilon_K)_{\text{SM}} = (17_{-1}^{+16}) \times 10^{-4}$ [83]. Theoretical calculations exhibit significant uncertainty.</p>	
<p>(2) Charge asymmetry in semilepton decays of K_L^0 (indirect CP violation):</p>	
$\delta(e) = \frac{(K_L^0 \rightarrow \pi^- e^+ \nu_e) - (K_L^0 \rightarrow \pi^+ e^- \bar{\nu}_e)}{(K_L^0 \rightarrow \pi^- e^+ \nu_e) + (K_L^0 \rightarrow \pi^+ e^- \bar{\nu}_e)} = (0.338 \pm 0.014) \times 10^{-2}$ (PDG [25]), $\delta(\mu) = (0.304 \pm 0.025) \times 10^{-2}$ (PDG [25]).	
<p>Averaged value is $\delta(l) = (0.327 \pm 0.012) \times 10^{-2}$. New data from KTeV [84]: $\delta(e) = (0.3322 \pm 0.0074) \times 10^{-2}$. CPT invariance is assumed to be valid, as is the rule $\Delta Q = \Delta S$; then $\delta(l) \simeq 2 \text{Re} \varepsilon_K$.</p>	
<p>(3) Indirect CP violation in the decay $K_L^0 \rightarrow \pi^+ \pi^- \gamma$:</p>	
$ \eta_{+-\gamma} = \left \frac{A(K_L^0 \rightarrow \pi^+ \pi^- \gamma; \text{CP violation})}{A(K_S^0 \rightarrow \pi^+ \pi^- \gamma)} \right = (2.35 \pm 0.07) \times 10^{-3}, \quad \varphi_{\pi^+ \pi^- \gamma} = 44^\circ \pm 4^\circ$ (PDG [25]).	
<p>(4) $K_L^0 \rightarrow \pi^+ \pi^- e^+ e^-$ asymmetry in the distribution over the angle φ between the planes ($\pi^+ \pi^-$) and ($e^+ e^-$) in the K_L^0 rest frame, due to violation of CP and T invariance:</p>	
$A_{\pi\pi ee}^L = \frac{N(\sin 2\varphi > 0) - N(\sin 2\varphi < 0)}{N(\sin 2\varphi > 0) + N(\sin 2\varphi < 0)}, \quad A_{\pi\pi ee}^L = 13.6 \pm 2.5 \pm 1.2\%$ (KTeV [85]), $A_{\pi\pi ee}^L = 13.9 \pm 2.7 \pm 2.0\%$ (NA48 [86]).	
<p>The asymmetry is due to interference between the CP-conserving amplitude M1 and the CP-violating amplitude with internal conversion of bremsstrahlung (IB). The experimental values of asymmetry [85, 86] are consistent with theoretical predictions [87, 88].</p>	
<p>(5) Violation of T invariance in $K^0 \rightleftharpoons \bar{K}^0$ mixing, manifested in the asymmetry of transition probabilities $[R(\bar{K}^0 \rightarrow K^0) - R(K^0 \rightarrow \bar{K}^0)] / [R(\bar{K}^0 \rightarrow K^0) + R(K^0 \rightarrow \bar{K}^0)]$ [88]:</p>	
<p>The asymmetry measured in the experiment CPLEAR [89]:</p>	
$A = \left(\frac{R[\bar{K}^0 _{t=0} \rightarrow (e^+ \pi^- \nu_e)_{t=\tau}] - R[K^0 _{t=0} \rightarrow (e^- \pi^+ \bar{\nu}_e)_{t=\tau}]}{R[\bar{K}^0 _{t=0} \rightarrow (e^+ \pi^- \nu_e)_{t=\tau}] + R[K^0 _{t=0} \rightarrow (e^- \pi^+ \bar{\nu}_e)_{t=\tau}]} \right)_{1 < \tau < 20\tau_s} = (6.6 \pm 1.3 \pm 1.0) \times 10^{-3}.$	
<p>The tagging of \bar{K}^0 (K^0) at the moment of production ($t = 0$) occurs in reactions $\bar{p}p \rightarrow \bar{K}^0 K^+ \pi^-$ ($K^0 K^- \pi^+$), while the tagging of K^0 (\bar{K}^0) takes place at the moment of decay ($t = \tau$) via channels $K^0 \rightarrow e^+ \pi^- \nu_e$ ($\bar{K}^0 \rightarrow e^- \pi^+ \bar{\nu}_e$) in accordance with the rule $\Delta Q = \Delta S$.</p>	

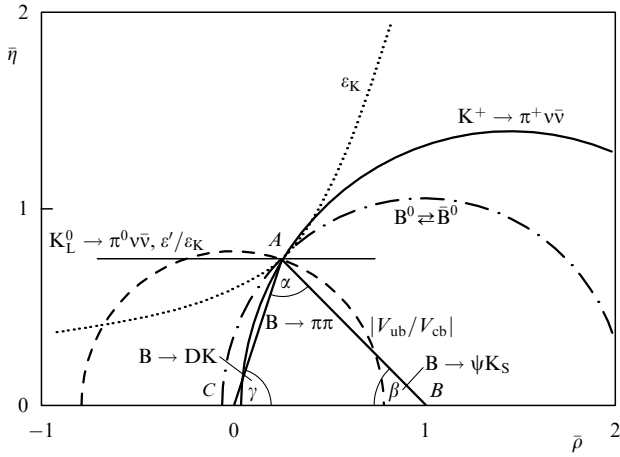


Figure 4. Idealized diagram for the dependence of a number of processes upon the parameters ρ, η of the quark mixing matrix: $\epsilon_K, |V_{ub}/V_{cb}|, \Delta M_d, \Delta M_s, K \rightarrow \pi\nu\bar{\nu}$. In the SM, the curves for all the processes must intersect at the vertex A of the unitary triangle.

determines its elements. This is illustrated in an idealized form with the aid of Fig. 4, while the actual situation determined by the accuracies achieved is reflected in Fig. 5. The concrete processes presented in these figures will be examined below.

Within the framework of the SM, joint analysis has been performed of the information on the quark mixing matrix and on the parameters of the unitary triangle (27). The results of these studies [25, 29, 45, 48, 90–95] differ somewhat among each other, which is mainly due to the differences in the approach to estimation of systematic and theoretical errors: more conservative (like, for instance, in PDG-2002 [25]) or more ‘aggressive’ (like in Refs [29, 45, 48]). Table 5, proceeded from these studies, reflects the differences in the results obtained; see also Fig. 5a from Ref. [25], and Fig. 5b from Ref. [45]. Most of the calculations in the present review are based on data pertaining to the more conservative approach which, from our point of view, still remains preferable.

In Table 5, presented are the values of the main parameters applied in subsequent sections of this review when analyzing the properties of the unitary triangle (27) [and of the so-called kaon unitary triangle depending on the unitarity relation (24)], in estimating the matrix elements of V_{CKM} , related to the decays of t-quarks, and in calculating probabilities for the loop FCNC processes. All the necessary definitions can be found in Table 5, although the meaning of some of the parameters introduced is explained in subsequent sections of the review. Nevertheless, we considered it expedient to put all these definitions in a single place for the convenience of the reader.

One must bear in mind that the loop processes of higher orders, utilized in the analysis, are due to the region of very small distances and may be sensitive to various NP effects going beyond the framework of the SM. In accordance with the SM, the data for all the decays examined must be consistent with each other and lead to one and the same form of the unitary triangle, i.e., to a certain position of its vertex A . The contribution of NP effects may be revealed as a divergence of the data on this vertex for different processes. Searches for such effects are of particular interest. As follows from Table 5, the presently available data can be seen not to contradict the SM, although they may need to be further refined.

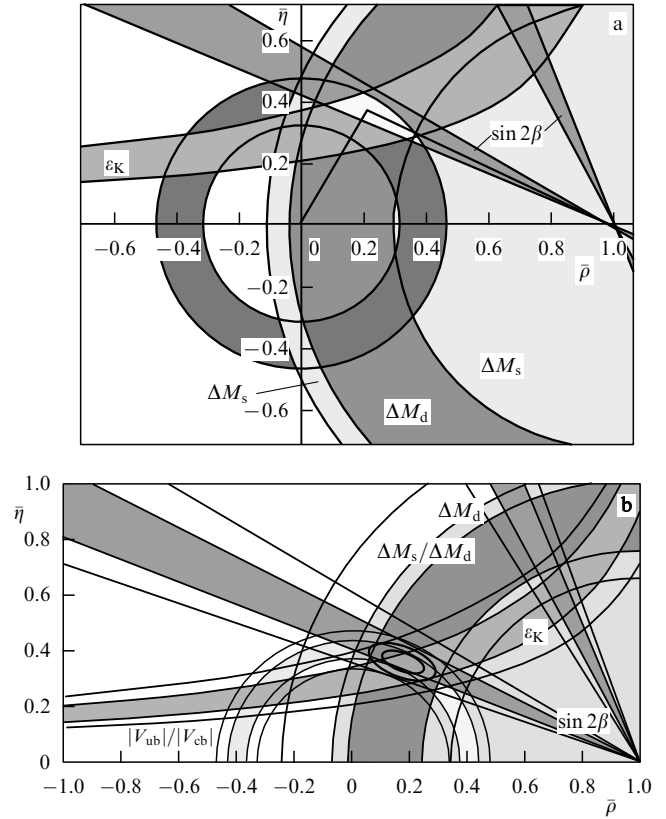


Figure 5. Restrictions on the parameters of the unitary triangle, arising from the available data on $\epsilon_K, \Delta M_d, \Delta M_s, |V_{ub}/V_{cb}|$, and the asymmetry $a_{\psi K} = \sin 2\beta$ in the decays $B^0(\bar{B}^0) \rightarrow (J/\psi) K_S^0$. (a) Restrictions based on the ‘conservative’ approach of PDG-2002 [25]. (b) Restrictions based on the ‘aggressive’ approach [45]; uncertainties in the determination of parameters corresponding to confidence levels of 68 and 95% are shown [45]. For the angle β , considering the data on $a_{\psi K} = \sin 2\beta$ in the angular square of interest, there exist two solutions shown in the figure: $\beta = (1/2) \arcsin a_{\psi K}$ and $\beta = \pi/2 - (1/2) \arcsin a_{\psi K}$. However, from the data on $R_b = (1/\lambda)|V_{ub}|/|V_{cb}|$ it is seen that within the SM only the first of these solutions satisfies the condition for finding the vertex of the unitary triangle.

For a complete understanding of Figs 4 and 5 and of the prospects of further studies in this field, we shall consider concrete processes and their characteristics in the (η, ρ) -plane.

4.1 Data on the CP-violation parameter ϵ_K in $K^0 \rightleftharpoons \bar{K}^0$ mixing

As was shown in Section 3, violation of CP invariance in $K^0 \rightleftharpoons \bar{K}^0$ mixing is determined by the parameter ϵ_K and results in eigenstates of the $(K^0 \rightleftharpoons \bar{K}^0)$ -system with definite masses and lifetimes; these eigenstates contain CP-even and CP-odd components $|K_1^0\rangle$ and $|K_2^0\rangle$ (see Table 3):

$$\begin{aligned} |K_S^0\rangle &= \frac{1}{\sqrt{2(1+|\epsilon_K|^2)}} [(1+\epsilon_K)|K^0\rangle + (1-\epsilon_K)|\bar{K}^0\rangle] \\ &= \frac{1}{\sqrt{1+|\epsilon_K|^2}} [|K_1^0\rangle + \epsilon_K|K_2^0\rangle], \\ |K_L^0\rangle &= \frac{1}{\sqrt{2(1+|\epsilon_K|^2)}} [(1+\epsilon_K)|K^0\rangle - (1-\epsilon_K)|\bar{K}^0\rangle] \\ &= \frac{1}{\sqrt{1+|\epsilon_K|^2}} [|K_2^0\rangle + \epsilon_K|K_1^0\rangle]. \end{aligned} \quad (68)$$

Table 5. Parameters of the quark mixing matrix V_{CKM} and the unitary triangle, and other data applied in the calculation of FCNC decays.

Experimental data	Calculated parameters	Data used in computing FCNC decays
<p>Matrix V_{CKM}:</p> <p>$V_{\text{ud}} = 0.9734 \pm 0.0008$,</p> <p>$V_{\text{us}} = 0.2196 \pm 0.0023$,</p> <p>$V_{\text{ub}} = (3.6 \pm 0.7) \times 10^{-3}$,</p> <p>$V_{\text{cd}} = 0.224 \pm 0.016$,</p> <p>$V_{\text{cs}} = 0.996 \pm 0.013$,</p> <p>$V_{\text{cb}} = (41.2 \pm 2.0) \times 10^{-3}$,</p> <p>$\frac{ V_{\text{ub}} }{ V_{\text{cb}} } = 0.087 \pm 0.017$.</p> <p>CP violation in decays $K^0 \rightarrow 2\pi$:</p> <p>$\varepsilon_K = (2.282 \pm 0.017) \times 10^{-3}$,</p> <p>$\text{Re} \frac{\varepsilon'}{\varepsilon_K} = (16.6 \pm 1.6) \times 10^{-4}$.</p> <p>CP asymmetry in decays $B_d^0(\bar{B}_d^0) \rightarrow J/\psi K_s^0$:</p> <p>$a_{\psi K} = (\sin 2\beta)_{\text{SM}} = 0.734 \pm 0.054$ [104],</p> <p>$\beta = 23.6^\circ \pm 2.3^\circ$ — angle of unitary triangle,</p> <p>$\beta_K = \beta + 1^\circ = 24.6^\circ \pm 2.3^\circ$ — angle in kaon unitary triangle [118],</p> <p>$M_W = 80.4 \text{ GeV}$ — mass of W^\pm boson,</p> <p>$\sin^2 \vartheta_W = 0.23143 \pm 0.00015$ — sine squared of Weinberg angle.</p> <p>Masses and mass differences for K^0- and $B_{d,s}^0$-mesons:</p> <p>$M_{K^0} = 497.672 \pm 0.031 \text{ MeV}$,</p> <p>$\Delta M_K = (0.5300 \pm 0.0012) \times 10^{10} \text{ s}^{-1}$ $= (3.489 \pm 0.008) \times 10^{-6} \text{ eV}$,</p> <p>$M_{B_d} = M_d = 5279.4 \pm 0.5 \text{ MeV}$,</p> <p>$\Delta M_{B_d} = \Delta M_d = (0.489 \pm 0.008) \times 10^{12} \text{ s}^{-1}$ $= (3.22 \pm 0.05) \times 10^{-4} \text{ eV}$,</p> <p>$M_B = M_s = 5369.6 \pm 2.4 \text{ MeV}$,</p> <p>$\Delta M_B = \Delta M_s > 14.4 \times 10^{-12} \text{ s}^{-1}$ (95% C.L.)</p>	<p>K^0-decay parameters:</p> <p>$f = 159.8 \pm 1.5 \text{ MeV}$ — decay constant,</p> <p>$\hat{B}_K = 0.86 \pm 0.06_G \pm 0.14_U$ — nonperturbative decay parameter (G — Gaussian errors, U — uniform distribution for errors).</p> <p>$B_{d,s}^0$-decay parameters:</p> <p>$f_d \sqrt{\hat{B}_d} = 226 \pm 36 \text{ MeV}$,</p> <p>$f_s \sqrt{\hat{B}_s} = 266 \pm 35 \text{ MeV}$.</p> <p>Parameter of SU(3) violation:</p> <p>$\xi = \frac{f_s \sqrt{\hat{B}_s}}{f_d \sqrt{\hat{B}_d}} = 1.16 \pm 0.06$ (old value).</p> <p>New values of ξ accounting for chiral extrapolation:</p> <p>$\xi = 1.32 \pm 0.10$ [101],</p> <p>$\xi = 1.18 \pm 0.04_{-0}^{+0.12}$ [103],</p> <p>$\xi = 1.22 \pm 0.07$ [102],</p> <p>$\xi = 1.24 \pm 0.07$ [8].</p> <p>Inami–Lim functions and QCD corrections for ε_K (see Table 2):</p> <p>$S_0(x_c) = (2.42 \pm 0.39) \times 10^{-4}$,</p> <p>$S_0(x_t, x_c) = (2.15 \pm 0.31) \times 10^{-3}$,</p> <p>$S_0(x_t) = 2.38 \pm 0.11$,</p> <p>$\eta_{\text{cc}} = 1.45 \pm 0.38$, $\eta_{\text{ct}} = 0.47 \pm 0.04$,</p> <p>$\eta_{\text{tt}} = 0.57 \pm 0.01$,</p> <p>$L = 3.837 \times 10^4$</p>	<p>Parameters of the unitary triangle:</p> <p>$\lambda = 0.222 \pm 0.002$.</p> <p>Set of ‘conservative’ parameters A [25]:</p> <p>$\bar{\rho} = 0.22 \pm 0.010$, $\bar{\eta} = 0.35 \pm 0.050$,</p> <p>$V_{\text{cb}} = (41.2 \pm 2.0) \times 10^{-3}$,</p> <p>$A = \frac{ V_{\text{cb}} }{\lambda^2} = 0.836 \pm 0.044$,</p> <p>$\text{Re} V_{\text{td}} = (7.1 \pm 0.8) \times 10^{-3}$,</p> <p>$\text{Im} V_{\text{td}} = (-3.2 \pm 0.4) \times 10^{-3}$,</p> <p>$V_{\text{td}} = (7.8 \pm 0.9) \times 10^{-3}$.</p> <p>Set of ‘aggressive’ parameters B [48]:</p> <p>$\bar{\rho} = 0.173 \pm 0.046$, $\bar{\eta} = 0.357 \pm 0.027$,</p> <p>$V_{\text{cb}} = (40.6 \pm 0.8) \times 10^{-3}$,</p> <p>$A = \frac{ V_{\text{cb}} }{\lambda^2} = 0.824 \pm 0.023$.</p> <p>Inami–Lim functions (see Table 2):</p> <p>for $K \rightarrow \pi \nu \bar{\nu}$ decays</p> <p>$X(x_t) = 1.52 \pm 0.05$,</p> <p>$F(x_c) = \frac{2}{3} X(x_c)_{e,\mu} + \frac{1}{3} X(x_c)_\tau$ $= (9.82 \pm 1.78) \times 10^{-4}$,</p> <p>$f = 1.03 \pm 0.02$ — nonperturbative correction,</p> <p>$\delta(x_c) = f \frac{F(x_c)}{X(x_t)} = (6.66 \pm 1.23) \times 10^{-4}$,</p> <p>$P_c(\nu \bar{\nu}) = \delta(x_c) \frac{X(x_t)}{\lambda^4} = f \frac{F(x_c)}{\lambda^4} = 0.42 \pm 0.06$,</p> <p>$\rho_0 = 1 + \Delta = 1 + \frac{\delta(x_c)}{ V_{\text{cb}} ^2} = 1.39 \pm 0.08$;</p> <p>for $K_L^0 \rightarrow \pi^0 e^+ e^-$ decay</p> <p>$\hat{Y}_{7A}^2 + \hat{Y}_{7V}^2 = 39.2 \pm 2.9$;</p> <p>for $K_L^0 \rightarrow \mu^+ \mu^-$ decay</p> <p>$Y(x_t) = 1.00 \pm 0.05$, $\rho'_0 = 1.23 \pm 0.03$</p>
<p><i>Note.</i> If no reference is given, the data were taken from PDG-2002 [25]. Calculations were based on the ‘conservative’ parameters (set A) [25], unless otherwise specified.</p>		

Indirect violation of CP invariance manifests itself in several decays of K-mesons, which are presented in Table 4. There, also, data are presented on the direct violation of CP invariance in the decays $K_L^0 \rightarrow 2\pi$.

The process of $K^0 \rightleftharpoons \bar{K}^0$ mixing is determined by the interaction operator $Q(\Delta S = 2) = (\bar{s}d)_{V-A}(\bar{s}d)_{V-A}$. The corresponding amplitude assumes the form

$$\langle \bar{K}^0 | (\bar{s}d)_{V-A} (\bar{s}d)_{V-A} | K^0 \rangle.$$

We shall investigate its structure, first of all, applying the completeness condition $\sum_n |n\rangle \langle n| = 1$, when summing over all the final states for the K-decays. Then, in the so-called vacuum saturation approximation [96], i.e., dominance of the contribution of the vacuum state $|0\rangle$ to the sum $\sum_n |n\rangle \langle n|$, we arrive at

$$\begin{aligned} & \langle \bar{K}^0 | (\bar{s}d)_{V-A} (\bar{s}d)_{V-A} | K^0 \rangle \\ &= \langle \bar{K}^0 | (\bar{s}d)_{V-A} \sum_n |n\rangle \langle n| (\bar{s}d)_{V-A} | K^0 \rangle \\ &\simeq \langle \bar{K}^0 | (\bar{s}d)_{V-A} | 0 \rangle \langle 0 | (\bar{s}d)_{V-A} | K^0 \rangle \propto f_K^2. \end{aligned} \quad (69)$$

Here, the K-meson constant $f_K = 159.8 \pm 1.5 \text{ MeV}$ is determined from the lepton decays $K^+ \rightarrow \mu^+ \nu_\mu$. The amplitude of this decay includes the hadron transition factor of kaons to vacuum: $\langle 0 | (\bar{s}u)_{V-A} | K^+ \rangle \simeq \langle 0 | (\bar{s}d)_{V-A} | K^0 \rangle$ (isotopic invariance). To account for the approximate character of vacuum saturation, an additional nonperturbative parameter $\hat{B}_K \simeq 0.86 \pm 0.15$ is introduced, so that

$$\langle \bar{K}^0 | Q(\Delta S = 2) | K^0 \rangle = \langle \bar{K}^0 | (\bar{s}d)_{V-A} (\bar{s}d)_{V-A} | K^0 \rangle \propto f_K^2 \hat{B}_K,$$

or, to be more accurate,

$$\langle \bar{K}^0 | Q(\Delta S = 2) | K^0 \rangle = \frac{8}{3} M_K^2 f_K^2 \hat{B}_K$$

(see, for instance, Refs [26, 27]). Computations of the parameter \hat{B}_K have been performed within lattice QCD.

The parameter ε_K of CP violation in $K^0 \rightleftharpoons \bar{K}^0$ mixing is determined by the imaginary part of the mixing box diagrams (see Fig. 3) and takes the form

$$\varepsilon_K \simeq \exp \frac{i\pi}{4} \cdot \frac{\text{Im} M_{12}}{\sqrt{2} \Delta m_K} \simeq \exp \frac{i\pi}{4} \cdot \frac{G_F^2 M_W^2 m_K}{12\sqrt{2} \pi^2 \Delta m_K} f_K^2 \hat{B}_K \text{Im} M'_{12} \quad (70)$$

(for the chosen normalization of $\text{Im } M'_{12}$). The dependence of $\text{Im } M'_{12}$ on the matrix elements of V_{CKM} can be determined from the diagrams for $(\text{K}^0 \rightleftharpoons \bar{\text{K}}^0)$ mixing according to the rules indicated in Figs 1 and 3e:

$$\begin{aligned} \text{Im } M'_{12} &= [\eta_{\text{cc}} S_0(x_c) \text{Im}(V_{\text{cs}} V_{\text{cd}}^*)^2 + \eta_{\text{tt}} S_0(x_t) \text{Im}(V_{\text{ts}} V_{\text{td}}^*)^2 \\ &\quad + 2\eta_{\text{ct}} S_0(x_c; x_t) \text{Im}(V_{\text{cs}} V_{\text{cd}}^* V_{\text{ts}} V_{\text{td}}^*)] \\ &= [\eta_{\text{cc}} S_0(x_c) \text{Im } \lambda_c^{*2} + \eta_{\text{tt}} S_0(x_t) \text{Im } \lambda_t^{*2} \\ &\quad + 2\eta_{\text{ct}} S_0(x_c; x_t) \text{Im}(\lambda_c^* \lambda_t^*)]. \end{aligned} \quad (71)$$

Here, the Inami–Lim functions S_0 for the box diagrams of $(\text{K}^0 \rightleftharpoons \bar{\text{K}}^0)$ mixing, the QCD corrections η_{cc} and so on, compiled in Tables 2 and 5, as well as the matrix elements λ_c and λ_t (see Table 1) are used.

Upon performing simple transformations, we obtain for the CP-violation parameter ε_{K} , in the case of $(\text{K}^0 \rightleftharpoons \bar{\text{K}}^0)$ mixing, the relation†

$$\begin{aligned} \varepsilon_{\text{K}} &= \exp(i\phi_\varepsilon) L \hat{B}_{\text{K}} \text{Im } \lambda_t \\ &\quad \times \{ \text{Re } \lambda_c [\eta_{\text{cc}} S_0(x_c) - \eta_{\text{ct}} S_0(x_c; x_t)] - \text{Re } \lambda_t \eta_{\text{tt}} S_0(x_t) \}, \end{aligned} \quad (72)$$

$$L = \frac{G_{\text{F}}^2 m_{\text{K}} M_{\text{W}}^2 f_{\text{K}}^2}{6\sqrt{2} \pi^2 \Delta m_{\text{K}}} = 3.837 \times 10^4, \quad (73)$$

$$\text{Re } \lambda_c = -\lambda \left(1 - \frac{\lambda^2}{2}\right) = -0.217 \pm 0.002. \quad (74)$$

Hence, and from data on the Inami–Lim functions for the $(\text{K}^0 \rightleftharpoons \bar{\text{K}}^0)$ -mixing box diagrams, it is possible to find the condition relating $\text{Re } \lambda_t$ and $\text{Im } \lambda_t$ and being determined by the experimental value of the parameter $|\varepsilon_{\text{K}}| = (2.282 \pm 0.017) \times 10^{-3}$:

$$\hat{B}_{\text{K}} \text{Im } \lambda_t [N_{\text{c}}(\varepsilon_{\text{K}}) - \text{Re } \lambda_t \eta_{\text{tt}} S_0(x_t)] = \frac{|\varepsilon_{\text{K}}|}{L} = 5.95 \times 10^{-8}, \quad (75)$$

where

$$\begin{aligned} N_{\text{c}}(\varepsilon_{\text{K}}) &= \text{Re } \lambda_c [\eta_{\text{cc}} S_0(x_c) - \eta_{\text{ct}} S_0(x_c; x_t)] \\ &= (1.43 \pm 0.44) \times 10^{-4} \end{aligned} \quad (76)$$

is the term determining the influence of c-quarks in Eqn (75).

Thus, the linkage between $\text{Re } \lambda_t$ and $\text{Im } \lambda_t$ is defined by relation (75), which may be represented in the numerical form as follows

$$\begin{aligned} \hat{B}_{\text{K}} \text{Im } \lambda_t \{ (1.43 \pm 0.44) \times 10^{-4} - \text{Re } \lambda_t (1.357 \pm 0.067) \} \\ = 5.95 \times 10^{-8}. \end{aligned} \quad (77)$$

Relations (75) and (77) represent equations of a hyperbola in the plane of the variables $\text{Re } \lambda_t$, $\text{Im } \lambda_t$.

† *Author's note added in English proofreading.* After issuing the Russian version of my review [*Usp. Fiz. Nauk* **173** 1025 (2003)] I got to know that loop vertex functions used for describing the CP-violation parameter ε_{K} in $\text{K}^0 \rightleftharpoons \bar{\text{K}}^0$ mixing and designated in this article as Inami–Lim loop functions $S_0(x_c)$, $S_0(x_t)$, and $S_0(x_c; x_t)$ as well as QCD corrections η_{c} , η_{t} , and η_{ct} to these functions were first introduced in the theory by M I Vysotskiĭ in 1980 already. The relevant article reads as “ $\text{K}^0 \rightleftharpoons \bar{\text{K}}^0$ transition within $\text{SU}(3) \times \text{SU}(2) \times \text{SU}(1)$ -scheme” (*Yad. Fiz.* **31** 1535 (1980) [*Sov. J. Nucl. Phys.* **31** 797 (1980)]). I offer here my apology to M I Vysotskiĭ for the lack of reference to his basic work.

Making use of the expressions for $\text{Re } \lambda_t$ and $\text{Im } \lambda_t$ in terms of the parameters $\bar{\eta}$, $\bar{\rho}$ for the plane of the unitary triangle (27), namely

$$\text{Re } \lambda_t = -A^2 \lambda^5 \left(1 - \frac{\lambda^2}{2}\right) (1 - \bar{\rho}) + O(\lambda^5), \quad (78)$$

$$\text{Im } \lambda_t = \frac{\bar{\eta} A^2 \lambda^5}{1 - \lambda^2/2} + O(\lambda^9)$$

(see Table 1), one can rewrite the expression for the ‘ ε_{K} -hyperbola’ (75) in the $(\bar{\eta}, \bar{\rho})$ -plane as

$$\begin{aligned} \bar{\eta} [(1 - \bar{\rho}) A^2 \eta_{\text{tt}} S_0(x_t) + P_{\text{c}}(\varepsilon_{\text{K}})] A^2 \hat{B}_{\text{K}} \\ = \frac{5.95 \times 10^{-8}}{\lambda^{10}} = 0.205 \pm 0.018. \end{aligned} \quad (79)$$

The influence of c-quarks is taken into account by the term

$$\begin{aligned} P_{\text{c}}(\varepsilon_{\text{K}}) &= \frac{-\eta_{\text{cc}} S_0(x_t) + \eta_{\text{ct}} S_0(x_c; x_t)}{\lambda^4} \\ &= \frac{(6.59 \pm 2.00) \times 10^{-4}}{\lambda^4} = 0.27 \pm 0.08. \end{aligned} \quad (80)$$

The hyperbola (79) is presented in an idealized form in Fig. 4. For the real situation (see Fig. 5), the errors in the parameter values (of which the most significant error is due to calculations of \hat{B}_{K} in lattice QCD) result in a ‘hyperbolic belt’ in the $(\bar{\rho}, \bar{\eta})$ -plane, which plays an essential role in determining the possible position of the vertex A of the unitary triangle (27).

The hyperbola (79) can also be represented in the form

$$\begin{aligned} \bar{\eta} |V_{\text{cb}}|^2 \hat{B}_{\text{K}} \left[(1 - \bar{\rho}) |V_{\text{cb}}|^2 + \frac{-\eta_{\text{cc}} S_0(x_c) + \eta_{\text{ct}} S_0(x_c; x_t)}{\eta_{\text{tt}} S_0(x_t)} \right] \\ = \frac{2.282 \times 10^{-3}}{L \eta_{\text{tt}} S_0(x_t) \lambda^2} \end{aligned} \quad (81)$$

or as

$$\begin{aligned} \bar{\eta} |V_{\text{cb}}|^2 \hat{B}_{\text{K}} [(1 - \bar{\rho}) |V_{\text{cb}}|^2 + (4.9 \pm 1.5) \times 10^{-4}] \\ = (8.90 \pm 0.44) \times 10^{-7} \end{aligned} \quad (82)$$

(we recall that $|V_{\text{cb}}| = A\lambda^2$).

4.2 Data on the side R_{b} of the triangle

The length of one of the sides of the unitary triangle, R_{b} , in Fig. 2 is determined by relation (28):

$$\begin{aligned} R_{\text{b}} &= \sqrt{\bar{\rho}^2 + \bar{\eta}^2} = \left(1 - \frac{\lambda^2}{2}\right) \frac{1}{\lambda} \left| \frac{V_{\text{ub}}}{V_{\text{cb}}} \right| \\ &= \frac{1}{\sqrt{\sigma} \lambda} \left| \frac{V_{\text{ub}}}{V_{\text{cb}}} \right| \simeq \frac{1}{\lambda} \left| \frac{V_{\text{ub}}}{V_{\text{cb}}} \right|. \end{aligned}$$

Thus, as one can see from the idealized Fig. 4, the vertex of the unitary triangle in the $(\bar{\eta}, \bar{\rho})$ -plane must lie on a circle of radius R_{b} . In reality, one obtains

$$R_{\text{b}} = \frac{1}{\sqrt{\sigma} \lambda} \left| \frac{V_{\text{ub}}}{V_{\text{cb}}} \right| = 0.40 \pm 0.08,$$

which defines the range of admissible values in the $(\bar{\eta}, \bar{\rho})$ -plane, shown in Fig. 5. Further revision of the matrix elements $|V_{ub}|$ and $|V_{cb}|$ and of their ratio is to be expected after new measurements are performed at B-factories and new lattice QCD calculations as well as those in the approximation of the effective model of heavy quarks are implemented (see discussion of this issue in Refs [94, 97, 98]).

The maximum value of $R_{b,\max} = 0.50$ (95% C.L.) also determines the maximum angle β of the unitary triangle. This angle corresponds to the position of the tangent to a circle of radius $R_{b,\max}$ with its center at the vertex C , leaving vertex B of the triangle, i.e., to an angle $\alpha = \pi/2$; see Fig. 4. Therefore, the following restriction [39] is imposed on the unitary triangle:

$$\sin 2\beta_{\max} = 2 \sin \beta_{\max} \cos \beta_{\max} = 2R_{b,\max} \sqrt{1 - R_{b,\max}^2} = 0.87, \\ \beta_{\max} = 30^\circ \text{ (95\% C.L.)}. \quad (83)$$

4.3 The mixing processes $B_d^0 \rightleftharpoons \bar{B}_d^0$ and $B_s^0 \rightleftharpoons \bar{B}_s^0$

The mixing of neutral B-mesons, $B_d^0 \rightleftharpoons \bar{B}_d^0$ and $B_s^0 \rightleftharpoons \bar{B}_s^0$, proceeds in a manner similar to $(K^0 \rightleftharpoons \bar{K}^0)$ mixing; see Table 3 and diagram in Fig. 3e. From this diagram estimates may be made of the corresponding mass differences for the two components of the B_d^0 - and B_s^0 -mesons:

$$\Delta M_{B_q} = \frac{G_F^2 M_W^2 M_{B_q} S_0(x_t) \eta_B}{6\pi^2} f_{B_q}^2 \hat{B}_q |V_{tq} V_{tb}^*|^2, \quad (84)$$

since the hadron matrix element \mathcal{M}_q determining $(B^0 \rightleftharpoons \bar{B}^0)$ mixing has the form

$$\mathcal{M}_q = \langle \bar{B}_q^0 | [\bar{b}\gamma^\mu(1 + \gamma_5)q] [\bar{b}\gamma_\mu(1 + \gamma_5)q] | B_q^0 \rangle \\ = \frac{8}{3} M_{B_q}^2 f_{B_q}^2 \hat{B}_q.$$

Here, $q = d, s$ for B_d^0 - or B_s^0 -mesons, and $\eta_B = 0.55 \pm 0.01$ is the QCD correction in perturbative calculations of the Inami–Lim loop function $S_0(x_t)$ for $(B^0 \rightleftharpoons \bar{B}^0)$ mixing.

Numerical values of the constants for B_q^0 -mesons are determined by lattice QCD calculations and have the disadvantage of significant theoretical uncertainties [99]:

$$f_{B_d} = 198 \pm 30 \text{ MeV}, \quad \hat{B}_{B_d} = 1.30 \pm 0.12, \\ f_{B_d} \sqrt{\hat{B}_{B_d}} = 226 \pm 36 \text{ MeV}, \\ f_{B_s} = 230 \pm 30 \text{ MeV}, \quad \hat{B}_{B_s} = 1.34 \pm 0.10, \\ f_{B_s} \sqrt{\hat{B}_{B_s}} = 266 \pm 35 \text{ MeV}. \quad (85)$$

Hereinafter, we shall make use of simplified notation: $M_{B_d} \equiv M_d$, $M_{B_s} \equiv M_s$, $\Delta M_{B_d} \equiv \Delta M_d$, $\Delta M_{B_s} \equiv \Delta M_s$, $f_{B_d} \equiv f_d$, $f_{B_s} \equiv f_s$, $\hat{B}_{B_d} \equiv \hat{B}_d$, and $\hat{B}_{B_s} \equiv \hat{B}_s$. To avoid misunderstanding, we recall that quark masses are denoted by small letters (m_u, m_c, m_t are the masses of ‘upper’ quarks with $q = +2/3$, and m_d, m_s, m_b are the masses of ‘lower’ quarks with $q = -1/3$).

The side of the unitary triangle, namely

$$R_t = \sqrt{(1 - \bar{\rho}^2) + \bar{\eta}^2} \simeq \frac{|V_{td}|}{A\lambda^3} \simeq \frac{1}{\lambda} \frac{|V_{td}|}{|V_{cb}|},$$

[see Eqn (28) and Fig. 2] may be determined from expression (84) for ΔM_{B_d} :

$$|V_{td}| = \frac{\sqrt{6} \pi}{G_F M_W} \left(\frac{\Delta M_d}{M_d S_0(x_t) \eta_B} \right)^{1/2} \frac{1}{f_d \sqrt{\hat{B}_d}} \\ = (8.20 \times 10^3 \text{ GeV}) \left(\frac{\Delta M_d}{M_d S_0(x_t) \eta_B} \right)^{1/2} \frac{1}{f_d \sqrt{\hat{B}_d}} \\ = (7.8 \pm 1.3) \times 10^{-3}, \quad (86)$$

$$R_t = \frac{|V_{td}|}{A\lambda^3} = \frac{|V_{td}|}{|V_{cb}|\lambda} = \frac{1.10}{A\sqrt{S_0(x_t)}} = 0.85 \pm 0.14.$$

Here, use is made of the parameters presented⁵ in Tables 1, 2, and 5.

The uncertainty in R_t is mainly due to the error in calculating the parameter $f_d \sqrt{\hat{B}_d}$ in lattice QCD. The corresponding circle of radius R_t determines the possible position of the vertex of the unitary triangle in the $(\bar{\rho}, \bar{\eta})$ -plane; see Figs 4 and 5. Since the elements of the matrix V_{CKM} , the mixing parameters, and other quantities are continuously being corrected, it is convenient to rewrite Eqn (86) in a somewhat different form

$$|V_{td}| = 7.8 \times 10^{-3} \frac{226 \text{ MeV}}{f_d \sqrt{\hat{B}_d}} \left(\frac{\Delta M_d}{0.489 \text{ ps}^{-1}} \right)^{1/2} \\ \times \left(\frac{0.55}{\eta_B} \right)^{1/2} \left(\frac{2.38}{S_0(x_t)} \right)^{1/2}, \quad (87)$$

$$R_t = 0.85 \frac{|V_{td}|}{7.8 \times 10^{-3}} \left(\frac{0.0412}{|V_{cb}|} \right) \left(\frac{0.222}{\lambda} \right).$$

The data for ε_K [hyperbola (70) in the $(\bar{\rho}, \bar{\eta})$ -plane] and the results derived from determination of R_t from measurement of ΔM_d [see Eqn (86)] permit us to find the value of $\sin 2\beta$ for the unitary triangle, albeit with a large uncertainty. Indeed, from Eqns (31), (79), and (86) we have

$$\sin 2\beta = \frac{2\bar{\eta}(1 - \bar{\rho})}{(1 - \bar{\rho})^2 + \bar{\eta}^2} = \frac{2\bar{\eta}(1 - \bar{\rho})}{R_t^2}, \\ \bar{\eta}(1 - \bar{\rho}) = \left[\frac{0.205}{A^2 \hat{B}_K} - \bar{\eta} P_c(\varepsilon_K) \right] \frac{1}{A^2 S_0(x_t) \eta_{tt}}, \\ R_t^2 = \frac{1.20}{A^2 S_0(x_t)}.$$

Hence follows

$$\sin 2\beta = \frac{1.66}{\eta_{tt}} \left[\frac{0.205}{A^2 \hat{B}_K} - \bar{\eta} P_c(\varepsilon_K) \right] = 0.75 \pm 0.29. \quad (88)$$

The accuracy of determining R_t will probably be enhanced significantly when the ratio $\Delta M_d/\Delta M_s$ is measured. From Eqn (84) it follows that

$$\frac{\Delta M_d}{\Delta M_s} = \frac{M_d}{M_s} \left| \frac{V_{td}}{V_{ts}} \right|^2 \frac{f_d^2 \hat{B}_d}{f_s^2 \hat{B}_s} = \frac{M_d}{M_s} \frac{1}{\xi^2} \left| \frac{V_{td}}{V_{ts}} \right|^2 \\ \simeq \frac{M_d}{M_s} \frac{1}{\xi^2} \frac{\lambda^2 R_t^2}{1 + \lambda^2 (2\bar{\rho} - 1)}. \quad (89)$$

⁵ In Table 5, a somewhat more precise value of $|V_{td}| = (7.8 \pm 0.9) \times 10^{-3}$ is shown, which resulted from a complete fit of the universal triangle (see data in Fig. 5b).

Here, the following relationships are valid:

$$\begin{aligned} \left| \frac{V_{td}}{V_{ts}} \right|^2 &= \frac{(A\lambda^3)^2 [(1-\bar{\rho})^2 + \bar{\eta}^2]}{(A\lambda^2)^2 [(1-\lambda^2/2 + \lambda^2\bar{\rho})^2 + \lambda^4\bar{\eta}^2]} \\ &\simeq \frac{\lambda^2 R_t^2}{1 + \lambda^2(2\bar{\rho} - 1)}, \\ \left| \frac{V_{td}}{V_{ts}} \right| &= \frac{\lambda R_t}{1 + (\lambda^2/2)(2\bar{\rho} - 1)}, \\ R_t &= \frac{\xi}{\lambda} \left(\frac{\Delta M_d}{\Delta M_s} \right)^{1/2} \left(\frac{M_s}{M_d} \right)^{1/2} \left[1 + \frac{\lambda^2}{2} (2\bar{\rho} - 1) \right] \\ &\simeq \frac{\xi}{\lambda} \left(\frac{\Delta M_d}{\Delta M_s} \right)^{1/2} \left(\frac{M_s}{M_d} \right)^{1/2}. \end{aligned} \quad (90)$$

In principle, the ratio $\xi = f_s \sqrt{\hat{B}_s} / f_d \sqrt{\hat{B}_d}$, due to SU(3) violation in processes of $(B_{d,s}^0 \rightleftharpoons B_{d,s}^0)$ mixing, can be determined from lattice QCD calculations with an essentially higher accuracy than the individual parameters $f_d \sqrt{\hat{B}_d}$ and $f_s \sqrt{\hat{B}_s}$. The calculated result for ξ usually referred to is $\xi = 1.16 \pm 0.06$. However, recently it has been revealed that the quantity ξ contains an additional theoretical error, which was hitherto not taken into account accurately enough. Indeed, in this ratio there occurs, to a certain extent, compensation of statistical errors and of uncertainties related to taking into account the region of small distances (on the order of m_B^{-1}) and of intermediate distances [on the order of $A_{\text{QCD}}^{-1} \simeq (250 \text{ MeV})^{-1}$]. But, for the quantity ξ , an essential role is played by uncertainties in the region of large distances. These uncertainties are related to the difference in mass between the light quarks: $m_s \simeq 100 \text{ MeV}$ and $m_d \simeq 2.5\text{--}5.5 \text{ MeV}$ in B_s^0 - and B_d^0 -mesons, respectively.

The mass range of light quarks, in which it has been possible till now to carry out lattice QCD calculations, lies within the limits $(1/2)m_s \lesssim m_q \lesssim (3/2)m_s$. In this region, the values of f_{B_q} and \hat{B}_{B_q} depend linearly upon m_q . This linear dependence was applied without sufficient grounds for extrapolation to the mass m_d , which led to the previous value $\xi = 1.16 \pm 0.06$. As is shown in Ref. [100], nonlinear effects may noticeably influence the value of ξ . Therefore, the uncertainty in ξ was increased ($\xi = 1.16_{-0.06}^{+0.13}$) in Refs [97, 99], just for estimation, but, apparently, this also turned out to be insufficient.

In Ref. [101], logarithmic chiral extrapolation based on CHPT calculations was applied for finding ξ . It turned out that logarithmic extrapolation significantly enhanced the value of ξ (Fig. 6a), which amounted to $\xi = 1.32 \pm 0.10$ [101]. In other studies [102, 103] taking into account logarithmic extrapolation, somewhat lower values were obtained for ξ (they are given in Table 5). At present, the existing uncertainty in determining ξ noticeably influences the evaluation of parameters of the unitary triangle (Fig. 6b). One can hope that this problem will be resolved by further development of the technique of lattice QCD calculations. A brief description of the existing difficulties in these calculations and of the prospects for essential enhancement of the precision in some of them is provided in Section 4.5.

At present, only the lower limit has been established experimentally for the mass difference: $\Delta M_s > 14.4 \text{ ps}^{-1}$, or $\Delta M_d / \Delta M_s < 0.035$ (95% C.L.). Then, from Eqn (90) and the

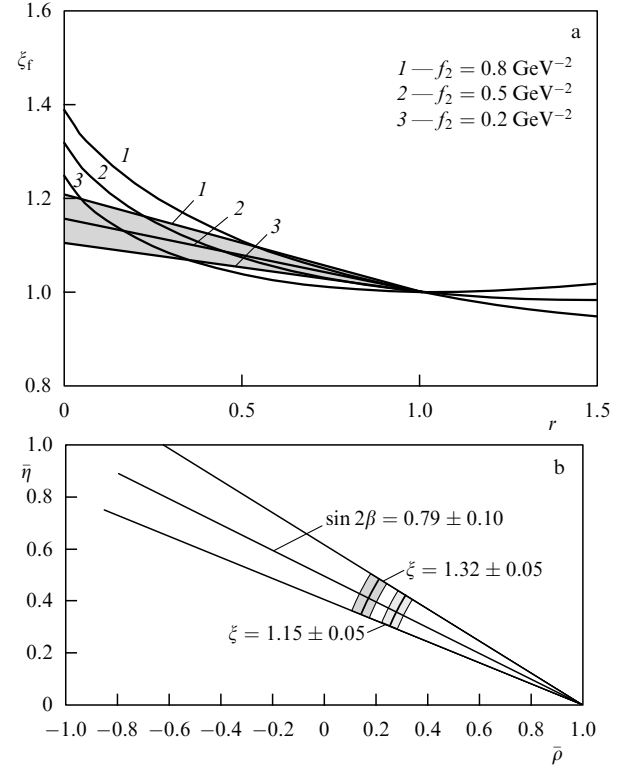


Figure 6. Chiral logarithmic extrapolation for the SU(3)-violation parameter ξ in the case of $B_{d,s}^0$ mixing [101]. (a) Influence of the chiral logarithmic extrapolation in $r = m_q/m_s$ to the mass m_d of the light quark on the quantity ξ . The following notation is used: $\xi = (f_s/f_d)\sqrt{\hat{B}_s}/\sqrt{\hat{B}_d} = \xi_r \xi_B$ (ξ_r depends strongly on the extrapolation procedure, and ξ_B depends weakly), f_2 represents the values of the low-energy constant in CHPT. Chiral logarithmic extrapolation results in the values of $\xi_r = 1.32 \pm 0.08$ and $\xi = 1.32 \pm 0.10$. The straight lines show the linear extrapolation resulting in $\xi_r = 1.15 \pm 0.05$. (b) Influence of the variation in ξ on the determination of the parameters $\bar{\rho}$ and $\bar{\eta}$ of the unitary triangle (and $R_t = [(1-\bar{\rho})^2 + \bar{\eta}^2]^{1/2}$). Calculations were carried out for $\sin 2\beta = 0.79 \pm 0.10$, $\Delta M_s = 20 \text{ ps}^{-1}$, $\xi = 1.32 \pm 0.05$ and $\xi = 1.15 \pm 0.05$.

two values of $\xi = 1.16$ and $\xi = 1.32$, it is possible to find the upper limits for R_t and $|V_{td}|$:

$$R_t \simeq \left(\frac{\Delta M_d}{\Delta M_s} \right)^{1/2} \left(\frac{M_s}{M_d} \right)^{1/2} \xi \frac{1}{\lambda} < 0.99 \quad (1.12),$$

$$\left| \frac{V_{td}}{V_{ts}} \right| < 0.22 \quad (0.25), \quad (91)$$

$$|V_{td}| < 8.9 \times 10^{-3} \quad (10.2 \times 10^{-3}).$$

The upper limit for R_t in formula (91) can also be represented as

$$R_t = 0.99 \left(\frac{\Delta M_d / \Delta M_s}{0.035} \right)^{1/2} \left(\frac{\xi}{1.16} \right) \left(\frac{0.222}{\lambda} \right).$$

In the coming years, the difference in mass ΔM_s is to be measured with an accuracy of approximately 1% in experiments using the installations D0 and CDF at the Fermilab collider. It is also very important to develop the theory of lattice QCD calculations so as to clarify the value of ξ .

4.4 Violation of CP invariance

and the measurement of asymmetry

in the decays $B_d^0 \rightarrow (J/\psi)K_S^0$ and $\bar{B}_d^0 \rightarrow (J/\psi)K_S^0$

Let us consider the decays $B_d^0 \rightarrow (J/\psi)K_S^0$ and $\bar{B}_d^0 \rightarrow (J/\psi)K_S^0$, i.e., decays to a state with definite CP parity:

$$\begin{aligned} \eta_{CP}((J/\psi)K_S^0) &= \eta_{CP}(J/\psi) \eta_{CP}(K_S^0) \cdot (-1)^L \\ &= (+1) \cdot (+1) \cdot (-1) = -1. \end{aligned}$$

Since J/ψ is a vector meson with $J^{PC} = 1^{--}$, $|K_S^0\rangle \simeq |K_1^0\rangle$ is a CP-even pseudoscalar state, and B_d^0 is a pseudoscalar meson, it is easy to verify that J/ψ and K_S^0 are in a state with orbital momentum $L = 1$. The decays $B_d^0 \rightarrow (J/\psi)K_S^0$ and $\bar{B}_d^0 \rightarrow (J/\psi)K_S^0$ are due to transitions $b \rightarrow c\bar{c}s$ and $\bar{b} \rightarrow c\bar{c}\bar{s}$, in which the dominant role is played by tree amplitudes, while the contribution of penguin amplitudes is very small (see diagrams in Fig. 3f). These processes are discussed in detail in Refs [7, 30–34, 44, 45, 47].

As has been shown in Section 3.3, the processes examined are determined by interference between the amplitude of direct decay to a final state of definite CP parity and the amplitude of a mixing process and subsequent decay to the same final state. These processes are characterized by the parameter [see formula (67)]

$$\lambda_{\psi K} = \frac{q}{p} \frac{\bar{A}}{A},$$

where

$$A = \langle (J/\psi)K_S^0 | H | B_d^0 \rangle, \quad \bar{A} = \langle (J/\psi)K_S^0 | H | \bar{B}_d^0 \rangle.$$

Violations of CP invariance occur, if $\lambda_{\psi K} \neq 1$ and $\text{Im } \lambda_{\psi K} \neq 0$, although here it is possible that $|q/p| \simeq 1$, $|\bar{A}/A| \simeq 1$ and $|\lambda_{\psi K}| \simeq 1$ (precisely this case is dealt with below). Violation of CP symmetry is manifested in the asymmetry (66):

$$a_{\psi K} = \frac{\Gamma(\bar{B}_d^0 \rightarrow (J/\psi)K_S^0) - \Gamma(B_d^0 \rightarrow (J/\psi)K_S^0)}{\Gamma(\bar{B}_d^0 \rightarrow (J/\psi)K_S^0) + \Gamma(B_d^0 \rightarrow (J/\psi)K_S^0)} \neq 0. \quad (92)$$

We recall the expressions for the time dependence of the states $B_d^0(t)$ and $\bar{B}_d^0(t)$, presented in Table 3:

$$\begin{aligned} B_d^0(t) &= \exp(-iM_d t) \exp\left(-\frac{1}{2} \Gamma_B t\right) \\ &\quad \times \left[|B_d^0\rangle \cos \frac{\Delta M_d t}{2} + i \frac{q}{p} |\bar{B}_d^0\rangle \sin \frac{\Delta M_d t}{2} \right], \\ \bar{B}_d^0(t) &= \exp(-iM_d t) \exp\left(-\frac{1}{2} \Gamma_B t\right) \\ &\quad \times \left[|\bar{B}_d^0\rangle \cos \frac{\Delta M_d t}{2} + i \frac{p}{q} |B_d^0\rangle \sin \frac{\Delta M_d t}{2} \right]. \end{aligned}$$

Hence, it is possible to obtain the decay widths

$$\begin{aligned} \Gamma[\bar{B}_d^0(t) \rightarrow (J/\psi)K_S^0] &\propto \left| \bar{A} \cos \frac{\Delta M_d t}{2} + i \frac{p}{q} A \sin \frac{\Delta M_d t}{2} \right|^2 \\ &= \left[\cos \frac{\Delta M_d t}{2} + i \frac{1}{\lambda_{\psi K}} \sin \frac{\Delta M_d t}{2} \right]^2 |\bar{A}|^2 \\ &= \left| \lambda_{\psi K} \cos \frac{\Delta M_d t}{2} + i \sin \frac{\Delta M_d t}{2} \right|^2 \frac{|\bar{A}|^2}{|\lambda_{\psi K}|^2} \end{aligned}$$

$$\begin{aligned} &\simeq \left| \lambda_{\psi K} \cos \frac{\Delta M_d t}{2} + i \sin \frac{\Delta M_d t}{2} \right|^2 |A|^2 \\ &= \left[\left(\text{Re } \lambda_{\psi K} \cos \frac{\Delta M_d t}{2} \right)^2 \right. \\ &\quad \left. + \left(\text{Im } \lambda_{\psi K} \cos \frac{\Delta M_d t}{2} + \sin \frac{\Delta M_d t}{2} \right)^2 \right] |A|^2 \\ &= \left[|\lambda_{\psi K}|^2 \cos^2 \frac{\Delta M_d t}{2} + \sin^2 \frac{\Delta M_d t}{2} \right. \\ &\quad \left. + \text{Im } \lambda_{\psi K} \sin(\Delta M_d t) \right] |A|^2, \end{aligned}$$

$$\begin{aligned} \Gamma[B_d^0(t) \rightarrow (J/\psi)K_S^0] &\propto \left| A \cos \frac{\Delta M_d t}{2} + i \frac{q}{p} \bar{A} \sin \frac{\Delta M_d t}{2} \right|^2 \\ &= \left| \cos \frac{\Delta M_d t}{2} + i \lambda_{\psi K} \sin \frac{\Delta M_d t}{2} \right|^2 |A|^2 \\ &= \left[\left(\cos \frac{\Delta M_d t}{2} - \text{Im } \lambda_{\psi K} \sin \frac{\Delta M_d t}{2} \right)^2 \right. \\ &\quad \left. + \left(\text{Re } \lambda_{\psi K} \sin \frac{\Delta M_d t}{2} \right)^2 \right] |A|^2 \\ &= \left[\cos^2 \frac{\Delta M_d t}{2} + |\lambda_{\psi K}|^2 \sin^2 \frac{\Delta M_d t}{2} \right. \\ &\quad \left. - \text{Im } \lambda_{\psi K} \sin(\Delta M_d t) \right] |A|^2, \end{aligned}$$

as well as their difference and their sum:

$$\begin{aligned} \Gamma[\bar{B}_d^0(t) \rightarrow (J/\psi)K_S^0] - \Gamma[B_d^0(t) \rightarrow (J/\psi)K_S^0] &\propto |A|^2 \left[(|\lambda_{\psi K}|^2 - 1) \cos^2 \frac{\Delta M_d t}{2} \right. \\ &\quad \left. + (1 - |\lambda_{\psi K}|^2) \sin^2 \frac{\Delta M_d t}{2} + 2 \text{Im } \lambda_{\psi K} \sin(\Delta M_d t) \right] \\ &= |A|^2 \left[-(1 - |\lambda_{\psi K}|^2) \left(\cos^2 \frac{\Delta M_d t}{2} - \sin^2 \frac{\Delta M_d t}{2} \right) \right. \\ &\quad \left. + 2 \text{Im } \lambda_{\psi K} \sin(\Delta M_d t) \right] \\ &= |A|^2 \left[-(1 - |\lambda_{\psi K}|^2) \cos(\Delta M_d t) + 2 \text{Im } \lambda_{\psi K} \sin(\Delta M_d t) \right], \\ \Gamma[\bar{B}_d^0(t) \rightarrow (J/\psi)K_S^0] + \Gamma[B_d^0(t) \rightarrow (J/\psi)K_S^0] &\propto |A|^2 \left[(1 + |\lambda_{\psi K}|^2) \left(\cos^2 \frac{\Delta M_d t}{2} + \sin^2 \frac{\Delta M_d t}{2} \right) \right] \\ &= |A|^2 [1 + |\lambda_{\psi K}|^2]. \end{aligned}$$

Therefore, the asymmetry in the decays $B_d^0(\bar{B}_d^0) \rightarrow (J/\psi)K_S^0$ is defined by the expression

$$\begin{aligned} a_{\psi K}(t) &= \frac{\Gamma(\bar{B}_d^0 \rightarrow (J/\psi)K_S^0) - \Gamma(B_d^0 \rightarrow (J/\psi)K_S^0)}{\Gamma(\bar{B}_d^0 \rightarrow (J/\psi)K_S^0) + \Gamma(B_d^0 \rightarrow (J/\psi)K_S^0)} \\ &= \frac{-(1 - |\lambda_{\psi K}|^2) \cos(\Delta M_d t) + 2 \text{Im } \lambda_{\psi K} \sin(\Delta M_d t)}{1 + |\lambda_{\psi K}|^2} \\ &= -\frac{1 - |\lambda_{\psi K}|^2}{1 + |\lambda_{\psi K}|^2} \cos(\Delta M_d t) + \frac{2 \text{Im } \lambda_{\psi K}}{1 + |\lambda_{\psi K}|^2} \sin(\Delta M_d t). \end{aligned} \quad (93)$$

As will be shown below, the experimental data suggest that the condition $|\lambda_{\psi K}| = 1$ is satisfied with a very high precision and Eqn (93) transforms into the relation

$$a_{\psi K}(t) = \text{Im } \lambda_{\psi K} \sin(\Delta M_d t). \quad (94)$$

In this case, the decay asymmetry is determined by a single weak-interaction phase, while the hadron corrections and uncertainties turn out to be very small, which makes possible a quite accurate quantitative test of the SM predictions for the violation of CP invariance in B_d^0 - and \bar{B}_d^0 -decays.

It is evident that relation (93) is readily generalized to the asymmetry of any rare decays $B_d^0(\bar{B}_d^0) \rightarrow f_{CP}$, where f_{CP} is a state with definite CP parity. The asymmetry coefficient $a_{f_{CP}}$ for these decays has the form

$$a_{f_{CP}}(t) = -\frac{1 - |\lambda_{f_{CP}}|^2}{1 + |\lambda_{f_{CP}}|^2} \cos(\Delta M_d t) + \frac{2 \text{Im } \lambda_{f_{CP}}}{1 + |\lambda_{f_{CP}}|^2} \sin(\Delta M_d t).$$

From the discussion in Section 3.4 it follows that

$$\lambda_{\psi K} = \lambda_{(J/\psi)K_S^0} = \left(\frac{q}{p}\right)_B \frac{\bar{A}((J/\psi)K_S^0)}{A((J/\psi)K_S^0)}. \quad (95)$$

In the decays of B^0 - and \bar{B}^0 -mesons, the states $K^0(\bar{b} \rightarrow \bar{s}c\bar{c})$ and $\bar{K}^0(b \rightarrow sc\bar{c})$ are produced. The production of K_S^0 -mesons in the final state proceeds via $(K^0 \rightleftharpoons \bar{K}^0)$ mixing. Since it follows from the data of Table 3 that

$$|K_0\rangle = \frac{|K_S^0\rangle + |K_L^0\rangle}{2p}, \quad |\bar{K}_0\rangle = \frac{|K_S^0\rangle - |K_L^0\rangle}{2q},$$

then one finds

$$|\bar{B}^0\rangle \rightarrow |\bar{K}^0\rangle + c\bar{c} \rightarrow \frac{|K_S^0\rangle}{2q} + c\bar{c},$$

$$|B^0\rangle \rightarrow |K^0\rangle + c\bar{c} \rightarrow \frac{|K_S^0\rangle}{2p} + c\bar{c}.$$

Therefore, the ratio of the respective amplitudes in Eqn (95) is determined by the expression

$$\begin{aligned} \frac{\bar{A}((J/\psi)K_S^0)}{A((J/\psi)K_S^0)} &= \eta_{\psi K_S^0} \left(\frac{p}{q}\right)_K \frac{\bar{A}(\bar{B}^0 \rightarrow c\bar{c}\bar{K}^0)}{A(B^0 \rightarrow c\bar{c}K^0)} \\ &= \eta_{\psi K_S^0} \left(\frac{p}{q}\right)_K \frac{\bar{A}(b \rightarrow c\bar{c}s)}{A(\bar{b} \rightarrow c\bar{c}\bar{s})}, \end{aligned}$$

and the CP-violation parameter in the decay $B_d^0(\bar{B}_d^0) \rightarrow (J/\psi)K_S^0$ takes the form

$$\begin{aligned} \lambda_{(J/\psi)K_S^0} &= \eta_{\psi K_S^0} \left(\frac{q}{p}\right)_B \left(\frac{p}{q}\right)_K \frac{\bar{A}(b \rightarrow c\bar{c}s)}{A(\bar{b} \rightarrow c\bar{c}\bar{s})} \\ &= -\left(\frac{V_{tb}^* V_{td}}{V_{tb} V_{td}^*}\right) \left(\frac{V_{cd}^* V_{cs}}{V_{cd} V_{cs}^*}\right) \left(\frac{V_{cb} V_{cs}^*}{V_{cb}^* V_{cs}}\right) \\ &= -\left(\frac{V_{tb}^* V_{td}}{V_{tb} V_{td}^*}\right) \underbrace{\left(\frac{V_{cd}^* V_{cb}}{V_{cd} V_{cb}^*}\right)}_{\simeq 1} \simeq -\frac{V_{tb}^* V_{td}}{V_{tb} V_{td}^*}. \quad (96) \end{aligned}$$

Here, the following notation is used:

$$\begin{aligned} \left(\frac{q}{p}\right)_B &\simeq -\left(\frac{M_{12}^*}{M_{12}}\right)_B = -\frac{(V_{tb}^* V_{td})^2}{|V_{tb} V_{td}^*|^2} \\ &= -\frac{(V_{tb}^* V_{td})(V_{tb}^* V_{td})}{(V_{td} V_{tb}^*)(V_{td} V_{tb}^*)} = -\frac{V_{td} V_{tb}^*}{V_{td}^* V_{tb}}, \\ \left(\frac{p}{q}\right)_K &\simeq -\frac{V_{cs} V_{cd}^*}{V_{cs}^* V_{cd}} \simeq -1 \end{aligned}$$

(as compared with the preceding formula for $(q/p)_K$, the substitution $b \rightarrow s$ and $t \rightarrow c$ has been made, since, in the corresponding box diagram for $(K^0 \rightleftharpoons \bar{K}^0)$ mixing, a special role is played by virtual c-quarks, but not t-quarks, as in $(B^0 \rightleftharpoons \bar{B}^0)$ mixing; see, for example, Refs [1, 2]), and also

$$\frac{\bar{A}(b \rightarrow c\bar{c}s)}{A(\bar{b} \rightarrow c\bar{c}\bar{s})} = \frac{V_{cb} V_{cs}^*}{V_{cb}^* V_{cs}},$$

$$\frac{V_{cb} V_{cd}^*}{V_{cb}^* V_{cd}} \simeq 1,$$

$$\eta_{\psi K_S^0} = -1$$

is the CP parity of the $(J/\psi)K_S^0$ -system in the state $L = 1$, i.e., with total spin equal to zero (B-meson), and finally

$$V_{cb} = A\lambda^2 = V_{cb}^*, \quad V_{cd} = -\lambda = V_{cd}^*$$

(see Table 1).

The dependences of the amplitudes on the elements of the V_{CKM} matrix are determined by the rules outlined in Figs 1 and 3e and in the captions to these figures. As one can see from Fig. 2, for the unitary triangle, the vector $\vec{A}\vec{B}$ in the $(\bar{\rho}, \bar{\eta})$ -plane is determined as $V_{tb}^* V_{td} = |\mathbf{c}| \exp(-i\beta)$. Then, we ultimately obtain the following relationships from Eqns (94) and (96):

$$\begin{aligned} \lambda_{(J/\psi)K_S^0} &= -\frac{|\mathbf{c}| \exp(-i\beta)}{|\mathbf{c}| \exp(i\beta)} = -\exp(-i2\beta) \\ &= -\cos 2\beta + i \sin 2\beta, \end{aligned}$$

$$\text{Im } \lambda_{(J/\psi)K_S^0} = \sin 2\beta, \quad (97)$$

$$a_{\psi K}(t) = \text{Im } \lambda_{(J/\psi)K_S^0} \sin(\Delta M_d t) = \sin 2\beta \sin(\Delta M_d t).$$

Thus, in the SM, the time-independent asymmetry in the decays $B_d^0(\bar{B}_d^0) \rightarrow (J/\psi)K_S^0$ has the form

$$a_{\psi K} = \text{Im } \lambda_{(J/\psi)K_S^0} = \sin 2\beta, \quad (98)$$

and its measurement permits us to determine the parameter $\sin 2\beta$ of the unitary triangle, and the result obtained is practically independent of hadron corrections related to taking into account the penguin diagrams. The angle 2β is determined by the relative phase between the amplitudes of $(B^0 \rightleftharpoons \bar{B}^0)$ mixing and the tree B^0 -decay. It must be emphasized that the latter assertion and formula (98) take place only in the SM. In the general case (accounting for NP effects), this phase changes, so that

$$\phi_d = \phi_d^{\text{CM}} + \phi_d^{\text{NP}} = 2\beta + \phi_d^{\text{NP}}.$$

Then formula (98) can be rewritten as

$$a_{\psi K} = \text{Im } \lambda_{(J/\psi)K_S^0} = \sin \phi_d = \sin(2\beta + \phi_d^{\text{NP}}).$$

The data for $a_{\psi K}$, obtained in experiments at the B-factories⁶ BaBar and Belle, as well as the first results achieved at the $\bar{p}p$ collider with the installation CDF are the following [104]:

$$a_{\psi K} = \begin{cases} 0.79_{-0.44}^{+0.41} \text{ (CDF)}, \\ 0.741 \pm 0.067 \pm 0.033 = 0.741 \pm 0.075 \text{ (BaBar)}, \\ 0.719 \pm 0.074 \pm 0.035 = 0.719 \pm 0.082 \text{ (Belle)}. \end{cases}$$

The weighted mean value of asymmetry (taking into account the previous data from OPAL and ALEPH) amounts to

$$\langle \text{Im } \lambda_{(J/\psi)K_S^0} \rangle = \langle a_{\psi K} \rangle = (\sin 2\beta)_{\text{SM, expt}} = 0.734 \pm 0.054. \quad (99)$$

The data of BaBar and Belle yield the parameter

$$|\lambda_{\psi K}| = 0.949 \pm 0.039,$$

which is indeed close to unity. As is shown in Ref. [30], the data of other independent measurements permit us to significantly enhance the accuracy of this assertion. In asymmetry measurements in semileptonic decays of B_d^0 -mesons, the following relationship holds true:

$$a_{\text{SL}} = \frac{\Gamma(\bar{B}_d^0 \rightarrow 1^+ X) - \Gamma(B_d^0 \rightarrow 1^- X)}{\Gamma(\bar{B}_d^0 \rightarrow 1^+ X) + \Gamma(B_d^0 \rightarrow 1^- X)} = \frac{1 - |q/p|^4}{1 + |q/p|^4};$$

it has been shown that

$$a_{\text{SL}} = 0.002 \pm 0.014, \quad \left| \frac{q}{p} \right| = 0.999 \pm 0.007.$$

From data on CP asymmetry in the decays of charged B_{\mp} -mesons, we have

$$\begin{aligned} a_{\psi K} &= \frac{\Gamma(B^- \rightarrow (J/\psi)K^-) - \Gamma(B^+ \rightarrow (J/\psi)K^+)}{\Gamma(B^- \rightarrow (J/\psi)K^-) + \Gamma(B^+ \rightarrow (J/\psi)K^+)} \\ &= \frac{|\bar{A}_{\psi K}/A_{\psi K}|^2 - 1}{|\bar{A}_{\psi K}/A_{\psi K}|^2 + 1} = 0.008 \pm 0.025, \end{aligned}$$

or

$$\left| \frac{\bar{A}_{\psi K}}{A_{\psi K}} \right| = 1.008 \pm 0.025.$$

Combining these data one can obtain

$$|\lambda_{\psi K}| = \left| \frac{q}{p} \right| \left| \frac{\bar{A}_{\psi K}}{A_{\psi K}} \right| = 1.007 \pm 0.025,$$

i.e., the relation $|\lambda_{\psi K}| = 1$, which was used earlier in analyzing the decays $B_d^0(\bar{B}_d^0) \rightarrow (J/\psi)K_S^0$ [see Eqn (94)], is satisfied with very good accuracy.

Thus, the determination of $(\sin 2\beta)_{\text{SM, expt}}$ from the CP-asymmetry $a_{\psi K}$ contains no uncertainties related to the influence of strong interactions, and can subsequently be made several times better.

⁶ The values for $\sin 2\beta$, obtained in the experiments BaBar and Belle, are based on the measurement of asymmetry not only in the decays $B^0(\bar{B}^0) \rightarrow (J/\psi)K_S^0$, but also in decays involving the production of other states of charmonium together with K_S^0 - and K_L^0 -mesons.

In fitting the parameters of the unitary triangle (27) within the framework of the SM, the prediction was made for $(\sin 2\beta)_{\text{SM}} = 0.59-0.88$, which is in good agreement with experimental data. New studies permit us to narrow this interval down to $(\sin 2\beta)_{\text{SM}} = 0.66-0.77$ [29, 48]. This is the first quite accurate test of the mechanism of CP-symmetry breaking within the SM. The good agreement between experimental data and SM theoretical predictions shows that the mechanism of CP violation, related to the complex character of the V_{CKM} matrix, plays an essential, maybe even dominant, role in the violation of CP symmetry in flavor changing processes at not too high energies.

We note that precise data concerning the quantitative test of CP nonconservation have only been obtained in a sole process, so one should not be too hasty in making more broad predictions, since the existing accuracy leaves sufficient room for the contribution of additional mechanisms of CP violation, related to NP. In this connection, the prospects of other experiments with B-decays may also turn out to be quite promising. One must also bear in mind that the preliminary data on asymmetry in the decays $B_d^0(\bar{B}_d^0) \rightarrow \pi^+\pi^-$, $B_d^0(\bar{B}_d^0) \rightarrow \phi K_S^0$, and $B_d^\pm \rightarrow \pi^\pm K_S^0$, obtained in experiments at Belle, point to possible manifestations of new significant effects of CP violation in B-physics (the statistical error of these results is still too high, and they have not been confirmed by measurements at BaBar).

It is also necessary to note that the data on $a_{\psi K}$ (see Fig. 5) yield a double solution for the angle β in the upper $(\bar{\eta}, \bar{\rho})$ -semiplane. From $\sin 2\beta = 0.734 \pm 0.054$ it follows that the angle β may lie in the region $21.5^\circ < \beta < 26^\circ$ or in the region $64^\circ < \beta < 67^\circ$, since $\sin 2\beta = \sin(\pi - 2\beta)$. The first solution is preferable, since it alone is consistent with the data on $|V_{ub}/V_{cb}|$ in the SM. However, new physical effects may also lead to the second solution. Therefore, it is important to carry out independent measurements of the sign of $\cos 2\beta$, so as to remove this ambiguity (for the first solution $\cos 2\beta = +0.7$, and for the second solution $\cos 2\beta = -0.7$). Such measurements are quite complicated, but they are already under way [48]. We shall again deal with the two-valued property for the angle β in Section 6.2.

An essential role in searches for NP effects may also be played by independent measurements of the angle γ which is more sensitive to searches for new effects than the angle β . Data on the angle γ can, for example, be obtained from measurements of $\Delta M_s/\Delta M_d$ at a fixed value of β (see Ref. [28]).

Measurements at the Belle and BaBar installations are developing rapidly and successfully. In the nearest future new results in B-physics are to be expected also from the installations D0 and CDF at the Fermilab collider, and, subsequently, from the collider B-meson superfactories LHCb (CERN) and BTeV (Fermilab) [44]. Therefore, studies of processes involving violation of CP invariance and searches for NP in B-decays are, at present, entering a new, very promising phase. At the same time, new experiments with K-mesons, which will permit us to carry out independent measurements of the parameters of the unitary triangle and realize very sensitive tests of the SM, may turn out to be very perspective. Of particular interest are future measurements of $\sin 2\beta$ and of other parameters in high-precision experiments with K-mesons, in which super-rare decays $K^+ \rightarrow \pi^+ \nu \bar{\nu}$ and $K_L^0 \rightarrow \pi^0 \nu \bar{\nu}$ and other close processes will be studied (see Section 5).

The results of determining the parameters of the unitary triangle from data of different experiments and their consistency with each other are analyzed in detail in Ref. [48] (see, also, Ref. [30], where the prospects of future experiments with B-mesons are discussed).

4.5 Prospects for further investigation of the parameters of the unitary triangle

We shall now briefly consider the further prospects of determining with greater accuracy the elements of the quark mixing matrix V_{CKM} and the parameters of the unitary triangle (27). Since the existing accuracies are to a great extent determined by theoretical uncertainties, progress in this field depends essentially on the development of theoretical methods and, first and foremost, on the improvement of the technique of lattice QCD calculations.

In recent years, significant progress has been made in understanding the existing problems in this field and in the development of the corresponding computational methods. It is to be expected that the next generation of lattice QCD calculations will permit the researchers to achieve the accuracy in many theoretical estimates that will be greater by several fold, and this will be related not only to enhancements in the power of supercomputers used for lattice calculations, but even more to the development of computational methods [99, 101, 103, 105].

Until now, mostly quenched lattice QCD calculations were performed, in which the processes of virtual quark pair production were not introduced directly. This led to badly controlled theoretical errors which amounted to 10–25%. At present, the first unquenched QCD calculations are being carried out taking into account polarization processes of the hadron vacuum. Table 6 presents the results of some quenched and unquenched calculations, for comparison. Hope is expressed that in the near future all calculations will be done in the unquenched approximation [101].

Table 6. Results of calculations of the decay constants for B- and D-mesons in the quenched and unquenched lattice QCD [99].

Decay constant	Quenched calculation, MeV	Unquenched calculation, MeV	Experimental value, MeV
f_B	173 ± 23	198 ± 30	—
f_{B_s}	200 ± 20	230 ± 30	—
f_D	203 ± 14	226 ± 15	—
f_{D_s}	230 ± 14	250 ± 30	280 ± 48
f_{B_s}/f_B	1.15 ± 0.03	1.16 ± 0.05	—
f_{D_s}/f_D	1.12 ± 0.02	1.12 ± 0.04	—

Development of the technique of lattice QCD calculations will closely interlace with the possibility of high-precision measurements of a number of quantities, which can be used as touchstones for elaborating improved computational methods and extending them to other processes. At present, a new program is being prepared at Cornell University (USA) for measurements in the physics of charmed mesons in experiments at intersecting e^+e^- storage rings at an energy of $\sqrt{s} = 3-5$ GeV (the collaboration CLEO-c at intersecting rings CESR-c [106]). In experiments at this $(c-\tau)$ -factory, detailed studies of the leptonic decays $D^- \rightarrow l^- \nu_l$, $D_s^- \rightarrow l^- \nu_l$ ($l = \mu, e$), $D_s^- \rightarrow \tau^- \nu_\tau$ and of similar decays of antiparticles are to be carried out, which will permit the determination of their

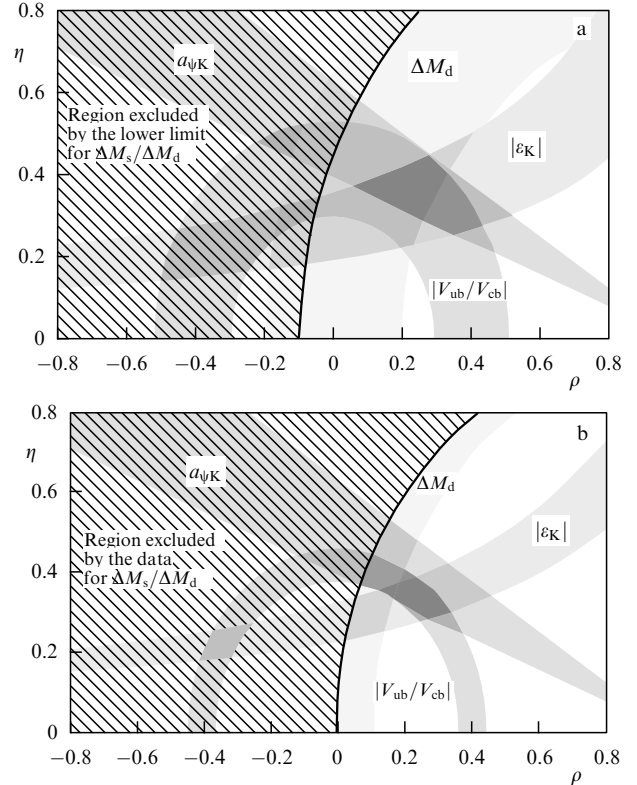


Figure 7. Expected enhancement in the accuracy of determining parameters of the unitary triangle, due to future measurements at B-factories, with the installation CLEO-c and, especially, due to progress in lattice QCD calculations connected to this experimental program [105]. (a) Present precision in determining parameters from the data on $|\epsilon_K|$, $|V_{ub}/V_{cb}|$, $B_{d,s}^0$ mixing and asymmetry $a_{\psi K}$. (b) Enhancement of accuracy expected during the nearest few years, which is to a significant extent due to the reduction of uncertainties in theoretical calculations (down to 2–3%).

branching ratios with an uncertainty of 3–4%, as well as the decay constants f_D and f_{D_s} with an uncertainty of 1.5–2%. Accurate data will also be obtained for the branching ratios and form factors of a series of semileptonic decays of charmed mesons. The branching ratios of the respective semileptonic and leptonic decays no longer depend on the matrix elements V_{CKM} and can be used for direct measurements of the form factors.

New data on f_D and f_{D_s} as well as on the form factors in the decays $D \rightarrow \pi l \nu_l$ and $D \rightarrow K l \nu_l$ will permit us to determine the matrix elements $|V_{cd}|$ and $|V_{cb}|$ with an accuracy of 1–1.5%. An important role in the test of the accuracies of QCD calculations will also be played by studies of the states of charmonium and beautionium.

It will be possible to successfully apply the theoretical methods, approved in high-precision experiments with D-mesons, in analyzing new improved data which will be obtained at the B-factories BaBar and Belle. Here, the expected error in determining the matrix elements $|V_{td}|$ and $|V_{ts}|$, obtained from the processes of $(B_{d,s}^0 \rightleftharpoons \bar{B}_{d,s}^0)$ mixing, will amount to 5%, while the error in measurements of $|V_{cb}|$ and $|V_{ub}|$ in decays of the tree type will, respectively, amount to 3 and 5%, or even less.

Enhancement of the accuracy in determining matrix elements and parameters of the unitary triangle can be illustrated with the aid of Fig. 7, in which existing data are compared with results expected during the nearest several

years. Further enhancement of the accuracy can be achieved in experiments at the hadron B-factories LHCb and BTeV [44]. The project Super BaBar, in which the luminosity of e^+e^- -collisions should be increased by two orders of magnitude, is also being discussed.

5. The decays $K^+ \rightarrow \pi^+ \nu \bar{\nu}$ and $K_L^0 \rightarrow \pi^0 \nu \bar{\nu}$

5.1 General considerations

The decays $K^+ \rightarrow \pi^+ \nu \bar{\nu}$ and $K_L^0 \rightarrow \pi^0 \nu \bar{\nu}$, represented by the diagrams in Fig. 8, play a special role among FCNC processes. They are sometimes called ‘golden decays’, since their probabilities can be predicted within the framework of the SM with a very great precision and depend weakly on theoretical assumptions. Let us point out some of the key aspects of these processes:

(1) The main contribution to the processes $K^+ \rightarrow \pi^+ \nu \bar{\nu}$ and $K_L^0 \rightarrow \pi^0 \nu \bar{\nu}$ are provided by the region of very small distances: $r \sim 1/m_t, 1/M_Z$. Therefore, it is possible to take into account quite accurately the strong interactions at a quark level within the framework of perturbative QCD in the leading logarithmic (LLA) and in the next in order to logarithmic (NLA) approximations. The new QCD calculations, which take into account approximations of higher orders, will permit the improvement of this accuracy even more.

(2) Passage from quark to hadron processes, as a rule, gives rise to difficulties in calculating matrix elements such as $\langle \pi | H_w | K \rangle_{\pi \nu \bar{\nu}}$, which require us to take into account the region of large distances. However, these difficulties can be avoided by applying an original ‘renormalization’ procedure which, within the framework of charge symmetry, allows us to relate the matrix element $\langle \pi | H_w | K \rangle_{\pi \nu \bar{\nu}}$ to the matrix element $\langle \pi | H_w | K \rangle_{\pi \nu e}$ for the well-studied semileptonic decay $K^+ \rightarrow \pi^0 e \nu_e$. Therefore, the ratio $\text{BR}(K \rightarrow \pi \nu \bar{\nu}) / \text{BR}(K^+ \rightarrow \pi^0 e \nu_e)$ depends very weakly on the uncertainties due to the consideration of hadron processes.

(3) Thus, within the framework of the SM, the decays $K \rightarrow \pi \nu \bar{\nu}$ are theoretically pure processes which can be calculated quite reliably and with good precision. The uncertainties in calculations of the $K^+ \rightarrow \pi^+ \nu \bar{\nu}$ -decay probability do not exceed 7% and are mainly due to the influence of the lighter c-quarks. One can hope that the accuracy of introducing the correction which takes into account the effect of c-quarks may be enhanced as the technique of QCD calculations develops. For the decay $K_L^0 \rightarrow \pi^0 \nu \bar{\nu}$, which is practically free from the influence of c-quarks (see below), the uncertainty in theoretical calculations does not exceed 1–2%.

(4) In the SM, the decays $K \rightarrow \pi \nu \bar{\nu}$ are strongly suppressed and are characterized by very small expected probabilities (not higher than 10^{-10}). This opens interesting prospects for searching the new effects going beyond the framework of the SM. The effective vertices $Z d \bar{s}$ of the diagrams shown in Fig. 8 are determined by the region of small distances: $r \sim 1/m_t, 1/M_Z$. Therefore, the decays $K \rightarrow \pi \nu \bar{\nu}$ turn out to be sensitive to the contribution from new heavy objects (for example, supersymmetric particles; see Fig. 8c) that are also manifested at small distances. Comparison of the results of experiments with reliable theoretical estimates within the framework of the SM permit us to search directly for manifestations of NP in the rare kaon decays.

5.2 The $K \rightarrow \pi \nu \bar{\nu}$ decays in the Standard Model

In the case of neutral and charged kaons, the decays $K \rightarrow \pi \nu \bar{\nu}$ have been considered comprehensively within the SM framework in numerous publications (see, for example, Refs [3, 5, 26–30, 32, 33, 35–37, 41, 42, 47] and references cited therein, as well as papers [55, 58, 107–119]).

As has been shown in Refs [107, 108] (see, also Refs [3, 32, 33, 35]), the decay $K_L^0 \rightarrow \pi^0 \nu \bar{\nu}$ is characterized by violation of CP invariance and is due to interference between the amplitude of the FCNC decay $s \rightarrow d \nu \bar{\nu}$ with direct CP violation and the amplitude of $(|K^0 \rangle \rightleftharpoons |\bar{K}^0 \rangle)$ mixing in which indirect CP violation takes place. Let us define the decay amplitudes

$$a = A(K^0 \rightarrow \pi^0 \nu \bar{\nu}), \quad (100)$$

$$\bar{a} = A(\bar{K}^0 \rightarrow \pi^0 \nu \bar{\nu}). \quad (101)$$

When the states $|K_{L,S}^0 \rangle = p|K^0 \rangle \mp q|\bar{K}^0 \rangle$ decay via the channel $\pi^0 \nu \bar{\nu}$, then the following relations hold valid for the amplitudes:

$$A(K_{L,S}^0 \rightarrow \pi^0 \nu \bar{\nu}) = pa \mp q\bar{a} = pa \left(1 \mp \frac{q}{p} \frac{\bar{a}}{a} \right) = pa(1 \mp \lambda_{\pi \nu \bar{\nu}}), \quad (102)$$

where, in accordance with formula (67), we put

$$\lambda_{\pi \nu \bar{\nu}} = \frac{q}{p} \frac{\bar{a}}{a}. \quad (103)$$

It follows from expression (59) that

$$\left| \frac{q}{p} \right| = \left| \frac{1-\varepsilon}{1+\varepsilon} \right| \simeq 1 - 2\text{Re}\varepsilon = 1 + O(10^{-3}),$$

and with an even greater accuracy we have for the ratio of the absolute values of the amplitudes: $|\bar{a}/a| = 1$. (The quantity

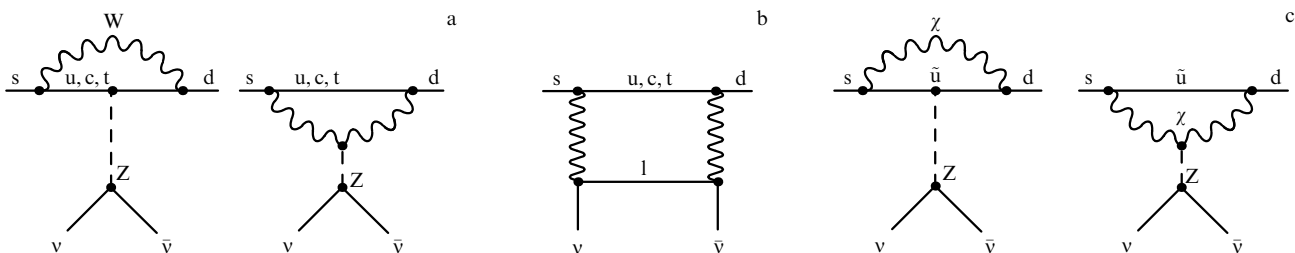


Figure 8. Loop diagrams for the FCNC processes $s \rightarrow d \nu \bar{\nu}$: (a) penguin diagrams; (b) box diagram, and (c) diagrams for the possible contribution of supersymmetric particles to the $Z d \bar{s}$ vertex.

$|\bar{a}/a|$ can differ from unity only if in the final state there are two or more components with distinct scattering phases; in the case of $\pi^0\nu\bar{\nu}$, this is not so.) Therefore, the following estimate may be given:

$$|\lambda_{\pi\nu\bar{\nu}}| = \left| \frac{q}{p} \right| \left| \frac{\bar{a}}{a} \right| = 1 + O(10^{-3}),$$

so that

$$\lambda_{\pi\nu\bar{\nu}} = \exp(2i\vartheta). \quad (104)$$

Then, from Eqn (102) we obtain

$$\begin{aligned} \frac{\Gamma(K_L^0 \rightarrow \pi^0\nu\bar{\nu})}{\Gamma(K_S^0 \rightarrow \pi^0\nu\bar{\nu})} &= \left| \frac{pa - q\bar{a}}{pa + q\bar{a}} \right|^2 = \left| \frac{1 - \lambda_{\pi\nu\bar{\nu}}}{1 + \lambda_{\pi\nu\bar{\nu}}} \right|^2 \\ &= \frac{1 - 2\text{Re} \lambda_{\pi\nu\bar{\nu}} + |\lambda_{\pi\nu\bar{\nu}}|^2}{1 + 2\text{Re} \lambda_{\pi\nu\bar{\nu}} + |\lambda_{\pi\nu\bar{\nu}}|^2} = \frac{1 - \cos 2\vartheta}{1 + \cos 2\vartheta} = \tan^2 \vartheta. \end{aligned} \quad (105)$$

If CP invariance holds valid, then $a = \bar{a}$ and $\vartheta = 0$, i.e., in this limit the decay $K_L^0 \rightarrow \pi^0\nu\bar{\nu}$ is forbidden. Thus, it can only proceed via the mechanism of CP-invariance violation resulting from the interference between the amplitudes of ($K^0 \rightleftharpoons \bar{K}^0$) mixing and the direct decay $s \rightarrow d\nu\bar{\nu}$. The quantity ϑ in Eqns (104) and (105) represents the relative CP-violating phase between these two amplitudes.

It can also be shown directly that in the decays $K_L^0 \rightarrow \pi^0\nu\bar{\nu}$ CP invariance is violated. Indeed, the CP parity of the $|\pi^0\nu\bar{\nu}\rangle$ system is determined as $\text{CP}|\pi^0\nu\bar{\nu}\rangle = (-1)^L \text{CP}|\pi^0\rangle \text{CP}|\nu\bar{\nu}\rangle$, where L is the relative angular momentum of π^0 and $\nu\bar{\nu}$. Since K^0 and π^0 are spinless particles, then $L = J$ (J is the total angular momentum of the $\nu\bar{\nu}$ system). In the rest frame of $\nu\bar{\nu}$, the left-handed neutrinos and right-handed antineutrinos have a total angular momentum $J = 1$. Therefore, we arrive at

$$\begin{aligned} \text{CP}|\pi^0\nu\bar{\nu}\rangle &= (-1)^J \text{CP}|\pi^0\rangle \text{CP}|\nu\bar{\nu}\rangle \\ &= (-1)(-1) \text{CP}|\nu\bar{\nu}\rangle = \text{CP}|\nu\bar{\nu}\rangle. \end{aligned}$$

If lepton flavors are assumed to be conserved ($\nu_e\bar{\nu}_e$ pairs, instead of $\nu_e\bar{\nu}_\mu$, are produced, etc. — that is, the system represents a particle and its antiparticle), then $|\nu\bar{\nu}\rangle$ will have the quantum numbers $J^{\text{PC}} = 1^{++}$ or 1^{--} . Consequently, $\text{CP}|\nu\bar{\nu}\rangle = +1$ and $\text{CP}|\pi^0\nu\bar{\nu}\rangle = +1$. Since

$$|K_L^0\rangle = \frac{|K_2^0\rangle + \varepsilon|K_1^0\rangle}{\sqrt{1 + |\varepsilon|^2}},$$

the main component of this state ($|K_2^0\rangle$) has $\text{CP} = -1$. Therefore, the decay $K_L^0 \rightarrow \pi^0\nu\bar{\nu}$ proceeds with CP-parity nonconservation, and its probability is determined by the imaginary components λ_c and λ_t .

We note that the analysis performed above is valid not only for the decays $K^0 \rightarrow \pi^0\nu\bar{\nu}$, but also for $K^0 \rightarrow \pi^0 I^+ I^-$ if the production of $I^+ I^-$ pairs is due to loop FCNC diagrams (the box diagram, electroweak penguin diagrams with Z^0 exchange or with one-photon exchange). In this case, the $\pi^0 I^+ I^-$ system is also produced in a state of positive CP parity: $\text{CP}|\pi^0(I^+ I^-)\rangle = +1$.

In the SM, the amplitudes of the decays $K \rightarrow \pi\nu\bar{\nu}$ are due to loop diagrams for FCNC processes (see Figs 8a and 8b) acting at small distances. As has already been noted, after application of the ‘renormalization’ procedure permitting us

to take into account the effects of hadron structure with the aid of normalization to the probability of the known decay $K^+ \rightarrow \pi^0 e^+ \nu_e$ [55], the influence of large-distance effects becomes negligible [109].

Applying the loop diagrams depicted in Figs 8a and 8b, it is possible, within the framework of the SM, to obtain the $K \rightarrow \pi\nu\bar{\nu}$ -decay amplitudes for each type of neutrino ν_j :

$$\begin{aligned} A(K^+ \rightarrow \pi^+ \nu_j \bar{\nu}_j) &= \frac{G_F}{\sqrt{2}} \langle \pi^+ \nu_j \bar{\nu}_j | H_w | K^+ \rangle \frac{\alpha}{2\pi \sin^2 \vartheta_W} \\ &\times [\lambda_c X(x_c) + \lambda_t X(x_t)], \end{aligned} \quad (106)$$

$$\begin{aligned} A(K^0 \rightarrow \pi^0 \nu_j \bar{\nu}_j) &= \frac{G_F}{\sqrt{2}} \langle \pi^0 \nu_j \bar{\nu}_j | H_w | K^0 \rangle \frac{\alpha}{2\pi \sin^2 \vartheta_W} \\ &\times [\lambda_c X(x_c) + \lambda_t X(x_t)], \end{aligned} \quad (107)$$

$$\begin{aligned} A(\bar{K}^0 \rightarrow \pi^0 \nu_j \bar{\nu}_j) &= \frac{G_F}{\sqrt{2}} \langle \pi^0 \nu_j \bar{\nu}_j | H_w | \bar{K}^0 \rangle \frac{\alpha}{2\pi \sin^2 \vartheta_W} \\ &\times [\lambda_c^* X(x_c) + \lambda_t^* X(x_t)], \end{aligned} \quad (108)$$

$$\begin{aligned} A(K_L^0 \rightarrow \pi^0 \nu_j \bar{\nu}_j) &\simeq A(K_2^0 \rightarrow \pi^0 \nu_j \bar{\nu}_j) \\ &= \frac{1}{\sqrt{2}} [A(K^0 \rightarrow \pi^0 \nu_j \bar{\nu}_j) - A(\bar{K}^0 \rightarrow \pi^0 \nu_j \bar{\nu}_j)] \\ &= \frac{G_F}{\sqrt{2}} \langle \pi^0 \nu_j \bar{\nu}_j | H_w | K^0 \rangle \frac{\alpha}{\sqrt{2} 2\pi \sin^2 \vartheta_W} \\ &\times 2i [\text{Im} \lambda_c X(x_c) + \text{Im} \lambda_t X(x_t)]. \end{aligned} \quad (109)$$

Here, $\lambda_i = V_{id} V_{is}^*$ ($i = c, t$) (see Table 1), $x_c = m_c^2/M_W^2$, and $x_t = m_t^2/M_W^2$, with $X(x_c)$ and $X(x_t)$ being the Inami–Lim functions for the loop diagrams presented in Figs 8a and 8b (see Tables 2 and 5).

To obtain the total $K \rightarrow \pi\nu\bar{\nu}$ -decay probability, one must sum up the respective partial probabilities over all the lepton flavors j of the neutrino pairs $\nu_j\bar{\nu}_j$ produced. As one can see from Fig. 8b, in the box diagrams for $K \rightarrow \pi\nu\bar{\nu}$ it is necessary to take into account the influence of virtual charged leptons. Since the mass of the t-quark is very large, as compared to lepton masses, the components $\lambda_t X(x_t)$ are independent of the lepton masses. However, in the case of the terms $\lambda_c X(x_c)$, the contributions for ν_e, ν_μ differ from the contribution for ν_τ : $X(x_c)_\tau \simeq 0.7X(x_c)_{\mu,e}$ [26]. Therefore, instead of $X(x_c)$, the function

$$F(x_c) = \frac{2}{3} X(x_c)_{e,\mu} + \frac{1}{3} X(x_c)_\tau$$

is introduced in Eqns (106)–(109) with the correction factor $f = 1.03 \pm 0.02$, which takes into account the nonperturbative contribution from additional quark operators of dimensionality 8 [115]. After this substitution, summing up the probabilities over the lepton flavors reduces to multiplication by a factor of 3:

$$\begin{aligned} \sum_{j=e,\mu,\tau} |A(K \rightarrow \pi\nu_j\bar{\nu}_j)|^2 &= 3 \left(\frac{G_F}{\sqrt{2}} \langle \pi\nu\bar{\nu} | H_w | K \rangle \right)^2 \\ &\times \left(\frac{\alpha}{2\pi \sin^2 \vartheta_W} \right)^2 |\lambda_c f F(x_c) + \lambda_t X(x_t)|^2. \end{aligned} \quad (110)$$

Perturbative QCD calculations for the Inami–Lim functions in the leading logarithmic approximation (LLA)

and the next-to-logarithmic approximation (NLA) result in the following values [26, 27, 58, 113]

$$X(x_t) = 1.52 \pm 0.05, \\ F(x_c) = \frac{2}{3} X(x_c)_{e,\mu} + \frac{1}{3} X(x_c)_\tau \simeq (9.8 \pm 1.8) \times 10^{-4}.$$

Since $F(x_c)/X(x_t) \sim 10^{-3}$, the contribution of terms due to c quarks turns out to be significant, only if the small function $F(x_c)$ is compensated by the relatively large factor in front of this function, i.e., for terms with the factor $\text{Re } \lambda_c$. (From Table 1 it follows that $\text{Re } \lambda_c \sim \lambda$, while $\text{Im } \lambda_c, \text{Im } \lambda_t, \text{Re } \lambda_t < \lambda^5$.)

As noted above, to take into account the matrix elements $\langle \pi v \bar{v} | H_w | K \rangle$, normalization is introduced to the known decay $K^+ \rightarrow \pi^0 e^+ \nu_e$. The amplitude of this decay has the form

$$A(K^+ \rightarrow \pi^0 e^+ \nu_e) = \frac{G_F}{\sqrt{2}} \langle \pi^0 e^+ \nu_e | H_w | K^+ \rangle \lambda. \quad (111)$$

Applying isotopic asymmetry, one can find the relation between the respective hadron matrix elements:

$$\left| \frac{\langle \pi^+ v \bar{v} | H_w | K^+ \rangle}{\langle \pi^0 e^+ \nu_e | H_w | K^+ \rangle} \right|^2 = 2r_+, \quad \left| \frac{\langle \pi^0 v \bar{v} | H_w | K^0 \rangle}{\langle \pi^0 e^+ \nu_e | H_w | K^+ \rangle} \right|^2 = r_0. \quad (112)$$

Here, $r_+ = 0.901$ and $r_0 = 0.944$ are correction factors taking into account violation of isotopic symmetry and the differences in phase volumes for $K^+ \rightarrow \pi^0 e^+ \nu_e$, $K^+ \rightarrow \pi^+ v \bar{v}$, and $K^0 \rightarrow \pi^0 v \bar{v}$ decays [112].

With account of relationship (112) for the ratio of amplitudes, we have

$$\frac{A(K^+ \rightarrow \pi^+ v \bar{v})}{A(K^0 \rightarrow \pi^0 v \bar{v})} = \sqrt{2r_+/r_0}.$$

From relations (100)–(104) for the decay amplitude $|K_L^0\rangle = p|K^0\rangle - q|\bar{K}^0\rangle$ it follows that

$$A(K_L^0 \rightarrow \pi^0 v \bar{v}) = pa - q\bar{a} = pa \left(1 - \frac{q\bar{a}}{p a} \right) \\ = pA(K^0 \rightarrow \pi^0 v \bar{v})(1 - \lambda_{\pi v \bar{v}}) \\ = pA(K^0 \rightarrow \pi^0 v \bar{v})(1 - \exp(2i\vartheta)), \\ \frac{A(K_L^0 \rightarrow \pi^0 v \bar{v})}{A(K^+ \rightarrow \pi^+ v \bar{v})} = \frac{pA(K^0 \rightarrow \pi^0 v \bar{v})}{A(K^0 \rightarrow \pi^0 v \bar{v})\sqrt{2r_+/r_0}} (1 - \exp(2i\vartheta)) \\ = \frac{1 - \cos 2\vartheta - i \sin 2\vartheta}{2\sqrt{r_+/r_0}},$$

where $p \simeq 1/\sqrt{2}$. Hence, it is possible to impose modelless restrictions on the ratios between widths and branching ratios of the two decays $K \rightarrow \pi v \bar{v}$:

$$\frac{\Gamma(K_L^0 \rightarrow \pi^0 v \bar{v})}{\Gamma(K^+ \rightarrow \pi^+ v \bar{v})} = \frac{1 - \cos 2\vartheta}{2r_+/r_0} = \frac{r_0}{r_+} \sin^2 \vartheta < \frac{r_0}{r_+} = 1.048, \\ \frac{\text{BR}(K_L^0 \rightarrow \pi^0 v \bar{v})}{\text{BR}(K^+ \rightarrow \pi^+ v \bar{v})} = \frac{r_0}{r_+} \frac{\tau(K_L^0)}{\tau(K^+)} \sin^2 \vartheta < \frac{r_0}{r_+} \frac{\tau(K_L^0)}{\tau(K^+)} = 4.37. \quad (113)$$

The decay probability for $K^+ \rightarrow \pi^+ v \bar{v}$ is determined from Eqns (106), (110)–(112):

$$\text{BR}(K^+ \rightarrow \pi^+ v \bar{v})_{\text{SM}} = \text{BR}(K^+ \rightarrow \pi^0 e^+ \nu_e) \frac{3\alpha^2}{4\pi^2 \sin^4 \vartheta_W} \cdot 2r_+ \\ \times \frac{1}{\lambda^2} \left\{ [fF(x_c) \text{Re } \lambda_c + X(x_t) \text{Re } \lambda_t]^2 + [X(x_t) \text{Im } \lambda_t]^2 \right\} \\ = K_+ \frac{X^2(x_t)}{\lambda^2} \left\{ [\delta(x_c) \text{Re } \lambda_c + \text{Re } \lambda_t]^2 + (\text{Im } \lambda_t)^2 \right\} \\ = K_+ B(\lambda_c; \lambda_t). \quad (114)$$

Here, $\alpha = 1/129$ is the value of electromagnetic constant $\alpha(M_W)$ at the Z -pole, $\sin^2 \vartheta_W = 0.23$ (ϑ_W is the Weinberg angle), and

$$\text{BR}(K^+ \rightarrow \pi^0 e^+ \nu_e) = 4.82 \times 10^{-2},$$

$$K_+ = \frac{3\alpha^2 r_+ \text{BR}(K^+ \rightarrow \pi^0 e^+ \nu_e)}{2\pi^2 \sin^4 \vartheta_W} = 7.50 \times 10^{-6}.$$

The factor taking into account the influence of virtual c -quarks takes the form

$$\delta(x_c) = f \frac{F(x_c)}{X(x_t)} = (6.65 \pm 1.23) \times 10^{-4}.$$

More often, the value

$$P_c(v\bar{v}) = \delta(x_c) \frac{X(x_t)}{\lambda^4} = f \frac{F(x_c)}{\lambda^4} = 0.42 \pm 0.06$$

is used.

The $K_L^0 \rightarrow \pi^0 v \bar{v}$ -decay probability is written down as

$$\text{BR}(K_L^0 \rightarrow \pi^0 v \bar{v}) = K_+ \frac{r_0}{r_+} \frac{\tau(K_L^0)}{\tau(K^+)} \frac{X^2(x_t)}{\lambda^2} (\text{Im } \lambda_t)^2 \\ = K_0 \frac{X^2(x_t)}{\lambda^2} (\text{Im } \lambda_t)^2, \quad (115)$$

where

$$K_0 = K_+ \frac{r_0}{r_+} \frac{\tau(K_L^0)}{\tau(K^+)} = 3.28 \times 10^{-5},$$

and the ratio of lifetimes of the K_L^0 - and K^+ -mesons amounts to $\tau(K_L^0)/\tau(K^+) = 4.17$.

Making use of the expressions for $\text{Re } \lambda_c$, $\text{Re } \lambda_t$, and $\text{Im } \lambda_t$ in terms of the variables of the unitary triangle in the plane of parameters $\bar{\rho}, \bar{\eta}$ (see Table 1), namely

$$\text{Re } \lambda_c = -\lambda \left(1 - \frac{\lambda^2}{2} \right) + O(\lambda^5),$$

$$\text{Re } \lambda_t = -A^2 \lambda^5 \left(1 - \frac{\lambda^2}{2} \right) (1 - \bar{\rho}) + O(\lambda^7),$$

$$\text{Im } \lambda_t = A^2 \lambda^5 \bar{\eta} + O(\lambda^9) = A^2 \lambda^5 \bar{\eta} \frac{1}{1 - \lambda^2/2} + O(\lambda^9),$$

one can obtain an expression for $B(\lambda_c; \lambda_t)$ in formula (114):

$$\begin{aligned}
 B(\lambda_c; \lambda_t) &= \frac{X^2(x_t)}{\lambda^2} \{ [\delta(x_c) \operatorname{Re} \lambda_c + \operatorname{Re} \lambda_t]^2 + (\operatorname{Im} \lambda_t)^2 \} \\
 &= X^2(x_t) \left\{ \left[-\left(1 - \frac{\lambda^2}{2}\right) \delta(x_c) - A^2 \lambda^4 \left(1 - \frac{\lambda^2}{2}\right) (1 - \bar{\rho}) \right]^2 \right. \\
 &\quad \left. + \left(A^2 \lambda^4 \bar{\eta} \frac{1}{1 - \lambda^2/2} \right)^2 \right\} \\
 &= X^2(x_t) A^4 \lambda^8 \frac{1}{\sigma} \left[\left(\frac{\delta(x_c)}{A^2 \lambda^4} + 1 - \bar{\rho} \right)^2 + (\sigma \bar{\eta})^2 \right] \\
 &= X^2(x_t) |V_{cb}|^4 \frac{1}{\sigma} [(1 + \Delta - \bar{\rho})^2 + (\sigma \bar{\eta})^2] \\
 &= X^2(x_t) |V_{cb}|^4 \frac{1}{\sigma} [(\rho_0 - \bar{\rho})^2 + (\sigma \bar{\eta})^2]. \tag{116}
 \end{aligned}$$

Here (for the data in Table 5), it is readily calculated that

$$\begin{aligned}
 \Delta &= \frac{\delta(x_c)}{A^2 \lambda^4} = \frac{\delta(x_c)}{|V_{cb}|^2} = \frac{f F(x_c)}{|V_{cb}|^2 X(x_t)} \\
 &= (6.66 \pm 1.23) \times 10^{-4} \frac{1}{|V_{cb}|^2} = 0.39 \pm 0.08, \\
 \rho_0 &= 1 + \Delta = 1.39 \pm 0.08, \\
 \sigma &= \frac{1}{(1 - \lambda^2/2)^2} = 1.051, \quad |V_{cb}| = A \lambda^2.
 \end{aligned}$$

As already mentioned, to take into account the influence of c-quarks on the probability $\operatorname{BR}(K^+ \rightarrow \pi^+ \nu \bar{\nu})$, one usually applies, instead of $\delta(x_c)$, the following value [58]

$$P_c(\nu \bar{\nu}) = f \frac{F(x_c)}{\lambda^4} = \delta(x_c) \frac{X(x_t)}{\lambda^4} = 0.42 \pm 0.06$$

(the factor f is often dropped, since it represents a small correction). Here, the expression for Δ does not change, naturally:

$$\Delta = \frac{P_c(\nu \bar{\nu}) \lambda^4}{|V_{cb}|^2 X(x_t)} = \frac{\delta(x_c)}{|V_{cb}|^2}.$$

A more accurate expression for the function $B(\lambda_c; \lambda_t)$ [114] is given in Appendix III.

Employing the conservative numerical values for the CKM parameters $|V_{cb}|, \bar{\eta}$, and $\bar{\rho}$ from PDG-2002 [25] (see Table 5), from Eqns (114)–(116) it is possible to obtain the final expressions and numerical estimates for the $K \rightarrow \pi \nu \bar{\nu}$ -decay probabilities in the SM:

$$\begin{aligned}
 \operatorname{BR}(K^+ \rightarrow \pi^+ \nu \bar{\nu})_{\text{SM}} &= K_+ A^4 \lambda^8 X^2(x_t) \frac{1}{\sigma} [(\rho_0 - \bar{\rho})^2 + (\sigma \bar{\eta})^2] \\
 &= K_+ |V_{cb}|^4 X^2(x_t) \frac{1}{\sigma} [(\rho_0 - \bar{\rho})^2 + (\sigma \bar{\eta})^2] \\
 &= 7.50 \times 10^{-6} [2.88 \times 10^{-6} \pm (19.4\%)] \\
 &\quad \times [2.31 \pm (6.6\%)] [1.43 \pm (20\%)] \\
 &= [7.14 \pm (28.6\%)] \times 10^{-11} = (7.1 \pm 2.0) \times 10^{-11}, \tag{117}
 \end{aligned}$$

$$\begin{aligned}
 \operatorname{BR}(K_L^0 \rightarrow \pi^0 \nu \bar{\nu})_{\text{SM}} &= K_0 A^2 \lambda^8 X^2(x_t) (\sigma \bar{\eta})^2 \\
 &= K_0 |V_{cb}|^4 X^2(x_t) (\sigma \bar{\eta})^2 \\
 &= 3.28 \times 10^{-5} [2.88 \times 10^{-6} \pm (19.4\%)] \\
 &\quad \times [2.31 \pm (6.6\%)] [0.129 \pm (28.6\%)] \\
 &= [2.8 \pm (35\%)] \times 10^{-11} = (2.8 \pm 1.0) \times 10^{-11}. \tag{118}
 \end{aligned}$$

The inaccuracies in estimations of $\operatorname{BR}(K \rightarrow \pi \nu \bar{\nu})$ by formulae (117) and (118) are dominated by current uncertainties of CKM parameters. They essentially exceed the intrinsic theoretical errors in these branching ratios, which are conditioned by the calculations of $F(x_c)$ and $X(x_t)$ and amount to 7% for $\operatorname{BR}(K^+ \rightarrow \pi^+ \nu \bar{\nu})$, and to 1–2% for $\operatorname{BR}(K_L^0 \rightarrow \pi^0 \nu \bar{\nu})$.

We stress that the estimates of uncertainties in Eqns (117) and (118) are of quite an approximate and illustrative character, since they do not take into account correlations between $\bar{\rho}, \bar{\eta}$, and $|V_{cb}|$. These estimates are intended mainly for demonstration of the influence of various factors on the values of decay probabilities and the uncertainties in their determination. They reveal, for example, a strong influence of the uncertainties in determining $|V_{cb}|$ on the final result, since the probabilities (117) and (118) contain the factor $|V_{cb}|^4$. Measurement of exclusive semileptonic decays of B-mesons in the CLEO experiment [120] yielded quite a large value

$$|V_{cb}| = (46.9 \pm 3.0) \times 10^{-3}$$

(as compared to the data in Table 5). If this value is correct, then it essentially increases the decay probabilities relative to estimates (117) and (118).

More accurate probability values

$$\operatorname{BR}(K^+ \rightarrow \pi^+ \nu \bar{\nu})_{\text{SM}} = (7.5 \pm 2.9) \times 10^{-11},$$

$$\operatorname{BR}(K_L^0 \rightarrow \pi^0 \nu \bar{\nu})_{\text{SM}} = (2.6 \pm 1.2) \times 10^{-11}$$

taking into account correlations were found in Ref. [28] by scanning the CKM parameters. A somewhat different fitting method applied in Ref. [119] gave the value

$$\operatorname{BR}(K^+ \rightarrow \pi^+ \nu \bar{\nu}) = (7.2 \pm 2.1) \times 10^{-11}.$$

All these estimates have turned out to be close to the simple estimates (117) and (118). In Refs [92, 121–123], the correlation effects were evident — they enhanced the accuracy in estimating the 95% limits for the $K \rightarrow \pi \nu \bar{\nu}$ probabilities, presented in these papers. Taking into account correlations for parameters of the unitary triangle in the $(\bar{\rho}, \bar{\eta})$ -plane happens to be somewhat difficult. Therefore, another method is applied below for calculations [118] of $\operatorname{BR}(K^+ \rightarrow \pi^+ \nu \bar{\nu})_{\text{SM}}$ and $\operatorname{BR}(K_L^0 \rightarrow \pi^0 \nu \bar{\nu})_{\text{SM}}$ in terms of variables of the so-called kaon unitary triangle, where the correlations are not so significant and are accounted for more readily.

We note that, when the ‘aggressive’ approach to estimating the CKM parameters [29, 45, 48] (see Table 5) is adopted, then from Eqns (117) and (118) it is possible to obtain more accurate values

$$\operatorname{BR}(K^+ \rightarrow \pi^+ \nu \bar{\nu})_{\text{SM}} = (7.6 \pm 1.2) \times 10^{-11},$$

$$\operatorname{BR}(K_L^0 \rightarrow \pi^0 \nu \bar{\nu})_{\text{SM}} = (2.9 \pm 0.5) \times 10^{-11}.$$

However, we think that, owing to the situation with the values of $|V_{cb}|$ and ζ (corrections due to SU(3)-symmetry breaking in $B_d^0 \rightleftharpoons \bar{B}_d^0$ and $B_s^0 \rightleftharpoons \bar{B}_s^0$ mixing; see Section 4 and Table 5) being unclear, the ‘conservative’ approach [25] at present seems to be more justified.

As was already noted, another approach has been developed in Ref. [118] to estimation of the $K \rightarrow \pi \nu \bar{\nu}$ -decay probabilities, which is free from the influence of $|V_{cb}|$ and $\Delta M_{d,s}$ (due to the B-mixing) and which simplifies taking into

account correlations between the SM parameters. In this method, direct estimations of $\text{Re } \lambda_t$ and $\text{Im } \lambda_t$ are performed, which determine the probabilities of the decays being studied [see Eqns (114) and (115)]. These estimations make use of the parameters of the kaon unitary triangle in the complex ($\text{Re } \lambda_t$, $\text{Im } \lambda_t$)-plane, based on unitarity relation (24) containing the matrix elements of kaon decays, but not the matrix elements of B-decays. The corresponding unitarity relation can be represented in the form

$$\lambda_u + \lambda_c + \lambda_t = 0, \quad \lambda_i = V_{id} V_{is}^*, \quad i = u, c, t. \quad (119)$$

The possibility of applying the kaon unitary triangle was discussed in Refs [41, 124]. In the strongly compressed triangle (Fig. 9a), $\lambda_u = V_{ud} V_{us}^* = \lambda(1 - \lambda^2/2)$ is a real quantity and serves as the base of the triangle. The other side $|\lambda_c| \simeq |\lambda_u|$ is characterized by a very small complex phase: $|\text{Im } \lambda_c / \text{Re } \lambda_c| \simeq \bar{\eta} \lambda^4 A^2 \simeq 6 \times 10^{-4}$. Estimations of $\text{BR}(\text{K} \rightarrow \pi \nu \bar{\nu})$ were carried out using the third side λ_t of the triangle. Data obtained in the kaon sector do not permit us to find λ_t , yet. Therefore, the $|\varepsilon_K|$ -hyperbola (75), (77) in the ($\text{Re } \lambda_t$, $\text{Im } \lambda_t$)-plane was used in Ref. [118] together with the theoretically clean (within the framework of the SM) results of determining $\sin 2\beta$ from measurements of the CP asymmetry $a_{\psi K}$ in the decays $\text{B}_d^0(\bar{\text{B}}_d^0) \rightarrow (\text{J}/\psi)\text{K}_S^0$.

The angle β_K in the kaon unitary triangle (Fig. 9a) can be obtained from the value of $\beta = 23.6^\circ \pm 2.3^\circ$ (the preferable solution in the SM; see Fig. 5 and Table 5):

$$\begin{aligned} \beta_K &= \pi - \varphi(\lambda_t) = \pi - \varphi(V_{td}) + \varphi(V_{ts}) \\ &= \beta + 1.0^\circ = 24.6^\circ \pm 2.3^\circ. \end{aligned} \quad (120)$$

Here, the phase $\varphi(V_{td}) = -\beta$ [see Eqn (29)], while the matrix element $V_{ts} \simeq -A\lambda^2(1 + i\eta\lambda^2)$ is characterized by the phase $\varphi(V_{ts}) = -\pi + \eta\lambda^2 = -\pi + 0.0172 \simeq -\pi + 1^\circ$ [V_{ts} lies in the third quadrant of the complex ($\text{Re } \lambda_t$, $\text{Im } \lambda_t$)-plane].

Thus, the vertex of the kaon unitary triangle ($\text{Re } \lambda_t^a$, $\text{Im } \lambda_t^a$) can be determined in the SM from the intersection of the $|\varepsilon_K|$ -hyperbola in the ($\text{Re } \lambda_t$, $\text{Im } \lambda_t$)-plane (77):

$$\begin{aligned} \hat{B}_K \text{Im } \lambda_t &[(1.43 \pm 0.44) \times 10^{-4} - (1.357 \pm 0.067) \text{Re } \lambda_t] \\ &= 5.95 \times 10^{-8} \end{aligned}$$

and the straight line with the slope $-\tan \beta_K$ (Fig. 9a):

$$\text{Im } \lambda_t = -\tan \beta_K \text{Re } \lambda_t = (-0.458 \pm 0.049) \text{Re } \lambda_t. \quad (121)$$

The set of equations has been solved and the respective uncertainties have been determined in Ref. [118] with the aid of the probability distribution function (PDF) in the Bayesian approach [48, 92] (in this approximation, theoretical errors are given by flat probability distributions) and are confirmed by the scanning method with Gauss probability distributions. Here, the position of the vertex of the kaon unitary triangle (we denote it by λ_t^a) was found:

$$\text{Re } \lambda_t^a = (-2.84 \pm 0.31) \times 10^{-4}, \quad (122)$$

$$\text{Im } \lambda_t^a = (1.30 \pm 0.13) \times 10^{-4}.$$

Hence, and from expressions (114), (115), the probability distributions for $\text{BR}(\text{K} \rightarrow \pi \nu \bar{\nu})$ (see, for example, Fig. 9b) were obtained, and the decay probabilities for $\text{K}^+ \rightarrow \pi^+ \nu \bar{\nu}$ and $\text{K}_L^0 \rightarrow \pi^0 \nu \bar{\nu}$ were ultimately established [118]:

$$\begin{aligned} \text{BR}(\text{K}^+ \rightarrow \pi^+ \nu \bar{\nu})_{\text{SM}} &= \frac{R_+}{\lambda^2} \left\{ [fF(x_c) \text{Re } \lambda_c + X(x_t) \text{Re } \lambda_t^a]^2 + [X(x_t) \text{Im } \lambda_t^a]^2 \right\} \\ &= (7.07 \pm 1.03) \times 10^{-11}, \end{aligned} \quad (123)$$

$$\begin{aligned} \text{BR}(\text{K}_L^0 \rightarrow \pi^0 \nu \bar{\nu})_{\text{SM}} &= R_0 \frac{X^2(x_t)}{\lambda^2} (\text{Im } \lambda_t^a)^2 \\ &= (2.60 \pm 0.52) \times 10^{-11}. \end{aligned} \quad (124)$$

In obtaining the result (123) account was taken of the correlations between the parameters of the ε_K -hyperbola (determining the vertex λ_t^a of the K-meson unitary triangle) and the Inami–Lim functions $F(x_c)$, $X(x_t)$ via the variables x_c , x_t and the QCD parameter $A_{\overline{\text{MS}}}$. Taking into account these correlations reduces the uncertainty in determining $\text{BR}(\text{K}^+ \rightarrow \pi^+ \nu \bar{\nu})$ by 20%. The results (123) and (124) are in good agreement with those in formulas (117) and (118), are independent of $|V_{cb}|$ and of the information about the mass differences $\Delta M_{d,s}$, and exhibit a higher precision.

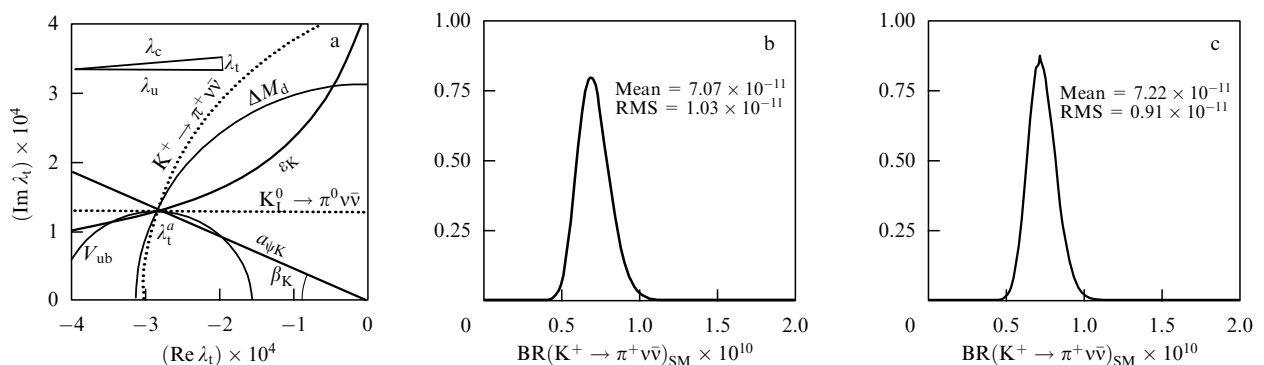


Figure 9. Analysis of $\text{K} \rightarrow \pi \nu \bar{\nu}$ decays in terms of the variables of the kaon unitary triangle [118]. (a) Determination of the vertex λ_t^a of the kaon unitary triangle. The solid curves ε_K and $a_{\psi K}$ show the method for finding λ_t^a [see Eqn (122)] as the intersection of the ε_K -hyperbola and the straight line determined by the $a_{\psi K}$ asymmetry (see text). The dotted circle corresponds to the $\text{K}^+ \rightarrow \pi^+ \nu \bar{\nu}$ decay. The circle V_{ub} is described by relation (128), while the circle ΔM_d is described by relation (127). In the SM, all the curves intersect at the vertex λ_t^a of the triangle. The kaon unitary triangle $\lambda_t + \lambda_c + \lambda_u = 0$ is shown (not to scale) in the upper corner of the figure. (b) Probability distribution for $\text{BR}(\text{K}^+ \rightarrow \pi^+ \nu \bar{\nu})_{\text{SM}}$, determined in the SM by the data on $|\varepsilon_K|$ and $a_{\psi K}$. The obtained 95% boundaries for the branching ratio of this decay are as follows: $5.6 \times 10^{-11} < \text{BR}(\text{K}^+ \rightarrow \pi^+ \nu \bar{\nu})_{\text{SM}} < 8.9 \times 10^{-11}$. (c) Probability distribution for $\text{BR}(\text{K}^+ \rightarrow \pi^+ \nu \bar{\nu})_{\text{SM}}$, obtained within the SM from the set of data for $|\varepsilon_K|$, $a_{\psi K}$, V_{ub} , and ΔM_d .

Naturally, if all the CKM parameters were determined reliably enough (without additional systematic errors related to the corresponding theoretical models for these parameters), then within the framework of the SM appropriate application of all the available information could only enhance the estimation accuracy of the respective $K \rightarrow \pi\nu\bar{\nu}$ -decay probabilities. However, at present, there exist systematic uncertainties and contradictory data, so that to obtain results free from part of these uncertainties would be very desirable. Moreover, in connection with the possible manifestations of NP in various processes of the K- and B-sectors, independent estimates of $BR(K \rightarrow \pi\nu\bar{\nu})_{SM}$ making use of diverse information may turn out to be extremely essential. These issues are discussed in greater detail in Section 6.

Although the main goal of work [118] was the estimation of $BR(K \rightarrow \pi\nu\bar{\nu})_{SM}$ without taking into account the contradictory information about $|V_{cb}|$ and ξ , the more transparent method proposed in this work for taking account of correlations between the parameters permitted us to submit estimates of $BR(K \rightarrow \pi\nu\bar{\nu})$, additionally making use of the data for $|V_{cb}|$, $|V_{ub}|$, and ΔM_d . To this end, the following relation for the mass difference

$$\begin{aligned} \Delta M_d &= \frac{G_F}{6\pi^2} M_W^2 M_d f_d^2 \hat{B}_{B_d} \eta_B S_0(x_t) |V_{td} V_{tb}^*|^2 \\ &= N^2 |V_{td} V_{tb}^*|^2 \simeq N^2 \frac{|\lambda_t|^2}{|V_{cb}|^2}, \end{aligned} \quad (125)$$

where

$$N^2 = \frac{G_F}{6\pi^2} M_W^2 M_d f_d^2 \hat{B}_{B_d} \eta_B S_0(x_t),$$

and the condition of unitarity (25) expressed in the form

$$\lambda_t = \left(1 - \frac{\lambda^2}{2}\right) V_{ub}^* V_{cb}^* - \lambda (V_{cb}^*)^2 \quad (126)$$

were considered. In these equations, the approximate values of the elements of the quark mixing matrix V_{CKM} were used:

$$\begin{aligned} V_{tb}^* &\simeq 1, \quad V_{us} = \lambda, \quad V_{ud} \simeq 1 - \frac{\lambda^2}{2}, \quad V_{cb} \simeq -V_{ts}, \\ |V_{td} V_{tb}^*|^2 &= \frac{|\lambda_t|^2}{|V_{cb}|^2}, \quad (V_{cb}^*)^2 \simeq |V_{cb}|^2, \quad V_{cd} \simeq -\lambda. \end{aligned}$$

Equations (125) and (126) can be represented as two circles in the $(\text{Re } \lambda_t, \text{Im } \lambda_t)$ -plane (Fig. 9a):

$$(\text{Re } \lambda_t)^2 + (\text{Im } \lambda_t)^2 = R_1^2 = \frac{\Delta M_d |V_{cb}|^2}{N^2} \quad (127)$$

(with its center at the origin of the reference system, and of radius $R_1 = \sqrt{\Delta M_d} |V_{cb}|/N$) and

$$(\text{Re } \lambda_t + |V_{cb}|^2 \lambda)^2 + (\text{Im } \lambda_t)^2 = R_2^2 = \left(1 - \frac{\lambda^2}{2}\right)^2 |V_{ub}^* V_{cb}^*|^2 \quad (128)$$

(with its center shifted to the point $-\lambda|V_{cb}|^2$, and of radius $R_2 \simeq |V_{ub}^* V_{cb}^*|$). The intersection of these circles permits us to determine independently the vertex of the kaon unitary triangle, although the respective accuracies turned out to be worse than in expressions (122).

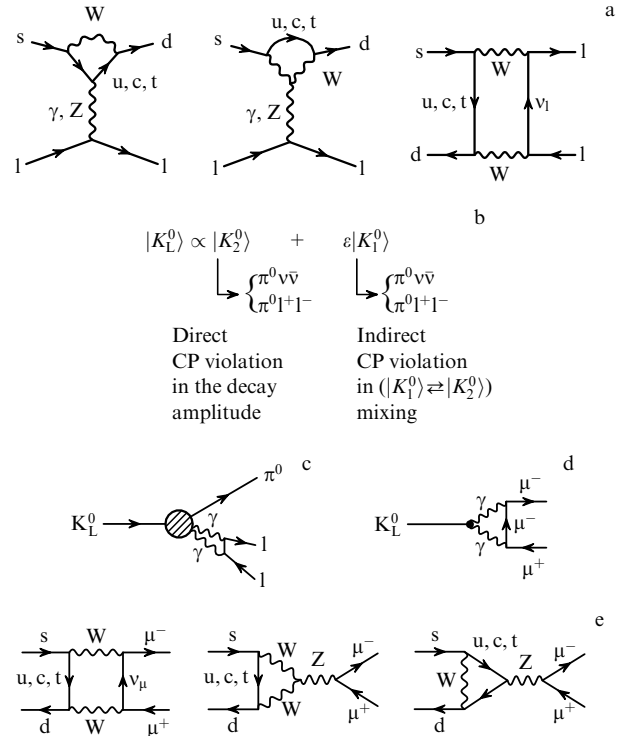


Figure 10. Diagrams for FCNC processes with neutral kaons. (a) Diagrams for FCNC processes $s \rightarrow dl^{+1-}$, manifested in decays $K_L^0 \rightarrow \pi^0 l^{+1-}$ with CP violation ($l = e, \mu$). (b) Processes of direct and of indirect CP violation in decays $K_L^0 \rightarrow \pi^0 l^{+1-}$ and $K_L^0 \rightarrow \pi^0 \nu\bar{\nu}$. Owing to the contribution of large distances to processes with one-photon exchange in the decays $K^0 \rightarrow \pi^0 l^{+1-}$, the CP-conserving amplitude of the $K_S^0 \rightarrow \pi^0 l^{+1-}$ decay may be much larger than the CP-violating amplitude of the $K_L^0 \rightarrow \pi^0 l^{+1-}$ decay, and the contribution from the indirect mechanism of CP violation may be significant. In the $K^0 \rightarrow \pi^0 \nu\bar{\nu}$ decays, the amplitudes of K_S^0 - and K_L^0 -decays are comparable, and the mechanism of indirect violation is negligible owing to the smallness of ϵ . (c) Diagram with two-photon exchange for the $K_L^0 \rightarrow \pi^0 l^{+1-}$ decay without violation of CP invariance. (d) Diagram for the decay $K_L^0 \rightarrow l^{+1-}$ proceeding via two-photon exchange (dominant in the region of large distances). (e) FCNC processes in the decay $K_L^0 \rightarrow \mu^+ \mu^-$ in the region of small distances.

The total information from all the processes dealt with here corresponds to

$$\begin{aligned} (\text{Re } \lambda_t^a)_{SM, \text{total}} &= (-2.91 \pm 0.22) \times 10^{-4}, \\ (\text{Im } \lambda_t^a)_{SM, \text{total}} &= (1.27 \pm 0.11) \times 10^{-4} \end{aligned}$$

and results in the following $K \rightarrow \pi\nu\bar{\nu}$ -decay probabilities (see also Fig. 9c):

$$BR(K^+ \rightarrow \pi^+ \nu\bar{\nu})_{SM, \text{total}} = (7.22 \pm 0.91) \times 10^{-11}, \quad (129)$$

$$BR(K_L^0 \rightarrow \pi^0 \nu\bar{\nu})_{SM, \text{total}} = (2.49 \pm 0.42) \times 10^{-11}. \quad (130)$$

Their precision is somewhat higher than in Eqns (123) and (124), but these results are related to the application of a large number of parameters.

5.3 Other rare FCNC decays of kaons

The $K^+ \rightarrow \pi^+ \nu\bar{\nu}$ and $K_L^0 \rightarrow \pi^0 \nu\bar{\nu}$ decays considered in the preceding section are not the only rare kaon processes due to loop FCNC diagrams. The decays $K_L^0 \rightarrow \pi^0 l^{+1-}$ and $K_L^0 \rightarrow l^{+1-}$, in which FCNC mechanisms are also manifested at small distances, are of significant interest. Regretfully, theoretical interpretation of decays involving charged leptons happens to be more complicated than interpretation of

Table 7. Data on the rare decays $K_L^0 \rightarrow \pi^0 l^+ l^-$ and $K_L^0 \rightarrow l^+ l^-$ (for details and references see review [42]).

Decay $K_L^0 \rightarrow \pi^0 l^+ l^-$ (see Figs 10a–10c)	
$K_L^0 \rightarrow \pi^0 e^+ e^-$ _{CP-dir} with direct CP violation. FCNC diagrams in the region of small distances (see Figs 10a, 10b)	$\text{BR}(K_L^0 \rightarrow \pi^0 e^+ e^-)_{\text{CP-dir, SM}} = \underbrace{\frac{1}{\lambda^2} \frac{\tau(K_L^0)}{\tau(K^+)}}_{K_e = 6.3 \times 10^{-6}} \left(\frac{\alpha}{2\pi} \right)^2 \text{BR}(K^+ \rightarrow \pi^0 e^+ \nu_e) \underbrace{[\tilde{Y}_{7A}^2 + \tilde{Y}_{7B}^2]}_{39.2 \pm 2.9} \underbrace{(\text{Im } \lambda_t)^2}_{\sigma \eta^2 V_{cb} ^4 \lambda^2} = (4.6 \pm 1.6) \times 10^{-12}$ ($\tilde{Y}_{7A}, \tilde{Y}_{7B}$ — Inami–Lim loop functions for $K_L^0 \rightarrow \pi^0 e^+ e^-$; see Tables 2 and 5)
$K_L^0 \rightarrow \pi^0 e^+ e^-$ _{CP-indir} with indirect CP violation in ($K_1^0 \rightleftharpoons K_2^0$) mixing	$\text{BR}(K_L^0 \rightarrow \pi^0 e^+ e^-)_{\text{CP-indir}} = \frac{\tau(K_L^0)}{\tau(K_S^0)} g_K ^2 \text{BR}(K_S^0 \rightarrow \pi^0 e^+ e^-) = 3.0 \times 10^{-3} \text{BR}(K_S^0 \rightarrow \pi^0 e^+ e^-).$ In the absence of direct measurements of $\text{BR}(K_S^0 \rightarrow \pi^0 e^+ e^-)$, the probability is estimated with a large uncertainty in the chiral model from data on $\text{BR}(K^+ \rightarrow \pi^+ e^+ e^-)$. Hence, $\text{BR}(K_L^0 \rightarrow \pi^0 e^+ e^-)_{\text{CP-indir}} \simeq (1-5) \times 10^{-12}$. To clarify this prediction, it is important to measure $\text{BR}(K_S^0 \rightarrow \pi^0 e^+ e^-)$.
$K_L^0 \rightarrow \pi^0 \gamma^* \gamma^* \rightarrow \pi^0 e^+ e^-$, CP is conserved	From new data [125] on the decay $K_L^0 \rightarrow \pi^0 \gamma \gamma$ in experiment NA48, the decay probability with CP conservation is estimated as $\text{BR}(K_L^0 \rightarrow \pi^0 e^+ e^-)_{\text{CP, inv}} \simeq (4.7_{-1.8}^{+2.2}) \times 10^{-13}$. The decay $K_L^0 \rightarrow \pi^0 e^+ e^-$ proceeds mainly with CP violation
$K_L^0 \rightarrow \pi^0 \mu^+ \mu^-$	The probability of the decay $K_L^0 \rightarrow \pi^0 \mu^+ \mu^-$ with CP violation is five times smaller than that of the decay $K_L^0 \rightarrow \pi^0 e^+ e^-$. No quantitative analysis has been performed for the CP-conserving component in $K_L^0 \rightarrow \pi^0 \mu^+ \mu^-$
Experimental data from KTeV	The existing sensitivity is restricted by the background (90% C.L.) [126]: $\text{BR}(K_L^0 \rightarrow \pi^0 e^+ e^-) < 2.8 \times 10^{-10}, \quad \text{BR}(K_L^0 \rightarrow \pi^0 \mu^+ \mu^-) < 3.4 \times 10^{-10}.$ The background situation is very complicated, especially owing to the background from the decay $K_L^0 \rightarrow e^+ e^- \gamma \gamma$ exhibiting a large probability ($\text{BR} \sim 6 \times 10^{-7}$)
Decay $K_L^0 \rightarrow l^+ l^-$ (see Figs 10d, 10e)	
$K_L^0 \rightarrow \mu^+ \mu^-$	Experimental result (see Refs [25, 127]): $\text{BR}(K_L^0 \rightarrow \mu^+ \mu^-)_{\text{expt}} = (7.15 \pm 0.16) \times 10^{-9}, \quad \text{BR}(K_L^0 \rightarrow \mu^+ \mu^-) = A_{\mu\mu} ^2 = (\text{Re } A_{\mu\mu})^2 + (\text{Im } A_{\mu\mu})^2.$ Absorptive contribution determined by the on-mass-shell intermediate state $K_L^0 \rightarrow \gamma \gamma$: $(\text{Im } A_{\mu\mu})^2 = \underbrace{\frac{\alpha^2 m_\mu^2}{2m_K^2 \beta_\mu} \left[\ln \frac{1 - \beta_\mu}{1 + \beta_\mu} \right]^2}_{1.20 \times 10^{-5}} \underbrace{\text{BR}(K_L^0 \rightarrow \gamma \gamma)}_{(5.92 \pm 0.15) \times 10^{-4}} = (7.09 \pm 0.18) \times 10^{-9}, \quad \beta_\mu = \sqrt{1 - \frac{4m_\mu^2}{m_K^2}} = 0.905.$ Absorptive contribution nearly saturates experimental probability. The dispersive amplitude $\text{Re } A_{\mu\mu}$ is determined by off-mass-shell $K_L^0 \rightarrow \gamma^* \gamma^*$ transitions. $\text{Re } A_{\mu\mu} = (\text{Re } A_{\mu\mu})_{\text{SD}} + (\text{Re } A_{\mu\mu})_{\text{LD}}$, where $(\text{Re } A_{\mu\mu})_{\text{SD}}$ is determined by FCNC processes at small distances, and the contribution of large distances, $(\text{Re } A_{\mu\mu})_{\text{LD}}$, depends on the form factor of the $K_L^0 \rightarrow \gamma^* \gamma^*$ vertex: $(\text{Re } A_{\mu\mu})_{\text{SM}} = \underbrace{\frac{\alpha^2 \text{BR}(K^+ \rightarrow \mu^+ \nu_\mu) \tau(K_L^0)}{\pi^2 \sin^4 \vartheta_W} \lambda^8}_{K_{\mu\mu} = 1.68 \times 10^{-9}} \left[\underbrace{\frac{\text{Re } \lambda_c}{\lambda} P_c(\mu\mu)}_{\text{contribution of c-quarks}} + \underbrace{\frac{\text{Re } \lambda_t}{\lambda^5} Y(X_t)}_{\text{contribution of t-quarks}} \right]^2 = (8.4 \pm 2.0) \times 10^{-10}.$ From $\text{BR}(K_L^0 \rightarrow \mu^+ \mu^-)_{\text{expt}}$, $(\text{Im } A_{\mu\mu})^2$, and estimates of $(\text{Re } A_{\mu\mu})_{\text{LD}}$ it is possible to obtain the restriction $ (\text{Re } A_{\mu\mu})_{\text{SD}} ^2 < 1.3 \times 10^{-9}$ (90% C.L.); see Ref. [128]†
$K_L^0 \rightarrow e^+ e^-$	The experimental result [129] $\text{BR}(K_L^0 \rightarrow e^+ e^-)_{\text{expt}} = (8.7_{-4.1}^{+5.7}) \times 10^{-12}$ is in good agreement with calculations within the chiral model. In the SM, the decay is fully due to the region of large distances, since $(\text{Re } A_{ee})_{\text{SD}}^2 \simeq (\text{Re } A_{\mu\mu})_{\text{SD}}^2 \frac{\text{BR}(K^+ \rightarrow e^+ \nu_e)}{\text{BR}(K^+ \rightarrow \mu^+ \nu_\mu)} \simeq 2 \times 10^{-14}$
† Author's note added in English proofreading. This estimation of $ (\text{Re } A_{\mu\mu})_{\text{SD}} ^2$ is model-dependent. In the recent paper by G Isidori and R Unterdorfer, hep-pub/031084, more conservative value ($< 2.5 \times 10^{-9}$) for this upper limit was obtained.	

the ‘golden decays’ $K \rightarrow \pi \nu \bar{\nu}$, owing to the essential contribution, due to photon exchanges, of the region of large distances to the processes involving $l^+ l^-$ pairs. Here, we shall only present a brief description of decays with charged leptons (Table 7, Fig. 10). A detailed analysis and references to original publications are to be found, for example, in reviews [39–42]; see also Refs [125–129].

5.4 Experimental studies of the decays $K^+ \rightarrow \pi^+ \nu \bar{\nu}$ and $K_L^0 \rightarrow \pi^0 \nu \bar{\nu}$ (state of affairs and prospects)

Investigation of the theoretically clean ‘golden decays’ $K^+ \rightarrow \pi^+ \nu \bar{\nu}$ and $K_L^0 \rightarrow \pi^0 \nu \bar{\nu}$ represents a very difficult experimental task. The expected probabilities of these processes in the SM are at the level of 10^{-10} or even lower.

Their reliable identification is rendered very difficult owing to the absence of rigorous kinematical selection criteria for the final $\pi \nu \bar{\nu}$ states and for numerous background processes, which are due to the decays $K^+ \rightarrow \mu^+ \nu_\mu$, $\pi^+ \pi^0$, $\mu^+ \nu \gamma$, $\pi^+ \pi^0 \gamma$, etc. At present, only the decay $K^+ \rightarrow \pi^+ \nu \bar{\nu}$ has been observed in the experiment BNL E787 [130–133], where two events have been found against a very low background. Let us consider the existing experimental situation and the prospects for further research.

5.4.1 Experiment BNL E787. In experiments (see Refs [130–133]), the decays of stopping K^+ -mesons are studied. The layout of the experiment E787 is presented in Fig. 11a. The experimental device is a solenoidal spectrometer with a

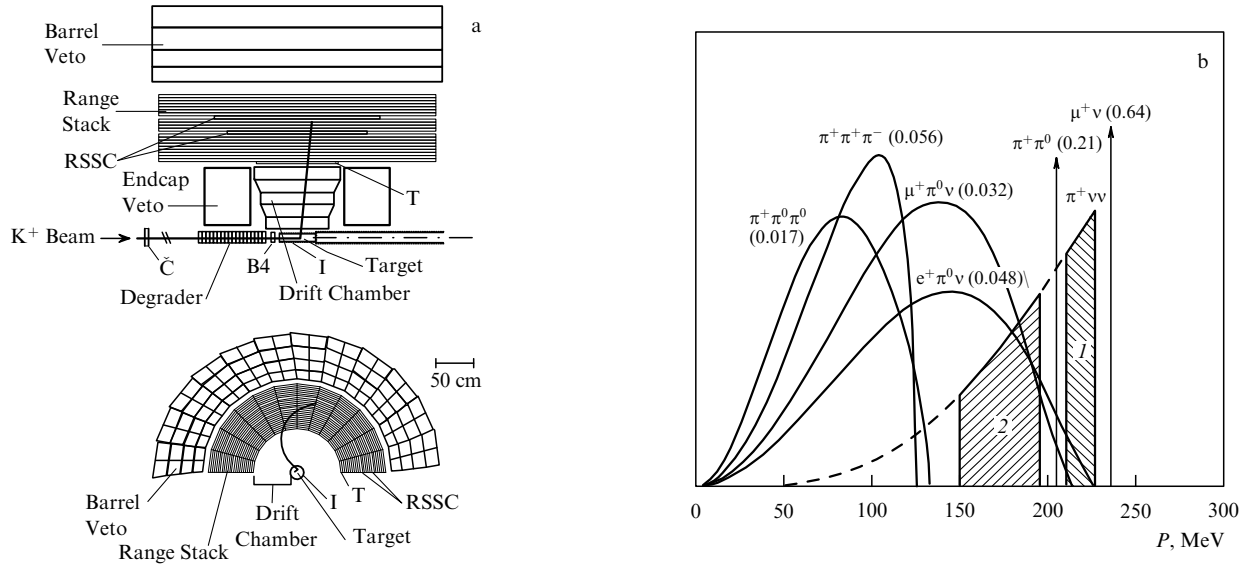


Figure 11. The layout of the experiment BNL E787 [130, 131]. (a) Lateral view (top) and rear view (bottom) for the upper half of the symmetric experimental device: K⁺ Beam — beam of separated kaons; C — Cherenkov counter for identification of the K⁺-mesons; B4, I, T — scintillation counters; Target — active target of scintillating fibre counters; Barrel Veto — lateral veto system of multisection calorimeters and scintillation counters, interlayered with lead; Endcap Veto — end part of the veto system consisting of CsI spectrometers; Drift Chamber — DC of magnetic spectrometer; Range Stack — scintillation range counters; RSSC — drift tubes. The veto system of the installation, which practically has a 4π-geometry, was very efficient in suppressing the photon background. Measurement of the pion momenta and path ranges in the magnetic spectrometer and the range counters, as well as registering of the decay chain π⁺ → μ⁺ → e⁺ permitted identification of pions in the fiducial region. (b) Momentum spectrum of secondary particles produced in the decays of stopped kaons: 1 and 2 — fiducial regions used in searches for K⁺ → π⁺ν̄ decays. The branching ratios for the respective decays are shown.

magnetic field of 1 T, directed along the axis of the incident beam. Upon being identified and slowed down, the K⁺-mesons from the separated beam are made to stop within the detector in a special active target consisting of scintillating fibres. For identifying the K⁺ → π⁺ν̄ decay, events were selected that corresponded to stops inside the target and to decays of K⁺-mesons involving the production of a single charged decay particle (with a time delay exceeding 2 ns relative to the stopping moment of the K⁺-mesons). The momentum, energy, and path range (in the Range Stack counters) of the decay particle were measured by a set of range counters.

The secondary particle stopped in a set of counters and was identified as π⁺-meson by its path range and the decay chain π⁺ → μ⁺ → e⁺. All this allowed the effective suppression of the background from the decay muons and from direct processes (without any delay) such as charge exchange or inelastic interaction of the incident particle. To identify the decay K⁺ → π⁺ν̄, events were selected, the kinematics of which differed from the kinematics of two-particle decays K⁺ → μ⁺ν_μ and K⁺ → π⁺π⁰. In Fig. 11b, two kinematical regions for searches of the decay K⁺ → π⁺ν̄ are shown. The background from additional particles and photons was suppressed by a very effective veto system with a 4π-geometry.

The most clean experimental conditions for revealing decays were realized in kinematical region 1 (211 < P_π < 229 MeV/c) lying above the pion peak from the K_{π2}-decay (Fig. 11b). A careful analysis of the background outside the signal region, carried out with the aid of uncorrelated selection criteria, has permitted ones to suppress its main sources and to verify that the expected background in the signal region is at the level of 0.1 event. Only after this was the signal region investigated, and two

K⁺ → π⁺ν̄ events were observed in it against an expected background not exceeding 0.15 event (Fig. 12a). This result corresponds to a decay probability [131]

$$\begin{aligned} \text{BR}(K^+ \rightarrow \pi^+ \nu \bar{\nu}) &= (1.57^{+1.75}_{-0.82}) \times 10^{-10}, \\ \text{BR}(K^+ \rightarrow \pi^+ \nu \bar{\nu}) &> 0.5 \times 10^{-10} \quad (90\% \text{ C.L.}), \\ \text{BR}(K^+ \rightarrow \pi^+ \nu \bar{\nu}) &< 3.9 \times 10^{-10} \quad (90\% \text{ C.L.}). \end{aligned} \quad (131)$$

Searches were also performed of K⁺ → π⁺ν̄ events in signal region 2 (140 < P_π < 195 MeV/c) lying below the peak from the K_{π2}-decay (Fig. 11b) [132]. Here, the background conditions were significantly worse than in region 1, owing to the background of K⁺ → π⁺π⁰ with subsequent interaction of the π⁺-meson, which reduced its apparent energy and path range. In signal region 2, one event was revealed against an expected background of 0.73 ± 0.18 event. This corresponds to the upper limit of the probability:

$$\text{BR}(K^+ \rightarrow \pi^+ \nu \bar{\nu}) < 4.2 \times 10^{-9}$$

for a weak (V-A)-interaction [which provides no new information as compared with formulas (131)], and

$$\text{BR}(K^+ \rightarrow \pi^+ \nu \bar{\nu}) < 4.7 \times 10^{-9} \quad (2.5 \times 10^{-9})$$

for the anomalous scalar (tensor) interaction causing the respective decay (all the boundaries given correspond to a 90% confidence level). As one can see from these data, making use of signal region 2 in future searches for K⁺ → π⁺ν̄ decays may be promising, if only it will be possible to suppress the background even more, which may be achieved by further enhancement of the efficiency of the veto system.

From the data of experiment E787, one can impose restrictions on the matrix element |V_{td}| and the parameter

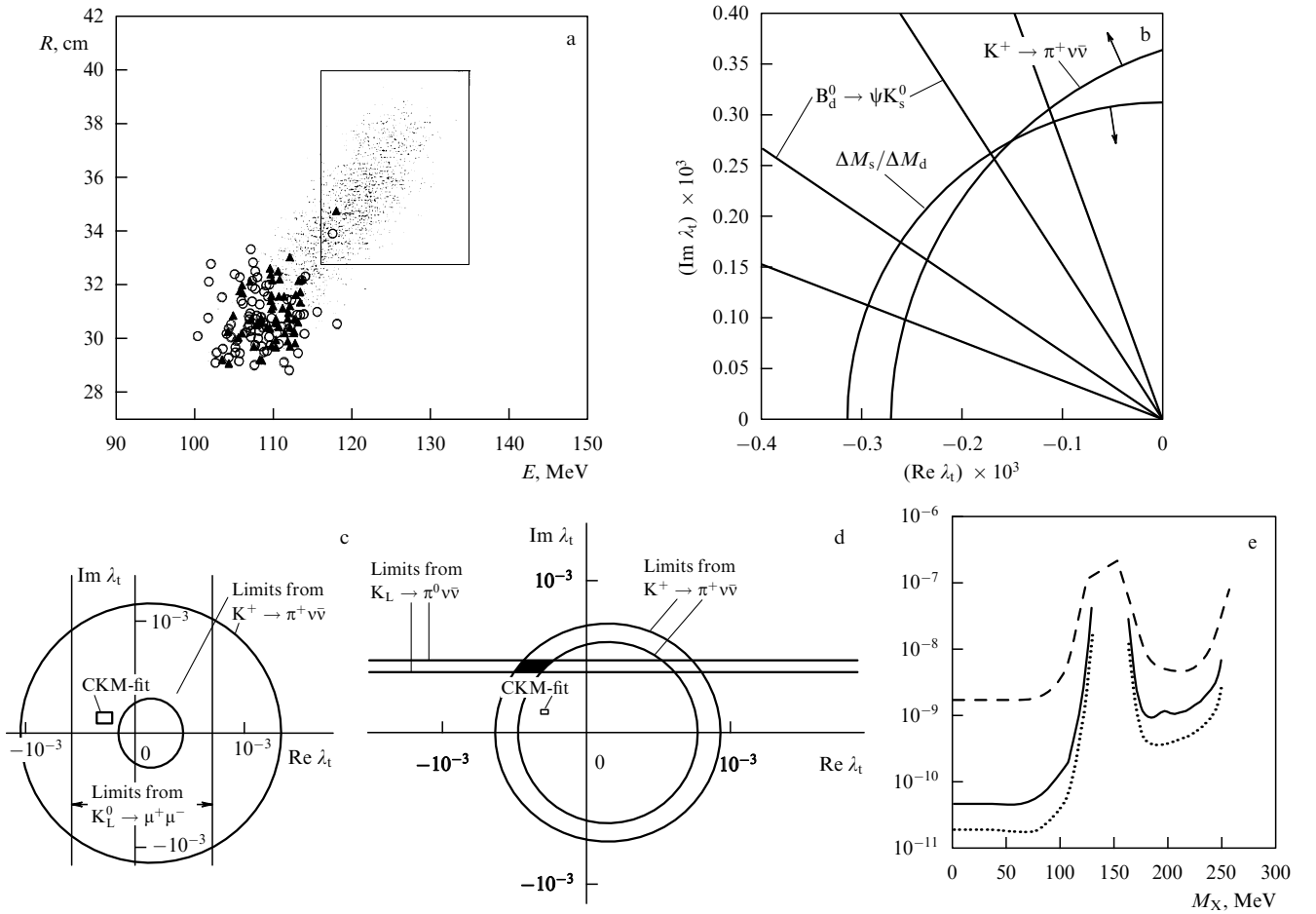


Figure 12. Results of experiment BNL E787 from the study of the rare decay $K^+ \rightarrow \pi^+ \nu \bar{\nu}$ [131, 132]. (a) Distribution of events selected at the concluding stage of data processing by the path range of π^+ -mesons, measured in the range counters, and by their energy determined from the momentum measurement in the magnetic spectrometer. The rectangle indicates the sensitivity region of the device for the decay $K^+ \rightarrow \pi^+ \nu \bar{\nu}$ (region I in Fig. 11b). Two registered $K^+ \rightarrow \pi^+ \nu \bar{\nu}$ events are shown, which were found during the processing of the exposures of 1998 (circles) and of 1995–1997 (small triangles). The group of events in the region of $E = 108$ MeV is due to the background from $K^+ \rightarrow \pi^+ \pi^0$. The points show the results of Monte Carlo simulation for the decays $K^+ \rightarrow \pi^+ \nu \bar{\nu}$. (b) Data on λ_t , obtained from measurements of $K^+ \rightarrow \pi^+ \nu \bar{\nu}$ and from experiments with B-mesons. The data from the asymmetry of $B_d^0(B_s^0) \rightarrow (J/\psi)K_S^0$ ($\sin 2\beta$) and from the $K^+ \rightarrow \pi^+ \nu \bar{\nu}$ -decay probability correspond to 90% C.L., and from $\Delta M_d/\Delta M_s$ to 95% C.L. The following experimental data are used in the plot: $\Delta M_s > 14.6 \text{ ps}^{-1}$; $0.56 \times 10^{-10} < \text{BR}(K^+ \rightarrow \pi^+ \nu \bar{\nu}) < 3.89 \times 10^{-10}$; $\sin 2\beta = 0.79 \pm 0.13$. (c) Data for $\text{Re } \lambda_t$ and $\text{Im } \lambda_t$, obtained from measurements of $\text{BR}(K^+ \rightarrow \pi^+ \nu \bar{\nu})$ in E787, and of $K_L^0 \rightarrow \mu^+ \mu^-$ in E871, and SM predictions (CKM-fit). (d) Expected results of measurements of $K^+ \rightarrow \pi^+ \nu \bar{\nu}$ and $K_L^0 \rightarrow \pi^0 \nu \bar{\nu}$ decays (given an accuracy in $|\lambda_t|$ and $\text{Im } \lambda_t$ of about 10%) under the assumption that the mean value of $\text{BR}(K^+ \rightarrow \pi^+ \nu \bar{\nu})$ will be the same as measured in experiments E787. The results of future experiments are compared with SM predictions (CKM-fit). (e) Limits imposed on the probabilities $\text{BR}(K^+ \rightarrow \pi^+ X^0)$ (90% C.L.) depending on the M_X mass. The solid curve corresponds to the result of Ref. [132], the dotted curve corresponds to the preceding result [134]. The points show the sensitivity of measurements [132] corresponding to a single observed event.

$\lambda_t = V_{ts}^* V_{td}$, which are independent of the restrictions following from experiments with B-mesons:

$$\begin{aligned}
 0.007 < |V_{td}| < 0.030 & \quad (68\% \text{ C.L.}), \\
 2.9 \times 10^{-4} < |\lambda_t| < 1.2 \times 10^{-3} & \quad (68\% \text{ C.L.}), \\
 -0.88 \times 10^{-4} < \text{Re } \lambda_t < 1.2 \times 10^{-3} & \quad (68\% \text{ C.L.}), \\
 \text{Im } \lambda_t < 1.1 \times 10^{-3} & \quad (90\% \text{ C.L.}).
 \end{aligned} \tag{132}$$

These measurements are illustrated in Fig. 12b, where for comparison the data of other experiments are also presented. In Figs 12c and 12d, the data for $\text{Re } \lambda_t$ and $\text{Im } \lambda_t$, obtained from experiments with the decays $K^+ \rightarrow \pi^+ \nu \bar{\nu}$ and $K_L^0 \rightarrow \mu^+ \mu^-$, are compared with predictions of the SM and possible prospects for future studies.

To conclude, we shall say a few words about decays such as $K^+ \rightarrow \pi^+ + X$, where X is a particle (or a pair of particles) that is not seen. Such processes could imitate decays

$K^+ \rightarrow \pi^+ \nu \bar{\nu}$. Thus, in models with extra dimensions, decays $K \rightarrow \pi + g$ that involved the emission of gravitons into space with extra dimensions, i.e., with a loss of energy and momentum in our space, were considered. However, estimation of the $K \rightarrow \pi + g$ -decay probabilities in models with extra dimensions leads to values of $\text{BR} < 10^{-12}$ (or even $\text{BR} \ll 10^{-12}$ [65]), i.e., they are practically unobservable. Most likely, there also exists a very small probability for a series of decays involving the emission of a pair of very light supersymmetric particles (photino, Goldstino); see Refs [110, 134–136]. Another hypothetical process of this type is represented by the so-called familon decays $K \rightarrow \pi + f$, where f is a neutral familon characterized by weak interaction and not manifested directly in the experiment [135]. Revelation of such decays is possible in studies of π -meson spectra (i.e., when a monochromatic line is identified).

From the BNL E787 experiment, restrictions have been obtained for the decay probability $\text{BR}(K^+ \rightarrow \pi^+ X^0)$ (where

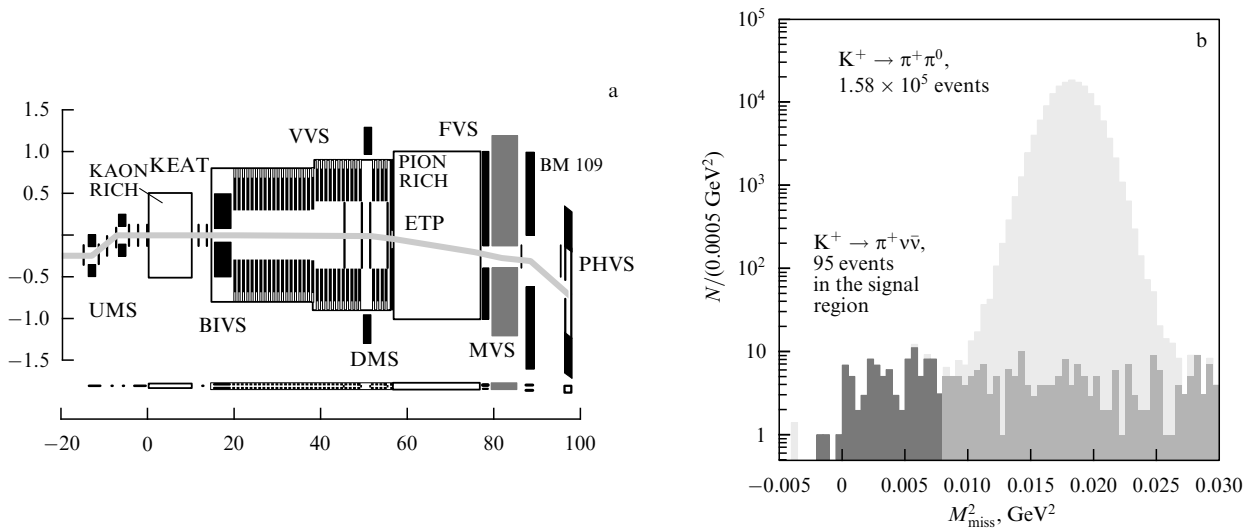


Figure 13. (a) Layout of the CKM detector [76]. The vertical and horizontal scales in the figure are in meters (the vertical and horizontal scales differ from each other). The lower part of the figure corresponds to a sole scale. The main elements of the detector are indicated in the figure (see text). (b) Expected results from the CKM experiment. The spectrum is shown of missing masses M_{miss}^2 in decays $K^+ \rightarrow \pi^+ + X_{\text{miss}}$ for combined results of measurements with magnetic spectrometers UMS and DMS and Cherenkov spectrometers KAON RICH and PION RICH (the results of calculations were obtained by GEANT–Monte Carlo for the CKM experiment). For the $(K^+ \rightarrow \pi^+ \nu \bar{\nu})$ decay, $M_{\text{miss}}^2 = M(\nu \bar{\nu})^2$. The region of registered $K^+ \rightarrow \pi^+ \nu \bar{\nu}$ events is shaded.

X^0 is a hypothetical stable weakly interacting particle) depending on the $m(X^0)$ mass; see Fig. 12e [132]. For a particle X^0 of very small mass (familon), the upper limit for the decay probability amounts to

$$\text{BR}(K^+ \rightarrow \pi^+ + f) < 5.9 \times 10^{-11} \text{ (90\% C.L.)}.$$

For the effective familon interaction characterized by the Lagrangian

$$L = \frac{1}{F} \partial^\mu f (\bar{u} \gamma_\mu s) + \text{h.c.}, \quad (133)$$

one can hence obtain the restriction $F > 7.6 \times 10^{11}$ GeV [134, 135]. A number of other results in the physics of rare K-decays, obtained with the experimental installation E787, are examined in reviews [39–41].

5.4.2 Experiment BNL E949. The successful results of BNL E787 experiment led to a certain modernization of this installation, with the purpose of enhancing its sensitivity and reducing the background, and gave rise, also, to a new experiment, BNL E949 [77], aimed at further studies of the $K^+ \rightarrow \pi^+ \nu \bar{\nu}$ decay and of a number of other rare kaon decays. The new experiment was initiated in 2001, had a very effective run in 2002 and is to continue in 2003–2004. Enhancement of the efficiency of the experimental facility and of its veto system, improvement of the beam, and prolongation of the data-taking runs lead ones to expect that the E949 experiment will succeed in registering about 10 decays $K^+ \rightarrow \pi^+ \nu \bar{\nu}$ and in measuring its probability with an accuracy of 30%.

5.4.3 Experiment CKM at Fermilab. A new stage in the investigation of $K^+ \rightarrow \pi^+ \nu \bar{\nu}$ decays may be achieved in the CKM experiment [76], recently approved at Fermilab, in which the detection of about 100 decays $K^+ \rightarrow \pi^+ \nu \bar{\nu}$ is expected. This experiment differs, in principle, from E787 and E949 in that in this experiment searches will be undertaken for $K^+ \rightarrow \pi^+ \nu \bar{\nu}$ decays in flight in a high-intensity

separated beam of K^+ -mesons with momenta of 22 GeV/ c and intensity of 3×10^7 K^+ -mesons per cycle (the repetition frequency amounts to 20 cycles/min with a cycle 1 s long). The general layout of the CKM detector is presented in Fig. 13a. The device includes the following main elements:

the system for identifying the primary K^+ -mesons in the beam and for double measurement of their kinematic parameters with the aid of the magnetic spectrometer UMS (with proportional chambers and the scintillation hodoscope KEAT) and a Cherenkov spectrometer KAON RICH for measuring the velocity of the incident particle;

a decay volume with a deep vacuum 30 m long, surrounded by a very effective veto system (the photon veto system VVS and the system BIVS for suppressing the background from interaction of the beam particles);

a system for identifying the decay pions with a magnetic spectrometer DMS with proportional tubes operating in the vacuum volume, two scintillation hodoscopes ETP, and a Cherenkov spectrometer PION RICH for measuring the velocities of secondary particles (double measurement of the kinematics of the secondary pion);

a highly efficient photon spectrometer MVS with scintillating CsI crystals, which serves as part of the photon veto system of the CKM detector (the spectrometer FVS also serves for the recording of photons in other kaon decays, which will be studied in the CKM experiment; see Ref. [76]);

the muon hodoscopic veto system MVS used for additional suppression of the muon background (at a level of 10^{-5});

the photon veto system PHVS situated at the end of the experimental device (after the additional magnet BM109), covering the beam region and intended for enhancing the hermeticity of the entire photon veto system of the installation (the beam is deviated by the magnet and does not impinge upon the PHVS system).

Thus, identification of the decay $K^+ \rightarrow \pi^+ \nu \bar{\nu}$ is realized by double measurement of the kaon decay kinematics in a vacuum (for suppression of the background from the decay

Table 8. Expected background conditions in the CKM experiment [76].

Source of background	Effective BR value in units of 10^{-12}
Decays:	
$K^+ \rightarrow \mu^+ \nu_\mu$	< 0.04
$K^+ \rightarrow \pi^+ \pi^0$	< 3.7
$K^+ \rightarrow \mu^+ \nu_\mu \gamma$	< 0.09
Random coincidences of two K^+ -decays	< 0.51
Interactions:	
$K^+ A \rightarrow K_L^0 X$ $\quad \quad \quad \downarrow$ $\quad \quad \quad \pi^+ e^- \nu_e$	< 0.14
$K^+ A \rightarrow \pi^+ X$ (within the matter of the tracking system)	< 4.0
$K^+ A \rightarrow \pi^+ X$ (in the residual gas at 10^{-6} Torr)	< 2.1
Total background	< 10.6
<i>Note.</i> The effective values of BR are presented for residual background processes. For the decay being studied, $BR(K^+ \rightarrow \pi^+ \nu \bar{\nu}) \sim 10^{-10}$.	

$K^+ \rightarrow \pi^+ \pi^0$) and by application of a highly effective veto system for suppression of the background of photons and muons from K -decays. Studies will be carried out at the new separated kaon beam with superconducting high-frequency resonators, presently under construction at Fermilab. The kaon beam is formed by the proton beam of the main injector with a proton energy $E_p = 120$ GeV. The beam momentum is 22 GeV/ c and its total intensity is 50 MHz (30 MHz — beam kaons, 7.5 MHz — pion contamination, and 7.5 MHz — muon contamination of the beam). In two years of measurements with the CKM detector, about 100 $K^+ \rightarrow \pi^+ \nu \bar{\nu}$ events are planned to be registered (Fig. 13b) against a background of less than 10 events (the capacity of the CKM detector for suppression of various background processes is presented in Table 8). Measurements in the CKM experiment are to be started in 2007–2008.

5.4.4 The decay $K^+ \rightarrow \pi^+ \nu \bar{\nu}$ for stopping kaons at the J-PARK accelerator. A new proposal for a study of the decay $K^+ \rightarrow \pi^+ \nu \bar{\nu}$ in the case of stopping K -mesons from the separated beam of the J-PARK (KEK) accelerator presently under construction was submitted in the form of a letter of intent [137] at the end of 2002. In its idea, this experiment should be very close to the E787 and E949 BNL experiments which were discussed in Sections 5.4.1 and 5.4.2. Expectations are that it will be possible to achieve a sensitivity several times higher in this method by introducing a series of improvements (a more powerful and compact superconducting solenoidal magnet, a higher degree of segmentation of the detecting instruments, a better quality of the kaon beam, new front-end electronics of the data acquisition system) and to register about 50 $K^+ \rightarrow \pi^+ \nu \bar{\nu}$ events. The experiment is supposed to start soon after the new high-intensity J-PARK accelerator will be commissioned.

5.4.5 Investigation of the decay $K_L^0 \rightarrow \pi^0 \nu \bar{\nu}$. As compared to the decay $K^+ \rightarrow \pi^+ \nu \bar{\nu}$ discussed above, identification of the very rare decay $K_L^0 \rightarrow \pi^0 \nu \bar{\nu}$ represents a task that is by an order of magnitude more difficult, owing to the expected

probability of the process being smaller in the SM [see Eqn (124)] and to more complicated identification of the decay, in which no charged particles are produced in the final state, being more complicated. Therefore, up to now only quite weak direct restrictions have been imposed on this decay (KTeV [138]):

$$BR(K_L^0 \rightarrow \pi^0 \nu \bar{\nu}) < 5.9 \times 10^{-7} \quad (90\% \text{ C.L.}).$$

However, from the modelless limit (113) and the data on the probability $BR(K^+ \rightarrow \pi^+ \nu \bar{\nu})$ (131), it is possible to obtain a stronger restriction

$$BR(K_L^0 \rightarrow \pi^0 \nu \bar{\nu}) < 4.37 BR(K^+ \rightarrow \pi^+ \nu \bar{\nu}) \\ = 1.7 \times 10^{-9} \quad (90\% \text{ C.L.}). \quad (134)$$

All these limits lie very far from the value expected within the framework of the SM [see Eqn (130)]:

$$BR(K_L^0 \rightarrow \pi^0 \nu \bar{\nu})_{SM} = (2.49 \pm 0.42) \times 10^{-11}.$$

It must be emphasized that joint measurement of $BR(K^+ \rightarrow \pi^+ \nu \bar{\nu})$ and $BR(K_L^0 \rightarrow \pi^0 \nu \bar{\nu})$ is very important, since from the kaon data it will be possible to determine independently the parameters of the unitary triangle. A more detailed discussion of the importance of these experiments for testing the SM and its possible extensions is presented in the next section.

The experimental prospects, however, of these studies are less clear than for studies of the decay $K^+ \rightarrow \pi^+ \nu \bar{\nu}$. First of all, it must be noted that the project KAMI [139], which was very promising from the point of view of studying the decay $K_L^0 \rightarrow \pi^0 \nu \bar{\nu}$, was not approved at Fermilab owing to its complexity and high cost. Within this project measurements were to be carried out in the high-intensity K_L^0 beam of average momentum 10 GeV/ c at the main Fermilab Main Injector. The installation KAMI, which was to represent a further development of the KTeV, was intended to include a high-precision photon spectrometer for the detection of π^0 -mesons and a high-efficiency veto system for suppression of the photon background. Estimates have shown that with the KAMI installation one could expect to register about 100 $K_L^0 \rightarrow \pi^0 \nu \bar{\nu}$ events in a year of running with a background of about 10–15 events. KAMI was also to include a magnetic spectrometer that would make it possible to study other rare K_L^0 -decays ($K_L^0 \rightarrow \pi^0 1^+ 1^-$, $\pi^+ \pi^- e^+ e^-$, $\mu^+ \mu^- e^+ e^-$, and others) simultaneously. Regrettably, this project will not be implemented in near future.

At present, BNL has approved the KOPIO project [140] which should be carried out in the low-energy K_L^0 beam of the AGS BNL accelerator (with an average momentum of 0.7 GeV/ c) involving time-of-flight measurement of the K_L^0 -meson energy (referred to the high-frequency system of the accelerator). The direction of the outgoing photons produced in the π^0 -decay and their energy will be measured with γ -spectrometers with preradiators. The high-efficiency veto system and kinematical selection criteria will permit the suppression of the background and the identification of the decay $K_L^0 \rightarrow \pi^0 \nu \bar{\nu}$. The general layout of the KOPIO experiment is presented in Fig. 14. It is assumed that in two years of measurements 50 $K_L^0 \rightarrow \pi^0 \nu \bar{\nu}$ events can be registered, given the signal-to-background ratio at a level of 2. Measurements are expected to start in this experiment approximately in 2007–2008.

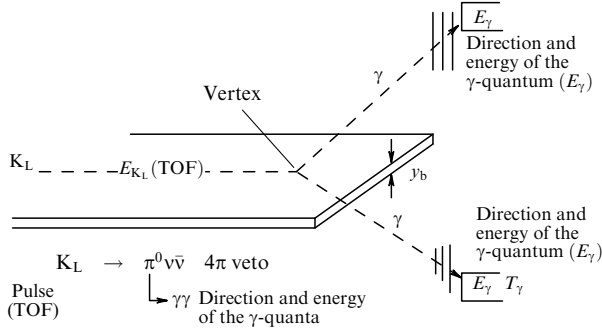
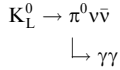


Figure 14. Layout of experiment KOPIO [140]. Identification of the decay



is performed by measurement of the energy of the K_L^0 -meson by the time-of-flight (TOF) technique, as well as energy and direction of the two outgoing photons. The vertical coordinate of the decay vertex is determined by the small vertical thickness (y_b) of the primary neutral beam. The mass m_{π^0} is determined from a 3C-fit.

In the experiment KEK E391A [141] in the K_L^0 -meson beam with average momentum 2 GeV/c, which is presently under way, only a limited sensitivity

$$\text{BR}(K_L^0 \rightarrow \pi^0 \nu \bar{\nu}) \lesssim 10^{-10}$$

will be achieved. However, at the next stage of the experiment, which is planned to be carried out at the new accelerator J-PARK (being presently under construction), a K_L^0 -meson beam of very high intensity is supposed to be prepared, which will permit the detection of about 10^3 $K_L^0 \rightarrow \pi^0 \nu \bar{\nu}$ events. It is still not clear whether such a high sensitivity will actually be achieved, since no project of this experiment exists yet. Nevertheless, one can hope that in experimental studies of $\text{BR}(K_L^0 \rightarrow \pi^0 \nu \bar{\nu})$ a sensitivity will be obtained, in the near future, of the same order of magnitude as in the $K^+ \rightarrow \pi^+ \nu \bar{\nu}$ experiments, i.e., that both probabilities will be measured with an error not exceeding 10%.

6. Rare decays of K- and B-mesons, CP violation in the Standard Model and beyond it

6.1 Joint analysis of the data from experiments with K- and B-mesons and searches for manifestations of New Physics

The investigation of rare decays of K- and B-mesons is entering a new phase that, in the nearest decade, will allow us to obtain high-precision data on a series of FCNC processes, the probabilities of which can be reliably predicted within the SM. Thus, great possibilities open up for testing the subtle predictions of this model for processes at small distances and the mechanisms of direct violation of CP invariance, and for searches of NP effects. Indeed, within the framework of the SM, theoretically clean kaon and B-meson measurements (first of all, studies of the decays $K^+ \rightarrow \pi^+ \nu \bar{\nu}$, $K_L^0 \rightarrow \pi^0 \nu \bar{\nu}$, of the ratio $\Delta M_d/\Delta M_s$ of the mixing parameters, and of CP-violating asymmetry in certain B-decays) will permit the researchers to determine independently the position of the vertex of the unitary triangle (see Fig. 4) and its parameters with better accuracy than we have now (see Fig. 5). If the data of independent experiments

are found to diverge, this will inevitably testify in favor of the existence of NP effects which were not taken into account in the analysis within the framework of the SM. In the present section we shall discuss redetermination of parameters and possible manifestations of new physical effects in rare FCNC processes. As a rule, the influence of new effects can be expected in the region of small distances, in the highest order (with respect to weak interaction) in the loop diagrams.

Since NP may manifest itself differently in FCNC processes changing flavors by $\Delta F = 2$ (mixing processes $K^0 \rightleftharpoons \bar{K}^0$, $B^0 \rightleftharpoons \bar{B}^0$, $D^0 \rightleftharpoons \bar{D}^0$) and by $\Delta F = 1$ (rare decays), independent studies of these two types of FCNC processes are needed. Here, the quantum number F characterizes a given flavor: strangeness S , beauty B , and charm C . For transitions with $\Delta F = 1$, the best prospects open up in high-precision studies of theoretically clean $K \rightarrow \pi \nu \bar{\nu}$ decays, for which quite accurate and reliable predictions can be made within the SM. Deviations from these predictions will unambiguously testify in favor of the existence of NP. The observation of $K^+ \rightarrow \pi^+ \nu \bar{\nu}$ in the BNL E787 experiment has demonstrated a real possibility for studying very rare decays, which are difficult to identify, and has opened the door to further high-precision studies of events of this class.

6.1.1 Independent determination of angle β of the unitary triangle in experimental studies of the decays $K^+ \rightarrow \pi^+ \nu \bar{\nu}$ and $K_L^0 \rightarrow \pi^0 \nu \bar{\nu}$ and CP asymmetry of $B_d^0(\bar{B}_d^0) \rightarrow (J/\psi)K_S^0$. From formula (117) one can see that the decay probability $\text{BR}(K^+ \rightarrow \pi^+ \nu \bar{\nu})$ is represented in the $(\bar{\rho}, \bar{\eta})$ -plane by an ellipse with its center on the $\bar{\rho}$ -axis. Indeed,

$$(\rho_0 - \bar{\rho})^2 + (\sigma\bar{\eta})^2 = c_0^2$$

is an equation of the ellipse

$$\frac{(\rho_0 - \bar{\rho})^2}{c_0^2} + \frac{\bar{\eta}^2}{(c_0/\sigma)^2}$$

with its center at point $\rho_0 = 1.39$ on the $\bar{\rho}$ -axis and with semiaxes c_0 and c_0/σ . Here,

$$c_0^2 = \frac{\sigma \text{BR}(K^+ \rightarrow \pi^+ \nu \bar{\nu})}{K_+ |V_{cb}|^4 X^2(x_t)}$$

can be found from measurements of $\text{BR}(K^+ \rightarrow \pi^+ \nu \bar{\nu})$. Since $\sigma = 1.051$, this ellipse is close to a circle. The vertex of the unitary triangle can be determined from the data on $\text{BR}(K^+ \rightarrow \pi^+ \nu \bar{\nu})$ and $\text{BR}(K_L^0 \rightarrow \pi^0 \nu \bar{\nu})$ decays as the intersection of the ellipse $(\rho_0 - \bar{\rho})^2 + (\sigma\bar{\eta})^2 = c_0^2$ [equation (117)] and the horizontal straight line $\bar{\eta} = \text{const}$ [from Eqn (118)] (see also Fig. 4).

The results of the two measurements will enable us to determine $\sin 2\beta$ from the data of the kaon experiments, and the respective measurement precisions are not distorted by the error in the determination of $|V_{cb}|^4$; for more details see Appendix I. We shall denote this result by $(\sin 2\beta)_K$. The uncertainty expected in the future K-meson experiments will amount to $\delta(\sin 2\beta)_K = \pm 0.07$, which is comparable to the measurement accuracy of $(\sin 2\beta)_B$ in experimental studies of the $B_d^0(\bar{B}_d^0) \rightarrow (J/\psi)K_S^0$ -decay asymmetry [see Eqn (99)]. The precision of B-meson measurements will be improved by that time.

Thus, from the data of kaon and B-meson experiments it will be possible to obtain independently information on the

direct processes of CP-invariance violation. The mechanisms manifested in K- and B-meson processes, considered here, are of a different nature. We recall that the FCNC decays $K^+ \rightarrow \pi^+ \nu \bar{\nu}$ and $K_L^0 \rightarrow \pi^0 \nu \bar{\nu}$ proceed in the higher orders in the weak interaction. As mentioned earlier, the vertex $Z\bar{s}$ for the diagrams of these decays may be especially sensitive to the contributions of new interactions. At the same time, the decays $B_d^0(\bar{B}_d^0) \rightarrow (J/\psi)K_S^0$, from the charge asymmetry $a_{\psi K}$ of which $(\sin 2\beta)_B$ is determined directly [see Eqn (98)] in the SM, proceed in first order in weak interactions (they are the decay processes $b \rightarrow c\bar{c}s$ and $\bar{b} \rightarrow \bar{c}c\bar{s}$).

The asymmetry $a_{\psi K}$ is due to the relative phase between the loop amplitude of $(B_d^0 \rightleftharpoons \bar{B}_d^0)$ mixing and the amplitude of the decay $b \rightarrow c\bar{c}s$ which proceeds in the tree approximation (see, for example, Ref. [32]). At the same time, as noted above, CP nonconservation in the decay $K_L^0 \rightarrow \pi^0 \nu \bar{\nu}$ is governed by the relative phase between the $(K^0 \rightleftharpoons \bar{K}^0)$ -mixing amplitude and the FCNC process $s \rightarrow d\nu \bar{\nu}$ related to the loop diagrams presented in Fig. 8. Within the framework of the SM, the asymmetry $a_{\psi K}$ and the relation between the probabilities $BR(K^+ \rightarrow \pi^+ \nu \bar{\nu})$ and $BR(K_L^0 \rightarrow \pi^0 \nu \bar{\nu})$ are determined by one and the same parameter $\sin 2\beta$ of the unitary triangle (see Appendix I). Therefore, in the SM, for which direct CP nonconservation is governed by a single phase in the CKM matrix, independent measurements with B- and K-mesons will result in the same value for the angle β : $(\sin 2\beta)_B = (\sin 2\beta)_K$.

It must once more be noted that the predictions for both the decays $K^+ \rightarrow \pi^+ \nu \bar{\nu}$ and $K_L^0 \rightarrow \pi^0 \nu \bar{\nu}$ as well as the decays $B_d^0(\bar{B}_d^0) \rightarrow (J/\psi)K_S^0$ are theoretically quite reliable within the SM. Therefore, the coincidence of the results of these two experimental cycles will permit us to test very rigorously the SM predictions for the mechanism of direct violation of CP invariance. At the same time, other mechanisms of CP nonconservation, related to supersymmetry, to additional Higgs doublets, etc., may alter the results of kaon and B-meson experiments in absolutely diverse ways. In the decays $B_d^0(\bar{B}_d^0) \rightarrow (J/\psi)K_S^0$, these mechanisms will, most likely, manifest themselves, first of all, in the amplitudes of $(B^0 \rightleftharpoons \bar{B}^0)$ mixing, determined by loop diagrams at small distances and sensitive to the contribution of new heavy particles. The first-order process $b \rightarrow c\bar{c}s$ may remain without any significant changes. The asymmetry $a_{\psi K}$ in B-decays will, now, be determined not only by the CKM phase (resulting in the angle β), but also by the new additional phase ϕ_d^{NP} (see Section 4.4). Therefore, the asymmetry of B-decays will alter and assume the form

$$a_{\psi K} = (\sin 2\beta)_B = \sin(2\beta + \phi_d^{\text{NP}}).$$

We now know from experiments that the phase ϕ_d^{NP} is, most likely, rather small.

In the case of decays $K \rightarrow \pi \nu \bar{\nu}$, new mechanisms, as mentioned earlier, may significantly affect loop FCNC processes which are sensitive to effects at small distances. Here, the ratio of the probabilities of $K^+ \rightarrow \pi^+ \nu \bar{\nu}$ and $K_L^0 \rightarrow \pi^0 \nu \bar{\nu}$ decay processes will, most likely, change, and then the quantity $(\sin 2\beta)_K$ will also change and become $\sin(2\beta + \phi_K^{\text{NP}})$, where ϕ_K^{NP} is the new phase manifested in kaon processes. Thus, if there do exist new mechanisms of CP nonconservation due to NP, the values of $(\sin 2\beta)_B$ and $(\sin 2\beta)_K$ may diverge significantly, and future experiments will permit the establishment of this fact unambiguously. The results to be obtained by future experiments are illustrated by the data presented in Fig. 15 (see Ref. [76]).

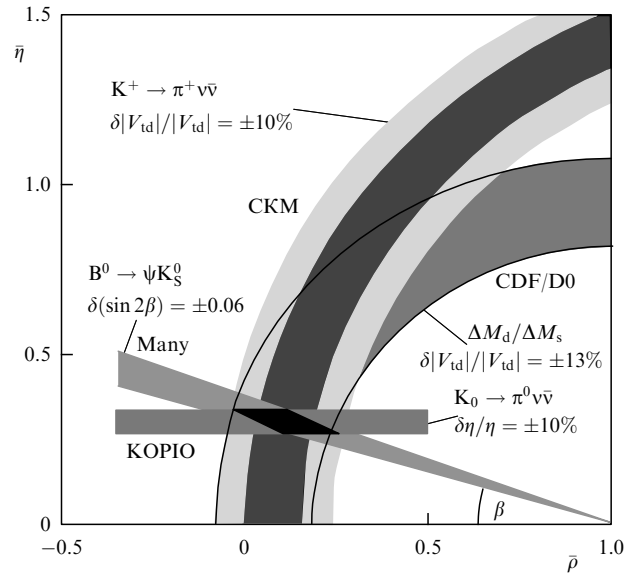


Figure 15. Expected values of the angle β and of the parameters $\bar{\rho}$, $\bar{\eta}$, which may be derived from the results of future experiments with kaons and B-mesons (see Ref. [76]).

6.1.2 Correlations between $BR(K^+ \rightarrow \pi^+ \nu \bar{\nu})$ and data on $|V_{ub}/V_{cb}|$, $\Delta M_d/\Delta M_s$, and $\sin 2\beta$ from B-decays. Within the framework of the SM, other correlations may be obtained between the results of experiments with B-mesons and data for the probabilities of rare $K \rightarrow \pi \nu \bar{\nu}$ decays (see, for example, Refs [58, 114, 119]). Thus, the position of the vertex of the unitary triangle can be determined from data on $BR(K^+ \rightarrow \pi^+ \nu \bar{\nu})$ and the ratio $|V_{ub}/V_{cb}| = R_b/\sqrt{\sigma} \lambda$ [see Eqn (28)] as the intersection of the ellipse $(\rho_0 - \bar{\rho})^2 + (\sigma\bar{\eta})^2 = c_0^2$ and the circle $\bar{\rho}^2 + \bar{\eta}^2 = R_b^2$ (see Fig. 4). Then one obtains

$$(\rho_0 - \bar{\rho})^2 + (\sigma\bar{\eta})^2 = c_0^2, \quad \sigma^2 \bar{\eta}^2 = \sigma^2 R_b^2 - \sigma^2 \bar{\rho}^2, \\ \bar{\rho} = \frac{1}{1 - \sigma^2} \left[\rho_0 \pm \sqrt{\sigma^2 \rho_0^2 + (1 - \sigma^2)(c_0^2 - \sigma^2 R_b^2)} \right].$$

The properties of the unitary triangle are only satisfied by the solution exhibiting the sign ‘-’ of the square root in this relationship.

Thus, from intersection of the ellipse ($K^+ \rightarrow \pi^+ \nu \bar{\nu}$) and the circle (R_b) one can find the following relations for the parameters of the unitary triangle:

$$\bar{\rho} = \frac{1}{1 - \sigma^2} \left[\rho_0 - \sqrt{\sigma^2 \rho_0^2 + (1 - \sigma^2)(c_0^2 - \sigma^2 R_b^2)} \right], \\ \bar{\eta} = \sqrt{R_b^2 - \bar{\rho}^2}, \\ c_0^2 = \frac{\sigma BR(K^+ \rightarrow \pi^+ \nu \bar{\nu})}{K_+ |V_{cb}|^4 X^2(x_t)}, \\ R_t^2 = (1 - \bar{\rho})^2 + \bar{\eta}^2 = 1 + R_b^2 - 2\bar{\rho}. \quad (135)$$

An essential test for the SM is the independent determination of the matrix element $|V_{td}|$ from measurement of the probability $BR(K^+ \rightarrow \pi^+ \nu \bar{\nu})$ and from data on $\Delta M_d/\Delta M_s$ [see Appendix II and Eqn (90)]. The uncertainty in determining $|V_{td}|$ within these two experimental approaches is expected to correspond to $\delta|V_{td}|/|V_{td}| \lesssim 0.1$.

Very interesting results can be obtained from data on the ratio $\Delta M_d/\Delta M_s$ between the mass differences, from measurements of $\sin 2\beta$ by the asymmetry of $B_d^0(\bar{B}_d^0) \rightarrow (J/\psi)K_S^0$ decays, and from data on the probability $\text{BR}(K^+ \rightarrow \pi^+ \nu\bar{\nu})$ [119]. Since from the properties of the unitary triangle it follows that $\bar{\rho} = 1 - R_t \cos \beta$, and $\bar{\eta} = R_t \sin \beta$, then

$$\begin{aligned} \text{BR}(K^+ \rightarrow \pi^+ \nu\bar{\nu}) &= K_+ |V_{cb}|^4 X^2(x_t) \frac{1}{\sigma} [(\sigma\bar{\eta})^2 + (\rho_0 - \bar{\rho})^2] \\ &= K_+ |V_{cb}|^4 X^2(x_t) \\ &\times \frac{1}{\sigma} [(\sigma R_t \sin \beta)^2 + (1 + \Delta - 1 + R_t \cos \beta)^2] \\ &= K_+ |V_{cb}|^4 X^2(x_t) \left[(\sigma R_t^2 \sin^2 \beta + \frac{1}{\sigma} (\Delta + R_t \cos \beta)^2 \right] \\ &\simeq K_+ |V_{cb}|^4 X^2(x_t) [R_t^2 + \Delta^2 + 2\Delta R_t \cos \beta] \end{aligned} \quad (136)$$

(if one neglects the factor $\sigma = 1.051$).

At the same time, it will subsequently be possible to determine the side of the unitary triangle (90):

$$R_t \simeq \frac{\xi}{\lambda} \left(\frac{\Delta M_d}{\Delta M_s} \right)^{1/2} \left(\frac{M_s}{M_d} \right)^{1/2}$$

from measurements of the ratio between the mixing parameters, $\Delta M_d/\Delta M_s$. Equation (136) represents a unique relationship which relates the results of three experiments: the measurement of $\text{BR}(K^+ \rightarrow \pi^+ \nu\bar{\nu})$, the measurement of $\sin 2\beta$ from the asymmetry of $B_d^0(\bar{B}_d^0) \rightarrow (J/\psi)K_S^0$ decays, and the measurement of the ratio of the mixing parameters for B_d^0 - and B_s^0 -mesons, which have a theoretically clean interpretation within the framework of the SM⁷. Therefore, in the next decade, during which new experimental data on $\text{BR}(K^+ \rightarrow \pi^+ \nu\bar{\nu})$ and $\Delta M_d/\Delta M_s$ will be obtained, relation (136) will permit us to implement one of the most important tests of the SM for the dynamics of quark flavors.

6.1.3 The quantity $\text{BR}(K^+ \rightarrow \pi^+ \nu\bar{\nu})$ and searches for New Physics. Searches for NP manifestations in the decay $K^+ \rightarrow \pi^+ \nu\bar{\nu}$ can be conducted by estimating the upper limit for the branching ratio of this decay in the SM and by comparison of this upper limit with existing and future data on $\text{BR}(K^+ \rightarrow \pi^+ \nu\bar{\nu})_{\text{expt}}$.

The upper limit $\text{BR}(K^+ \rightarrow \pi^+ \nu\bar{\nu})_{\text{SM, max}}$ is determined by two methods that, to a significant extent, are independent. One of them (proposed in Ref. [58]) takes advantage of relation (136), in which the upper limit for R_t is found from the presently available lower limit for the $(B_s^0 \rightleftharpoons \bar{B}_s^0)$ -mixing parameter $\Delta M_s > 14.4 \text{ ps}^{-1}$ (95% C.L.), the respective upper limit for $\Delta M_d/\Delta M_s < 0.035$ (95% C.L.), and relation (90):

$$\begin{aligned} R_t &= \frac{\xi}{\lambda} \left(\frac{\Delta M_d}{\Delta M_s} \right)^{1/2} \left(\frac{M_s}{M_d} \right)^{1/2} \left[1 - \frac{\lambda^2}{2} (1 - 2\bar{\rho}) \right] \\ &\simeq \frac{\xi}{\lambda} \left(\frac{\Delta M_d}{\Delta M_s} \right)^{1/2} \left(\frac{M_s}{M_d} \right)^{1/2}. \end{aligned}$$

⁷ We note that it will be possible to consider the predictions for $\Delta M_d/\Delta M_s$ theoretically clean only after resolving the problem of ξ , which originated in connection with the uncertainty in chiral extrapolation to the mass m_d of the light quark (see Section 4.3 and Table 5).

Representing the factor $[(\sigma\bar{\eta})^2 + (\rho_0 - \bar{\rho})^2]$ in Eqn (136) in the following approximate form

$$\begin{aligned} [(\sigma\bar{\eta})^2 + (\rho_0 - \bar{\rho})^2] &\simeq [\bar{\eta}^2 + (1 - \bar{\rho})^2] + 2(1 - \bar{\rho})\Delta + \Delta^2 \\ &= R_t^2 + 2(1 - \bar{\rho})\Delta + \Delta^2, \end{aligned}$$

one can show that for a given side R_t of the unitary triangle the decay branching ratio $\text{BR}(K^+ \rightarrow \pi^+ \nu\bar{\nu})$ increases with $(1 - \bar{\rho})$ — that is, its maximum corresponds to $\bar{\eta} = 0$ in the expression for $R_t = [\bar{\eta}^2 + (1 - \bar{\rho})^2]^{1/2}$ [or $\sin \beta = 0, \cos \beta = 1$ in Eqn (136)]. Then, it is readily calculated that

$$\begin{aligned} \text{BR}(K^+ \rightarrow \pi^+ \nu\bar{\nu})_{\text{max}} &= K_+ |V_{cb}|^4 X^2(x_t) \frac{1}{\sigma} [(1 - \bar{\rho})^2 + 2(\bar{\rho} - 1)\Delta + \Delta^2] \\ &= K_+ |V_{cb}|^4 X^2(x_t) \frac{1}{\sigma} [(1 - \bar{\rho}) + \Delta]^2 \\ &= K_+ |V_{cb}|^4 X^2(x_t) \frac{1}{\sigma} [R_t + \Delta]^2. \end{aligned} \quad (137)$$

Applying various estimates for the limits of the parameters present in Eqns (136) and (137), it is possible to derive the upper limit for the decay probability [119]:

$$\text{BR}(K^+ \rightarrow \pi^+ \nu\bar{\nu})_{\text{SM, max}; R_t} < 13.2 \times 10^{-11} \quad (138)$$

(this complies with the requirement that relation (137) be saturated with the upper limits $(\Delta M_d/\Delta M_s)^{1/2} < 0.18$, $|V_{cb}| < 0.044$, $\xi < 1.3$, $\Delta < 0.48$, and $X(x_t) < 1.57$). The upper limit (138) is independent of the uncertainties related to the ε_K -hyperbola (i.e., is independent of \hat{B}_K) and of the ratio $|V_{ub}|/|V_{cb}|$. It corresponds to three standard deviations from the value

$$\text{BR}(K^+ \rightarrow \pi^+ \nu\bar{\nu})_{\text{SM}} = (7.72 \pm 2.10) \times 10^{-11}$$

obtained in the same work [119] by fitting the CKM parameters for formula (117). This limit, however, depends on ξ and $|V_{cb}|$. It was obtained for the previous value of $\xi = 1.16 \pm 0.06$. For $\xi = 1.32 \pm 0.10$ [101], limit (138) increases up to 16×10^{-11} . The accuracy of this method for determining the upper limit will be essentially enhanced in the future (after the measurement of ΔM_s and resolution of the ξ -problem).

In the other method, proposed in Ref. [118] and discussed in Section 5, the upper limit for the probability $\text{BR}(K^+ \rightarrow \pi^+ \nu\bar{\nu})_{\text{SM, max}}$ is obtained from the probability distribution in Fig. 9b and from the data (123) determined by applying the technique of the K-meson unitary triangle. In this method, the upper limit comes to

$$\text{BR}(K^+ \rightarrow \pi^+ \nu\bar{\nu})_{\text{SM, max}} < 10 \times 10^{-11} \quad (99\% \text{ C.L.}), \quad (139)$$

and this quantity is independent of $|V_{cb}|, |V_{ub}|, \Delta M_{d,s}$, and ξ . Application of additional information on $|V_{cb}|, |V_{ub}|$, and ΔM_d [see formula (129)] permits us to somewhat lower the upper limit (down to $\text{BR}(K^+ \rightarrow \pi^+ \nu\bar{\nu})_{\text{SM, max}} < 9.8 \times 10^{-11}$), but enhances its dependence upon existing systematic uncertainties. The accuracy of this method increases with the precision of lattice QCD calculations of the parameter \hat{B}_K and the measurement accuracy of a_{ψ_K} .

Although the upper limit (139) does not yet contradict the experimental value

$$\text{BR}(\text{K}^+ \rightarrow \pi^+ \nu \bar{\nu})_{\text{expt}} = (15.7_{-8.2}^{+17.5}) \times 10^{-11}$$

($\text{BR} > \text{BR}_{\text{min}} = 5 \times 10^{-11}$) [131], the question naturally arises concerning the new interpretation of the physics of the decay $\text{K}^+ \rightarrow \pi^+ \nu \bar{\nu}$, if the limit (139) is actually violated in subsequent, more accurate, experiments. The interest in such a possibility is also aroused by the mean value of this branching ratio presently being greater than twice the SM prediction. The first essential test of the anomalous increase in the branching ratio is expected in the BNL E949 experiment, in which the probability $\text{BR}(\text{K}^+ \rightarrow \pi^+ \nu \bar{\nu})$ may be measured with an error of 30–40%. In the subsequent CKM FNAL experiment, the uncertainty of these measurements will be reduced to 10%, which will make possible a critical test of the restriction (139) and investigation of the correlations between the data of different measurements, based on the analysis of relations (136) and (137).

If the future, more accurate, experiments BNL E949 and CKM FNAL result in a statistically reliable value of $\text{BR}(\text{K}^+ \rightarrow \pi^+ \nu \bar{\nu})$ exceeding the limit (139), this will unambiguously testify in favor of the existence of NP. Then, comparison of various results considered in this section will permit us to draw certain conclusions concerning the nature of these effects. Thus, in Ref. [119], where in estimating the upper limit (138) use was made of data on $\Delta M_d/\Delta M_s$ and ξ , two scenarios were considered. In the first, the large value of $\text{BR}(\text{K}^+ \rightarrow \pi^+ \nu \bar{\nu})$ was explained by the manifestation of NP in the decay $s \rightarrow d \nu \bar{\nu}$ owing to modification of the Z ds vertex, and certain difficulties are pointed out, which are encountered by such an explanation. In the other scenario, the manifestation of NP is attributed to the ($\text{B}^0 \rightleftharpoons \bar{\text{B}}^0$)-mixing process. In this case, a large value of $\text{BR}(\text{K}^+ \rightarrow \pi^+ \nu \bar{\nu})$ can be obtained if $\bar{\rho} < 0$ [this is seen from the structure of formulas (117) and (137)].

A positive value of $\bar{\rho}$ is related, within the framework of the SM, to the general global fit of information in the $(\bar{\eta}, \bar{\rho})$ -plane. If the data on $\text{B}^0 \rightleftharpoons \bar{\text{B}}^0$ are excluded from this fit (they may be distorted by NP effects), values of $\bar{\rho} < 0$ become possible and even more probable (see Fig. 16). The necessity of obtaining independent information about the sign of $\bar{\rho}$ from data on the decays $\text{B} \rightarrow \text{K}\pi$, $\text{b} \rightarrow \text{d}l^+l^-$, and $\text{b} \rightarrow \text{s}l^+l^-$ is stressed. We shall again raise the issue of possible negative $\bar{\rho}$ values in Section 6.2.2.

The upper limit (139) obtained in Ref. [118], which is independent of data on $|\Delta M_{d,s}|$ and ξ , permits us to approach the interpretation of NP effects in a different manner. In this case, a large value of $\text{BR}(\text{K}^+ \rightarrow \pi^+ \nu \bar{\nu})$ may be attributed either to new effects in $s \rightarrow d \nu \bar{\nu}$, or to ε_{K} , i.e., $\text{K}^0 \rightleftharpoons \bar{\text{K}}^0$, or to $\text{B}_d^0(\bar{\text{B}}_d^0) \rightarrow (\text{J}/\psi)\text{K}_S^0$ decays (via the new phase between the amplitudes of the decay $\text{b} \rightarrow \text{c}\bar{\text{s}}$ and the $\text{B}_d^0 \rightleftharpoons \bar{\text{B}}_d^0$ amplitude). However, as has already been pointed out, this phase is quite small. Then, the large value of $\text{BR}(\text{K}^+ \rightarrow \pi^+ \nu \bar{\nu})$ requires, for its explanation, NP manifestations in the K-sector. Another possibility, related to the angle β having two values when $\sin 2\beta = 0.734 \pm 0.054$ [see formula (99)], is dealt with in Section 6.2.

One can hope that in the future more complete information on the decays $\text{K}^+ \rightarrow \pi^+ \nu \bar{\nu}$ and $\text{K}_L^0 \rightarrow \pi^0 \nu \bar{\nu}$ as well as on a number of B-decays will permit us to clarify this picture and to achieve significant success in searching for NP effects in rare FCNC processes.

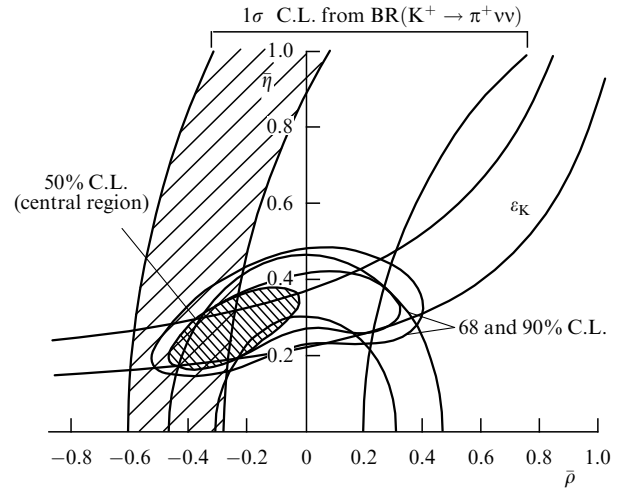


Figure 16. Admissible region of parameters for the vertex of the unitary triangle in the $(\bar{\rho}, \bar{\eta})$ -plane under the assumption that B^0 -mixing processes are determined by NP mechanisms and that their data cannot be applied for studying the unitary triangle [119]. Shown are the regions of the ε_{K} -hyperbola, the $|V_{\text{ub}}/V_{\text{cb}}|$ circle, and the shaded region determined by data on $\text{K}^+ \rightarrow \pi^+ \nu \bar{\nu}$. Contours are shown of the admissible $\bar{\rho}, \bar{\eta}$ region that correspond to 68 and 90% C.L., and also shown are the restrictions imposed by the region of central values for $\text{K}^+ \rightarrow \pi^+ \nu \bar{\nu}$ in E787 [131] (50% C.L.) assuming the accuracy of future E949 experiments [77] to be enhanced by a factor of two.

6.2 Models with New Physics and their influence on the $\text{K} \rightarrow \pi \nu \bar{\nu}$ -decay probabilities

In this section we shall briefly consider some models with NP and compare their predictions for the decay probabilities of $\text{K} \rightarrow \pi \nu \bar{\nu}$ and $\text{K}_L^0 \rightarrow \pi^0 l^+ l^-$ with the respective SM estimates and with available experimental data. The below-discussed NP effects illustrate the broad spectrum of new ideas to be found in the literature (see Refs [142–177]). The results of these discussions are presented in Tables 9–11 and, in particular, in the resultant Table 12 (see below), that sums up the predictions of various models.

Table 9. Modified loop functions $X(x_i)_{\text{SM}}(x_i; 1/R)$ and $S_0(x_i)_{\text{SM}} \rightarrow F_{\text{tt}}(x_i; 1/R)$ in the MFV model with universal extra dimensions and compactification radius R [144].

$1/R, \text{ GeV}$	$F_{\text{tt}}(x_i; 1/R)$	$X(x_i; 1/R)$
200	2.813	1.826
250	2.664	1.731
300	2.582	1.674
400	2.500	1.613
SM	$S_0(x_i)_{\text{SM}} = 2.38$	$X(x_i)_{\text{SM}} = 1.52$

As shown in Ref. [43], the effective Hamiltonian describing $\text{K} \rightarrow \pi \nu \bar{\nu}$ decays has the following form in practically all models with NP with left-handed neutrinos:

$$H_{\text{eff}} = \frac{2G_{\text{F}}}{\sqrt{2}} \frac{\alpha}{\pi \sin^2 \vartheta_{\text{W}}} \lambda_i \bar{\nu} \gamma^\mu (X_{\text{L}} P_{\text{L}} + X_{\text{R}} P_{\text{R}}) d \bar{\nu}_l \gamma_\mu P_{\text{L}} \nu_l + \text{h.c.} \quad (140)$$

Here, $P_{\text{L}} = (1 + \gamma_5)/2$ and $P_{\text{R}} = (1 - \gamma_5)/2$ in the notation adopted in this review correspond to left and right currents (with respective amplitudes X_{L} and X_{R}).

Table 10. Data on the characteristics of certain decays in the vectorlike model [153] with singlet exotic quarks of the ‘upper’ (T) or ‘lower’ (B) types.

Quantity	Model 1 (mixing with singlet T-quark)		Model 2 (mixing with singlet B-quark)		SM
	Minimum value	Maximum value	Minimum value	Maximum value	
$ V_{td} $	4×10^{-5}	44×10^{-3}	6×10^{-3}	13×10^{-3}	7×10^{-3}
$ V_{ts} $	0.2×10^{-2}	6.0×10^{-2}	5×10^{-2}	4.4×10^{-2}	3.9×10^{-2}
$\Delta M_s/\Delta M_d$	26.7	77	26.7	67	36
$\text{BR}(K_L^0 \rightarrow \pi^0 \nu \bar{\nu})$	~ 0	4.4×10^{-10}	~ 0	1.6×10^{-10}	$(2.60 \pm 0.52) \times 10^{-11}$
$\frac{\text{BR}(K_L^0 \rightarrow \pi^0 \nu \bar{\nu})}{\text{BR}(K^+ \rightarrow \pi^+ \nu \bar{\nu})}$	~ 0	4.35	~ 0	4.34	0.37 ± 0.09
Asymmetry $a_{D_s^+ D_s^-}$ in decays $B_s^0(\bar{B}_s^0) \rightarrow D_s^+ D_s^-$	-1	+1	-1	+1	$\simeq 0.03$

Table 11. Upper limits on the branching ratios for the decays $K \rightarrow \pi \nu \bar{\nu}$ and $K_L^0 \rightarrow \pi^0 e^+ e^-$ CP-dir versus the parameters λ_t and A_t in the supersymmetric model [72, 157].

A_t	Probability	λ_t (SM)	λ_t from unitarity of the CKM matrix
$A_t > 0$	$\text{BR}(K_L^0 \rightarrow \pi^0 \nu \bar{\nu})$	0.7×10^{-10}	0.9×10^{-10}
	$\text{BR}(K_L^0 \rightarrow \pi^0 e^+ e^-)_{\text{CP-dir}}$	1.1×10^{-11}	1.3×10^{-11}
	$\text{BR}(K^+ \rightarrow \pi^+ \nu \bar{\nu})$	1.7×10^{-10}	2.0×10^{-10}
$A_t < 0$	$\text{BR}(K_L^0 \rightarrow \pi^0 \nu \bar{\nu})$	0.8×10^{-10}	4.0×10^{-10}
	$\text{BR}(K_L^0 \rightarrow \pi^0 e^+ e^-)_{\text{CP-dir}}$	2.0×10^{-11}	5.9×10^{-11}
	$\text{BR}(K^+ \rightarrow \pi^+ \nu \bar{\nu})$	1.7×10^{-10}	2.7×10^{-10}

Hamiltonian (140) results in the following probabilities of $K \rightarrow \pi \nu \bar{\nu}$ decays:

$$\text{BR}(K^+ \rightarrow \pi^+ \nu \bar{\nu}) = 4.42 \times 10^{-11} \left| \frac{\lambda_t(X_L + X_R)}{\lambda^5} \right|^2, \tag{141}$$

$$\text{BR}(K_L^0 \rightarrow \pi^0 \nu \bar{\nu}) = 1.93 \times 10^{-10} \left| \text{Im} \frac{\lambda_t(X_L + X_R)}{\lambda^5} \right|^2.$$

As can be seen from comparison of Eqn (141) with Eqns (114) and (115), in the SM $X_R = 0$, and $X_L = X(x_t)(1 + \delta(x_c)\lambda_c/\lambda_t)$. In various models with NP, the expressions for X_L and/or X_R are modified (this is illustrated below by several examples).

In analyzing predictions in models with NP it is necessary to take into account restrictions on the parameters of these models, obtained from comparison with available experimental data for rare K- and B-decays, $(K^0 \rightleftharpoons \bar{K}^0)$ - and $(B^0 \rightleftharpoons \bar{B}^0)$ -mixing processes, CP-nonconservation parameters ε_K , $\varepsilon'/\varepsilon_K$, and $a_{\psi K}$, and, also, from the upper limits for particle dipole moments and studies of electroweak processes in experiments at colliders. These requirements have not always been fulfilled, especially because a number of predictions for new effects were made before recent experimental data became available.

As we shall see below, existing experimental data for $\text{BR}(K^+ \rightarrow \pi^+ \nu \bar{\nu})$ play an important role. They significantly restrict the possibility for new physical effects to manifest themselves, which should not contradict the restrictions [131]

$$5 \times 10^{-11} < \text{BR}(K^+ \rightarrow \pi^+ \nu \bar{\nu})_{\text{expt}} < 39 \times 10^{-11} \quad (90\% \text{ C.L.}).$$

A different situation occurs in the case of the decays $K_L^0 \rightarrow \pi^0 \nu \bar{\nu}$. The expected probabilities for this decay are

only limited by the modelless upper limit (113):

$$\frac{\text{BR}(K_L^0 \rightarrow \pi^0 \nu \bar{\nu})_{\text{SM}}}{\text{BR}(K^+ \rightarrow \pi^+ \nu \bar{\nu})_{\text{SM}}} = \frac{K_0}{K_+} \frac{(\text{Im} \lambda_t)^2}{[\sigma(x_c) \text{Re} \lambda_c + \text{Re} \lambda_t]^2 + (\text{Im} \lambda_t)^2} < \frac{r_0}{r_+} \frac{\tau(K_L^0)}{\tau(K^+)} = 4.37. \tag{142}$$

Hence, and from Eqns (117) and (118), it follows that the manifestation of new contributions to the decay $K_L^0 \rightarrow \pi^0 \nu \bar{\nu}$, which proceeds with violation of CP invariance, may result in an increase of the probability of this process by more than an order of magnitude ($|\text{Im} \lambda_t|^2 \rightarrow (\text{Im} \lambda_t + S)^2 \gtrsim 10 |\text{Im} \lambda_t|^2$), while altering the value of $\text{BR}(K^+ \rightarrow \pi^+ \nu \bar{\nu})$ by a factor not exceeding two, which does not contradict experimental data.

As noted in Section 2.3, for the effects of NP to be manifested, it is necessary to consider two different scenarios:

(1) A limited modification of the SM takes place (so-called MFV models with minimum flavor violation [72–74]), in which case there exist no new types of interactions or new CP-violating weak phases, while all NP manifestations reduce to modification of the Inami–Lim loop functions: $F_{\text{SM}}^i \rightarrow F_{\text{SM}}^i + F_{\text{NP}}^i$ [see Eqn (35)]. To be more concrete, the substitution $S_0(x_t) \rightarrow F_{tt}$ is made in expressions (79), (84), (86), and (87) due to $K^0 \rightleftharpoons \bar{K}^0$ - and $B^0 \rightleftharpoons \bar{B}^0$ -mixing processes, while the substitution $X(x_t) \rightarrow \bar{X}$ is made in the relations (114), (115), (117), and (118) for probabilities of decays $K \rightarrow \pi \nu \bar{\nu}$. Here F_{tt} and \bar{X} are the respective modified loop functions.

(2) More complex extensions of the SM are realized by taking into account changes in the quark dynamics, possible manifestations of new types of interactions, new flavors, and new CP-nonconserving complex phases. Such manifestations of NP bring about the modification of the amplitudes of the processes dealt with in accordance with relation (36).

An interesting property of the class of models with minimum flavor violation consists in the possibility of finding for them a so-called universal unitary triangle common to all MFV models and the SM [48, 74]. To determine the universal unitary triangle, measurements are used of quantities that are weakly influenced by NP and permit us, therefore, to find the parameters of the universal triangle in a modelless manner. The best variables for such an analysis happen to be the data on R_t , which are to be obtained from measurements of the ratio $\Delta M_d/\Delta M_s$ of mass differences (upon removal of uncertainties in ξ), the data on R_b from measurement of the ratio $|V_{ub}/V_{cb}|$, and the data for $\sin 2\beta$, found from the CP-odd asymmetry of

$B_d^0(\bar{B}_d^0) \rightarrow (J/\psi)K_S^0$ decays. At the same time, the values of R_t , obtained only from measuring ΔM_d , and the data for ε_K cannot be applied to determining the parameters of the universal unitary triangle, since they are described by the modified loop function F_{tt} and are model-dependent. The most detailed analysis of methods for determining parameters of the universal unitary triangle and its comparison with the unitary triangle in the SM can be found in Ref. [48].

6.2.1 New Physics models of the MFV type. In an MFV model with minimum supersymmetric extension of the SM (MFV MSSM) [142], the main corrections to the new generalized Inami–Lim functions are due to the contribution from charged Higgs bosons H^\pm and supersymmetric charginos χ_j^\pm ($j = 1, 2$) interacting with the lower quarks d, s, b and upper superquarks $\tilde{u}, \tilde{c},$ and \tilde{t} (Fig. 8c). In this case, the contribution of supersymmetric particles reduces, as a rule, the probabilities of $K \rightarrow \pi\nu\bar{\nu}$ and $K_L^0 \rightarrow \pi^0 e^+ e^-$ decays. Indeed, the influence of virtual supersymmetric particles results in modification of the Inami–Lim loop functions present in the expressions for the $K \rightarrow \pi\nu\bar{\nu}$ -decay probabilities and for $|\varepsilon_K|$:

$$\begin{aligned} X(x_t) &\rightarrow \tilde{X}(x_t; \text{SUSY}) = \tilde{X}, \\ S_0(x_t) &\rightarrow F_{tt}(x_t; \text{SUSY}) = F_{tt}. \end{aligned} \quad (143)$$

Here, the relations (75), (114), and (115) for $|\varepsilon_K|$ and $\text{BR}(K \rightarrow \pi\nu\bar{\nu})$ are also altered:

$$\begin{aligned} |\varepsilon_K| &= L\hat{B}_K \text{Im } \lambda_t [N_c(\varepsilon_K) - \eta_{tt} S_0(x_t) \text{Re } \lambda_t] \\ &\rightarrow L\hat{B}_K \text{Im } \lambda_t [N_c(\varepsilon_K) - \eta_{tt} F_{tt} \text{Re } \lambda_t], \\ \text{BR}(K^+ \rightarrow \pi^+ \nu\bar{\nu}) &= \frac{K_+ X^2(x_t)}{\lambda^2} \{ [f(x_c) + \text{Re } \lambda_t]^2 + (\text{Im } \lambda_t)^2 \} \\ &\rightarrow \frac{K_+ \tilde{X}^2}{\lambda^2} \{ [f(x_c) + \text{Re } \lambda_t]^2 + (\text{Im } \lambda_t)^2 \}, \\ \text{BR}(K_L^0 \rightarrow \pi^0 \nu\bar{\nu}) &= \frac{K_0 X^2(x_t)}{\lambda^2} (\text{Im } \lambda_t)^2 \rightarrow \frac{K_0 \tilde{X}^2}{\lambda^2} (\text{Im } \lambda_t)^2. \end{aligned} \quad (144)$$

As is shown by the analysis in Ref. [142], processes with $\Delta S = 2$ modify $S_0(x_t)$ so that $F_{tt} > S_0(x_t)$. Since the value of $|\varepsilon_K|$ is fixed ($|\varepsilon_K| = 2.282 \times 10^{-3}$), an increase in F_{tt} results in a decrease in $\text{Re } \lambda_t, \text{Im } \lambda_t$, which in turn reduces the $K \rightarrow \pi\nu\bar{\nu}$ -decay probability. The influence of processes with $\Delta S = 1$ on the function \tilde{X} may in part compensate, or even somewhat overcompensate, for such a reduction of $\text{BR}(K \rightarrow \pi\nu\bar{\nu})$. In accordance with calculations [142], the expected values of decay probabilities lie within the range

$$\begin{aligned} 0.65 &\leq \frac{\text{BR}(K^+ \rightarrow \pi^+ \nu\bar{\nu})_{\text{MSSM}}}{\text{BR}(K^+ \rightarrow \pi^+ \nu\bar{\nu})_{\text{SM}}} \leq 1.03, \\ 0.41 &\leq \frac{\text{BR}(K_L^0 \rightarrow \pi^0 \nu\bar{\nu})_{\text{MSSM}}}{\text{BR}(K_L^0 \rightarrow \pi^0 \nu\bar{\nu})_{\text{SM}}} \leq 1.03, \\ 0.48 &< \frac{\text{BR}(K_L^0 \rightarrow \pi^0 e^+ e^-)_{\text{MSSM}}}{\text{BR}(K_L^0 \rightarrow \pi^0 e^+ e^-)_{\text{SM}}} \Big|_{\text{CP-dir}} < 1.1. \end{aligned} \quad (145)$$

The minimum and maximum values of the kaon decay probabilities are determined by the parameters of the

MSSM model. A more detailed investigation of the model has been carried out in Ref. [113].

In Ref. [142], the signs of the generalized loop functions \tilde{X} and F_{tt} were assumed to be the same as in the SM ($F_{tt}, \tilde{X} > 0$). In MFV models, however, a more complex modification of the loop functions can be expected, in which case their signs are altered (i.e., $F_{tt}, \tilde{X} < 0$ become possible [47, 143]). In Appendix II, the modified expressions are presented for a number of quantities considered above, which take into account possible changes in the signs of F_{tt} and \tilde{X} .

In MFV theories with loop functions of different signs, broader limits have been obtained for possible predictions of the $K \rightarrow \pi\nu\bar{\nu}$ -decay probabilities. Thus, in the phenomenological model [47, 143], differing values of $\text{BR}(K_L^0 \rightarrow \pi^0 \nu\bar{\nu})$ have been obtained for $\tilde{X} > 0$ and $\tilde{X} < 0$ depending on $\text{BR}(K^+ \rightarrow \pi^+ \nu\bar{\nu})$ and the asymmetry $a_{\psi K}$ in $B_d^0(\bar{B}_d^0) \rightarrow (J/\psi)K_S^0$ decays. Existing experimental data permit ones to obtain the absolute upper limit for all versions of MFV models:

$$\text{BR}(K_L^0 \rightarrow \pi^0 \nu\bar{\nu}) < 70 \times 10^{-11} \text{ (90\% C.L.)}.$$

Note, also, that for each pair of $\text{BR}(K^+ \rightarrow \pi^+ \nu\bar{\nu})$ and $a_{\psi K}$ values, two values for $\text{BR}(K_L^0 \rightarrow \pi^0 \nu\bar{\nu})$, corresponding to $\tilde{X} > 0$ and to $\tilde{X} < 0$, can be predicted (see Fig. 17). For

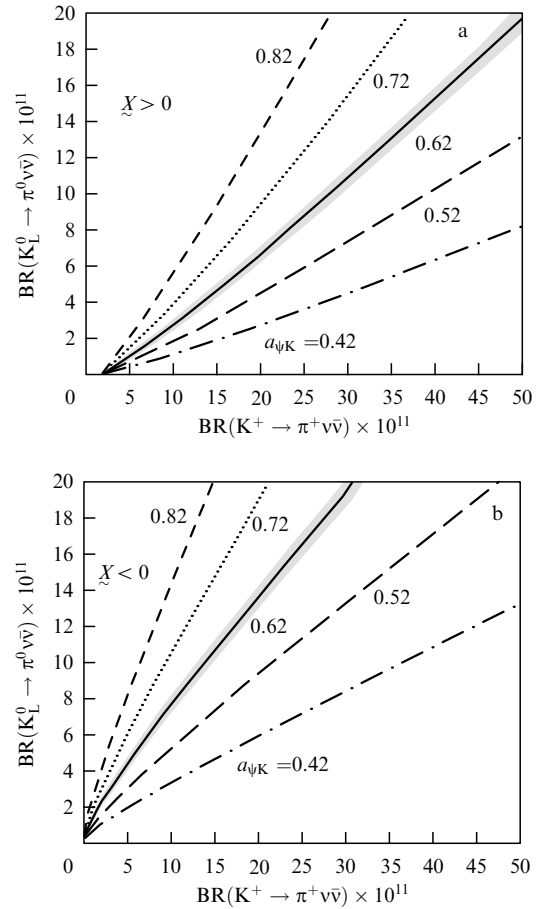


Figure 17. Dependence of $\text{BR}(K_L^0 \rightarrow \pi^0 \nu\bar{\nu})$ on $\text{BR}(K^+ \rightarrow \pi^+ \nu\bar{\nu})$ in the MFV model [143] for various values of the asymmetry $a_{\psi K}$ in $B_d^0(\bar{B}_d^0) \rightarrow (J/\psi)K_S^0$ decays for $\tilde{X} > 0$ (a) and $\tilde{X} < 0$ (b). The belts for $a_{\psi K} = 0.62$ illustrate the influence of uncertainties: they correspond to $P_c(\nu\bar{\nu}) = 0.40 \pm 0.06$.

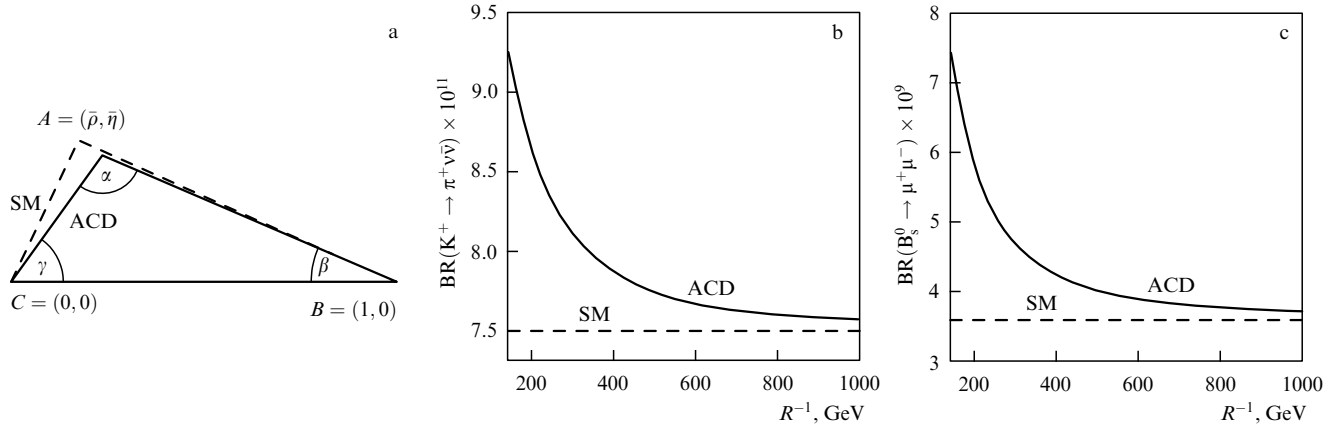


Figure 18. Predictions of the MFV model with extra dimension [144]: (a) unitary triangle in the SM and in the ACD model; (b, c) dependences of BR(K⁺ → π⁺νν̄) and BR(B_s⁰ → μ⁺μ⁻) predictions upon the energy scale of compactification R⁻¹.

example, for BR(K⁺ → π⁺νν̄) = 10 × 10⁻¹¹ and a_{ψK} = 0.7, the predicted values are the following:

$$\text{BR}(K_L^0 \rightarrow \pi^0 \nu \bar{\nu}) = \begin{cases} 3.8 \times 10^{-11} & (\tilde{\chi} > 0), \\ 10.0 \times 10^{-11} & (\tilde{\chi} < 0). \end{cases}$$

Thus, the sign ambiguity for the generalized loop functions $\tilde{\chi}$ in MFV models can be resolved with the aid of future data for BR(K⁺ → π⁺νν̄) and BR(K_L⁰ → π⁰νν̄).

For the upper limit of BR(K⁺ → π⁺νν̄)_{expt} ≤ 39 × 10⁻¹¹ (90% C.L.) [131], the following absolute upper limits of BR(K_L⁰ → π⁰νν̄) in MFV have been found [143]:

$$\text{BR}(K_L^0 \rightarrow \pi^0 \nu \bar{\nu})_{\text{MFV, max}} \leq \begin{cases} 27 \times 10^{-11} & (\tilde{\chi} > 0), \\ 45 \times 10^{-11} & (\tilde{\chi} < 0). \end{cases} \quad (146)$$

In the MFV models considered, the relation is established between the K_L⁰ → π⁰νν̄- and B → X_sνν̄-decay probabilities [27, 47, 143]:

$$\text{BR}(K_L^0 \rightarrow \pi^0 \nu \bar{\nu}) = 42.3 (\text{Im } \lambda_t)^2 \frac{0.104}{\text{BR}(B \rightarrow X_c e \bar{\nu}_e)} \times \left| \frac{V_{cb}}{V_{ts}} \right|^2 \left| \frac{f(z)}{0.54} \right| \text{BR}(B \rightarrow X_s \nu \bar{\nu})$$

(f(z) = 0.54 ± 0.04). From this relation, estimates of Im λ_t in MFV models with F_{tt} > 0 and F_{tt} < 0 (based on data for |ε_K| and ΔM_{d,s}), and the experimental upper limit

$$\text{BR}(B \rightarrow X_s \nu \bar{\nu}) < 6.4 \times 10^{-4} \quad (90\% \text{ C.L.}),$$

the following upper restriction

$$\text{BR}(K_L^0 \rightarrow \pi^0 \nu \bar{\nu})_{\text{MFV}} < 92 \times 10^{-11} \quad (90\% \text{ C.L.}).$$

has been obtained. Although this restriction is weaker than that given in Eqn (146), this limit may be significantly lowered as experiments with B-mesons will be developed.

One more model with NP, pertaining to the MFV type, was considered in Ref. [144]. In this work, the influence is estimated of the theory with extra dimensions (the so-called ACD model with one universal extra dimension [145]) on the parameters of the unitary triangle and the probabilities of some rare decays of K- and B-mesons. In

ACD theory, it is an extra dimension that has the compactification radius R corresponding to the energy scale 1/R ≳ 200–250 GeV.

The model under consideration also pertains to the class of MFV models, since the influence of the Kaluza–Klein structures in ACD theory modifies the Inami–Lim loop functions for FCNC processes. The modified loop functions now depend on the compactification radius:

$$X(x_t) \rightarrow \tilde{X}\left(x_t; \frac{1}{R}\right), \quad S_0(x_t) \rightarrow F_{tt}\left(x_t; \frac{1}{R}\right). \quad (147)$$

The dependence of the modified functions (147) upon 1/R is presented in Table 9. The quantity F_{tt}(x_t; 1/R) increases as compared with S₀(x_t), and this growth results in a decrease of Re λ_t and Im λ_t (as in Ref. [142]; see above). Here, the form of the SM unitary triangle is somewhat altered (see Fig. 18a). The side R_{t,ACD} of the unitary triangle is reduced, which corresponds to a change in the angles γ and α (γ_{ACD} < γ_{SM} and α_{ACD} > α_{SM}). The growth of $\tilde{X}(x_t; 1/R)$ overcompensates for the decrease in Re λ_t and Im λ_t and leads to a certain increase in the probabilities of a number of rare decays (Fig. 18b). As the compactification radius R decreases, the probability values also decrease and approach the SM predictions.

Extension of the SM, satisfying MFV criteria, is considered from a general viewpoint in Refs [146, 147]. Such an extension represents a low-energy effective field theory, in which the same fundamental fields, as in the SM, take part. A version of MFV has also been considered with two doublets of Higgs bosons. Flavor nonconservation and violation of CP invariance are described in this theory by the V_{CKM} matrix, as in the SM. Deviations from the SM are of a universal character in the K- and B-meson sectors of the theory.

Predicted violations of the SM are determined by local FCNC operators of dimensionality 6. Their amplitudes turn out to be proportional to universal parameters for FCNC transitions between external quarks of the ‘lower’ type:

$$(\lambda_{\text{FC}})_{ij} = \begin{cases} \lambda_t^2 V_{it}^* V_{tj}, & i \neq j; \quad i, j = d, s, b, \\ 0, & i = j. \end{cases} \quad (148)$$

Here, deviations from the SM in the effective low-energy theory are characterized by the energy cutoff scale A. Their

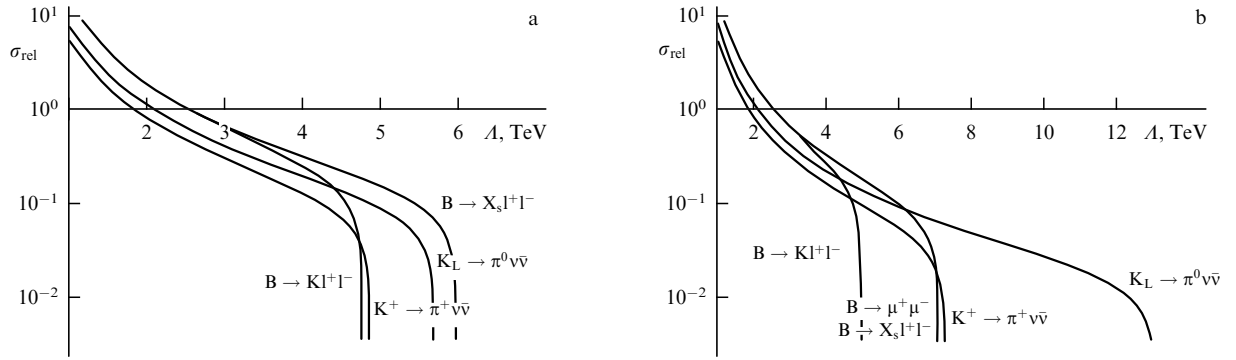


Figure 19. Comparison of the effectiveness of various rare decays of K- and B-mesons for determining the cutoff parameter A in MFV models under the assumption that the precision (with which the respective matrix elements V_{CKM} are known) amounts to 10% (a) and 1% (b) [146, 147]. The vertical scale shows the relative accuracy in measurement of decay branching ratios for values expected within the SM.

amplitudes turn out to be proportional to $\pm 1/A^2$ and vanish as $A \rightarrow \infty$ (the signs ‘ \pm ’ are governed by the constructive or destructive character of interference of these additional amplitudes with the SM amplitudes). The quantity A should not exceed several TeV (for the removal of dangerous divergences in the masses of Higgs bosons).

As a rule, violations of the SM in MFV theory do not exceed 10–30%. Therefore, theoretically clean (within the framework of the SM) rare decays such as $K \rightarrow \pi \nu \bar{\nu}$ may turn out to be especially promising in searching for such comparatively small effects. In Fig. 19, the boundaries of the cutoff parameter A of the theory are presented, which may be obtained in future studies of these and of other rare decays. It is also mentioned that some theoretically clean quantities (the CP asymmetry $a_{\psi K}$ in $B^0(\bar{B}^0) \rightarrow (J/\psi)K_S^0$ decays and the ratio $\Delta M_d/\Delta M_s$ of mass differences) are determined by the ratios between FCNC amplitudes and are therefore not very sensitive to the effects of NP.

6.2.2 More complex models with New Physics. In the preceding section, it was shown that MFV models give rise, as a rule, to insignificant corrections to the probabilities of rare decays, as compared with predictions of the SM. Meanwhile, although the experimental limits for these probabilities do not contradict such predictions, they still do leave significant space for searching more essential manifestations of NP in rare processes.

If the experimental data for rare kaon decays $K^+ \rightarrow \pi^+ \nu \bar{\nu}$, $K_L^0 \rightarrow \pi^0 \nu \bar{\nu}$, and $K_L^0 \rightarrow \pi^0 1^+ 1^-$ diverge essentially from the predictions of the SM and of its development in the class of MFV models, this will signify that more complex mechanisms for violating CP invariance are realized in nature, which are not governed by a single CKM phase, as happens in MFV models. Here, then, one should consider models in which a broad spectrum of new interactions and of new aspects of quark flavor dynamics may exist (see beginning of Section 6.2).

As was noted in Section 2.3, New Physics includes a large number of new models and new ideas. It contains new heavy particles and new interactions at small distances, and new mechanisms for violating CP invariance, which are characterized by additional complex parameters (new phases). Diverse versions of models with supersymmetric particles, new families of fundamental quarks, multi-Higgs structures, lepto-quarks, and other exotic objects have become widespread.

First of all, we shall consider quite a broad class of models related to the possible existence of new families of fundamental particles. In this case, additional transitions to new quark states violate the unitary conditions of the quark mixing matrix V_{CKM} for the three known quark generations. (Such a violation of unitarity was briefly discussed in Section 2.1.) In models with additional fundamental quark multiplets, the unitarity condition $V_{\text{CKM}}^+ V_{\text{CKM}} = 1$ will be replaced by the relations

$$\begin{aligned}
 \sum_i |V_{id}|^2 &= 1 - D_d^2 = U_{dd}, \\
 \sum_i |V_{is}|^2 &= 1 - D_s^2 = U_{ss}, \\
 \sum_i |V_{ib}|^2 &= 1 - D_b^2 = U_{bb}, \\
 \sum_i V_{is}^* V_{id} &= U_{sd} \neq 0, \\
 \sum_i V_{ib}^* V_{id} &= U_{bd} \neq 0, \\
 \sum_i V_{ib}^* V_{is} &= U_{bs} \neq 0
 \end{aligned} \tag{149}$$

($i = u, c, t$). Here, the unitary triangles of the SM transform into quadrangles.

As follows from experimental data, the following restrictions characterizing possible violation of the V_{CKM} -matrix unitarity hold valid:

$$D_k^2 \lesssim O(\lambda^3) \sim 10^{-2}, \quad U_{kj} \lesssim O(\lambda^4) \sim 2 \times 10^{-3} \tag{150}$$

($k, j = d, s, b$). Unitarity violation may lead to FCNC transitions of the tree type and significantly affect the probabilities of the respective decays. The influence of new fundamental generations will manifest itself in the estimates of matrix elements V_{td} , V_{ts} , and V_{tb} , which were not measured directly but were determined from the properties of loop processes and the unitarity relation for V_{CKM} .

Two types of models with additional quarks are distinguished. For so-called models with sequential fundamental multiplets, additional generations of upper (t') and lower (b') quarks, which have the same structure as the three already known quark generations, are introduced (see Section 2.1). Models of this type were dealt with, for example, in Refs [148–150]. In these models, for unitary

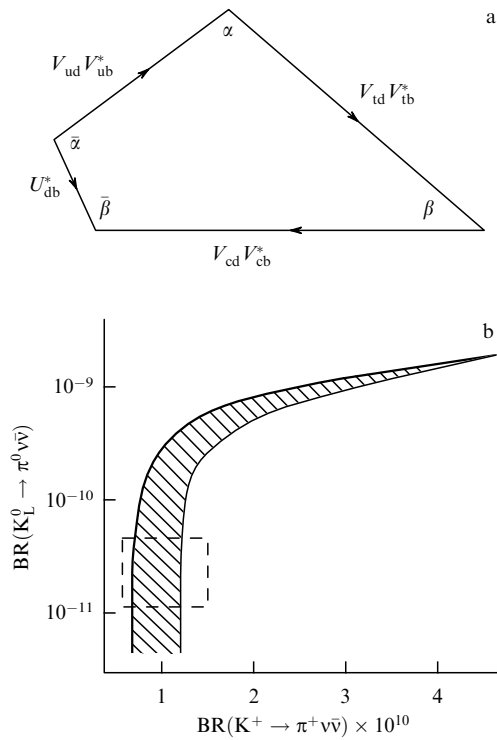


Figure 20. Model with four fundamental doublets of fermions (additional doublet with heavy quarks)

$$\begin{pmatrix} t' \\ b' \end{pmatrix}$$

[149]: (a) unitary quadrangle of the model (see text); (b) possible region for the probabilities of $K^+ \rightarrow \pi^+ \nu \bar{\nu}$ and $K_L^0 \rightarrow \pi^0 \nu \bar{\nu}$ decays in the model with four fundamental quark doublets (the rectangle represents the region of SM predictions). The mass region of quarks of the fourth generation is specified by $m_{t'} \approx 400$ GeV, and $m_{b'} \approx 350$ GeV.

quadrangles (149) one finds the equalities $U_{sd} = V_{t'd} V_{t'b}$, and so on (Fig. 20a). Here, the amplitude X_L in formulas (140) and (141) acquires an additional term:

$$X_L = (X_L)_{\text{SM}} + \frac{\lambda_{t'}}{\lambda_t} F(x_{t'}).$$

Depending on the mass $m_{t'}$, the value of $F(x_{t'})$ lies within the limits $1.5 \leq F(x_{t'}) \leq 5$, and if the value of $\lambda_{t'}/\lambda_t$ is sufficiently large, the contribution from the fourth quark generation to the probabilities (141) may be quite significant and result in essential deviations in the estimates of $K \rightarrow \pi \nu \bar{\nu}$ -decay probabilities from SM predictions. Thus, in Ref. [149], in a model with four generations of fundamental fermions taking into account the restrictions originating in ΔM_K , ΔM_d , ΔM_s , ΔM_D and other data, the following limits were obtained for the probabilities of FCNC decays of K-mesons (Fig. 20b):

$$\text{BR}(K^+ \rightarrow \pi^+ \nu \bar{\nu}) \simeq (0.7 - 4.4) \times 10^{-10},$$

$$\text{BR}(K_L^0 \rightarrow \pi^0 \nu \bar{\nu}) \simeq (0.05 - 10) \times 10^{-10}.$$

In a series of publications (see, for example, Refs [33, 151–153]), models were considered with additional exotic heavy quark singlets — only ‘lower’ (B, $q = -1/3$) or only ‘upper’ (T, $q = 2/3$). These exotic quarks take part in weak

interactions with their left-handed and right-handed components. They transform like SU(2)-singlets, and their introduction into the theory does not violate the compensation for triangular anomalies. Models with exotic quark singlets are termed vectorlike. We shall examine the results of one of the most recent works with exotic quarks [153], in which the peculiarities of such models are analyzed in detail, taking into account the restrictions imposed on their parameters and determined by a large body of experimental data.

In Ref. [153], rare decay processes [$K^+ \rightarrow \pi^+ \nu \bar{\nu}$, $K_L^0 \rightarrow \mu^+ \mu^-$, ε_K , $\varepsilon'/\varepsilon_K$, $b \rightarrow s l^+ l^-$, mass differences ΔM_d , ΔM_s , ΔM_D due to $(B_d^0 \rightleftharpoons \bar{B}_d^0)$ -, $(B_s^0 \rightleftharpoons \bar{B}_s^0)$ -, $(D^0 \rightleftharpoons \bar{D}^0)$ -mixing processes, the CP asymmetry $a_{\psi K}$ in $B_d^0(\bar{B}_d^0) \rightarrow (J/\psi) K_S^0$ decays] and high-precision measurements of electroweak parameters in collider experiments [$R_b = \Gamma(Z \rightarrow b\bar{b})/\Gamma(Z \rightarrow \text{hadrons})$, $A_{b,c}$ — the forward–backward asymmetry in b- and c-quark production in e^+e^- interactions, etc.] have been considered. In the case of models with exotic mixing, satisfying these restrictions, many expected decay probabilities were shown to be close to the SM predictions. There may, however, arise significant differences in the case of certain processes (see Table 10). Thus, in the models involving mixing with singlet T-quarks, the branching ratios for the decay $K_L^0 \rightarrow \pi^0 \nu \bar{\nu}$ may lie within the interval $0 - 4.4 \times 10^{-10}$, and in the case of mixing with B-singlets, within the interval $0 - 1.6 \times 10^{-10}$.

The model-independent relation (134) may be saturated throughout nearly all the admissible region of parameters for models with exotic mixing:

$$\frac{\text{BR}(K_L^0 \rightarrow \pi^0 \nu \bar{\nu})}{\text{BR}(K^+ \rightarrow \pi^+ \nu \bar{\nu})} < 4.37.$$

Thus, from Table 10 it is seen that for models reaching a good agreement with high-precision experimental data on the CP asymmetry $a_{\psi K}$ in $B_d^0(\bar{B}_d^0) \rightarrow (J/\psi) K_S^0$ decays, there nevertheless turn out to be possible strong violations of SM predictions and manifestations of NP for certain processes with violation of CP invariance and, first and foremost, in the case of $K_L^0 \rightarrow \pi^0 \nu \bar{\nu}$ decays. This once more confirms the importance of further studies of CP nonconservation in the kaon sector.

Possible extensions of the SM with a more complex structure of lepton and quark multiplets, based on the gauge group

$$SU(3)_C \otimes SU(3)_L \otimes U(1)_N \quad (3-3-1),$$

were investigated in Ref. [154]. In these models, leptons and quarks form triplets and singlets, with one of the quark generations being considered separately from the other two (two quark generations compose antitriplets, and the third generation represents a triplet). Such a model is natural for considering the heavy t-quark. The model contains a composite system of gauge bosons, including the additional heavy Z' -boson. The nonuniversal structure of generations in this model gives rise to FCNC processes with the exchange of Z' , proceeding in the tree approximation [155]. This 3-3-1 model predicts NP manifestations at an energy scale of several TeV.

The decay $K^+ \rightarrow \pi^+ \nu \bar{\nu}$ has been studied [155] as an example of an FCNC process proceeding at the tree level with Z' -boson exchange. The following relation was obtained

for the decay probability in the model considered:

$$\begin{aligned} \text{BR}(K^+ \rightarrow \pi^+ \nu \bar{\nu}) &= A \left(\frac{M_W^2}{M_{Z'}^2} \right)^2 \frac{m_d m_s}{m_b^2 |V_{us}|^2} \text{BR}(K^+ \rightarrow \pi^0 e^+ \nu_e) \\ &= 4.0 \times 10^{-5} A \left(\frac{M_W^2}{M_{Z'}^2} \right)^2. \end{aligned} \quad (151)$$

The parameters used in the calculations were as follows

$$\begin{aligned} \text{BR}(K^+ \rightarrow \pi^0 e^+ \nu_e) &= 4.42 \times 10^{-2}, \\ M_W &= 80.41 \text{ GeV}, \quad |V_{us}| = \lambda = 0.222, \end{aligned}$$

and the quark masses $m_b = 4.3 \text{ GeV}$, $m_s = 115 \text{ MeV}$, and $m_d = 7 \text{ MeV}$. The constant A depends on the version of the 3-3-1 model. Thus, in the model with a heavy right-handed neutrino representing the third term of the lepton triplet, the constant $A = 6$. In the minimal 3-3-1 model without new leptons, one has $A = 2/3$. The value

$$\text{BR}(K^+ \rightarrow \pi^+ \nu \bar{\nu}) = (1.57_{-0.82}^{+1.75}) \times 10^{-10}$$

was used for estimating the lower limit of the Z' -boson mass:

$$\begin{aligned} M_{Z'} &> 1.3\text{--}3.5 \text{ TeV} \quad (A = 6), \\ M_{Z'} &> 0.8\text{--}2 \text{ TeV} \quad (A = 2/3). \end{aligned}$$

These lower limits are higher than estimates based on the ΔM_K data for $(K^0 \rightleftharpoons \bar{K}^0)$ mixing.

We shall now consider the consequences of a broad class of models with supersymmetry, which are not restricted by the conditions of MFV models and thus admit significant manifestations of new physical effects in processes with CP nonconservation. In these models with SUSY there may occur new mechanisms for violation of CP invariance and for changing quark flavors, differing from the ones in the SM. Here, the influence of supersymmetric particles may significantly modify the contribution of various four-quark and penguin operators, which will be reflected in an essential manner in the probabilities of kaon FCNC decays [156]. In a general form, such processes are described by four-fermion operators $(1/M^2)(\bar{f}f)(\bar{f}f)$ (where M is a certain dimensional scale characterizing the supersymmetric contribution, and f are quark or lepton fermion fields). Another supersymmetric effect is due to so-called chromomagnetic operators such as $(1/M)\bar{q}\sigma^{\mu\nu}f_{\mu\nu}q$, related to the emission of photons or gluons (i.e., to the fields $f_{\mu\nu}$). It is manifested in estimates of the probability $\text{BR}(K_L^0 \rightarrow \pi^0 1^+ 1^-)_{\text{CP-dir}}$ and of the ratio $\varepsilon'/\varepsilon_K$. Particular sensitivity to supersymmetric effects may be exhibited by the $Zd\bar{s}$ vertex ('Z penguin'), where their contribution may not be suppressed by the introduction of a new scale of large masses M ; see Refs [72, 157–159].

Supersymmetric models lead to the following modification of the amplitude X_L in Eqn (141):

$$X_L = X_{\text{LSM}} + \frac{\tilde{\lambda}_t}{\lambda_t} H(x_s), \quad (152)$$

where $\tilde{\lambda}_t$ and $H(x_s)$ are determined by the masses and mixing coefficients of supersymmetric particles which provide an additional contribution to the amplitudes of FCNC processes. This contribution depends on three effective constants: constant A_t accounts for modification of the $Zd\bar{s}$ vertex, and constants A_g^\pm take into account the contribution from chromomagnetic operators. In this case, $A_t = \tilde{\lambda}_t H(x_s)$.

Similar expressions for A_g^\pm are determined by loop functions describing chromomagnetic penguin diagrams.

In other words, the supersymmetric contribution to the expressions for FCNC decay probabilities results in the modification

$$\lambda_t O(x_t) \rightarrow \lambda_t O(x_t) + A_t \text{ (or } A_g^\pm), \quad (153)$$

where the parameter $\lambda_t = V_{td} V_{ts}^*$ is related to the CKM matrix, the constant A_t characterizes the contribution of new processes to the $Zd\bar{s}$ vertex, and the constants A_g^\pm represent contributions from chromomagnetic operators.

Some upper estimates for these effective constants have been obtained:

$$|A_t| \lesssim 3 \times 10^{-3} \frac{500 \text{ GeV}}{m_{\tilde{q}}}, \quad |A_g^\pm| < 10^{-4} \frac{500 \text{ GeV}}{m_{\tilde{q}}}. \quad (154)$$

The supersymmetric contribution to the X_L amplitudes exhibits quite a complex character, and it changes depending on the different versions of supersymmetric models characterized by various masses and mixing mechanisms of new particles and by other peculiarities. Various scenarios have been considered that lead to essentially diverse results. In doing so, account was taken of additional restrictions on the parameters of the models, which are due to the experimental data for $\varepsilon'/\varepsilon_K$ and $\text{BR}(K_L^0 \rightarrow \mu^+ \mu^-)_{\text{SD}}$.

Different supersymmetric contributions affect the decay probabilities $\text{BR}(K^+ \rightarrow \pi^+ \nu \bar{\nu})$, $\text{BR}(K_L^0 \rightarrow \pi^0 \nu \bar{\nu})$, and $\text{BR}(K_L^0 \rightarrow \pi^0 1^+ 1^-)_{\text{CP-dir}}$ in differing ways. Thus, chromomagnetic penguin operators only contribute to the probability $\text{BR}(K_L^0 \rightarrow \pi^0 1^+ 1^-)_{\text{CP-dir}}$ and do not alter the predictions for the $K \rightarrow \pi \nu \bar{\nu}$ -decay probabilities. At the same time, the decay $K_L^0 \rightarrow \pi^0 \nu \bar{\nu}$ exhibits particular sensitivity to the concrete versions of supersymmetric models, in which direct CP nonconservation is no longer determined by the CKM phase (which in certain models may be small), but by new mechanisms. Therefore, it is important to perform experimental studies of all three rare K-meson processes and to compare the results obtained with the theoretical predictions based on different versions of the supersymmetric model.

We shall present here the results of the most consistent and conservative analysis performed in Refs [72, 159]. In this analysis, various phenomenological scenarios of CP nonconservation were considered:

$$\begin{aligned} \text{Im } A_t &= 0, \quad \text{Im } A_g^\pm \neq 0, \\ \text{Im } A_t &\neq 0, \quad \text{Im } A_g^\pm = 0, \\ \text{Im } A_t &\neq 0, \quad \text{Im } A_g^\pm \neq 0. \end{aligned}$$

Various assumptions were made concerning λ_t , which now could differ from the respective SM values, but satisfied the unitarity condition of the CKM matrix (for example, the above-mentioned case was considered, where $\text{Im } \lambda_t = 0$). The quantitative influence of parameters λ_t and A_t on the probabilities of rare kaon FCNC decays is characterized by the estimates presented in Table 11 [159].

The following restrictions on the decay probabilities were obtained within different scenarios of the model [72, 159]:

$$\begin{aligned} \text{BR}(K^+ \rightarrow \pi^+ \nu \bar{\nu}) &< 2.7 \times 10^{-10} \quad (1.7 \times 10^{-10}), \\ \text{BR}(K_L^0 \rightarrow \pi^0 \nu \bar{\nu}) &< 4 \times 10^{-10} \quad (1.2 \times 10^{-10}), \\ \text{BR}(K_L^0 \rightarrow \pi^0 e^+ e^-)_{\text{CP-dir}} &< 6 \times 10^{-11} \quad (2 \times 10^{-11}). \end{aligned} \quad (155)$$

Table 12. Data on the probabilities of decays $K^+ \rightarrow \pi^+ \nu \bar{\nu}$, $K_L^0 \rightarrow \pi^0 \nu \bar{\nu}$, and $K_L^0 \rightarrow \pi^0 e^+ e^-$ in the SM and in models with NP

	$BR(K^+ \rightarrow \pi^+ \nu \bar{\nu})$	$BR(K_L^0 \rightarrow \pi^0 \nu \bar{\nu})$	$BR(K_L^0 \rightarrow \pi^0 e^+ e^-)_{CP-dir}$	Comments
SM predictions	$(7.22 \pm 0.91) \times 10^{-11}$; see Eqn (129), $< 10 \times 10^{-11}$	$(2.49 \pm 0.42) \times 10^{-11}$; see Eqn (130)	$(4.6 \pm 1.6) \times 10^{-12}$; see Table 7	
Experimental data	$(1.57_{-0.82}^{+1.75}) \times 10^{-10}$, $> 0.5 \times 10^{-10}$ $< 3.9 \times 10^{-10}$ } (90% C.L.); see Eqn (131) [131]	$< 5.9 \times 10^{-7}$ (90% C.L.) [138]	$< 2.8 \times 10^{-10}$ (90% C.L.) [126]	Modelless upper limit: $BR(K_L^0 \rightarrow \pi^0 \nu \bar{\nu})$ $< 4.4 BR(K^+ \rightarrow \pi^+ \nu \bar{\nu})$ $\leq 1.7 \times 10^{-9}$ (90% C.L.); see Eqn (134)
Change in probabilities of rare kaon decays in models with NP: $R_{(1)} = \frac{BR(K^+ \rightarrow \pi^+ \nu \bar{\nu})}{BR(K^+ \rightarrow \pi^+ \nu \bar{\nu})_{SM}}$, $R_{(2)} = \frac{BR(K_L^0 \rightarrow \pi^0 \nu \bar{\nu})}{BR(K_L^0 \rightarrow \pi^0 \nu \bar{\nu})_{SM}}$, $R_{(3)} = \frac{BR(K_L^0 \rightarrow \pi^0 e^+ e^-)_{CP-dir}}{BR(K_L^0 \rightarrow \pi^0 e^+ e^-)_{CP-dir, SM}}$				
Models with NP	$R_{(1)}$	$R_{(2)}$	$R_{(3)}$	Comments
MFV model with minimal SUSY extension in SM (MSSM) [142]. No new mechanisms for violation of CP invariance and flavor changing	0.65–1.03	0.41–1.03	0.48–1.1	Decay probabilities change owing to supersymmetric corrections in loop diagrams [modified Inami–Lim functions $S_0(x_t) \rightarrow F_{tt}$, $X(x_t) \rightarrow \tilde{X}$]. The main corrections to the new generalizations of loop functions are contributed by charged Higgs bosons and charginos, interacting with lower quarks d, s, b and upper superquarks \tilde{u} , \tilde{c} , \tilde{t}
Further development of MFV models with generalized Inami–Lim loop functions both for positive and negative signs ($\tilde{X}, F_{tt} > 0$ and $\tilde{X}, F_{tt} < 0$) [143]		< 12 ($\tilde{X} > 0$), < 20 ($\tilde{X} < 0$) (absolute upper limits)		Probability $BR(K_L^0 \rightarrow \pi^0 \nu \bar{\nu})$ is represented as function of asymmetry $a_{\psi K}$ and of $BR(K^+ \rightarrow \pi^+ \nu \bar{\nu})$; see Fig. 17 (two predictions: for $\tilde{X} > 0$ and for $\tilde{X} < 0$)
MFV model with universal extra dimensions [144]	1.16	1.17		All probabilities are given for compactification scale $R^{-1} \simeq 200$ GeV. For $R^{-1} = 250$ (300) GeV, the effect of extra dimensions is reduced by a factor of 1.5 (2.0); see Fig. 18
Model with four generations of fundamental fermions [149]; see also Refs [148, 150]	0.9–6	0.2–36		Fourth generation of fundamental quarks t' , b' with the same structure as the three preceding generations. Unitarity of V_{CKM} matrix is violated; instead of unitary triangle, in this model there appears a unitary quadrangle; see Fig. 20
Models with additional exotic quark singlets: lower (B with $q = -1/3$) or upper (T with $q = +2/3$) [153] — vectorlike models. These models are also discussed in Refs [151, 152] and in other works (see references in papers [151–153])		$\lesssim 0-6$ (B-mixing) $\lesssim 0-17$ (T-mixing)		Unitarity of V_{CKM} matrix is violated and there appear FCNC processes of the tree type. Limits for the model parameters are determined from a large body of experimental data [including $BR(K^+ \rightarrow \pi^+ \nu \bar{\nu})$, $BR(K_L^0 \rightarrow \mu^+ \mu^-)$, $\Delta M_{d,s}$, CP-odd asymmetry $a_{\psi K}$ in $B_d^0(\bar{B}_d^0) \rightarrow (J/\psi)K_s^0$]. The probabilities for most FCNC processes are close to SM predictions. In the case of some decays ($K_L^0 \rightarrow \pi^0 \nu \bar{\nu}$, $B^0 \rightarrow \mu^+ \mu^-$), however, the probabilities may significantly exceed the SM predictions; see Table 10
Model with complex structure of lepton and quark multiplets based on the gauge group $SU(3)_C \times SU(2)_L \times U(1)_N$ (3-3-1) [154, 155]				Leptons and quarks form triplets and singlets. The model contains a composite system of gauge bosons, including the heavy Z' boson leading to FCNC processes at a tree level. The probability $BR(K^+ \rightarrow \pi^+ \nu \bar{\nu})$ was used for estimating the lower limit of the Z' -boson mass, which in different versions of the model lies in the region of 1.3–3.5 and 0.8–2 TeV
Supersymmetric models with new mechanisms of CP violation and flavor changing. In these models there may exist modified $Z\bar{d}s$ vertices [72, 159]	< 4	$< 14-18$ $< 4 \times 10^{-4}$	$< 22-29$	The most probable restrictions are $R_{(1)} < 2.2$, $R_{(2)} < 4.3$, $R_{(3)} < 10$. The large value of $R_{(3)}$ is due to the contribution of chromomagnetic operators; see also Table 11 For version of model with $\text{Im } \lambda_t \simeq 0$
Ref. [157]	< 12	< 130	< 120	In version of model with strengthened $Z\bar{d}s$ vertex

Table 12 (continued)

Models with NP	$R_{(1)}$	$R_{(2)}$	$R_{(3)}$	Comments
Ref. [158]	< 3 < 6.5	< 8 < 45	< 7 < 45	In version of model with additional mechanisms enhancing meson mixing effects ($\Delta F = 2$). Unitarity of V_{CKM} is assumed. Very high upper limits in Refs [157] and [158] either do not take into account all limits from other measurements (first and foremost, the data for $\varepsilon'/\varepsilon_K$), or require special compensation mechanisms and are not very probable
SUSY models with real matrix V_{CKM} and new mechanisms of CP nonconservation (sd transition with gluino exchange) [162]	0.2–2	$\ll 1$		Value of $R_{(2)}$ is very small, since CP-nonconserving phase in CKM matrix is close to zero, and the mechanism of CP violation with gluino exchange makes very little contribution to $K_L^0 \rightarrow \pi^0 \nu \bar{\nu}$
Further development of model posed in Ref. [162], when two mechanisms of CP nonconservation act: SUSY mechanism with gluino exchange and complex phase differing from zero in CKM matrix [163]	2–3 $\ll 1$	2–3 $\ll 1$	$\gg 1$ $\ll 1$	$K \rightarrow \pi \nu \bar{\nu}$ -decay probabilities may be two–three times larger than SM predictions, but may also be much smaller than these predictions. For $\text{BR}(K_L^0 \rightarrow \pi^0 e^+ e^-)_{\text{CP-dir}}$, a significant increase (decrease) is possible in comparison with SM prediction in case of constructive (destructive) interference between SUSY and SM amplitudes
Analysis of reasons for possible excess of $K^+ \rightarrow \pi^+ \nu \bar{\nu}$ -decay probability as compared to SM predictions [119]	$\gtrsim 1.5$ –2			Possibilities are discussed for NP manifestations in decays $s \rightarrow d \nu \bar{\nu}$ and in mechanisms of ($B^0 \leftrightarrow \bar{B}^0$) mixing, resulting in increase of $K^+ \rightarrow \pi^+ \nu \bar{\nu}$ -decay probability, for example, owing to $\bar{\rho} < 0$
Model with essential NP manifestation in meson mixing processes ($\Delta F = 2$). Here, amplitude of decays ($\Delta F = 1$) practically coincides with SM predictions (even for loop processes) [167]	0.5–1.7 0.9–2.8	$\left. \begin{array}{l} \\ \\ \end{array} \right\} 0.15$ –2.4		Meson mixing processes cannot be used for determining parameters of unitary triangle. It changes strongly. For $a_{\psi K} = \sin \phi_d = 0.734 \pm 0.54$ ($\phi_d = \phi_d^{\text{SM}} + \phi_d^{\text{NP}} = 2\beta + \phi_d^{\text{NP}}$) there may exist two values of ϕ_d , to which there correspond two sets of parameters of the unitary triangle: for $\phi_d^{(1)} \simeq 47^\circ$ $\beta^{(1)} = (19 \pm 8)^\circ$, $\gamma^{(1)} = (59 \pm 26)^\circ$, $\bar{\rho}^{(1)} = 0.20 \pm 0.18$, $\eta^{(1)} = 0.31 \pm 0.15$, i.e., $\gamma < 90^\circ$ and $\bar{\rho} > 0$; for $\phi_d^{(2)} \simeq 133^\circ$ $\beta^{(2)} = (16 \pm 8)^\circ$, $\gamma^{(2)} = (121 \pm 26)^\circ$, $\bar{\rho}^{(2)} = -0.20 \pm 0.18$, $\bar{\eta}^{(2)} = 0.31 \pm 0.15$, i.e., $\gamma > 90^\circ$ and $\bar{\rho} < 0$
SUSY model with effective $Z\bar{d}s$ -interaction $Z^\mu \bar{d}_j \gamma_\mu P_{L(R)} s$ (penguin diagrams with gluino exchange) [161]	$\lesssim 3$	$\lesssim 5$	$\lesssim 5$	Discussed are various versions of the model and conditions in which it leads to a significant increase in $R_{(1)}$, $R_{(2)}$, and $R_{(3)}$
Model with nonconservation of lepton flavors in the decay $K_L^0 \rightarrow \pi^0 \nu_i \bar{\nu}_j$ [108]		In this decay, a dominant role may be assumed by processes with CP conservation (if $i \neq j$)		The $K_L^0 \rightarrow \pi^0 \nu \bar{\nu}$ decay with CP conservation has very small probability in the SM — on the order of 10^{-14} [160]
Connection between NP manifestations, in generation of neutrino masses, in quark sector and in K-decays [165, 166]	$\lesssim 2.5$			Model leads to modification of $\text{Re}(Z\bar{d}s)$ and is manifested in the amplification of $K^+ \rightarrow \pi^+ \nu \bar{\nu}$
Model with technicolor [168]	< 1 –10	< 1 –10		Data for $K^+ \rightarrow \pi^+ \nu \bar{\nu}$ can be used to restrict parameters of model with technicolor
(L–R) model with intermediate bosons W_L and W_R and amplitudes X_L and X_R [see Eqn (140)]. In this model there is an additional scalar interaction [173]	1	1.3		Scalar operator leads to additional contribution of CP-conserving processes to $K_L^0 \rightarrow \pi^0 \nu \bar{\nu}$ decays. This contribution modifies the soft part of the π^0 -meson spectrum and increases $R_{(2)}$ approximately by 30%
Anomalous interaction at three-boson vertices WWZ [174]	0.1–2.8			When the anomalous constant Δg_1^Z of WWZ interaction changes from -0.2 to $+0.2$, the value of $R_{(1)}$ changes from 0.1 to 2.8. The value of $R_{(1)}$ is not very sensitive to the constant Δg_5^Z

Table 12 (continued)

Models with NP	$R_{(1)}$	$R_{(2)}$	$R_{(3)}$	Comments
Supersymmetric SU(5) model with heavy Majorana neutrino with right helicity and mass $m(\nu_R) \sim 10^{14}$ GeV [175]. Consequences are considered of this model in the quark sector, and, in particular, in kaon decays		0.25–2.5		The quantity ε_K may contain a large supersymmetric contribution, and therefore it should be excluded from analysis of unitary triangle and determination of parameters $\bar{\eta}$, $\bar{\rho}$. The range of possible values of $\bar{\eta}$ is somewhat extended as compared with SM predictions and amounts to $0.17 \leq \bar{\eta} \leq 0.53$, which is reflected in the $K_L^0 \rightarrow \pi^0 \nu\bar{\nu}$ branching ratio
Model with several Higgs doublets [171]	$\lesssim 3$			In models with several Higgs doublets, an essential role may be assumed by box diagrams with t-quarks and τ -leptons. This results in a significant increase in the $K^+ \rightarrow \pi^+ \nu\bar{\nu}$ -decay probability due to box diagrams and penguin diagrams with the contribution of Higgs fields
Top-color model [172] with significant violation of the GIM mechanism owing to the dynamic properties of the third generation of fundamental particles	$R \gtrsim 4$			This mechanism significantly increases the contribution from amplitudes of the $K^+ \rightarrow \pi^+ \nu\bar{\nu}$ decay with the emission of ν_τ
Models posed in Refs [43, 62, 147, 164, 176, 177]	$\simeq 1$	$\simeq 1$	$\simeq 1$	In these models and in a number of models of the MFV type, NP effects very weakly influence the probabilities of $K \rightarrow \pi \nu\bar{\nu}$ and $K_L^0 \rightarrow \pi^0 e^+ e^-$ decays

Here, the most probable restrictions, not requiring extreme assumptions, are presented in parentheses. We note that the probability $\text{BR}(K_L^0 \rightarrow \pi^0 \nu\bar{\nu})$ is very small in the version of the model with $\text{Im}\lambda_t = 0$: it is not higher than 10^{-14} [160]. Although the less rigorous restrictions presented in Refs [157, 158] cannot be totally excluded owing to possible compensations for various supersymmetric contributions, they seem quite artificial and hardly probable.

The possible enhancement of rare kaon FCNC-decay probabilities in the generalized supersymmetric model with the effective interaction $Z^\mu \bar{d}_{i\mu} P_{L(R)} s$ at the $Zd\bar{s}$ vertex for penguin diagrams with gluino exchange was considered in Ref. [161]. The respective estimates of decay probabilities in this model are presented in the summary Table 12, where all the data on possible NP manifestations in the kaon decays mentioned in this section are summarized.

In the supersymmetric model [162], violation of CP invariance in K-decays is related to (s–d) transitions with gluino exchange, and the CKM matrix contains no complex elements. This mechanism does not contribute to the CP-violating amplitude of the decay $s \rightarrow d\nu\bar{\nu}$. Therefore, the $K_L^0 \rightarrow \pi^0 \nu\bar{\nu}$ -decay probability will be very small in the model considered. At the same time, the probability expected for the decay $K^+ \rightarrow \pi^+ \nu\bar{\nu}$, due to both the CP-conserving and the CP-violating amplitudes, comes out to

$$\text{BR}(K^+ \rightarrow \pi^+ \nu\bar{\nu}) = (8.8 \pm 7.2) \times 10^{-11},$$

i.e., it may be comparable with the SM prediction.

In Ref. [163], it is shown that the predictions for the $K \rightarrow \pi \nu\bar{\nu}$ -decay probabilities, as well as for the contribution from the region of small distances to the decay $K_L^0 \rightarrow \mu^+ \mu^-$ (i.e., $|\text{Re} A_{\mu\mu}|_{\text{SD}}^2$; see Table 7) may be expected to increase by a factor of two or three as compared with the respective SM expectations, as the supersymmetric model considered [162] undergoes development (with inclusion into it of the non-vanishing complex CKM phase). However, for certain parameter values of the model, the probabilities may be significantly smaller than the SM quantities; this, first of all, concerns the decay $K_L^0 \rightarrow \pi^0 \nu\bar{\nu}$. In the case of the decays $K_L^0 \rightarrow \pi^0 1^+ 1^-$ involving direct violation of CP invariance, the model [163] predicts both a significant increase and a

significant decrease in the respective probabilities, depending on whether the interference between the SM amplitudes and the supersymmetric amplitudes of these processes is constructive or destructive.

One more mechanism of possible amplification of FCNC processes at the $Zd\bar{s}$ vertex was examined in Refs [165, 166]. In these works, the connections were discussed between lepton and quark generations, and possible NP manifestations were considered, which lead to the generation of neutrino masses and to neutrino oscillations, to some effects in the quark sector of the theory and in K-meson decays. The parameter of the model, which describes neutrino masses and oscillations, turned out to play an essential role for penguin diagrams responsible for FCNC processes at the $Zd\bar{s}$ vertex. The upper limit for the parameter of the model was obtained from data on the upper limit for $\text{BR}(K_L^0 \rightarrow \mu^+ \mu^-)_{\text{SD}}$. The mechanism considered contributes to $\text{Re}(Zd\bar{s})$ and may result in an increase of $\text{BR}(K^+ \rightarrow \pi^+ \nu\bar{\nu})$ up to 2×10^{-10} . In the work dealt with, however, the upper limit $\text{BR}(K_L^0 \rightarrow \mu^+ \mu^-)_{\text{SD}} < 2.8 \times 10^{-9}$ used was overestimated by a factor greater than two, instead of 1.3×10^{-9} (90% C.L.) (see Table 7). For this reason, the data for $\text{BR}(K^+ \rightarrow \pi^+ \nu\bar{\nu})$ may also be somewhat overestimated.†

As was said in Section 6.1.3, two nonstandard lines of the development of theory were considered in Ref. [119] that were proposed for explaining the possible excess of the probability $\text{BR}(K^+ \rightarrow \pi^+ \nu\bar{\nu})$ over the limit (138) [or (139)] obtained in the SM. Along one of these lines of development, NP is manifested in the process $s \rightarrow d\nu\bar{\nu}$ (for example, in supersymmetric modernizations of the SM, considered above). However, there exists still another possibility related to the manifestations of NP in ($B^0 \rightleftharpoons \bar{B}^0$)-mixing processes and leading to a nonstandard solution of the unitary triangle with vertex parameters $\bar{\rho} < 0$. This results in an increase of the $K^+ \rightarrow \pi^+ \nu\bar{\nu}$ branching ratio.

In Ref. [167], the discussion of the possible NP effects on ($B^0 \rightleftharpoons \bar{B}^0$)-mixing processes was continued. Quite a broad spectrum of models was considered, for which a significant

† Author's note added in English proofreading. But see the note on page 1026.

manifestation of NP occurs only in flavor changing processes with $\Delta F = 2$, i.e., in the case of meson mixing, $P^0 \rightleftharpoons \bar{P}^0$. The amplitudes of decays with $\Delta F = 1$ (including loop processes) are practically not modified here, as compared with SM predictions. In models of this type, data on $(B^0 \rightleftharpoons \bar{B}^0)$ mixing cannot be used for determining parameters of the SM unitary triangle. Now, it is no longer possible to restrict oneself to dealing with a single solution for the angle ϕ_d , determined from measurement of the asymmetry $a_{\psi K}$ in $B_d^0(\bar{B}_d^0) \rightarrow (J/\psi)K_S^0$ decays.

We recall that in models with NP one has

$$a_{\psi K} = \sin \phi_d = \sin(\phi_d^{\text{SM}} + \phi_d^{\text{NP}}) = \sin(2\beta + \phi_d),$$

and from $\sin \phi_d = 0.734 \pm 0.054$ [see Eqn (99)] there follow two possible solutions for the upper half of the $(\bar{\eta}, \bar{\rho})$ -plane:

$$21.5^\circ < \frac{\phi_d^{(1)}}{2} < 26^\circ, \quad 64^\circ < \frac{\phi_d^{(2)}}{2} < 68.5^\circ.$$

In the SM only the first solution $\phi_d^{(1)}/2 = \beta_{\text{SM}}$ satisfies the entire set of data for the unitary triangle. But in models with NP of the type considered in Ref. [167], one must consider both possible solutions: $\phi_d^{(1)}$ and $\phi_d^{(2)}$.

In Ref. [167] it is shown that one can find two solutions for the unitary triangle when analyzing data for R_b , determined by the ratio $|V_{ub}|/|V_{cb}|$, and the preliminary results of research of asymmetry in $B_d^0(\bar{B}_d^0) \rightarrow \pi^+\pi^-$ decays for two values of ϕ_d :

$$\begin{aligned} \beta_1 &\simeq 19^\circ \pm 8^\circ, \quad \gamma_1 = 59^\circ \pm 26^\circ, \\ \bar{\rho}_1 &= +0.20 \pm 0.18, \quad \bar{\eta}_1 = 0.31 \pm 0.15 \quad (\phi_d^{(1)} = 47^\circ); \\ \beta_2 &\simeq 16^\circ \pm 8^\circ, \quad \gamma_2 = 121^\circ \pm 26^\circ, \\ \bar{\rho}_2 &= -0.20 \pm 0.18, \quad \bar{\eta}_2 = 0.31 \pm 0.15 \quad (\phi_d^{(2)} = 133^\circ). \end{aligned}$$

Thus, the second solution corresponds to an angle $\gamma > 90^\circ$ and to negative values of the parameter $\bar{\rho}$. NP in the model of Ref. [167] does not directly influence the amplitudes of the $K \rightarrow \pi\nu\bar{\nu}$ processes, but their probabilities depend on parameters $\bar{\rho}$ and $\bar{\eta}$ in accordance with Eqns (117) and (118). For the two solutions ϕ_d , possible limits on the probabilities were found:

$$\begin{aligned} 3.3 \times 10^{-11} &\leq \text{BR}^{(1)}(K^+ \rightarrow \pi^+\nu\bar{\nu}) < 11.9 \times 10^{-11} \quad (\phi_d^{(1)}), \\ 6.5 \times 10^{-11} &\leq \text{BR}^{(2)}(K^+ \rightarrow \pi^+\nu\bar{\nu}) < 19.7 \times 10^{-11} \quad (\phi_d^{(2)}). \end{aligned} \quad (156)$$

The increase in the $K^+ \rightarrow \pi^+\nu\bar{\nu}$ -decay probability for the second solution is related to the value of $\bar{\rho} < 0$. In the case of the $K_L^0 \rightarrow \pi^0\nu\bar{\nu}$ decay, the probability does not depend on the choice of $\phi_d^{(1)}$ or $\phi_d^{(2)}$ and amounts to

$$0.4 \times 10^{-11} < \text{BR}(K_L^0 \rightarrow \pi^0\nu\bar{\nu}) < 6.2 \times 10^{-11}. \quad (157)$$

The accuracy of such an analysis is expected to improve as the measurement precision of angle γ is enhanced in studies of B-decays.

In models with technicolor, the $K \rightarrow \pi\nu\bar{\nu}$ -decay probabilities may exceed SM predictions significantly [168], owing to the influence of new interactions on the $Zd\bar{s}$ vertex. At the same time, existing data for the decay $K^+ \rightarrow \pi^+\nu\bar{\nu}$ permit us to obtain restrictions on the parameters of models with technicolor. Here, the upper limits for the $K^+ \rightarrow \pi^+\nu\bar{\nu}$ - and $K_L^0 \rightarrow \pi^0\nu\bar{\nu}$ -decay probabilities may be several times greater than SM predictions.

Large changes in the $K \rightarrow \pi\nu\bar{\nu}$ -decay probabilities may occur in other exotic theories: in supersymmetric models with nonconservation of R -parity [169, 170], in models with multi-Higgs multiplets [171], in the top-color model with significant violation of the GIM mechanism owing to the dynamic properties of the third generation of fundamental particles [172], in models with leptoquarks, and in some other theories in which significant modification of FCNC processes takes place [43, 62].

Nonconservation of lepton flavors may, in principle, also influence the $K_L^0 \rightarrow \pi^0\nu\bar{\nu}$ -decay probability. Within the SM framework, this decay is due to direct nonconservation of CP invariance, and the contributions of all other mechanisms turn out to be negligible. The hierarchy of processes with direct, indirect, and no violation of CP invariance corresponds, in terms of the $\text{BR}(K_L^0 \rightarrow \pi^0\nu\bar{\nu})$ probability, to the ratio $1:10^{-2}:(\lesssim 10^{-4})$ [160]. However, if new physical phenomena exist, the situation may be essentially changed. Thus, in models with nonconservation of lepton flavor, in which the $K_L^0 \rightarrow \pi\nu_i\bar{\nu}_j$ decay may proceed with the production of diverse types of neutrinos, the decays without violation of CP invariance can also take place, and their contribution may even be dominant [108].

In Ref. [173], $K \rightarrow \pi\nu\bar{\nu}$ decays were studied within the so-called left–right (LR) model, in which there appear scalar and tensor operators due to ‘box’ LR diagrams with left and right intermediate bosons W_L and W_R , respectively. [The Hamiltonian of this model contains the amplitudes X_L and X_R ; see Eqn (140).] It is shown that an essential role may be assumed by CP-conserving processes related to the scalar operator $(\bar{s}d)(\bar{\nu}_\tau\nu_\tau)$ and enhanced in the matrix element $\langle\pi|\bar{s}d|K\rangle$ by the factor M_K/m_s (m_s is the mass of the s -quark). Here, the $\text{BR}(K^+ \rightarrow \pi^+\nu\bar{\nu})$ probability varies very little, and for the decay $K_L^0 \rightarrow \pi^0\nu\bar{\nu}$ there arises an additional CP-conserving component. This component is manifested mainly in the region of low π^0 -meson energies and thus enhances the $\text{BR}(K_L^0 \rightarrow \pi^0\nu\bar{\nu})$ probability by 30% as compared with SM predictions.

The influence of anomalous interactions on the FCNC decay probabilities of K - and B -mesons at the three-particle vertices for gauge bosons was studied in Ref. [174]. It was shown, for example, that the $\text{BR}(K^+ \rightarrow \pi^+\nu\bar{\nu})$ probability may vary within broad limits depending on the anomalous constant Δg_1^z at the WWZ vertex and that it depends weakly on the constant Δg_2^z . High-precision measurements of FCNC decays will permit the researchers to supplement and refine searches for anomalous three-boson interactions, which are presently under way at e^+e^- - and $\bar{p}p$ -colliders.

It must be noted that in a number of cases NP effects are quite weakly reflected in the characteristics of $K \rightarrow \pi\nu\bar{\nu}$ decays. As a rule, this occurs in models, in which the violation of CP invariance and quark mixing processes are, as usual, determined by the properties of the CKM matrix, like in the SM. This is so, for example, in some versions of MSSM, in models with two Higgs doublets and in a number of other cases (see Refs [43, 62, 147, 164, 176, 177]).

The main predictions of various models with NP, dealt with in this section, are presented in the summary Table 12.

7. Conclusions

Violation of CP invariance was discovered in the famous experiment performed by Christenson, Cronin, Fitch, and

Turley [178] nearly forty years ago. For many years, even though new interesting results did appear (see Table 4), the situation changed little in essence, and the interpretation of CP nonconservation on the whole remained very vague. Recently, however, significant changes have taken place.

The first: in 1999 it became clear that there indeed exists direct violation of CP invariance in $K_L^0 \rightarrow \pi\pi$ decays with $\Delta S = 1$ and that it proceeds with quite a high probability [80, 81]; see Table 4. Thus, the result presented in Ref. [78] and met by the physics community with deep mistrust was confirmed with very good statistical accuracy. The data for $\text{Re}(\varepsilon'/\varepsilon_K)_{\text{expt}} = (16.8 \pm 1.8) \times 10^{-4}$ are in qualitative agreement with SM predictions

$$\text{Re}\left(\frac{\varepsilon'}{\varepsilon_K}\right)_{\text{SM}} \simeq (5-30) \times 10^{-4},$$

although theoretical difficulties do not permit checking whether the experimental data comply with this model or not.

The second: works at the electron B-factories BaBar and Belle were drastically accelerated in 1999, and in 2001–2002 an accurate result was obtained for the asymmetry $a_{\psi K} = \sin 2\beta = 0.734 \pm 0.054$ [104], which is in good agreement with SM predictions: $(\sin 2\beta)_{\text{SM}} = 0.59-0.88$. This was the first quantitative test of the CKM mechanism for the violation of CP invariance. The result obtained reveals that this mechanism may turn out to be the principal one and that the role of other possible mechanisms may not be so great, as it still seemed several years ago.

And, finally, the third: multi-years efforts of the BNL E787 collaboration led in 1997 to the observation of one of the two superrare ‘golden’ kaon decays, namely $K^+ \rightarrow \pi^+ \nu\bar{\nu}$ [130]. At present, already two events of this decay have been found. This clears the way for the future program of quantitative studies of $K^+ \rightarrow \pi^+ \nu\bar{\nu}$ and $K_L^0 \rightarrow \pi^0 \nu\bar{\nu}$ decays, which will permit in the next decade the independent investigation of the mechanisms of CP violation in K-decays. Comparison of these data with presently available and new data on CP nonconservation in B-decays and on $B_d^0 \rightleftharpoons \bar{B}_d^0$ - and, especially, $B_s^0 \rightleftharpoons \bar{B}_s^0$ -mixing processes will lead to essentially new tests of SM predictions for rare FCNC processes at small distances, which are very sensitive to NP manifestations.

One of the most interesting results, which is likely to be obtained relatively soon, consists in a quite accurate measurement of the $\text{BR}(K^+ \rightarrow \pi^+ \nu\bar{\nu})$ probability and its comparison with SM predictions. If it is shown that $\text{BR}(K^+ \rightarrow \pi^+ \nu\bar{\nu})$ exceeds the limit (139), this will unambiguously be interpreted as a manifestation of NP. In the future, various theoretical models may be studied on the basis of analysis of correlations between the results of theoretically clean measurements: the probabilities $\text{BR}(K^+ \rightarrow \pi^+ \nu\bar{\nu})$ and $\text{BR}(K_L^0 \rightarrow \pi^0 \nu\bar{\nu})$, the asymmetry $a_{\psi K}$, and the ratio $\Delta M_d/\Delta M_s$ [see, for example, relation (136)]. The predictions for many new models are illustrated by the data presented in Table 12, which once more reveal that future experiments for studying the decays $K^+ \rightarrow \pi^+ \nu\bar{\nu}$, $K_L^0 \rightarrow \pi^0 \nu\bar{\nu}$, and $K_L^0 \rightarrow \pi^0 e^+ e^-$ represent a very important and sensitive instrument for testing subtle predictions of the Standard Model and searching for effects of New Physics.

8. Appendices

I. Determination of $\sin 2\beta$ in the SM from measurements of the branching ratios for $K^+ \rightarrow \pi^+ \nu\bar{\nu}$ and $K_L^0 \rightarrow \pi^0 \nu\bar{\nu}$

From Eqns (117) and (118) it follows that within the framework of the SM the relations are valid:

$$\begin{aligned} \text{BR}(K^+ \rightarrow \pi^+ \nu\bar{\nu}) &= (K_+ \lambda^8) A^4 X^2(x_t) \left[\frac{1}{\sigma} (\rho_0 - \bar{\rho})^2 + \sigma \bar{\eta}^2 \right], \\ \text{BR}(K_L^0 \rightarrow \pi^0 \nu\bar{\nu}) &= (K_0 \lambda^8) A^4 X^2(x_t) (\sigma \bar{\eta}^2). \end{aligned} \quad (I.1)$$

We denote the reduced K $\rightarrow \pi \nu\bar{\nu}$ -decay widths (for $\lambda = 0.222$) by

$$\begin{aligned} B_1 &= \frac{\text{BR}(K^+ \rightarrow \pi^+ \nu\bar{\nu})}{K_+ \lambda^8} = \frac{\text{BR}(K^+ \rightarrow \pi^+ \nu\bar{\nu})}{4.425 \times 10^{-11}}, \\ B_2 &= \frac{\text{BR}(K_L^0 \rightarrow \pi^0 \nu\bar{\nu})}{K_0 \lambda^8} = \frac{\text{BR}(K_L^0 \rightarrow \pi^0 \nu\bar{\nu})}{1.935 \times 10^{-10}}. \end{aligned} \quad (I.2)$$

Accounting for Eqns (I.1) and (I.2) we arrive at

$$\begin{aligned} B_1 &= \frac{1}{\sigma} (\rho_0 - \bar{\rho})^2 A^4 X^2(x_t) + A^4 X^2(x_t) + (\sigma \bar{\eta})^2 \\ &= \frac{1}{\sigma} (\rho_0 - \bar{\rho})^2 A^4 X^2(x_t) + B_2 \\ &= \frac{1}{\sigma} \left(1 - \bar{\rho} + \frac{P_c(\nu\bar{\nu})}{A^2 X(x_t)} \right)^2 A^4 X^2(x_t) + B_2, \end{aligned} \quad (I.3)$$

$$\begin{aligned} (\rho_0 - \bar{\rho}) &= 1 + \Delta - \bar{\rho} = \left(1 - \bar{\rho} + \frac{P_c(\nu\bar{\nu})}{A^2 X(x_t)} \right) \\ &= \pm \frac{\sqrt{(B_1 - B_2)\sigma}}{A^2 X(x_t)}. \end{aligned} \quad (I.4)$$

Since $\bar{\rho} < 1$ and $1 + \Delta - \bar{\rho} > 0$ in the SM (see Fig. 2), the solution with the ‘-’ sign does not satisfy this condition and must be discarded. We recall that

$$\begin{aligned} \Delta &= \frac{P_c(\nu\bar{\nu})}{A^2 X(x_t)} = \frac{fF(x_c)}{A^2 \lambda^4 X(x_t)} = \frac{\delta(x_c)}{A^2 \lambda^4}, \\ \sigma &= \frac{1}{(1 - \lambda^2/2)^2} = 1.051 \end{aligned}$$

(see Section 5.2).

Data on the branching ratios of decays $K^+ \rightarrow \pi^+ \nu\bar{\nu}$ and $K_L^0 \rightarrow \pi^0 \nu\bar{\nu}$ will eventually permit determination of the parameters of the unitary triangle independently of the data on B-decays and ($K^0 \rightleftharpoons \bar{K}^0$)- and ($B^0 \rightleftharpoons \bar{B}^0$)-mixing processes:

$$\begin{aligned} \bar{\rho} &= 1 - \frac{\sqrt{(B_1 - B_2)\sigma} - P_c(\nu\bar{\nu})}{A^2 X(x_t)}, \\ \bar{\eta} &= \frac{\sqrt{B_2}}{A^2 X(x_t) \sqrt{\sigma}}. \end{aligned} \quad (I.5)$$

$$\begin{aligned} r_s = \cot \beta &= \frac{1 - \bar{\rho}}{\bar{\eta}} = \frac{\sqrt{\sigma} [\sqrt{(B_1 - B_2)\sigma} - P_c(\nu\bar{\nu})]}{\sqrt{B_2}}, \\ \cos \beta &= \frac{\cot \beta}{\sqrt{1 + \cot^2 \beta}} = \frac{r_s}{\sqrt{1 + r_s^2}}, \\ \sin \beta &= \frac{1}{\sqrt{1 + \cot^2 \beta}} = \frac{1}{\sqrt{1 + r_s^2}}. \end{aligned} \quad (I.6)$$

Applying the notation adopted earlier for the measurements of $\sin 2\beta$, from the data on the $K \rightarrow \pi\nu\bar{\nu}$ decay probabilities we find

$$(\sin 2\beta)_K = 2 \sin \beta_K \cos \beta_K = \frac{2r_s}{1+r_s^2}. \quad (\text{I.7})$$

As one can see from Eqns (I.3) and (I.4), the value of $(\sin 2\beta)_K$ is independent of $X(x_t)$, i.e., of the measurement accuracy of the t-quark mass, and, also, of A , V_{cb} , and λ . The precision in finding $(\sin 2\beta)_K$ will be determined only by the measurement precision of $\text{BR}(K^+ \rightarrow \pi^+\nu\bar{\nu})$ and $\text{BR}(K_L^0 \rightarrow \pi^0\nu\bar{\nu})$ and by calculations of the correction $fF(x_c)$ which takes into account the influence of c-quarks. The dependences of B_1 , B_2 , and $P_c(\nu\bar{\nu}) = fF(x_c)/\lambda^4$ on the high powers of λ are mutually cancelled out and do not appear in the final results (I.6) and (I.7) for r_s and $(\sin 2\beta)_B$.

Comparison of formula (I.7) with the result of measurement of CP-odd asymmetry in the $B_d^0(\bar{B}_d^0) \rightarrow (J/\psi)K_S^0$ decays, which we previously denoted by $a_{\psi K} = (\sin 2\beta)_B$, will permit us to check one of the most important predictions of the SM:

$$(\sin 2\beta)_K = \frac{2r_s}{1+r_s^2} = a_{\psi K} = (\sin 2\beta)_B. \quad (\text{I.8})$$

Denoting the asymmetry, for reasons of brevity, by $a_{\psi K} = a$, from formula (I.8) we obtain $r_s = (1 \pm \sqrt{1-a^2})/a$. The conditions $\bar{\rho} < 1$ and $\cot \beta > 1.7$ [see Eqn (83)] are satisfied by only one solution with the ‘+’ sign in front of $\sqrt{1-a^2}$:

$$\cot \beta = \frac{1 + \sqrt{1-a^2}}{a},$$

$$\begin{aligned} \bar{\eta} &= R_t \sin \beta = \frac{R_t}{\sqrt{1 + (1 + \sqrt{1-a^2})^2/a^2}} \\ &= \frac{R_t}{\sqrt{2}} \frac{a}{\sqrt{1 + \sqrt{1-a^2}}} = \frac{R_t}{\sqrt{2}} (1 - \sqrt{1-a^2})^{1/2}, \end{aligned} \quad (\text{I.9})$$

$$\bar{\rho} = 1 - \bar{\eta} \cot \beta = 1 - \frac{1 + \sqrt{1-a^2}}{a} \bar{\eta}.$$

II. Modified formulas for mixing processes and for FCNC decays in MFV models

According to the discussion in Section 6.2.1, the absence of new mechanisms for CP nonconservation (new ‘weak’ phases) and of new processes involving quark flavor changing, as compared to the SM, is assumed in MFV models. The influence of NP may manifest itself in modifications of the Inami–Lim loop functions due to the contribution from new heavy virtual particles (gluinos, charginos, charged Higgs fields, etc.). Here, transformation takes place [see Eqn (143)]:

$$S_0(x_t) \rightarrow F_{tt}, \quad X(x_t) \rightarrow \tilde{X}.$$

The loop functions taking into account the contributions of c-quarks, i.e., $P_0(\varepsilon_K)$, $P_c(\nu\bar{\nu})$, are determined by the region of comparatively large distances (on the order of magnitude of $1/m_c$) and are practically not modified, owing to the influence of heavy virtual objects. In generalized MFV models, the assumption is made that the modified loop functions F_{tt} and \tilde{X} can be either positive or negative. (In the SM, the signs of $S_0(x)$ and of $X(x_t)$ are positive.)

The modification of formulas for $\bar{\rho}$, $\bar{\eta}$, $\sin 2\beta$, R_t , ε_K -hyperbola, and others with the aid of functions F_{tt} and \tilde{X} with arbitrary signs, is illustrated in Table I.1. The main changes, here, are related to the change in sign of the parameters $\bar{\eta}$ and $\sin 2\beta$, and of interference terms between the amplitudes taking into account the contributions of t- and c-quarks to loop processes.

To conclude this section, we present relations for the branching ratios $\text{BR}(K^+ \rightarrow \pi^+\nu\bar{\nu})$ and $\text{BR}(K_L^0 \rightarrow \pi^0\nu\bar{\nu})$ in MFV models with arbitrary signs of the modified Inami–Lim functions \tilde{X} and F_{tt} . Applying the corresponding modifications of $\bar{\eta}$ and $\cot \beta$, presented in Table I.1, and introducing the following substitution in Eqn (I.3):

$$X(x_t) \rightarrow |\tilde{X}|, \quad P_c(\nu\bar{\nu}) = \text{sgn } \tilde{X} \cdot P_c(\nu\bar{\nu}),$$

where $\text{sgn } \tilde{X}$ is the sign of the respective function, it is possible to obtain the expression for B_1 in such a model. As a result, relations (I.3), (I.5), and (I.6) assume the form

$$B_1 = \frac{1}{\sigma} \left[1 - \bar{\rho} + \text{sgn } \tilde{X} \cdot \frac{P_c(\nu\bar{\nu})}{A^2|\tilde{X}|} \right]^2 A^4 |\tilde{X}|^2 + B_2, \quad (\text{II.1})$$

$$\bar{\rho} = 1 - \left[\frac{\pm \sqrt{\sigma(B_1 - B_2)} - \text{sgn } \tilde{X} \cdot P_c(\nu\bar{\nu})}{A^2|\tilde{X}|} \right], \quad (\text{II.2})$$

$$\bar{\eta} = \frac{\sqrt{B_2} \text{sgn } F_{tt}}{\sqrt{\sigma} A^2 |\tilde{X}|}, \quad (\text{II.3})$$

$$\begin{aligned} \text{sgn } F_{tt} \cdot r_s &= \text{sgn } F_{tt} \cdot \cot \beta = |\cot \beta| = f(\beta) \\ &= \frac{1 - \bar{\rho}}{|\bar{\eta}|} = \frac{\sqrt{\sigma}}{\sqrt{B_2}} \left[\pm \sqrt{\sigma(B_1 - B_2)} - \text{sgn } \tilde{X} \cdot P_c(\nu\bar{\nu}) \right]. \end{aligned} \quad (\text{II.4})$$

Here, it is easy to verify that

$$\text{sgn } F_{tt} \cdot \cot \beta = |\cot \beta| = f(\beta) = \frac{1 + \sqrt{1-a^2}}{a} > 0. \quad (\text{II.5})$$

In the case of $\tilde{X} > 0$, the solution with sign ‘-’ in front of $\sqrt{\sigma(B_1 - B_2)}$ in formulas (II.2) and (II.4) does not satisfy the condition $1 - \bar{\rho} \geq 0$ and must be discarded. If $\tilde{X} < 0$ and $B_1 - B_2 < P_c(\nu\bar{\nu})^2/\sigma \simeq 0.17$, in formulas (II.2) and (II.4) there may be two solutions corresponding to both signs in front of $\sqrt{\sigma(B_1 - B_2)}$.

However, this region corresponds to very small branching ratios $\text{BR}(K^+ \rightarrow \pi^+\nu\bar{\nu})$ and $\text{BR}(K_L^0 \rightarrow \pi^0\nu\bar{\nu})$ (inferior to 10^{-11} [143]), which is hardly probable and even contradicts the data of E781 for the $(K^+ \rightarrow \pi^+\nu\bar{\nu})$ -decay: $\text{BR}(K^+ \rightarrow \pi^+\nu\bar{\nu}) > 5 \times 10^{-11}$. Therefore, if $\tilde{X} < 0$ in the formulas for $\bar{\rho}$ and $\text{sgn } F_{tt} \cdot r_s$, there should be the sign ‘+’ in front of $\sqrt{\sigma(B_1 - B_2)}$. If B_1 and $a_{\psi K}$, i.e., $f(\beta)$, are known, then from Eqns (II.2) and (II.4) it follows that

$$\begin{aligned} \text{sgn } F_{tt} \cdot r_s &= f(\beta) \\ &= \frac{1}{\sqrt{B_2}} \left[\pm \sqrt{\sigma} \sqrt{B_1 - B_2} - \text{sgn } \tilde{X} \cdot P_c(\nu\bar{\nu}) \sqrt{\sigma} \right], \end{aligned}$$

or

$$B_1 - B_2 = \frac{1}{\sigma^2} \left[f(\beta) \sqrt{B_2} + \text{sgn } \tilde{X} \cdot P_c(\nu\bar{\nu}) \sqrt{\sigma} \right]^2. \quad (\text{II.6})$$

The calculated results for $\text{BR}(K_L^0 \rightarrow \pi^0\nu\bar{\nu})$ in MFV models with $\tilde{X} > 0$ and $\tilde{X} < 0$ were presented above (see Fig. 17).

We note that the minimum value of $a_{\psi K}$ in models with $F_{tt} > 0$ corresponds to $\sin 2\beta_{\min} = a_{\psi K, \min} = 0.42$, while in

Table I.1. Main relationships for parameters $\bar{\rho}$ and $\bar{\eta}$ of the unitary triangle, for asymmetry $a_{\psi K}$, for mass differences ΔM_d , $\Delta M_d/\Delta M_s$, and ε_K obtained within the SM and in MFV models with modified Inami–Lim loop functions $S_0(x_t) \rightarrow F_{tt}$, $\tilde{X}(x_t) \rightarrow \tilde{X}$ with $\tilde{X}, F_{tt} > 0$, and $\tilde{X}, F_{tt} < 0$.

Parameter	Standard Model	MFV models with $\tilde{X}, F_{tt} > 0$ and $\tilde{X}, F_{tt} < 0$
R_t from measurements of ΔM_d	$R_t = \sqrt{(1 - \bar{\rho})^2 + \bar{\eta}^2} = \frac{1.10}{A\sqrt{S_0(x_t)}}$; see Eqn (86)	$R_t = \sqrt{(1 - \bar{\rho})^2 + \bar{\eta}^2} = \frac{1.10}{A\sqrt{ F_{tt} }}$
ε_K -hyperbola in $(\bar{\rho}, \bar{\eta})$ -plane	$\bar{\eta}[(1 - \bar{\rho})A^2\eta_{tt}S_0(x_t) + P_c(\varepsilon_K)]A^2\hat{B}_K = 0.205$; see Eqn (79)	$\bar{\eta}[(1 - \bar{\rho})A^2\eta_{tt}F_{tt} + P_c(\varepsilon_K)]A^2\hat{B}_K = 0.205$
$\sin 2\beta$ from data on ε_K and R_t (i.e., on ΔM_d)	$\sin 2\beta = \frac{1.66}{\eta_{tt}} \left[\frac{0.205}{A^2\hat{B}_K} - \bar{\eta}P_c(\varepsilon_K) \right]$; see Eqn (88), $\bar{\eta} = R_t \sin \beta$	$\sin 2\beta = \frac{1.66}{\eta_{tt}} \left[\frac{0.205}{A^2\hat{B}_K} - \bar{\eta}P_c(\varepsilon_K) \right] \frac{F_{tt}}{ F_{tt} }$ $= \text{sgn } F_{tt} \cdot \frac{1.66}{\eta_{tt}} \left[\frac{0.205}{A^2\hat{B}_K} - \bar{\eta}P_c(\varepsilon_K) \right] = \text{sgn } F_{tt} \cdot \sin 2\beta $, $\bar{\eta} = \text{sgn } F_{tt} \cdot R_t \sin \beta = \text{sgn } F_{tt} \cdot \bar{\eta} $
Signs of $\sin 2\beta$ and $\bar{\eta}$	Signs of $\sin 2\beta$ and $\bar{\eta}$ are positive	Signs of $\sin 2\beta$ and $\bar{\eta}$ are negative in models with $F_{tt} < 0$
$\sin 2\beta_{\min}$	$\sin 2\beta_{\min} = \begin{cases} 0.42 [27, 143], \\ 0.52 [114]. \end{cases}$ There exists an absolute lower limit for $\sin 2\beta$, determined by relationship between ε_K and ΔM_d (R_t) and depending on parameters $V_{cb}, V_{ub}/V_{cb} , \hat{B}_K, F_{B_d}, (\hat{B}_{B_d})^{1/2}$, and ξ (it is found in the course of scanning these parameters)	$-\sin 2\beta_{\min} = 0.69 [143]$ in models with $F_{tt} < 0$. Destructive interference between contributions of t- and c-quarks in the expression for the ε_K -hyperbola in models with $F_{tt} < 0$ leads to an increase in the absolute value of the minimum angle β , necessary for describing the data concerning ε_K
$\sin 2\beta_{\max}$	$\sin 2\beta_{\max} = R_{b,\max} \sqrt{1 - R_{b,\max}^2} = 0.87$; see Eqn (83), $\beta < 30^\circ$ or $\cot \beta \gtrsim 1.7$	$ \sin 2\beta_{\max} = 0.87$, $ \beta < 30^\circ$ or $ \cot \beta \gtrsim 1.7$
Asymmetry $a_{\psi K} = a$ and $\sin 2\beta$	Phase $\phi_d = 2\beta + \arg S_0(x_t)$, $a_{\psi K} = \sin \phi_d = \sin 2\beta$ (in the SM)	$\phi_d = 2\beta + \arg F_{tt}$, $a_{\psi K} = \sin \phi_d = \text{sgn } F_{tt} \cdot \sin 2\beta$, $\sin 2\beta = \text{sgn } F_{tt} \cdot \sin 2\beta $, $a_{\psi K} = \sin 2\beta $ and is independent of the sign of F_{tt} . This is in agreement with the positive value of $a_{\psi K}$, found in experiments [104]
$\bar{\rho}$ and $\bar{\eta}$ from data on $a_{\psi K} = a$ and R_t (i.e., on $\Delta M_d, \Delta M_d/\Delta M_s$)	$r_s = \frac{1 - \bar{\rho}}{\bar{\eta}} = \cot \beta$, $(\sin 2\beta)_K = \frac{2r_s}{1 + r_s^2} = a = (\sin 2\beta)_B$; see Eqn (I.8), $\cot \beta = \frac{1 + \sqrt{1 - a^2}}{a}$, $\bar{\eta} = R_t \sin \beta = R_t \left(\frac{1 - \sqrt{1 - a^2}}{2} \right)^{1/2}$, $\bar{\rho} = 1 - R_t \cos \beta = 1 - \bar{\eta} \cot \beta$ $= 1 - \frac{1 + \sqrt{1 - a^2}}{a} \bar{\eta}$; see Eqn (I.9)	$\text{sgn } F_{tt} \cdot \cot \beta = f(\beta) > 0$, i.e. $\text{sgn } F_{tt} = -1$ corresponds to $\cot \beta < 0$, $\text{sgn } F_{tt} \cdot \cot \beta = \frac{1 - \bar{\rho}}{ \bar{\eta} } = f(\beta) = \frac{1 + \sqrt{1 - a^2}}{a} > 1.7$, $R_t^2 = (1 - \bar{\rho})^2 + \bar{\eta}^2 = [1 + f(\beta)^2] \bar{\eta}^2$, $\bar{\eta} = \text{sgn } F_{tt} \cdot \frac{R_t}{\sqrt{1 + f(\beta)^2}} = \text{sgn } F_{tt} \cdot R_t \left(\frac{1 - \sqrt{1 - a^2}}{2} \right)^{1/2}$, $\bar{\rho} = 1 - f(\beta) \bar{\eta} = 1 - \frac{1 + \sqrt{1 - a^2}}{a} \bar{\eta} $

models with $F_{tt} < 0$ it corresponds to $|\sin 2\beta_{\min}| = a_{\psi K, \min} = 0.69$ (see Table I.1). For all MFV models and the SM, the maximum value of $|\sin 2\beta_{\max}| = a_{\psi K, \max} = 0.87$ [see Eqn (83)]. All these limits do not contradict the experimental value of $a_{\psi K} = 0.734 \pm 0.054$ [104]. Applying relation (II.6), from the maximum value of $\text{BR}(K^+ \rightarrow \pi^+ \nu \bar{\nu})_{\max} = 3.9 \times 10^{-10}$, obtained from experiments E787 [131], one can determine the absolute upper limits

$$\text{BR}(K_L^0 \rightarrow \pi^0 \nu \bar{\nu})_{\text{MFV, max}} = \begin{cases} 27 \times 10^{-11} & (\tilde{X} > 0), \\ 45 \times 10^{-11} & (\tilde{X} < 0), \end{cases}$$

presented in Section 6.2.1 [see formulas (146)].

III. More precise relationship for $\text{BR}(K^+ \rightarrow \pi^+ \nu \bar{\nu}) = K_+ B(\lambda_c; \lambda_t)$

We shall now obtain a corrected expression for the function

$$B(\lambda_c; \lambda_t) = \frac{X(x_t)}{\lambda^2} [(\delta(x_c) \text{Re } \lambda_c + \text{Re } \lambda_t)^2 + (\text{Im } \lambda_t)^2], \quad (\text{III.1})$$

in which, unlike Eqn (116), use is made of the expansion of $\text{Re } \lambda_t$, taking into account all terms up to $O(\lambda^9)$ (see Table 1):

$$\begin{aligned} \text{Re } \lambda_t &= -A^2 \lambda^5 \left(1 - \frac{\lambda^2}{2} \right) (1 - \bar{\rho}) \\ &\quad - A^2 \lambda^7 [\bar{\rho} - (\bar{\rho}^2 + \bar{\eta}^2)] + O(\lambda^9). \end{aligned} \quad (\text{III.2})$$

Earlier, the less precise expression

$$\text{Re } \lambda_t = -A^2 \lambda^5 \left(1 - \frac{\lambda^2}{2} \right) (1 - \bar{\rho}) + O(\lambda^7)$$

was used. Now, the expressions for $\text{Re } \lambda_c$ and $\text{Im } \lambda_t$ will remain the same as before (see Table 1):

$$\text{Re } \lambda_c = -\lambda \left(1 - \frac{\lambda^2}{2} \right) + O(\lambda^5), \quad (\text{III.3})$$

$$\text{Im } \lambda_t = A^2 \lambda^5 \left(1 + \frac{\lambda^2}{2} \right) \bar{\eta} + O(\lambda^9). \quad (\text{III.4})$$

Expansion of $\text{Re } \lambda_c$ is justified only up to the terms $O(\lambda^5)$, since Eqn (114) contains the product

$$\delta(x_c) \text{Re } \lambda_c = -\delta(x_c) \lambda \left(1 - \frac{\lambda^2}{2}\right) + \delta(x_c) O(\lambda^5),$$

exhibiting a precision

$$\delta(x_c) O(\lambda^5) = 6.7 \times 10^{-4} O(\lambda^5) \lesssim O(\lambda^9).$$

Thus, the modified expression for $B(\lambda_c; \lambda_t)$ assumes the form

$$\begin{aligned} B(\lambda_c; \lambda_t) &= \frac{X^2(x_t)}{\lambda^2} [(\delta(x_c) \text{Re } \lambda_c + \text{Re } \lambda_t)^2 + (\text{Im } \lambda_t)^2] \\ &= \frac{X^2(x_t)}{\lambda^2} \lambda^2 \left(1 - \frac{\lambda^2}{2}\right)^2 \left\{ \left[-\delta(x_c) - A^2 \lambda^4 (1 - \bar{\rho}) \right. \right. \\ &\quad \left. \left. - \frac{A^2 \lambda^6 [\bar{\rho} - (\bar{\rho}^2 + \bar{\eta}^2)]}{1 - \lambda^2/2} \right]^2 + \frac{A^4 \lambda^8 \bar{\eta}^2}{(1 - \lambda^2/2)^4} \right\} \\ &= X^2(x_t) A^4 \lambda^8 \frac{1}{\sigma} \left\{ \left[\frac{\delta(x_c)}{A^2 \lambda^4} + 1 - \bar{\rho} \right. \right. \\ &\quad \left. \left. + \lambda^2 [\bar{\rho} - (\bar{\rho}^2 + \bar{\eta}^2)] \left(1 + \frac{\lambda^2}{2}\right) \right]^2 + (\sigma \bar{\eta})^2 \right\} \\ &= \lambda^8 A^4 X^2(x_t) \frac{1}{\sigma} \{ (\rho_0 - \bar{\rho})^2 + (\sigma \bar{\eta})^2 \\ &\quad + 2\lambda^2 (\rho_0 - \bar{\rho}) [\bar{\rho} - (\bar{\rho}^2 + \bar{\eta}^2)] + O(\lambda^4) \}. \end{aligned} \quad (\text{III.5})$$

It differs from Eqn (116) by the third term in the curly brackets, which is on the order of $O(\lambda^2)$.

Hence, one ultimately obtains the corrected expression for $\text{BR}(\text{K}^+ \rightarrow \pi^+ \nu \bar{\nu})$ (see, also, Ref. [114]):

$$\begin{aligned} \text{BR}(\text{K}^+ \rightarrow \pi^+ \nu \bar{\nu})_{\text{SM}} &= K_+ \lambda^8 A^4 X^2(x_t) \frac{1}{\sigma} [(\rho_0 - \bar{\rho})^2 + (\sigma \bar{\eta})^2] \\ &\quad \times \left(1 + \frac{2\lambda^2 (\rho_0 - \bar{\rho}) [\bar{\rho} - (\bar{\rho}^2 + \bar{\eta}^2)]}{(\rho_0 - \bar{\rho})^2 + (\sigma \bar{\eta})^2} \right). \end{aligned} \quad (\text{III.6})$$

Estimation of the correction factor in Eqn (III.6) with respect to the usually applied standard relation (117) for $\text{BR}(\text{K}^+ \rightarrow \pi^+ \nu \bar{\nu})_{\text{SM}}$ reveals that it differs from unity by less than 0.5%, so, as a rule, it need not be taken into account:

$$\begin{aligned} 1 + \frac{2\lambda^2 (\rho_0 - \bar{\rho}) [\bar{\rho} - (\bar{\rho}^2 + \bar{\eta}^2)]}{(\rho_0 - \bar{\rho})^2 + (\sigma \bar{\eta})^2} \\ = 1 + 4.0 \times 10^{-3} = 1.004 \simeq 1. \end{aligned} \quad (\text{III.7})$$

9. Notes added in proof

1. New data have been obtained on the element $|V_{us}| = \lambda$ of the quark mixing matrix.

1.1 Investigation of the $\text{K}^+ \rightarrow \pi^0 e^+ \nu_e$ decay in experiment BNL E865 (Sher A et al., hep-ex/0305042) has permitted the researchers to obtain the value of $|V_{us}| = 0.2272 \pm 0.0023 \pm 0.0007 \pm 0.0018 = 0.2272 \pm 0.0027$.

1.2 A new analysis of the set of data on the semilepton decays of hyperons (Cabibbo N et al., hep-ph/0307214; hep-ph/0307298) has resulted in the value of $|V_{us}| = 0.2250 \pm 0.0027$.

A certain increase in the value of $|V_{us}|$, as compared to the previous value (see Table 5), apparently resolves the known problem of possible violating one of the unitarity conditions of the quark mixing matrix, namely $|V_{ud}|^2 + |V_{us}|^2 + |V_{ub}|^2 = 1$.

2. Corrected predictions have been made for the $\text{K} \rightarrow \pi \nu \bar{\nu}$ -decay probabilities in the SM (Isidori G, hep-ph/0307014). Here, the relations used for probabilities were of the type (117), (118), while the parameter values in these expressions were determined by fitting data for the unitary triangle in the $(\bar{\rho}, \bar{\eta})$ -plane, given in Ref. [8] (they are close to set B in Table 5). The following decay probabilities have been determined:

$$\text{BR}(\text{K}^+ \rightarrow \pi^+ \nu \bar{\nu})_{\text{SM}} = (0.82 \pm 0.12) \times 10^{-10},$$

$$\text{BR}(\text{K}_L^0 \rightarrow \pi^0 \nu \bar{\nu})_{\text{SM}} = (0.27 \pm 0.05) \times 10^{-10}.$$

The accuracy of these predictions approach the results (123), (124) and (129), (130), obtained using the variables of the kaon unitary triangle (see Section 5.2).

3. A somewhat more precise value has been established for the CP-odd asymmetry in decays $\text{B}_d^0(\bar{\text{B}}_d^0) \rightarrow (\text{J}/\psi) \text{K}_S^0$ (Golob B, hep-ph/0300806). The results of measurements performed at the Belle and BaBar installations have approached each other even closer. The averaged value of asymmetry amounts to $\langle a_{\psi \text{K}} \rangle = 0.736 \pm 0.049$. In the SM, one has $a_{\psi \text{K}} = \sin 2\beta$ and $\beta = (23.7_{-2.0}^{+2.2})^\circ$.

4. The decay $\text{K}_S^0 \rightarrow \pi^0 e^+ e^-$ has been revealed in experiment NA48 (Batley J et al., hep-ex/0309075), and its probability has been determined: $\text{BR}(\text{K}_S^0 \rightarrow \pi^0 e^+ e^-) = (5.8_{-2.4}^{+2.9}) \times 10^{-9}$. Hence, one can predict (see Table 7) that

$$\begin{aligned} \text{BR}(\text{K}_L^0 \rightarrow \pi^0 e^+ e^-)_{\text{CP-indir}} \\ = 3.0 \times 10^{-3} \text{BR}(\text{K}_S^0 \rightarrow \pi^0 e^+ e^-) \simeq (1.7_{-0.7}^{+0.9}) \times 10^{-11}. \end{aligned}$$

References

1. Okun' L B *Leptony i Kvarki* (Leptons and Quarks) 2nd ed. (Moscow: Nauka, 1990) [Translated into English (Amsterdam: North-Holland, 1984)]; *Fizika Elementarnykh Chastits* (The Physics of Elementary Particles) 2nd ed. (Moscow: Nauka, 1988)
2. Commins E D, Bucksbaum P H *Weak Interactions of Leptons and Quarks* (Cambridge: Cambridge Univ. Press, 1983) [Translated into Russian (Moscow: Energoatomizdat, 1987)]
3. Branco G C, Lavoura L, Silva J P *CP Violation* (Oxford: Clarendon Press, 1999)
4. Kane G L *Modern Elementary Particle Physics* (Redwood City, CA: Addison Wesley, 1987) [Translated into Russian (Moscow: Mir, 1990)]
5. Bigi I I, Sanda A I *CP Violation* (Cambridge: Cambridge Univ. Press, 2000)
6. Buras A J, Linder M (Eds) *Heavy Flavours II* (Adv. Ser. Directions in High Energy Physics, Vol. 15) (Singapore: World Scientific, 1997)
7. Harrison P F, Quinn H R (Eds) *The BaBar Physics Book*, SLAC Report, SLAC-R-504 (1998)
8. Battaglia M et al. (Eds) *The CKM Matrix and the Unitarity Triangle: Proc. of the Workshop on CKM Unitarity Triangle Parameter Determination, Geneva, Switzerland, Feb. 13–16, 2002* (in press); hep-ph/0304132
9. Rosner J L, Winstein B D (Eds) *Kaon Physics: Proc. of the Workshop on K Physics (KAON-99), Chicago, USA, Jan. 21–26, 1999* (Chicago: Univ. of Chicago Press, 2000)
10. Costantini F, Isidori G, Sozzi M (Eds) *Proc. of the KAON-2001 Intern. Conf. on CP Violation, Pisa, Italy, June 12–17, 2001* (Frascati Phys. Ser., Vol. 26) (Frascati: INFN, 2001)

11. Jaros J, Peskin M (Eds) *Lepton Photon-99: XIX Intern. Symp. on Lepton and Photon Interactions at High Energies, Stanford, CA, USA, 9–14 Aug. 1999* (Singapore: World Scientific, 2000; *Int. J. Mod. Phys. A* **15** (Suppl. 1) (2000))
12. Sugimoto S, Yamanaka T (Eds) *Proc. of the Intern. Workshop on CP Violation in K, KEK, Dec. 18–19, 1998*, KEK Proc. 99-3 (1999)
13. Bianco S et al. (Eds) *Physics and Detectors for DAΦNE: Proc. of the 3rd DAΦNE Workshop on Physics and Detectors, Frascati, Nov. 16–19, 1999* (Frascati Phys. Ser., Vol. XVI) (Rome: INFN, 2000)
14. Cheng H-Y, Hou W-S (Eds) *Proc. of the 3rd Intern. Conf. on B Physics and CP Violation, Taipei, Taiwan, Dec. 3–7, 1999* (Singapore: World Scientific, 2000)
15. Huitu K et al. (Eds) *Proc. of the Intern. Europhysics Conf. on High-Energy Physics (EPS-HEP-99), Tampere, Finland, July 15–21, 1999* (Bristol: IOP Publ., 2000)
16. Kuno Y, Shinkawa T (Eds) *Proc. of the Intern. KEK Workshop “Kaons, Muons, Neutrino Physics and Future”, Oct. 31–Nov. 1, 1997*, KEK Proc. 97–24 (1998)
17. Lim C S, Yamanaka T (Eds) *Proc. of the XXX Intern. Conf. on High Energy Physics (ICHEP-2000), Osaka, Japan, July 27–Aug. 2, 2000* Vols 1, 2 (Singapore: World Scientific, 2001)
18. *Proc. of the Intern. Conf. on CP Violation Physics, Ferrara, Italy, Sept. 18–22, 2000*; *Nucl. Phys. B: Proc. Suppl.* **99B** (2001)
19. Bentvelsen S et al. (Eds) *Proc. of the XXXI Intern. Conf. on High Energy Physics (ICHEP-2002), Amsterdam, Holland, July 25–31, 2002* (Amsterdam: North-Holland, 2003); *Nucl. Phys. B: Proc. Suppl.* **117** (2003)
20. Lee-Franzini J, Franzini P, Bossi F (Eds) *Proc. of the XX Intern. Symp. on Lepton and Photon Interactions at High Energies (Lepton–Photon-01), Rome, Italy, July 23–28, 2001* (New Jersey: World Scientific, 2002)
21. Davies C T H, Playfer S M (Eds) *Heavy Flavour Physics: Theory and Experimental Results in Heavy Quark Physics* (Scottish Universities Summer School in Physics, 55) (Bristol: IOP, 2002)
22. *Proc. of the 5th Intern. Conf. on Hyperons, Charm, and Beauty Hadrons, Vancouver, BC, Canada, July 25–29, 2002*; *Nucl. Phys. B: Proc. Suppl.* **115** (2003)
23. Hashimoto S, Komatsubara T K (Eds) *Frontiers in Flavor Physics: Proc. of the 5th KEK Topical Conf. on Frontiers in Flavor Physics, Tsukuba, Japan, Nov. 20–22, 2001*; *Nucl. Phys. B: Proc. Suppl.* **111** (2002)
24. Belyaev A et al., hep-ph/0107046
25. Hagiwara K et al. (PDG 2002 Collab.) *Phys. Rev. D* **66** 010001 (2002)
26. Buchalla G, Buras A J, Lautenbacher M E *Rev. Mod. Phys.* **68** 1125 (1996)
27. Buras A J, Fleischer R, hep-ph/9704376; see also Ref. [6] p. 65; Buras A J, hep-ph/9806471; hep-ph/9905437; hep-ph/0101336
28. Buras A J, hep-ph/0109197; see also Ref. [10]
29. Buras A J, hep-ph/0210291
30. Nir Y *Nucl. Phys. B: Proc. Suppl.* **117** 111 (2003); hep-ph/0208080
31. Nir Y, hep-ph/0109090; see also Ref. [21] p. 147
32. Nir Y, in *Particle Physics: Proc. of the 1999 Summer School, Trieste, Italy, 21 June–9 July, 1999* (Eds G Senjanovic, A Yu Smirnov) (Singapore: World Scientific, 2000) p. 165; hep-ph/9911321; hep-ph/9810520; in *Proc. 1998 European School of High-Energy Physics, St. Andrews, Scotland, Aug. 23–Sept. 3, 1998* (CERN, 99-04, Eds N Ellis, J March-Russel) (Geneva: European Organization for Nuclear Research, 1999)
33. Grossman Y, Nir Y, Rattazzi R, hep-ph/9701231; see also Ref. [6] p. 755
34. Neubert M, in *Proc. 1995 European School of High-Energy Physics, Dubna, Aug. 27–Sept. 9, 1995* (CERN, 96-04, Eds N Ellis, M Neubert) (Geneva: CERN, 1996) p. 121; hep-ph/0207327; see Ref. [20] p. 14
35. D’Ambrosio G, Isidori G *Int. J. Mod. Phys. A* **13** 1 (1998)
36. Isidori G, hep-ph/9902235; hep-ph/9908399; see also Ref. [9] p. 355
37. Isidori G *Int. J. Mod. Phys. A* **17** 3078 (2002); hep-ph/0110255; see also Ref. [20] p. 160
38. Buchalla G, hep-ph/9912369; see also Ref. [15] p. 1; hep-ph/0002207; see also Ref. [13] p. 121; hep-ph/0103166
39. Littenberg L, hep-ex/0010048; *Frascati Phys. Ser.* **XI** 317 (1998); Littenberg L, Valencia G *Annu. Rev. Nucl. Part. Sci.* **43** 729 (1993)
40. Littenberg L, hep-ex/0212005
41. Barker A R, Kettell S H *Annu. Rev. Nucl. Part. Sci.* **50** 249 (2000); hep-ex/0009024
42. Landsberg L G *Yad. Fiz.* **64** 1811 (2001) [*Phys. Atom. Nucl.* **64** 1729 (2001)]
43. Rizzo T G, hep-ph/9809526
44. Stone S, see Ref. [21] p. 237; Nakada T, see Ref. [21] p. 373
45. Stocchi A *Nucl. Phys. B: Proc. Suppl.* **117** 145 (2003); hep-ph/0211245; *eConf C020805 TTH04* (2002); hep-ph/0304237
46. Shabalin E P *Usp. Fiz. Nauk* **171** 951 (2001) [*Phys. Usp.* **44** 895 (2001)]
47. Fleischer R *Phys. Rep.* **370** 537 (2002); hep-ph/0207108; hep-ph/0210323
48. Buras A J et al. *JHEP* **0301** 029 (2003); hep-ph/0207101
49. Cabibbo N *Phys. Rev. Lett.* **10** 531 (1963); Kobayashi M, Maskawa T *Prog. Theor. Phys.* **49** 652 (1973)
50. Glashow S L, Iliopoulos J, Maiani L *Phys. Rev. D* **2** 1285 (1970)
51. Wolfenstein L *Phys. Rev. Lett.* **51** 1945 (1983)
52. Randhawa M et al. *Mod. Phys. Lett. A* **15** 2363 (2000); hep-ph/0002217
53. Vainshtein A I, Zakharov V I, Shifman M A *Zh. Eksp. Teor. Fiz.* **72** 1275 (1977) [*Sov. Phys. JETP* **45** 670 (1977)]
54. Vainshtein A *Int. J. Mod. Phys. A* **14** 4705 (1999)
55. Inami T, Lim G S *Prog. Theor. Phys.* **65** 297 (1981)
56. Buras A J, Jamin M, Weisz P H *Nucl. Phys. B* **347** 491 (1990)
57. Herrlich S, Nierste U *Nucl. Phys. B* **419** 292 (1994); *Phys. Rev. D* **52** 6505 (1995); *Nucl. Phys. B* **476** 27 (1996)
58. Buchalla G, Buras A J *Nucl. Phys. B* **412** 106 (1994); *Phys. Rev. D* **54** 6782 (1996); *Nucl. Phys. B* **548** 309 (1999); hep-ph/9901288
59. Sakharov A D *Pis'ma Zh. Eksp. Teor. Fiz.* **5** 32 (1967) [*JETP Lett.* **5** 24 (1967)]
60. Brown H N et al. (Muon (g-2) Collab.) *Phys. Rev. Lett.* **86** 2227 (2001)
61. Peskin M E, hep-ph/0212204; SLAC-PUB-9613 (2002)
62. Hewett J L, Takeuchi T, Thomas S, hep-ph/9603391; SLAC-PUB-7088 (1996); CERN-TH/96-56
63. Abe F et al. (CDF Collab.) *Phys. Rev. Lett.* **79** 2198 (1997)
64. Abbott B et al. (D0 Collab.) *Phys. Rev. Lett.* **80** 666 (1998); **82** 2457 (1999); Landsberg G, hep-ex/9910034; see also Ref. [15] p. 793
65. Arkani-Hamed N, Dimopoulos S, Dvali G *Phys. Lett. B* **429** 263 (1998); *Phys. Rev. D* **59** 086004 (1999); hep-ph/9807344
66. Cheung K, Landsberg G *Phys. Rev. D* **62** 076003 (2000); hep-ph/9909218; Cheung K, hep-ph/0003306; Landsberg G, hep-ex/0009038; see also Ref. [17] Vol. 2, p. 1150
67. Abbott B et al. (D0 Collab.) *Phys. Rev. Lett.* **86** 1156 (2001); hep-ex/0008065
68. Hawking S W *Nature* **248** 30 (1974)
69. Dimopoulos S, Landsberg G *Phys. Rev. Lett.* **87** 161602 (2001); Giddings S B, Thomas S *Phys. Rev. D* **65** 056010 (2002)
70. Landsberg G *Phys. Rev. Lett.* **88** 181801 (2002); hep-ph/0112061; hep-ph/0211043
71. Anchordoqui L, Goldberg H *Phys. Rev. D* **67** 064010 (2003); hep-ph/0209337
72. Silvestrini L *Nucl. Phys. B: Proc. Suppl.* **93** 247 (2001); hep-ph/0009284; *Nucl. Phys. B: Proc. Suppl.* **99B** 181 (2001)
73. Ciuchini M et al. *Nucl. Phys. B* **534** 3 (1998)
74. Buras A J et al. *Phys. Lett. B* **500** 161 (2001); hep-ph/0007085
75. Landsberg L G, Obraztsov V F, see Ref. [9] p. 619; Obraztsov V F, Landsberg L G *Nucl. Phys. B: Proc. Suppl.* **99B** 257 (2001); hep-ex/0011033
76. Coleman R et al. (CKM Collab.) “A proposal for a precision measurement of the decay $K^+ \rightarrow \pi^+ \bar{\nu}$ and other rare K^+ processes at Fermilab using the main injector”, Fermilab, P-905 (1998); Frank G et al. (CKM Collab.) “A proposal for a precision measurement of the decay $K^+ \rightarrow \pi^+ \bar{\nu}$ and other rare K^+ processes at Fermilab using the main injector”, Fermilab, P-921 (2001); Tschirhard R S, see Ref. [12] pp. 85, 141, 151; Milsteine C et al. (CKM Collab.) *Nucl. Phys. B: Proc. Suppl.* **93** 348 (2001); hep-ex/0009046; Cooper P S *Nucl. Phys. B: Proc. Suppl.* **99B** 121 (2001); Landsberg L G *Yad. Fiz.* **65** 1795 (2002) [*Phys. Atom. Nucl.* **65** 1749 (2002)]
77. Bassalleck B et al. “E949: An experiment to measure $B(K^+ \rightarrow \pi^+ \bar{\nu})$ at BNL”, BNL-67247 (1999); Kettell S, see

- Ref. [12] p. 75; Komatsubara T K, *ibid.*, p. 133; Shinkawa T, *ibid.*, p. 137
78. Burkhardt H et al. (NA-31 Collab.) *Phys. Lett. B* **206** 169 (1988); Barr G D et al. (NA-31 Collab.) *Phys. Lett. B* **317** 233 (1993)
 79. Gibbons L K et al. (E731 Collab.) *Phys. Rev. Lett.* **70** 1203 (1993)
 80. Alavi-Harati A et al. (KTeV Collab.) *Phys. Rev. Lett.* **83** 22 (1999); Glazov A, see Ref. [10] p. 113; Alavi-Harati A et al. (KTeV Collab.) *Phys. Rev. D* **67** 012005 (2003); *Phys. Rev. D* **67** 012005 (2003); hep-ex/0208007
 81. Fanti V et al. (NA48 Collab.) *Phys. Lett. B* **465** 335 (1999); Mikulee L, see Ref. [10] p. 121; Batley J R et al. (NA48 Collab.) *Phys. Lett. B* **544** 97 (2002); hep-ex/0208009
 82. Buras A J, Gérard J-M *Phys. Lett. B* **517** 129 (2001); hep-ph/0106104
 83. Pich A, in *Astronomy, Cosmology, and Fundamental Physics: Proc. of the ESO/CERN/ESA Symp., Garching, Germany, 4–7 March 2002* (ESO Astrophys. Symp., Eds P A Shaver, L Dilella, A Giménez) (New York: Springer-Verlag, 2003) p. 105; hep-ph/0206011
 84. Alavi-Harati A et al. (KTeV Collab.) *Phys. Rev. Lett.* **88** 181601 (2002)
 85. Alavi-Harati A et al. (KTeV Collab.) *Phys. Rev. Lett.* **84** 408 (2000)
 86. Mazzucato E (NA48 Collab.) *Nucl. Phys. B: Proc. Suppl.* **99B** 81 (2001)
 87. Heiliger P, Sehgal L M *Phys. Rev. D* **48** 4146 (1993); Sehgal L M, see Ref. [9] p. 181
 88. Kabir P K *Phys. Rev. D* **2** 540 (1970); Aharony A *Lett. Nuovo Cimento* **3** 791 (1970)
 89. Bloch P (CPLEAR Collab.), see Ref. [9] p. 223
 90. Bertin A et al. *Riv. Nuovo Cimento* **23** (3) 1 (2000); Faccioli P *Nucl. Instrum. Meth. A* **462** 313 (2001); hep-ph/0011269
 91. Ciuchini M et al. *JHEP* **0107** 013 (2001); hep-ph/0012308; Stocchi A *Nucl. Instrum. Meth. A* **462** 318 (2001); hep-ph/0012215; Ciuchini M *Nucl. Phys. B: Proc. Suppl.* **109** (2–3) 307 (2002); hep-ph/0112133
 92. Höcker A et al. *Eur. Phys. J. C* **21** 225 (2001); hep-ph/0104062; *AIP Conf. Proc.* **618** 27 (2002); hep-ph/0112295
 93. Anikeev K et al., hep-ph/0201071; Fermilab-Pub-01/197
 94. (ALEPH, CDF, DELPHI, L3, OPAL, SLD Collab.), hep-ex/0112028
 95. Rosner J L *Nucl. Phys. B: Proc. Suppl.* **115** 385 (2003); hep-ph/0208243
 96. Gaillard M K, Lee B W *Phys. Rev. D* **10** 897 (1974)
 97. Falk A F *Nucl. Phys. B: Proc. Suppl.* **111** 3 (2002); hep-ph/0201094
 98. Uraltsev N, hep-ph/0010328; Lellouch L *Nucl. Phys. B: Proc. Suppl.* **117** 127 (2003); hep-ph/0211359
 99. Ryan S *Nucl. Phys. B: Proc. Suppl.* **106–107** 86 (2002); hep-lat/0111010
 100. Yamada N et al. (JLQCD Collab.) *Nucl. Phys. B: Proc. Suppl.* **106–107** 397 (2002); hep-lat/0110087
 101. Kronfeld A S, Ryan S M *Phys. Lett. B* **543** 59 (2002); hep-ph/0206058; Kronfeld A S *eConf C020620* FRBT05 (2002); hep-ph/0209231
 102. Bečirević D et al., hep-lat/0209131; *Phys. Lett. B* **563** 150 (2003); hep-ph/0211271
 103. Lellouch L *Nucl. Phys. B: Proc. Suppl.* **117** 127 (2003); hep-ph/0211359
 104. Affolder T et al. (CDF Collab.) *Phys. Rev. D* **61** 072005 (2000); hep-ex/9909003; see also Ref. [17]; Aubert B et al. (BaBar Collab.) *Phys. Rev. Lett.* **89** 201802 (2002); hep-ex/0207042; Karyotakis Y *Nucl. Phys. B: Proc. Suppl.* **117** 98 (2003); Abe K et al. (Belle Collab.), hep-ex/0207098; Yamauchi M *Nucl. Phys. B: Proc. Suppl.* **117** 83 (2003)
 105. Mackenzie P “The tevatron, the lattice, and the unitarity triangle: 21st Century lattice QCD”, Fermilab Joint Experimental-Theoretical Seminar, 27 September (2002); Cassel D G, hep-ex/0307038
 106. Briere R A et al., CLNS-01-1742 (2001)
 107. Littenberg L G *Phys. Rev. D* **39** 3322 (1989)
 108. Grossman Y, Nir Y *Phys. Lett. B* **398** 163 (1997); hep-ph/9701313
 109. Hagelin J S, Littenberg L S *Prog. Part. Nucl. Phys.* **23** 1 (1989); Rein D, Sehgal L M *Phys. Rev. D* **39** 3325 (1989); Lu M, Wise M B *Phys. Lett. B* **324** 461 (1994); Geng C Q, Hsu I J, Lin Y C *Phys. Lett. B* **355** 569 (1995); Fajfer S *Nuovo Cimento A* **100** 397 (1997)
 110. Ellis J, Hagelin J S, Rudaz S *Phys. Lett. B* **192** 201 (1987); Ellis J, Hagelin J S *Nucl. Phys. B* **217** 189 (1983)
 111. Dib C O et al. *Mod. Phys. Lett. A* **6** 3573 (1991)
 112. Marciano W J, Parsa Z *Phys. Rev. D* **53** R1 (1996)
 113. Bobeth C et al. *Nucl. Phys. B* **630** 87 (2002); hep-ph/0112305
 114. Bergmann S, Perez G *JHEP* **0008** 034 (2000); hep-ph/0007170
 115. Falk A F, Lewandowski A, Petrov A A *Phys. Lett. B* **505** 107 (2001); hep-ph/0012099
 116. Falk A, see Ref. [11] p. 174
 117. Bigi I I, Gabbiani F *Nucl. Phys. B* **367** 3 (1991)
 118. Kettell S H, Landsberg L G, Nguyen H, hep-ph/0212321
 119. D’Ambrosio G, Isidori G *Phys. Lett. B* **530** 108 (2002); hep-ph/0112135
 120. Briere R A et al. (CLEO Collab.) *Phys. Rev. Lett.* **89** 081803 (2002)
 121. Atwood D, Soni A, hep-ph/0212071
 122. Atwood D, Soni A *Phys. Lett. B* **508** 17 (2001); hep-ph/0103197
 123. Laplace S, hep-ph/0209188
 124. Marciano W, see Ref. [9] p. 603
 125. Lai A et al. (NA48 Collab.) *Phys. Lett. B* **514** 253 (2001); *Phys. Lett. B* **536** 229 (2002); hep-ex/0205010
 126. Alavi-Harati A et al. (KTeV Collab.) *Phys. Rev. Lett.* **86** 397 (2001); hep-ex/0009030; *Phys. Rev. Lett.* **84** 5279 (2000); hep-ex/0309072
 127. Ambrose D et al. (BNL E871 Collab.) *Phys. Rev. Lett.* **84** 1389 (2000)
 128. Wah Y W (KTeV Collab.), see Ref. [17] p. 767
 129. Ambrose D et al. (BNL E871 Collab.) *Phys. Rev. Lett.* **81** 4309 (1998)
 130. Adler S et al. (E787 Collab.) *Phys. Rev. Lett.* **79** 2204 (1997); **84** 3768 (2000)
 131. Adler S et al. (E787 Collab.) *Phys. Rev. Lett.* **88** 041803 (2002); hep-ex/0111091
 132. Adler S et al. (E787 Collab.) *Phys. Lett. B* **537** 211 (2002); hep-ex/0201037
 133. Kettell S H, hep-ex/0207044; *Nucl. Phys. B: Proc. Suppl.* **111** 232 (2002); hep-ex/0205029; Littenberg L, hep-ex/0010048; *AIP Conf. Proc.* **618** 89 (2002); hep-ex/0201026; Bryman D, hep-ex/0206072; Diwan M V, hep-ex/0205089
 134. Atiya M S et al. *Phys. Rev. Lett.* **70** 2521 (1993)
 135. Wilczek F *Phys. Rev. Lett.* **49** 1549 (1982)
 136. Gorbunov D S, Rubakov V A *Phys. Rev. D* **64** 054008 (2001)
 137. Komatsubara T K, Nakano T, Nomura T “Study of the rare decay $K^+ \rightarrow \pi^+ \bar{\nu} \nu$ with stopped kaon beam at J-PARC”, Lett. of Intent, KEK, December 27, 2002; <http://kaon.kek.jp/~kpwg/>
 138. Alavi-Harati A et al. *Phys. Rev. D* **61** 072006 (2000)
 139. Alexopoulos T et al., KAMI Proposal, Fermilab (2001); Yamana-ka T *Nucl. Phys. B: Proc. Suppl.* **99B** 104 (2001)
 140. Chiang L H et al., KOPIO — a Search for $K^0 \rightarrow \pi^0 \bar{\nu} \nu$ BNL Proposal (1999); Bryman D A, Littenberg L *Nucl. Phys. B: Proc. Suppl.* **99B** 61 (2001)
 141. Inagaki T et al. (KEK E391A Collab.) Proposal, KEK Internal 96-13 (1996); Inagaki T, in *Proc. of KEK Workshop 1997*, KEK Proc. 97-24, p. 205
 142. Buras A J et al. *Nucl. Phys. B* **592** 55 (2001); hep-ph/0007313
 143. Buras A J, Fleischer R *Phys. Rev. D* **64** 115010 (2001); hep-ph/0104238
 144. Buras A J, Spranger M, Weiler A *Nucl. Phys. B* **660** 225 (2003); hep-ph/0212143
 145. Appelquist T, Cheng H-C, Dobrescu B A *Phys. Rev. D* **64** 035002 (2001); hep-ph/0012100
 146. D’Ambrosio G et al. *Nucl. Phys. B* **645** 155 (2002); hep-ph/0207036
 147. Isidori G, hep-ph/0301159
 148. Türke U *Phys. Lett. B* **168** 296 (1986); Eilam G, Hewett J L, Rizzo T G *Phys. Lett. B* **193** 533 (1987)
 149. Hattori T, Hasuike T, Wakaizumi S *Phys. Rev. D* **60** 113008 (1999); hep-ph/9804412
 150. Huang C-S, Huo W-J, Wu Y-L *Phys. Rev. D* **64** 016009 (2001); hep-ph/0005227
 151. Barenboim G, Botella F J, Vives O *Nucl. Phys. B* **613** 285 (2001); hep-ph/0105306
 152. Hawkins D, Silverman D *Phys. Rev. D* **66** 016008 (2002); hep-ph/0205011
 153. Aguilar-Saavedra J A *Phys. Rev. D* **67** 035003 (2003); hep-ph/0210112

154. Dumm D G, Pisano F, Pleitez V *Mod. Phys. Lett. A* **9** 1609 (1994); Liu J T, Ng D *Phys. Rev. D* **50** 548 (1994); Long H N, Van V T *J. Phys. G: Nucl. Part. Phys.* **25** 2319 (1999)
155. Long H N, Trung L P, Van V T *Zh. Eksp. Teor. Fiz.* **119** 633 (2001) [*JETP* **92** 548 (2001)]; hep-ph/0104007
156. Ellis J *Nucl. Phys. B: Proc. Suppl.* **99B** 331 (2001); hep-ph/0011396
157. Colangelo G, Isidori G *JHEP* **9809** 009 (1998); hep-ph/9808487
158. Buras A J, Silvestrini L *Nucl. Phys. B* **546** 299 (1999); Silvestrini L, hep-ph/9906202
159. Buras A J et al. *Nucl. Phys. B* **546** 3 (2000); hep-ph/9908371
160. Buchalla G, Isidori G *Phys. Lett. B* **440** 170 (1998); hep-ph/9806501
161. Chen C-H *J. Phys. G: Nucl. Part. Phys.* **28** L33 (2002); hep-ph/0202188
162. Baek S et al. *Phys. Rev. D* **62** 117701 (2000); hep-ph/9907572; hep-ph/0009105
163. Baek S et al. *Nucl. Phys. B* **609** 442 (2001); hep-ph/0105028
164. Goto T, Okada Y, Shimizu Y *Phys. Rev. D* **58** 094006 (1998); hep-ph/9804294
165. Hung P Q *Phys. Rev. D* **62** 053015 (2000)
166. Hung P Q, Soddu A *Phys. Rev. D* **65** 054035 (2002); hep-ph/0108119
167. Fleischer R, Isidori G, Matias J *JHEP* **0305** 053 (2003); hep-ph/0302229
168. Xiao Z J et al. *Eur. Phys. J. C* **7** 487 (1998); Xiao Z, Li C, Chao K *Eur. Phys. J. C* **10** 51 (1999)
169. Agashe K, Graesser M *Phys. Rev. D* **54** 4445 (1996)
170. Bhattacharyya G, Raychaudhuri A *Phys. Rev. D* **57** R3837 (1998)
171. Grossman Y *Nucl. Phys. B* **426** 355 (1994)
172. Buchalla G et al. *Phys. Rev. D* **53** 5185 (1996)
173. Kiyo Y, Morozumi T, Tanimoto M, hep-ph/9805307
174. Burdman G *Phys. Rev. D* **59** 035001 (1999); hep-ph/9806360; hep-ph/9811457
175. Akama N et al. *Phys. Rev. D* **64** 095012 (2001); hep-ph/0104263
176. Perez G *JHEP* **0002** 043 (2000); hep-ph/0001037
177. Cho G-C *Eur. Phys. J. C* **5** 525 (1998); hep-ph/9804327
178. Christenson J H et al. *Phys. Rev. Lett.* **13** 138 (1964)